**NOAA Project**
Report

# Development of Four Additional Tsunami Inundation Maps with Revision of Port Aransas, TX and Updating Existing Ones with Maritime Products

*Final Report to the*
*National Tsunami Hazard Mitigation Program (NTHMP)*
*in Completion of Project Awards*
*NA15NWS4670031 and NA16NWS4670039*


Authors

| | |
|---|---|
| Juan J Horrillo | Texas A&M University at Galveston |
| Wei Cheng | |
| Jens Figlus | |

Collaborators:

| | |
|---|---|
| Chayne Sparagowski | Coastal Bend Council of Governments |
| | NTHMP Mitigation and Education Subcommittee |


Under the guidance of
**NTHMP Mapping and Modeling Subcommittee**

**National Tsunami Hazard Mitigation Program**

**National Oceanic and Atmospheric Administration**

OCEAN ENGINEERING
TEXAS A&M UNIVERSITY


Ocean Engineering
Texas A&M University at Galveston
Galveston, Texas, 77553


November 2017

# Contents

# List of Figures

# List of Tables

# 1 Executive Summary

Potential tsunami sources for the GOM are local submarine landslides, which have been examined in the past by the Atlantic and Gulf of Mexico Tsunami Hazard Assessment Group [ten Brink et al., 2009b]. In their findings, they stated that submarine landslides in the GOM are considered a potential tsunami hazard. However, the probability of such an event (tsunamis generated by large landslides) is low. The probability of occurrence is related to ancient (historical) massive landslides which were probably active prior to 7,000 years ago when large quantities of sediments were emptied into the Gulf of Mexico. Nowadays, sediment continues to empty into the Gulf of Mexico mainly from the Mississippi River. This sediment supply contributes to the slope steepening and the increase of fluid pore pressure in sediments, which may lead to further landslide activities and hence, the reason for this study in determining the potential tsunami hazard and its effects in the Gulf of Mexico.

For the triggering mechanism (tsunami generation) we use 3 historical sources, i.e., the Eastbreaks, Mississippi Canyon and West Florida landslides. A probabilistic approach was implemented in our previous study, see [Horrillo et al., 2015], to fill gaps along the continental shelf between the historical landslide sources by adding synthetic landslide sources (4 in total) to cover the entire northern part of the GOM. Our probabilistic studies confirmed a recurrence period of major landslide events of around 8000 years, consistent with findings by [Geist et al., 2013].

These historical and probabilistic tsunami sources (7 in total) are used as the maximum credible events that could happen in the region according to the local bathymetry, seafloor slope, and sediment information. These credible events are then used to determine the inundation impact on selected communities along the GOM. The extent and magnitude of the tsunami inundation in those selected locations are achieved by using a combination of 3D and 2D coupled-numerical models. For instance, the 3D model, TSUNAMI3D, is used for tsunami generation to determine the initial dynamic wave or initial source and results are passed as an input to the 2D non-hydrostatic model, NEOWAVE, to determine the tsunami wave propagation and the detailed runup and inundation extent in each of the communities. Tsunami flooding inland-extent, maximum inundation water depth, momentum flux and direction, current velocity and vorticity can then be determined within the inundation-prone areas of the selected communities. Also, tsunami inundation and hurricane category flooding can be compared to access tsunami hazard in unmapped locations.

This project focused on the implementation of recent developments in the tsunami science recommended by the National Tsunami Hazard Mitigation Program Modeling - Mapping Subcommittee - Strategic Plan (NTHMP-MMS-SP) into our current Gulf of Mexico (GOM) tsunami mitigation products. Three main developments for tsunami mitigation have been created under this project for communities in the GOM that will provide guidance to state emergency managers for tsunami hazard mitigation and warning purposes.

The first is the development of four tsunami inundation maps in Pensacola, FL, Key West, FL Okaloosa County, FL and Santa Rosa County, FL, with revision of Port Aransas, TX (Mustang Island, TX) to account for new landslide sources. Maximum tsunami inundation extent, water height, and momentum flux magnitude and direction are determined from each landslide sources, as well as the maximum of maximum inundation maps from all landslide

sources. The four new tsunami inundation map products add to the existing six mapped locations, which provide so far good coverage of the most populous coastal areas along the GOM.

The second is a continuing study of the comparison between existing SLOSH hurricane flooding data and our tsunami inundation result, in order to provide temporal-low-order estimate for tsunami hazard areas (community) where inundation studies have not yet been assigned/executed or where little bathymetric and elevation data exists. The adopted approach to define a quick estimate of tsunami vulnerability areas in the GOM has been taken from the existing hurricane storm surge flooding results along coastal areas, in which storm flooding map products are based on hurricane category. The existing storm surge flooding maps cover almost the entire GOM coastal regions and thus they are very well known among GOM regional emergency managers and other parties. This study was first carried out in Horrillo et al. [2016] (award number NA14NWS4670049) where five locations were studied, namely South Padre Island, TX, Galveston, TX, Mobile, AL, Panama City, FL, and Tampa, FL. In this project, the comparison was performed in Pensacola, FL, Key West, FL, Okaloosa County, FL, Santa Rosa County, FL and Mustang Island, TX.

The third is to produce the velocity field and velocity magnitude maps for all the landslide scenarios, for South Padre Island, TX, Mobile, AL, Panama City, FL, and Tampa, FL, which were mapped in project NA13NWS4670018 [Horrillo et al., 2015], and Pensacola, FL, Key West, FL, Okaloosa County, FL, Santa Rosa County, FL and Mustang Island, TX, which are the newly mapped areas in this project. Galveston, TX was already completed in project NA14NWS4670049 [Horrillo et al., 2016] as a pilot study. Based on these velocity maps, location of strong currents and their damaging levels are identified. The tsunami hazard maritime products such as tsunami current magnitude, vorticity, safe/hazard zones would be central for future developments of maritime hazard maps, maritime emergency response and as well as infrastructure planning. We hope that the results herein may assist the maritime communities, port managers and other NTHMP's interested parties.

Although the recurrence of destructive tsunami events have been verified to be quite low in the GOM, our work has confirmed that submarine landslide events with similar characteristics to those used here, have indeed the potential to cause severe damage to GOM coastal communities. Therefore, this work is intended to provide guidance to local emergency managers to help managing urban growth, evacuation planning, and public education with final objective to mitigate potential tsunami hazards in the GOM.

# 1 Introduction

## 1.1 Background

The U.S. Tsunami Warning System has included Gulf of Mexico (GOM) coasts since 2005 in order to enable local emergency management to act in response to tsunami warnings. To plan for the warning response, emergency managers must understand what specific areas within their jurisdictions are threatened by tsunamis. Coastal hazard areas susceptible to tsunami inundation can be determined by historical events, by modeling potential tsunami

events (worst-case scenarios), or by using a probabilistic approach to determine the rate of recurrence or likelihood of exceeding a certain threshold. As the GOM coastal regions have no significant recent historical tsunami records, numerical modeling and probabilistic methodologies for source identification must be used to determine coastal hazard zones.

Potential tsunami sources for the GOM are local submarine landslides [ten Brink et al., 2009b]; sources outside the GOM are considered a very low threat and may not significantly impact GOM coastal communities or infrastructure [Knight, 2006]. Although a massive tsunamigenic underwater landslide in the GOM is considered a potential hazard, the frequency of such events (though not well-constrained) is probably quite low based on historical evidence [Dunbar and Weaver, 2008] and available data on ages of failures which suggest they were probably active prior to 7,000 years ago when large quantities of sediments were emptied into the GOM [ten Brink et al., 2009b]. However, sediments continue to empty into the GOM, mainly from the Mississippi River, contributing to slope steepening and the increase of fluid pore pressure in sediments which may lead to unstable slopes that can be subsequently triggered to failure by seismic loading [Masson et al., 2006, ten Brink et al., 2009a, Dugan and Stigall, 2010, Harbitz et al., 2014]. In addition, the unique geometry of the GOM basin makes even unlikely tsunami events potentially hazardous to the entire Gulf Coast. Waves tend to refract along continental slopes; thus, given the curved geomorphology of the GOM shelf and the concave shape of the coastline, any outgoing tsunami wave could potentially affect the opposite coast in addition to the coast close to the landslide source.

Three large-scale historical (ancient) submarine landslides with tsunamigenic potential have been identified within the GOM [ten Brink et al., 2009b], representing possible worst-case tsunami scenarios affecting GOM coasts in the past. In order to generate a more complete picture of landslide tsunami potential in the GOM, a probabilistic approach has been implemented to develop four additional synthetic landslide sources which fill gaps along the continental shelf between the historical landslide sources [Pampell-Manis et al., 2016]. These probabilistic tsunami sources are considered to be the maximum credible events that could happen in a particular region of the GOM according to the local bathymetry, seafloor slope, sediment information, and seismic loading. The probabilistic maximum credible events together with the historical sources form a suite of tsunami sources that have been used within coupled 3D and 2D numerical models to model tsunami generation and propagation throughout the GOM and to develop high-resolution inundation maps for the inundation-prone areas of four selected communities along the Gulf Coast: Pensacola, FL, Key West, FL, Okaloosa County, FL and Santa Rosa County, FL, with revision of Port Aransas, TX (Mustang Island, TX). These inundation studies showed that tsunamis triggered by massive submarine landslides have the potential to cause widespread and significant inundation of coastal cities. All of the ten communities and seven landslide sources are shown in Fig. 1.

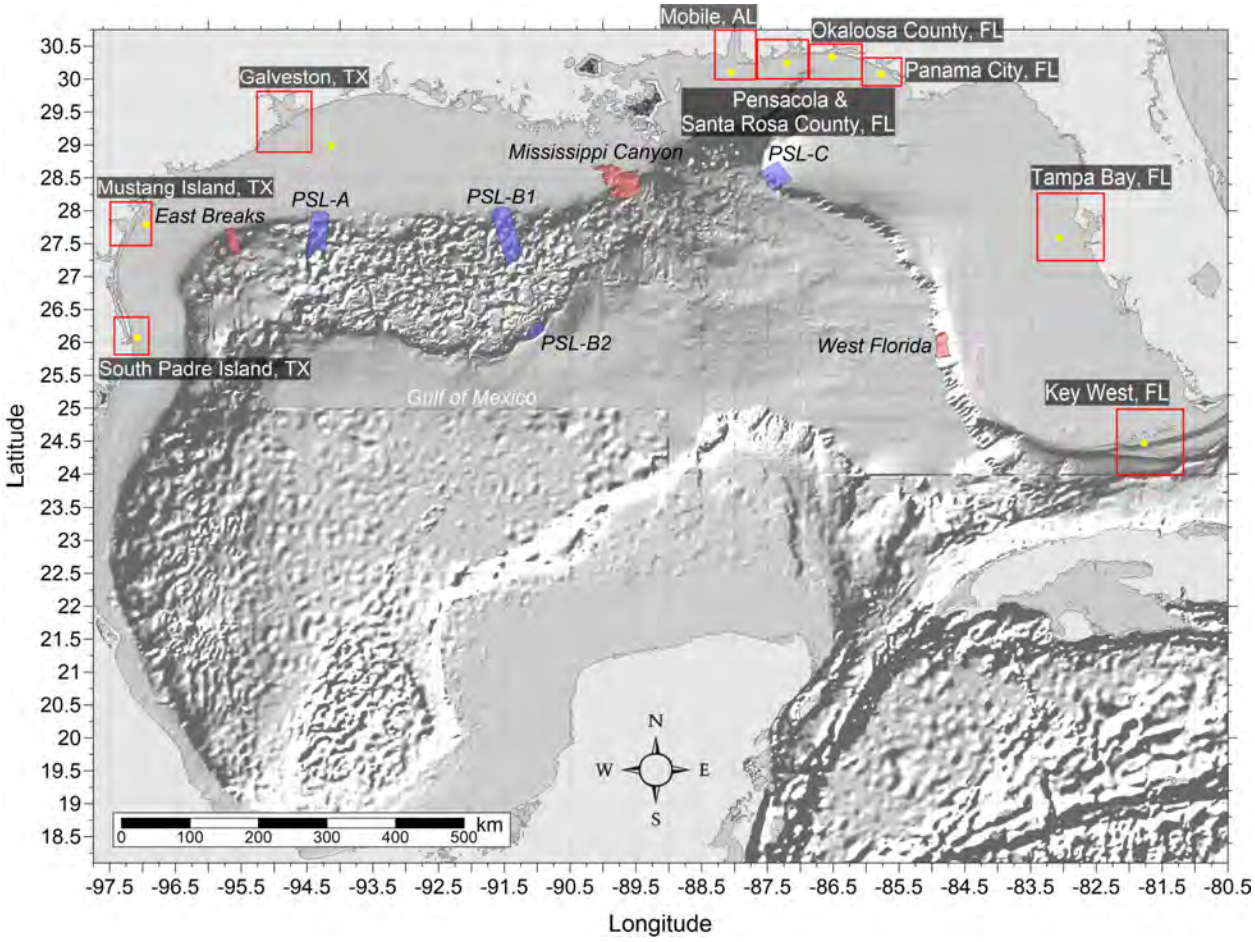


Figure 1: Selected communities or geography regions along the US GOM coastline where tsunami maps have been developed. Red rectangles indicate 3 arcsecond (∼90m) domains of each coastal community where tsunami inundation is modeled; red hatched areas are historical landslide sources; blue hatched areas are Probabilistic Submarine Landslide (PSL) sources; yellow dots are locations of numerical wave gauges. The contour drawn is the zero-meter contour for land elevation.

While high-resolution tsunami inundation studies have been completed for these ten communities and are planned for additional locations, vulnerability assessments are still essential for coastal locations where inundation studies have not yet been performed or planned, or where there is a lack of high-resolution bathymetric and/or elevation data. Therefore, we aim to extend the results of the completed mapping studies in order to provide estimates of tsunami inundation zones for hazard mitigation efforts in un-mapped locations. Inundation maps with even low resolution are useful to emergency managers to create first-order evacuation maps, and some methods currently exist to provide low-resolution estimates of hazard zones for regions which do not currently have or warrant high-resolution maps. For example, guidance given by the National Tsunami Hazard Mitigation Program (NTHMP) Mapping and Modeling Subcommittee in "Guidelines and Best Practices to Establish Areas of Tsunami Inundation for Non-modeled or Low-hazard Regions" (available from `http://nws.weather.gov/nthmp/documents/Inundationareaguidelinesforlowhazardareas.pdf`) recommends that coastal areas and areas along ocean-connected waterways that are below 10 m (33 ft) elevation are at risk for most tsunamis, and rare and large tsunamis may inundate above this elevation. However, in low-lying coastal regions such as along the Gulf Coast, the 10 m (33 ft) elevation contour is too far inland to be reasonably applicable for estimating potential tsunami inundation zones. The guidance additionally suggests that low-lying areas are prone to inundation within 3 km (1.9 mi) inland for locally-generated tsunamis and within 2 km (1.3 mi) inland for distant sources. While these distances may be reasonable for some regions of the Gulf Coast, prevalent bathymetric and topographic features such as barrier islands/peninsulas complicate the method of delineating inundation-prone areas based on distance from the shoreline. As a result, the purpose of the current work is to improve the methodology which compares modeled tsunami inundation to modeled/predicted hurricane storm surge. Specifically, we aim to identify the hurricane category which produces modeled maximum storm surge that best approximates the maximum tsunami inundation modeled in this project. Even though many physical aspects of storm surge inundation are completely different from those of tsunamis (time scale, triggering mechanism, inundation process, etc.), good agreement or clear trends between tsunami and storm surge flooding on a regional scale can be used to provide first-order estimates of potential tsunami inundation in communities where detailed inundation maps have not yet been developed or are not possible due to unavailability of high-resolution bathymetry/elevation data. Additionally, since tsunamis are not well-understood as a threat along the Gulf Coast, while hurricane hazards are well-known, this method of predicting tsunami inundation from storm surge provides a way for GOM emergency managers to better prepare for potential tsunami events based on more understandable and accessible information.

Recent tsunamis have shown that the maritime community requires additional information and guidance about tsunami hazards and post-tsunami recovery [Wilson et al., 2012, 2013]. To accomplish mapping and modeling activities to meet NTHMP's planning/response purposes for the maritime community and port emergency management and other customer requirements, it is necessary to continue the process to include maritime products in our current inundation map development. These activities will include tsunami hazard maritime products generated by GOM's tsunami sources (submarine landslides) that may impact specifically ship channels, bay inlets, harbors, marinas, and oil infrastructures (e.g., des-

ignated lightering and oil tanker waiting zones), which has already been applied in other tsunami risk regions, e.g., California, Oregon and Washington. It is worth noting that Galveston was the first city where we implemented the maritime products [Horrillo et al., 2016]. The other nine locations, South Padre Island, TX, Mobile, AL, Panama City, FL, and Tampa, FL, mapped during [Horrillo et al., 2015] (project NA13NWS4670018), and Pensacola, FL, Key West, FL, Okaloosa County, FL, Santa Rosa County, FL and Mustang Island, TX are added to the maritime portfolio in this project.

Although the probability of a large-scale tsunami event in the GOM is low, this and previous studies have indicated that tsunami events with characteristics similar to those detailed in Horrillo et al. [2015] have the potential to cause severe flooding and damage to GOM coastal communities that is similar to or even greater than that seen from major hurricanes, particularly in open beach and barrier island regions. The tsunami hazard maritime products such as tsunami current magnitude, vorticity, safe/hazard zones would be central for future developments of maritime hazard maps, maritime emergency response as well as infrastructure planning. The results of this work are intended to provide guidance to local emergency managers to help with managing urban growth, evacuation planning, and public education with the vision to mitigate potential GOM tsunami hazards.

This report is organized as follows. Section 2 briefly describes the tsunami sources used for tsunami modeling (2.1) and the numerical models used for calculation (2.2). Section 3 covers the inundation and momentum flux maps for Pensacola, FL, Key West, FL, Okaloosa County, FL and Santa Rosa County, FL, with revision of Port Aransas, TX (Mustang Island, TX). The comparison of tsunami inundation with hurricane storm surge inundation is given in Section 4 for the five selected Gulf Coast communities. The current velocity and vorticity maps are described in Section 5 for nine communities (South Padre Island, TX, Mobile, AL, Panama City, FL, Tampa, FL, Pensacola, FL, Key West, FL, Okaloosa County, FL, Santa Rosa County, FL, and Mustang Island, TX). Concluding remarks on general trends seen among the communities and practical applications for other regions are given in Section 6.

## 1.2 Regional and Historical Context

### Pensacola, FL

Pensacola is a mainland city north of the Pensacola Bay, which is shielded by the Santa Rosa barrier island and the Fairpoint Peninsula from the GOM. Pensacola is the westmost city in the state of Florida. It is 95 km east of Mobile, Alabama, and 315 km west of the capital of Florida, Tallahassee. Pensacola has an area of 105.4 $km^2$. Via Pensacola Bay Bridge, Pensacola is connected to the city of Gulf Breeze on the Fairpoint Peninsula, which is connected to the Santa Rosa Island by the Pensacola Beach Road. Pensacola is a sea port on the Pensacola Bay and a large naval air station is located in Warrington, just southwest of Pensacola. As of the 2010 census, the population of Pensacola was 51,923, and the population density was 2,303.5 people per square mile (956.8/$km^2$). In this study, the finest grid (grid level 4, 1/3 arcsecond resolution) covers mainland Pensacola, Gulf Breeze (west portion of the Fairpoint Peninsula) and western part of Santa Rosa Island (west of Pensacola Beach).

Many major hurricanes have made landfall in the vicinity of Pensacola, among which the most devastating is the 2004 Hurricane Ivan. Hurricane Ivan was a category 3 storm when it moved across the Gulf of Mexico to hit Florida [Panchang and Li, 2006]. Ivan destroyed most of the Escambia Bay Bridge on I-10 with 400 m of the bridge collapsing into the bay, destroyed more than 10000 houses, and resulted in over six billion damage in metro Pensacola. Rain reached 15.75 inches in Pensacola, with a 12 feet storm surge in Escambia Bay. In addition, the 2005 Hurricane Dennis and Hurricane Katrina caused only minor to moderate damage.

**Key West, FL**

Key West is an island city in the Florida Keys archipelago which extends from the southwest tip of the state of Florida. Key West is also the southernmost city in the continental United States, just 90 miles from Cuba. Key West and its nearby keys form the dividing line between the Atlantic Ocean and the Gulf of Mexico. Key West is connected to the mainland by Highway 1. As of the 2010 census, the population of Key West was 24,649, and the population density was 4,411.8 people per square mile (1,832.5/km$^2$). In this study, our high resolution grid covers Key West and the Stock Island to the east, as well as the Big Coppitt Key, Geiger Key, and the East Rockland Key.

Unlike the other study locations, Key West has been relatively unaffected by major storms, except for Hurricane Georges and Hurricane Wilma, until September 2017, when Category 4 Hurricane Irma destroyed an estimated 25 percent of homes on the islands. In 1998, the Category 2 Hurricane Georges damaged many houseboats near Cow Key channel on the east side of the island. The 2005 Hurricane Wilma was a Category 5 hurricane, the second most destructive of the 2005 season. It resulted in two meter inundation of a large portion of the lower keys, which damaged thousands of cars and flooded many houses.

**Okaloosa County, FL**

Our study area includes Destin and Okaloosa Island by the GOM, and Walton Beach, Ocean City, Lake Lorraine, etc., on the mainland separated by Choctawhatchee Bay. U.S. Highway 98 connects Okaloosa Island to Fort Walton Beach via the Brooks Bridge and to Destin via the Destin Bridge, to the west and east respectively. Destin is located on a peninsula, originated as a barrier island which was later connected to the mainland gradually by hurricanes and sea level changes. Destin is connected to southern Niceville, FL via Spence Parkway. As of the census of 2000, there were 11,455 people in Destin, 19507 in Fort Walton Beach, 5550 in Ocean City and 7010 in Lake Lorraine. The 3 arcsecond study area sits right between our previous mapping locations, Pensacola, FL and Panama City, FL (Fig. 1).

The 2004 Hurricane Ivan caused heavy damage in Fort Walton Beach.

**Santa Rosa County, FL**

Santa Rosa County study area shares the same 3 arcsecond computational grid with Pensacola, FL. The area include the Santa Rosa Island, East Gulf Breeze and Navarre. Santa Rosa Island is connected to Gulf Breeze through Pensacola Beach Road, and Gulf Breeze is

connected to Pensacola through Pensacola Bay Bridge, and to Milton through Avalon Blvd. As of the census of 2000, there were 5763 people in Gulf Breeze City, Fl and 31378 in Navarre CDP, FL.

The 2004 Hurricane Ivan caused heavy damage in Gulf Breeze and Navarre Beach. Hurricane Dennis made landfall as a Category 3 hurricane on Santa Rosa Island on July 10, 2005. Sustained winds of 158 km/h were reported at Navarre Beach. On Santa Rosa Island, the hurricane resulted in a storm surge of 2.1 m.

### Mustang Island, TX

Port Aransas, Texas is a resort and fishing community on Mustang Island, located 24 miles northeast of Corpus Christi in the northeastern corner of Nueces County. Port Aransas' early economic reliance was on ranching, but as time progressed the town became more reliant on tourist attractions such as fishing and beaches. Port Aransas currently remains as a relatively small community with a total population of 3,370 per the census 2000 demographic profile obtained from 2010 U.S. Census Bureau data. However, during the summer months the population grows significantly to well over 20,000 during peak tourism.

Port Aransas was almost completely wiped out by the 1919 hurricane, which came on land between Brownsville and Corpus Christi. A storm surge of approximately 20 ft (6 m) high passed over the town wiping out most of the buildings and the dune systems [Myers et al., 2006]. Many of the residents, who survived the hurricane, left Port Aransas. It took many years for the islanders to rebuild the town. According to the report written by Myers, et al. (2006), the 1925 census shows that the Port Aransas population grew to 250 permanent residents. Since then, many hurricanes have come and gone. One of the largest hurricanes to hit Port Aransas was Hurricane Carla, which came ashore in 1961, causing massive destruction to the island, see Figure 2. Many other hurricanes had cause severe inundation and destruction; once again, rebuilding Port Aransas was a slow process. In August 2017, Category 4 Hurricane Harvey inflicted tremendous damage across Aransas County. Wind gusts were observed up to 212 km/h near Port Aransas. Almost every structure in Port Aransas suffered damage. More than 510 mm of rain was recorded in the Corpus Christi metropolitan area.

# 2 Tsunami Inundation Modeling

## 2.1 Landslide Tsunami Sources

Seven large-scale landslide configurations were created assuming an unstable (gravity-driven) sediment deposit condition. Three of these landslide configurations are historical events identified by ten Brink et al. [2009b]: the Eastbreaks, Mississippi Canyon, and West Florida submarine landslides, which are shown as red hatched regions in Fig. 1. The other four were obtained using a probabilistic methodology based on work by Maretzki et al. [2007] and Grilli et al. [2009] and extended for the GOM by Pampell-Manis et al. [2016]. The probabilistic landslide configurations were determined based on distributions of previous GOM submarine landslide dimensions through a Monte Carlo Simulation (MCS) approach. The MCS methodology incorporates a statistical correlation method for capturing trends seen in observational data for landslide size parameters while still allowing for randomness in the generated landslide dimensions. Slope stability analyses are performed for the MCS-generated trial landslide configurations using landslide and sediment properties and regional seismic loading (Peak Horizontal ground Acceleration, PHA) to determine landslide configurations which fail and produce a tsunami. The probability of each tsunamigenic failure is calculated based on the joint probability of the earthquake PHA and the probability that the trial landslide fails and produces a tsunami wave above a certain threshold. Those failures which produce the largest tsunami amplitude and have the highest probability of occurrence are deemed the most extreme probabilistic events, and the dimensions of these events are averaged to determine maximum credible probabilistic sources. The four maximum credible Probabilistic Submarine Landslides (PSLs) used as tsunami sources for this study are termed PSL-A, PSL-B1, PSL-B2, and PSL-C and are shown as blue hatched regions in Fig. 1. A complete discussion of the submarine landslide sources used here is given in Horrillo et al. [2015] and Pampell-Manis et al. [2016]. Specific details on the size parameters of each landslide source are given in Tables 7-20 of Horrillo et al. [2015].

## 2.2 Numerical Models

For the seven landslide tsunami sources considered here, tsunami wave development and subsequent propagation and inundation of coastal communities was modeled using coupled 3D and 2D numerical models [Horrillo et al., 2015]. The tsunami generation phase was modeled using the 3D model TSUNAMI3D [Horrillo, 2006, Horrillo et al., 2013], which solves the finite difference approximation of the full Navier-Stokes equations and the incompressibility (continuity) equation. Water and landslide material are represented as Newtonian fluids with different densities, and the landslide- water and water-air interfaces are tracked using the Volume of Fluid (VOF) method of Hirt and Nichols [1981], which is simplified to account for the large horizontal/vertical aspect ratio of the tsunami wave and the selected computational cell size required to construct an efficient 3D grid. The pressure term is split into hydrostatic and non-hydrostatic components. Although TSUNAMI3D has the capability of variable grids, the nesting capability necessary for modeling detailed inundation of coastal regions is too computationally intensive within the fully 3D model; thus, detailed inundation

modeling is achieved by coupling the 3D model to a 2D model. Once the tsunami wave generated by the 3D model is fully developed, the wave is passed as an initial condition to the 2D model for modeling wave propagation and coastal inundation. The generated wave is considered fully developed when the total wave energy (potential plus kinetic) reaches a maximum and before the wave leaves the computational domain, as discussed in López-Venegas et al. [2015]. The 2D model used here is NEOWAVE [Yamazaki et al., 2008], a depth-integrated and non-hydrostatic model built on the nonlinear shallow water equations which includes a momentum-conserved advection scheme to model wave breaking and two-way nested grids for modeling higher-resolution wave runup and inundation. Propagation and inundation are calculated via a series of nested grids of increasing resolution, from 15 arcsecond (450 m) resolution for a domain encompassing the entire northern GOM (Fig. 1), to finer resolutions of 3 arcseconds (90 m, from NOAA NCEI Coastal Relief Models), 1 arcsecond (30 m), and 1/3 arcsecond (10 m, from NOAA NCEI Tsunami Inundation Digital Elevation Models [DEMs]) to model detailed inundation of the most populated/ inundation-prone areas of each coastal community. The 3 arcsecond (90 m) subdomains encompassing each coastal community studied here are shown by red rectangles in Fig. 1.

# 3 Tsunami Maps

In this section, the numerical results are presented for each location, first the table of maximum wave amplitude and arrival time after landslide failure, then the inundation and momentum flux maps for each landslide source, and finally the assembly of inundation result to obtain the maximum of maximum inundation map from all sources and the maximum inundation map by source.

## 3.1 Pensacola, FL

Table 1: Maximum tsunami wave amplitude and corresponding arrival time after landslide failure at Pensacola, FL numerical wave gauge: 30°14'45.00"N, 87°12'30.00"W (Fig. 1), approximate water depth 21 m.

| Tsunami Source | Maximum Wave Amplitude (m) | Arrival Time After Landslide Failure (hr) |
|---|---|---|
| East Breaks | 0.26 | 2.7 |
| PSL-A | 0.41 | 2.3 |
| PSL-B1 | 0.38 | 1.5 |
| PSL-B2 | 0.10 | 6.0 |
| Mississippi Canyon | 4.49 | 1.0 |
| PSL-C | 1.60 | 1.3 |
| West Florida | 0.36 | 1.6 |

**Pensacola, FL**
**East Breaks submarine landslide**
**Maximum Inundation Depth**

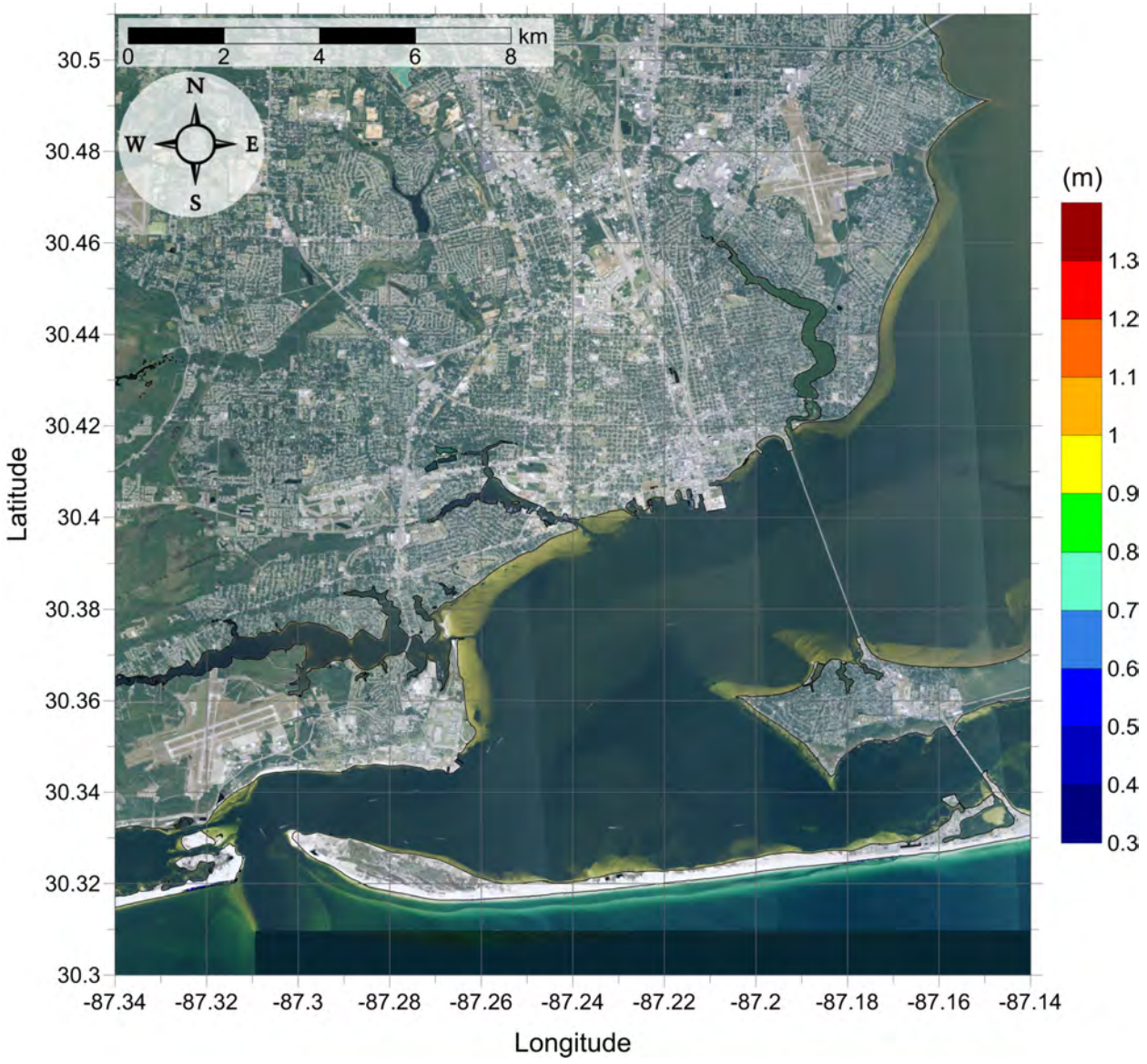


Figure 2: Maximum inundation depth (m) caused by the East Breaks submarine landslide in Pensacola, FL. Contour drawn is the zero-meter contour for land elevation.

**Pensacola, FL**
**East Breaks submarine landslide**
**Maximum Momentum Flux**

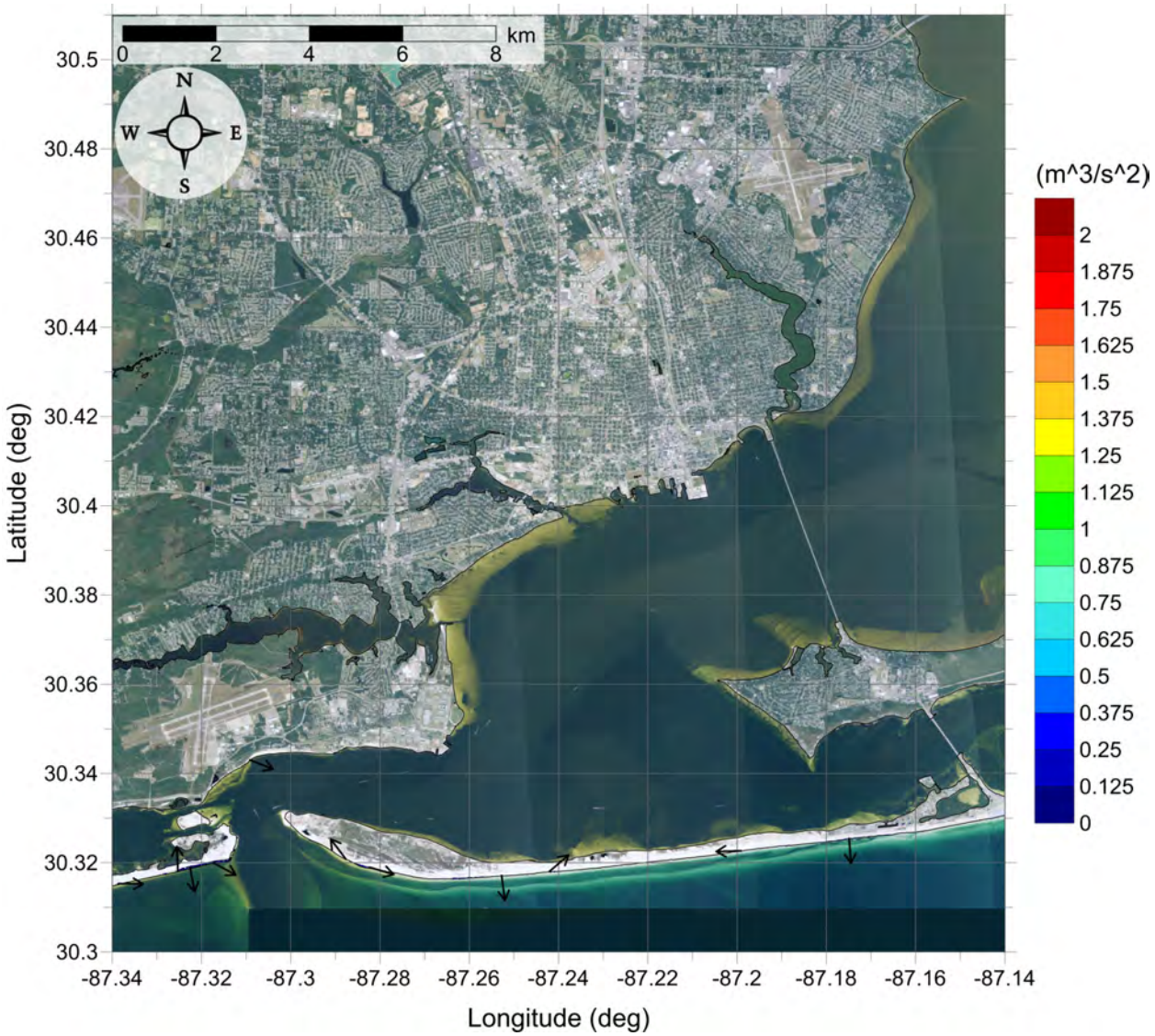


Figure 3: Maximum momentum flux ($m^3/s^2$) caused by the East Breaks submarine landslide in Pensacola, FL. Arrows represent direction of maximum momentum flux. Contour drawn is the zero-meter contour for land elevation.

**Pensacola, FL**
**Probabilistic Submarine Landslide A**
**Maximum Inundation Depth**

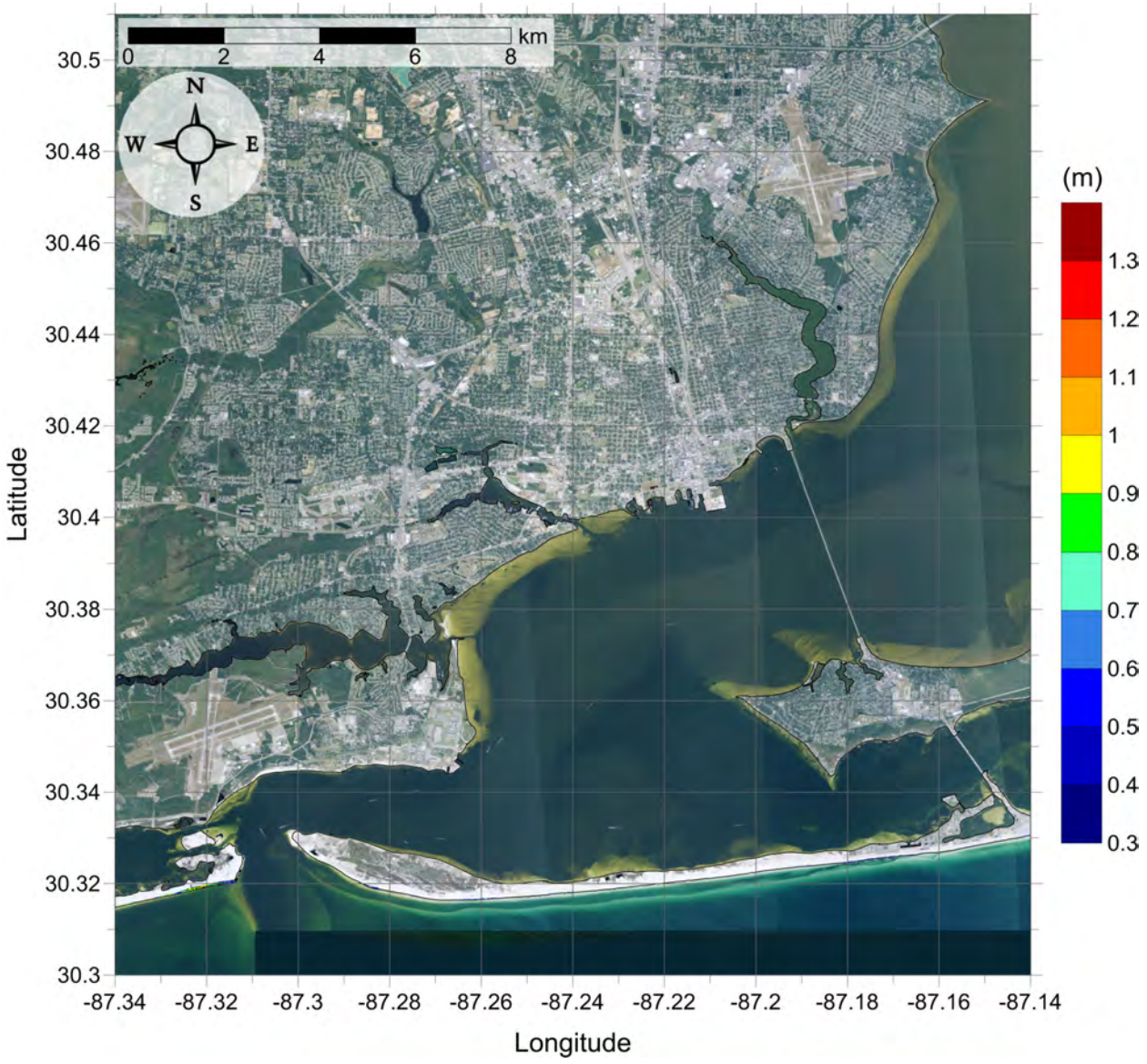


Figure 4: Maximum inundation depth (m) caused by the Probabilistic Submarine Landslide A in Pensacola, FL. Contour drawn is the zero-meter contour for land elevation.

**Pensacola, FL**
**Probabilistic Submarine Landslide A**
**Maximum Momentum Flux**

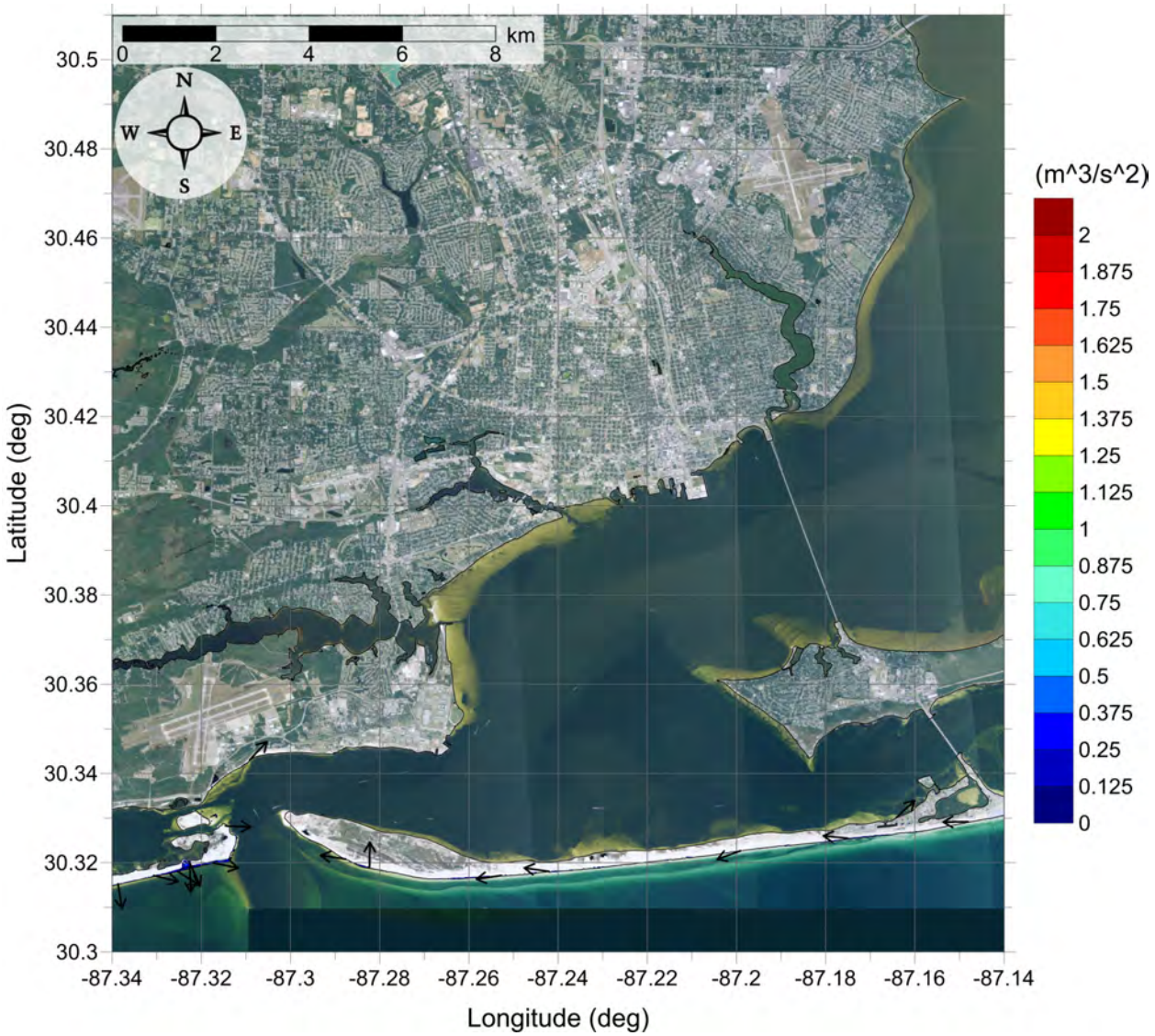


Figure 5: Maximum momentum flux ($m^3/s^2$) caused by the Probabilistic Submarine Landslide A in Pensacola, FL. Arrows represent direction of maximum momentum flux. Contour drawn is the zero-meter contour for land elevation.

**Pensacola, FL**
**Probabilistic Submarine Landslide B1**
**Maximum Inundation Depth**

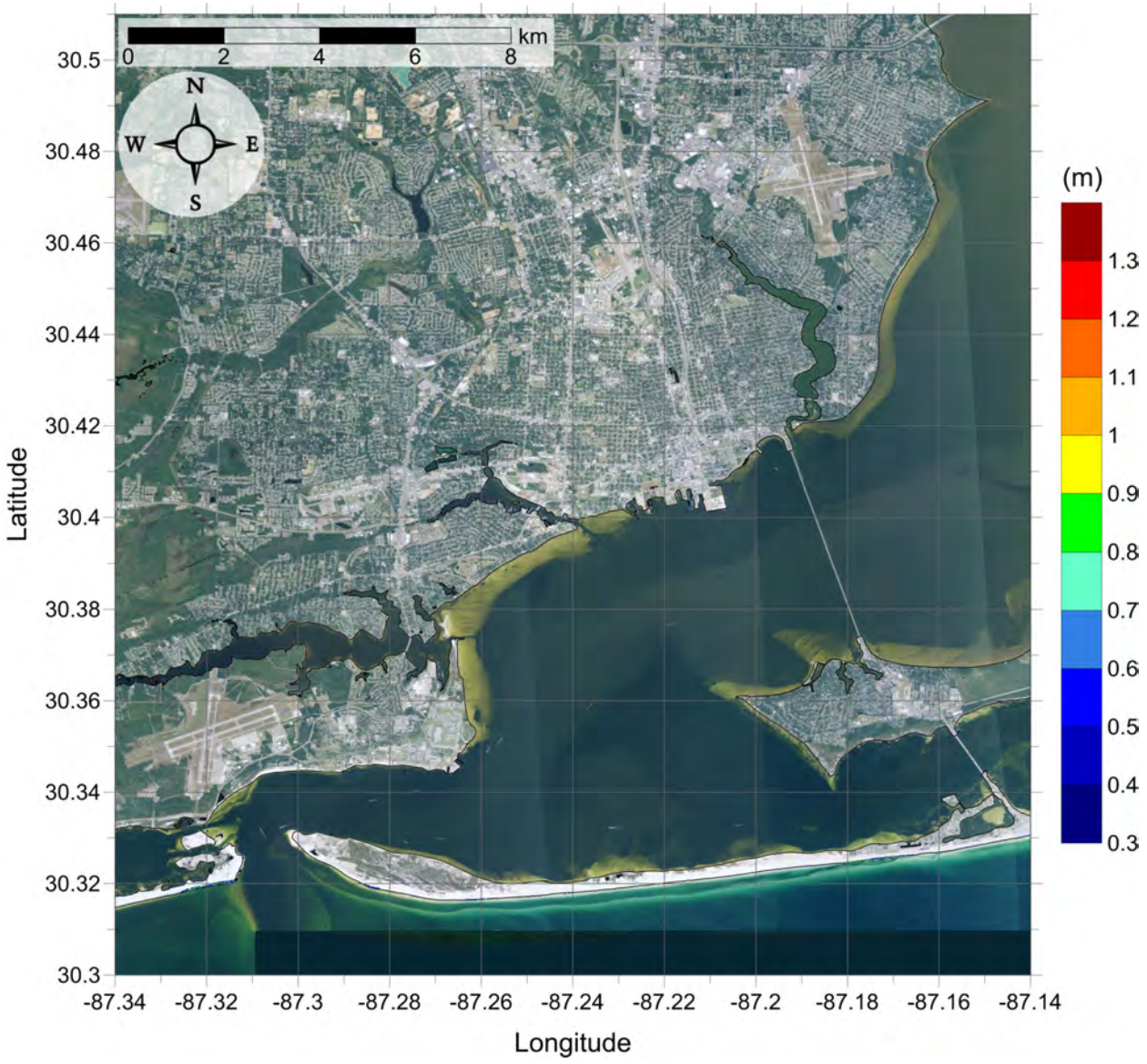


Figure 6: Maximum inundation depth (m) caused by the Probabilistic Submarine Landslide B1 in Pensacola, FL. Contour drawn is the zero-meter contour for land elevation.

**Pensacola, FL**
**Probabilistic Submarine Landslide B1**
**Maximum Momentum Flux**

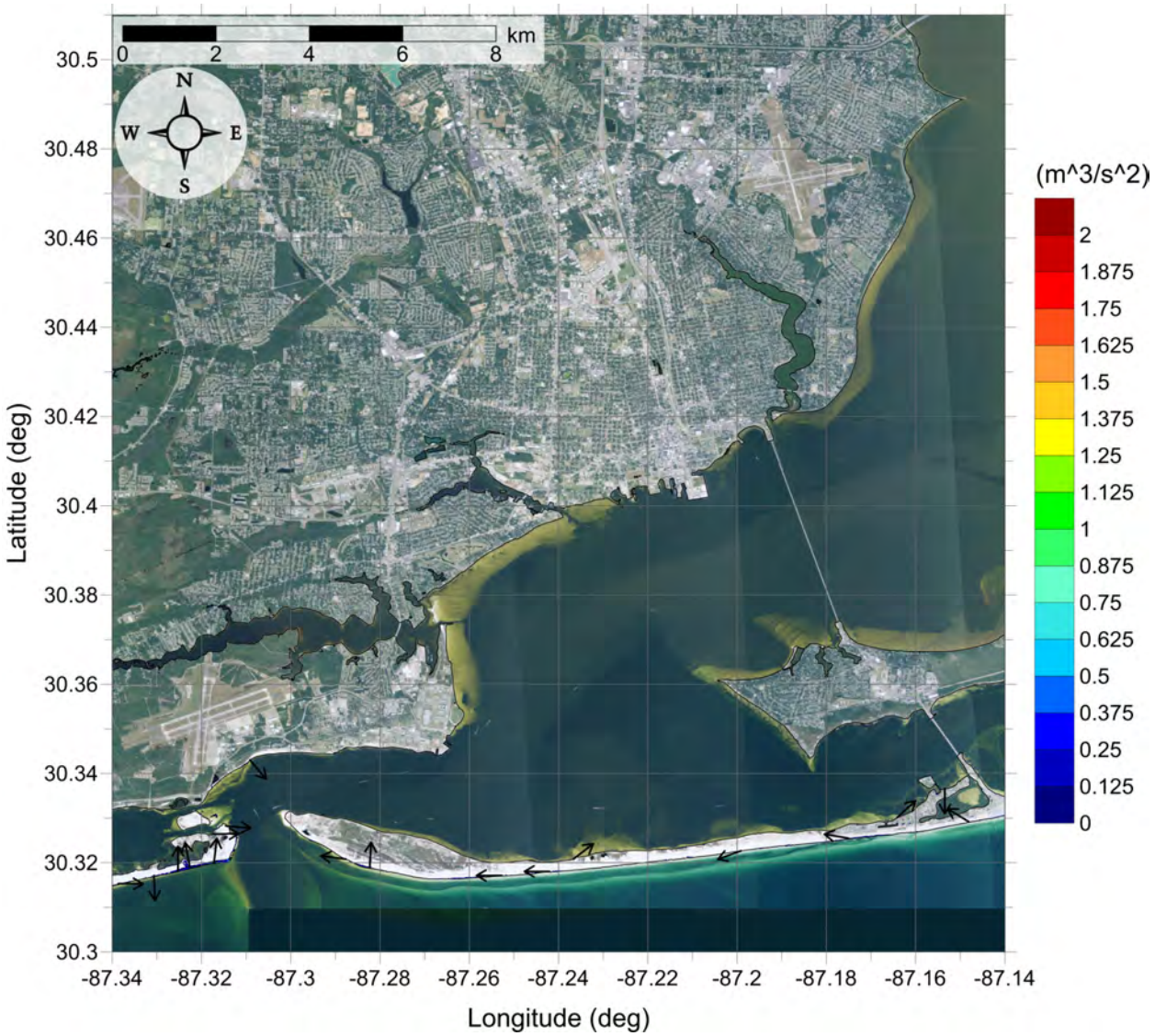


Figure 7: Maximum momentum flux ($m^3/s^2$) caused by the Probabilistic Submarine Landslide B1 in Pensacola, FL. Arrows represent direction of maximum momentum flux. Contour drawn is the zero-meter contour for land elevation.

**Pensacola, FL**
**Probabilistic Submarine Landslide B2**
**Maximum Inundation Depth**

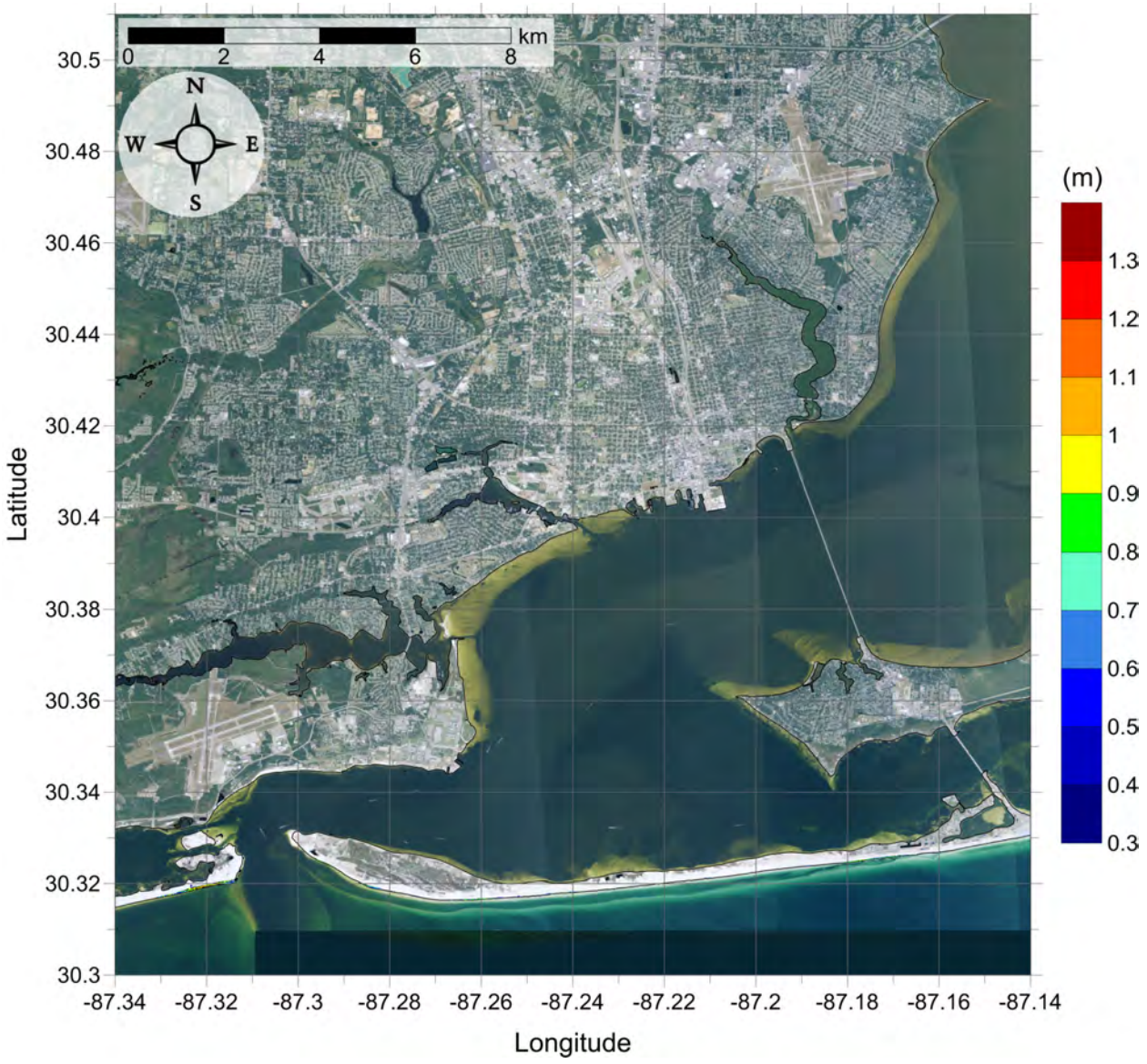


Figure 8: Maximum inundation depth (m) caused by the Probabilistic Submarine Landslide B2 in Pensacola, FL. Contour drawn is the zero-meter contour for land elevation.

**Pensacola, FL**
**Probabilistic Submarine Landslide B2**
**Maximum Momentum Flux**

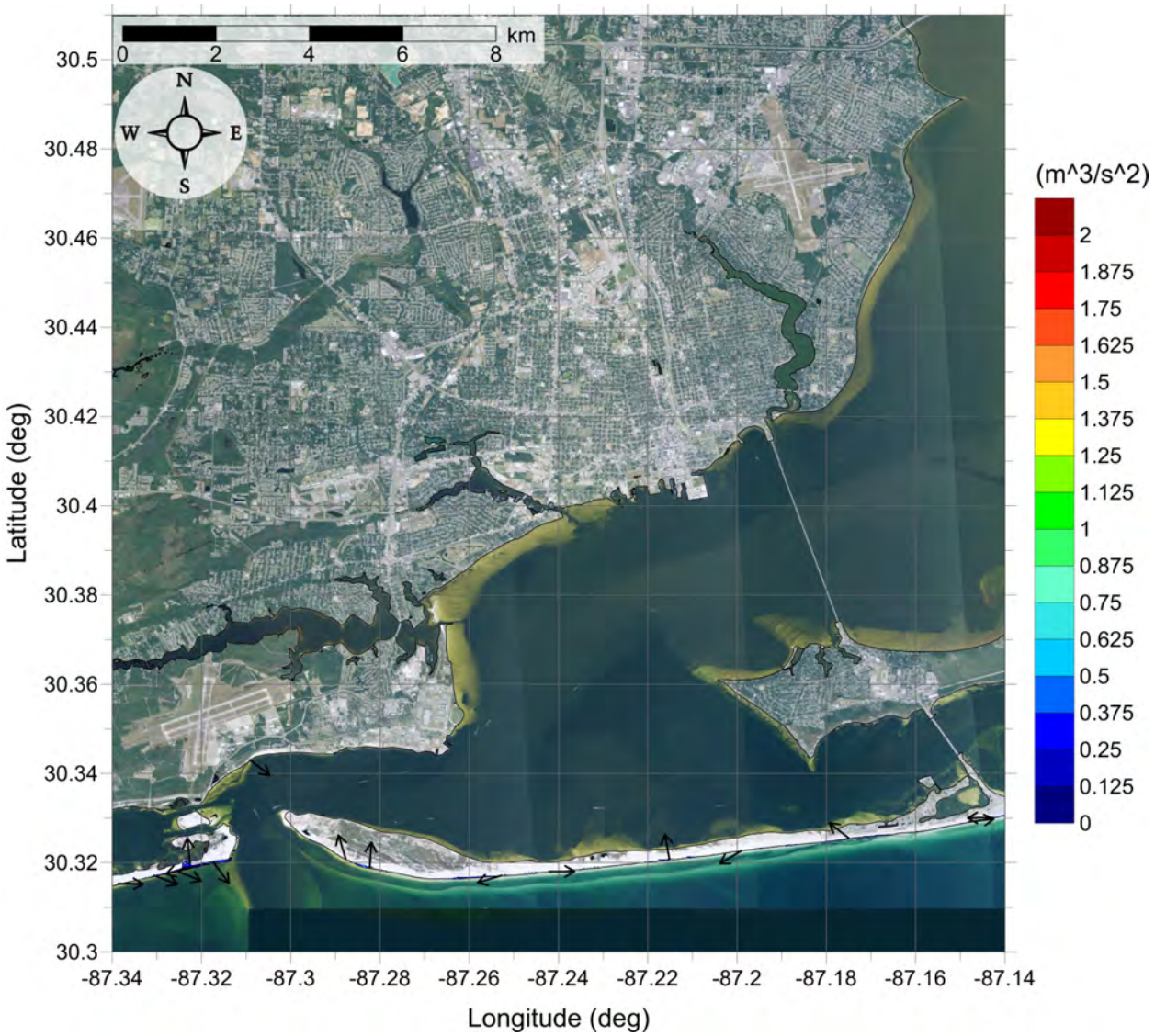


Figure 9: Maximum momentum flux ($m^3/s^2$) caused by the Probabilistic Submarine Landslide B2 in Pensacola, FL. Arrows represent direction of maximum momentum flux. Contour drawn is the zero-meter contour for land elevation.

**Pensacola, FL**
**Mississippi Canyon submarine landslide**
**Maximum Inundation Depth**

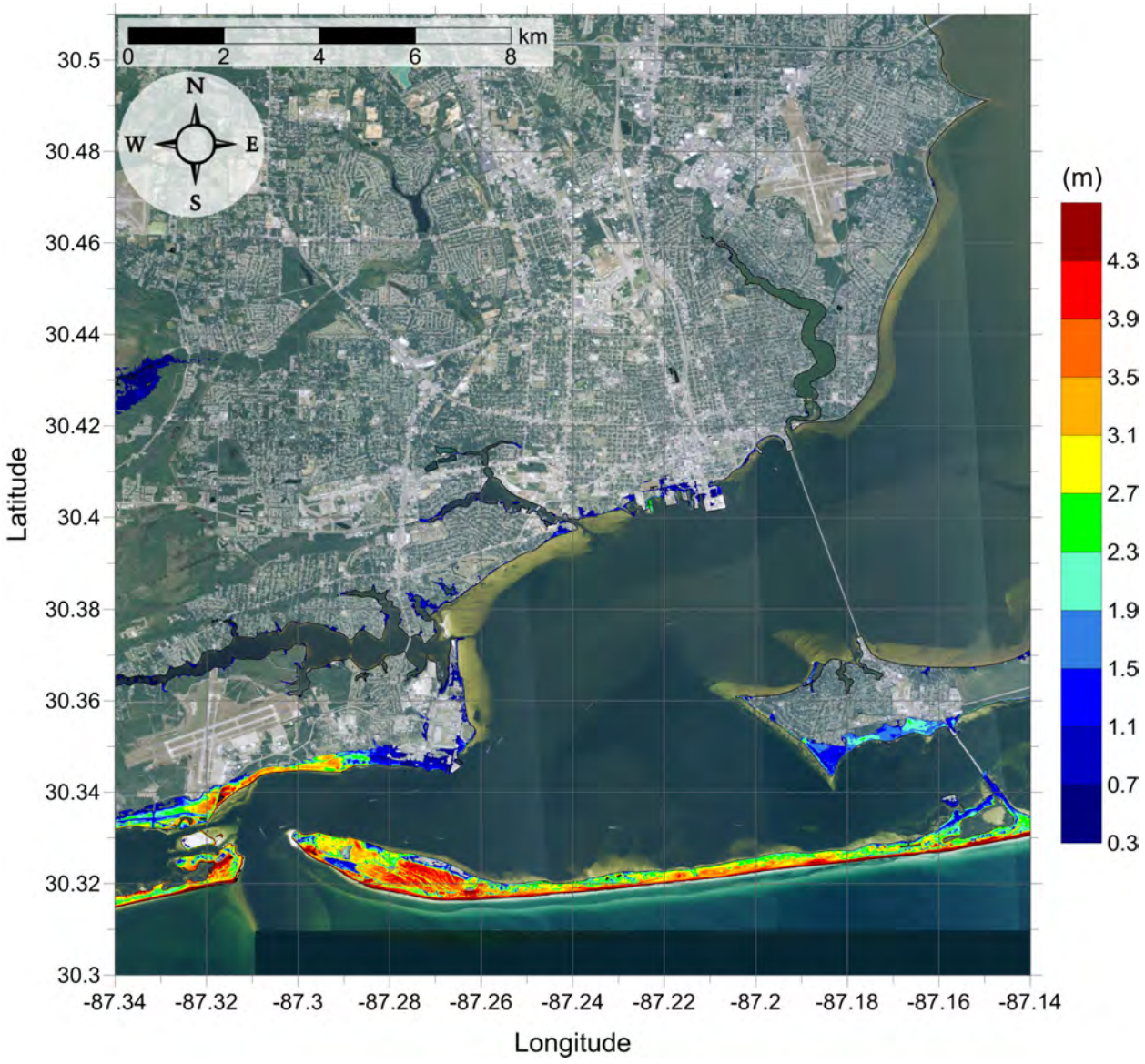


Figure 10: Maximum inundation depth (m) caused by the Mississippi Canyon submarine landslide in Pensacola, FL. Contour drawn is the zero-meter contour for land elevation.

**Pensacola, FL**
**Mississippi Canyon submarine landslide**
**Maximum Momentum Flux**

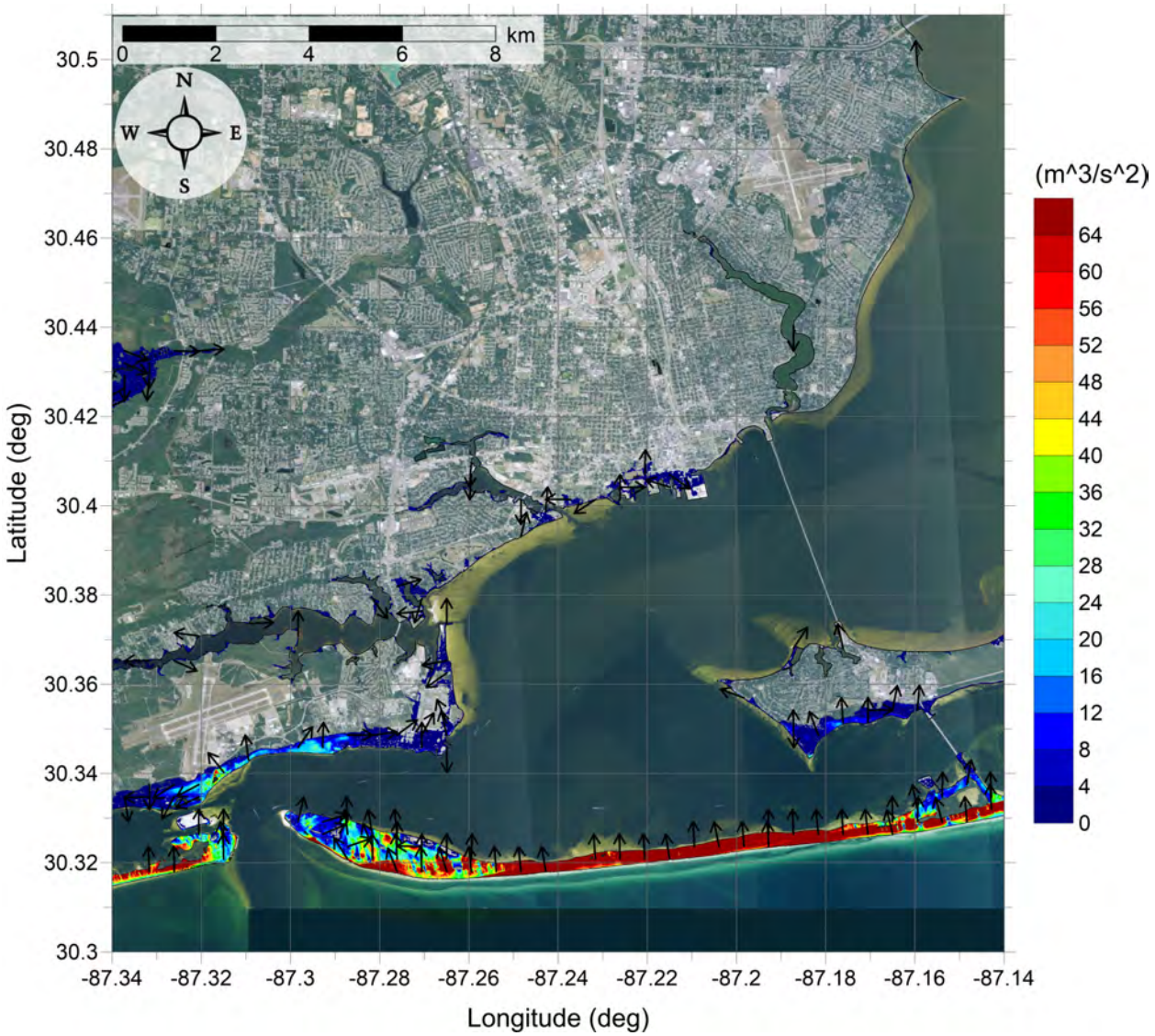


Figure 11: Maximum momentum flux ($m^3/s^2$) caused by the Mississippi Canyon submarine landslide in Pensacola, FL. Arrows represent direction of maximum momentum flux. Contour drawn is the zero-meter contour for land elevation.

**Pensacola, FL**
**Probabilistic Submarine Landslide C**
**Maximum Inundation Depth**

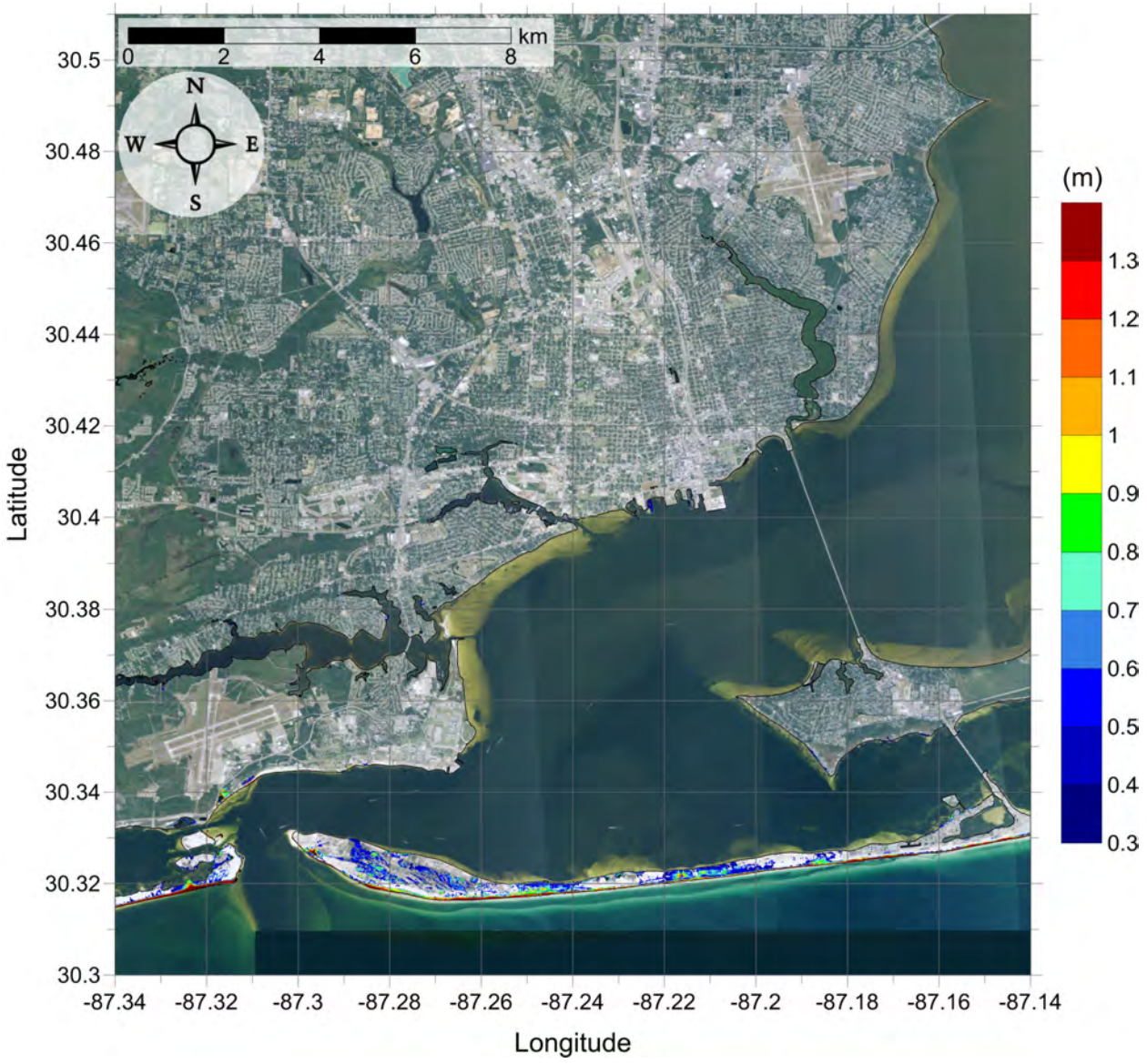


Figure 12: Maximum inundation depth (m) caused by the Probabilistic Submarine Landslide C in Pensacola, FL. Contour drawn is the zero-meter contour for land elevation.

**Pensacola, FL**
**Probabilistic Submarine Landslide C**
**Maximum Momentum Flux**

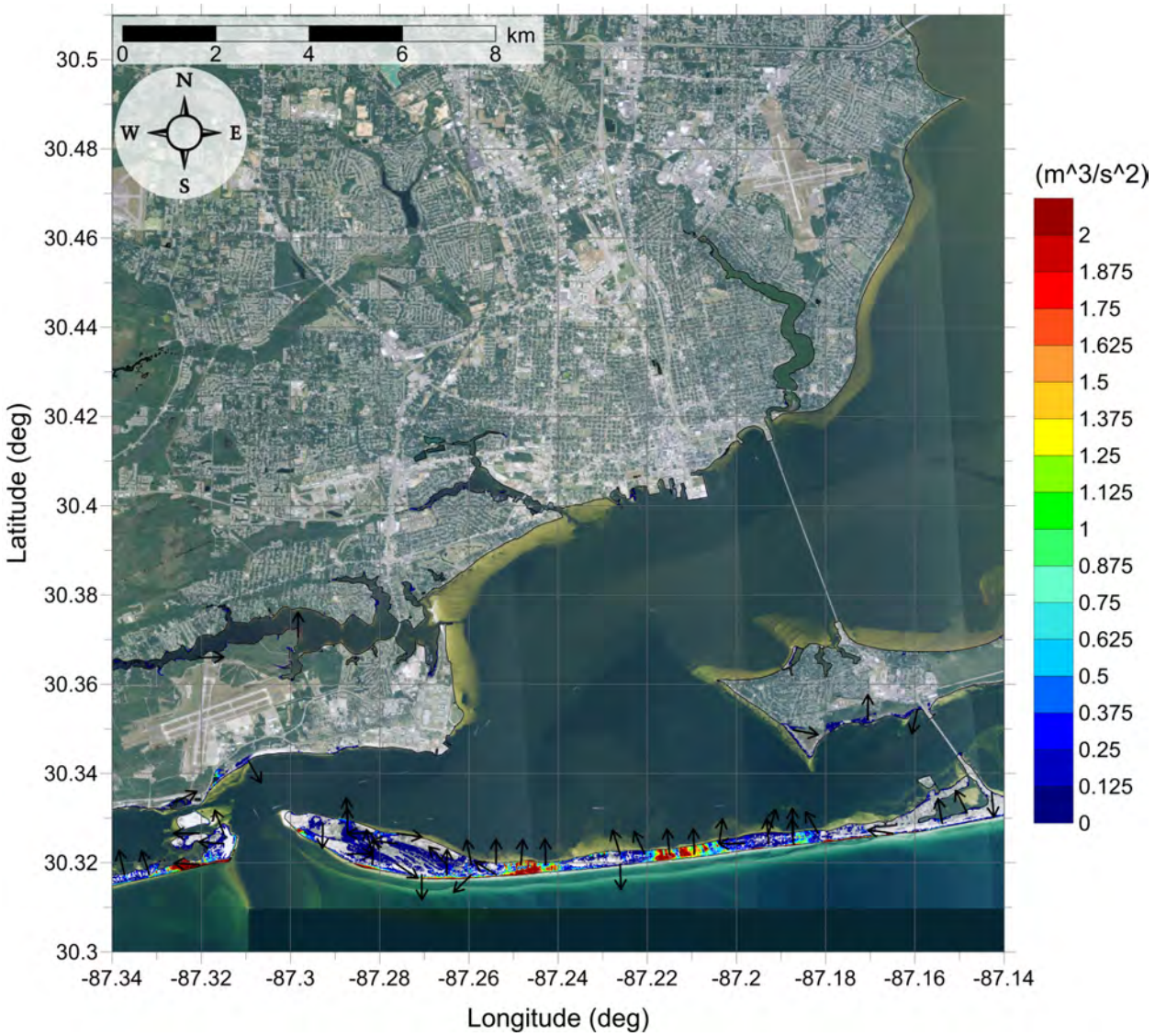


Figure 13: Maximum momentum flux ($m^3/s^2$) caused by the Probabilistic Submarine Landslide C in Pensacola, FL. Arrows represent direction of maximum momentum flux. Contour drawn is the zero-meter contour for land elevation.

**Pensacola, FL**
**West Florida submarine landslide**
**Maximum Momentum Flux**

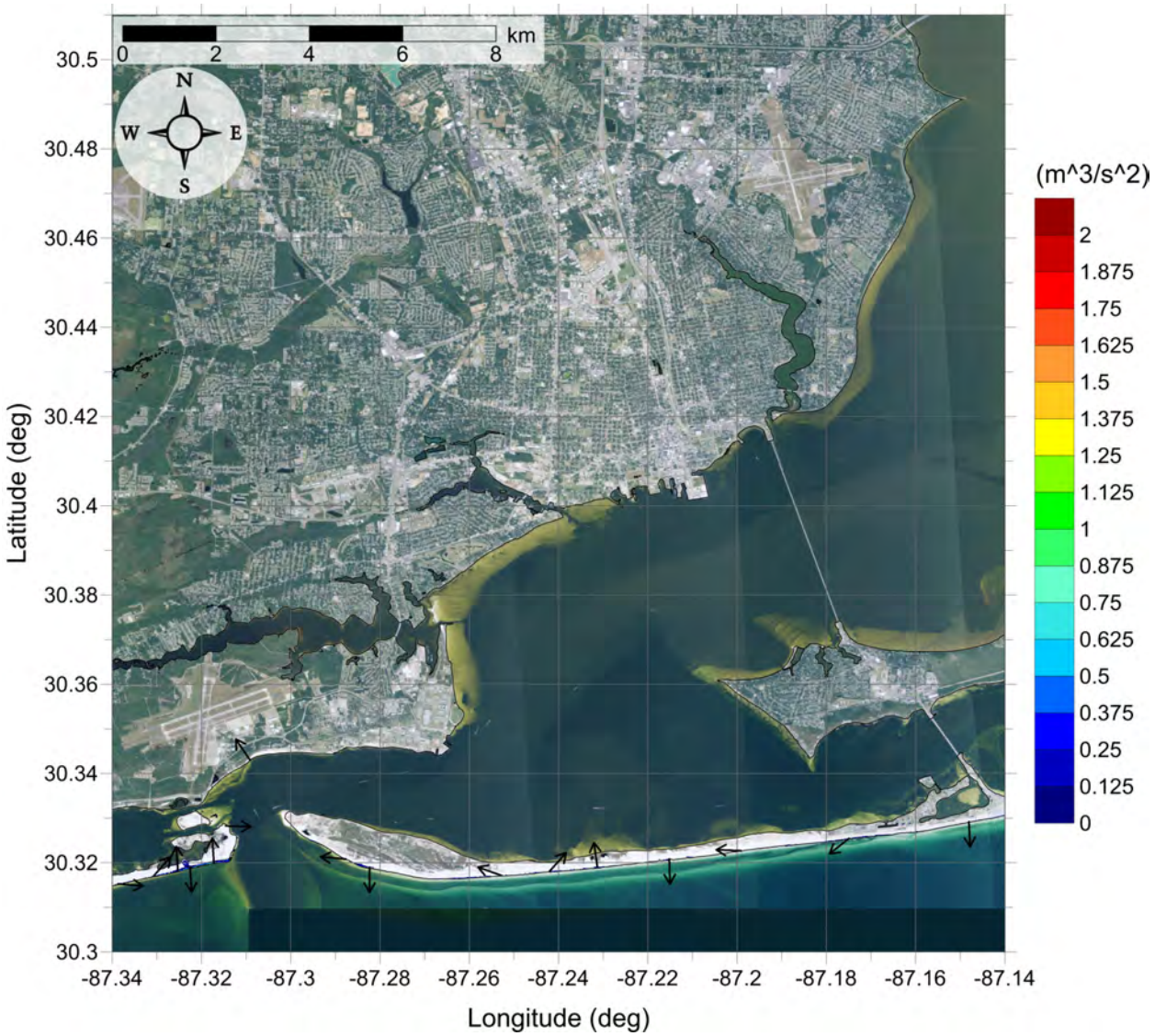


Figure 14: Maximum momentum flux ($m^3/s^2$) caused by the West Florida submarine landslide in Pensacola, FL. Arrows represent direction of maximum momentum flux. Contour drawn is the zero-meter contour for land elevation.

**Pensacola, FL**
**All Sources**
**Maximum of Maximum Inundation Depth**

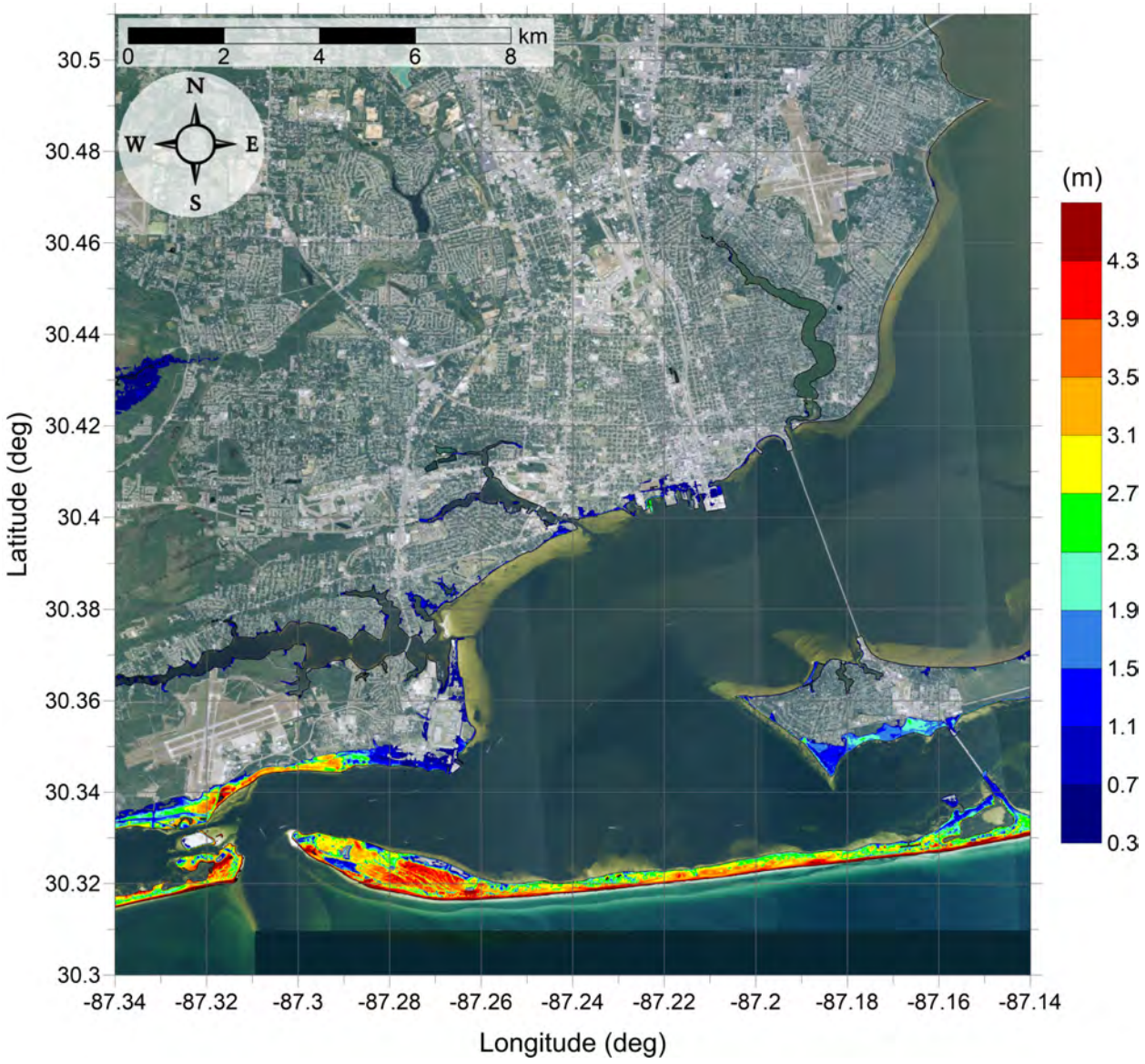


Figure 15: Maximum of maximums inundation depth (m) in Pensacola, FL, calculated as the maximum inundation depth in each grid cell from an ensemble of all tsunami sources considered. Contour drawn is the zero-meter contour for land elevation.

## Pensacola, FL
## All Sources
## Maximum Inundation Depth by Source

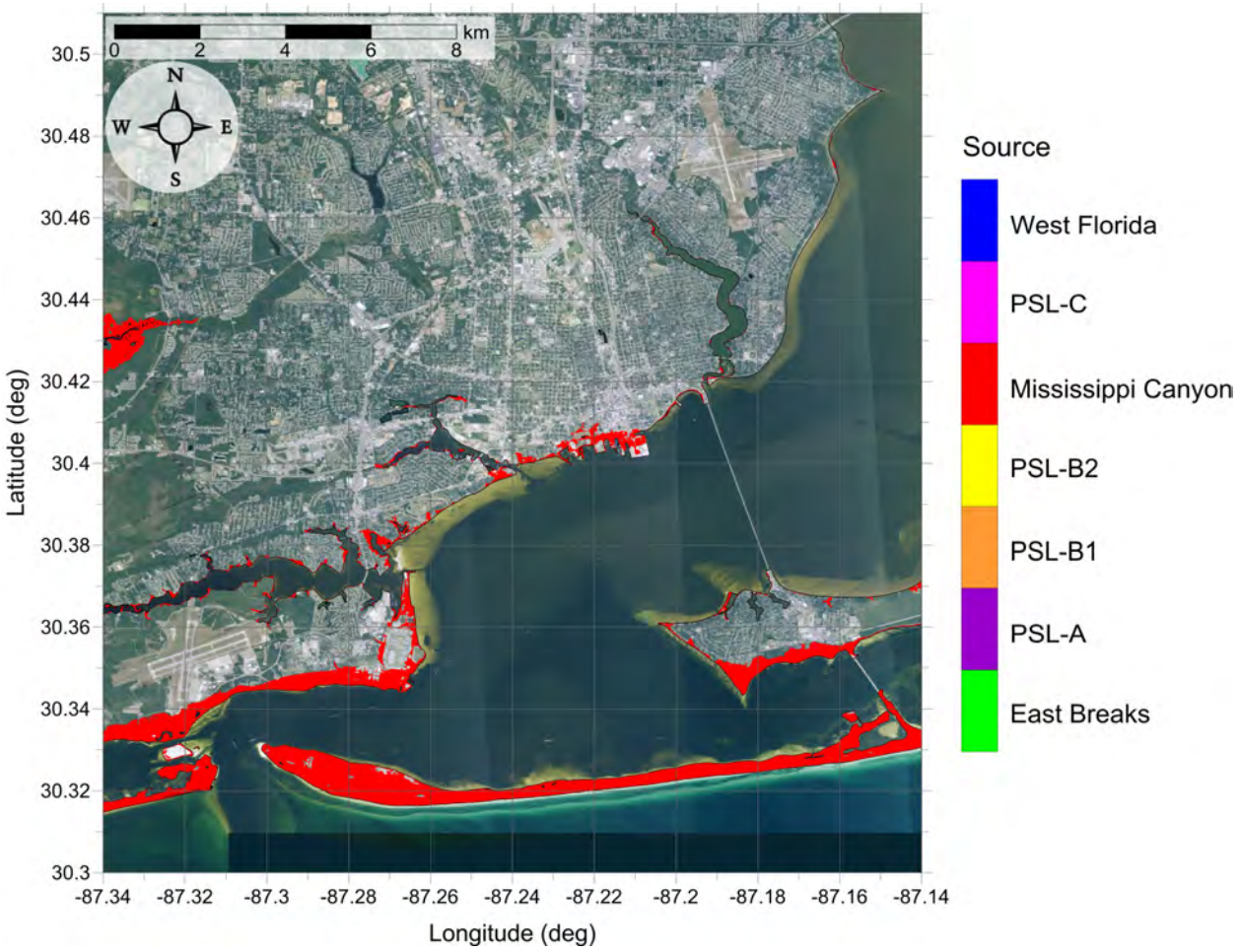


Figure 16: Indication of the tsunami source which causes the maximum of maximums inundation depth (m) in each grid cell from an ensemble of all tsunami sources in Pensacola, FL. Contour drawn is the zero-meter contour for land elevation.

## 3.2 Key West, FL

Table 2: Maximum tsunami wave amplitude and corresponding arrival time after landslide failure at Key West, FL numerical wave gauge: 24°28'15.00"N, 81°46'16.00"W (Fig. 1), approximate water depth 10 m.

| Tsunami Source | Maximum Wave Amplitude (m) | Arrival Time After Landslide Failure (hr) |
|---|---|---|
| East Breaks | 0.10 | 2.6 |
| PSL-A | 0.25 | 2.3 |
| PSL-B1 | 0.33 | 1.7 |
| PSL-B2 | 0.48 | 1.7 |
| Mississippi Canyon | 4.28 | 1.5 |
| PSL-C | 0.87 | 1.5 |
| West Florida | 0.19 | 1.1 |

## Key West, FL
## East Breaks submarine landslide
## Maximum Inundation Depth

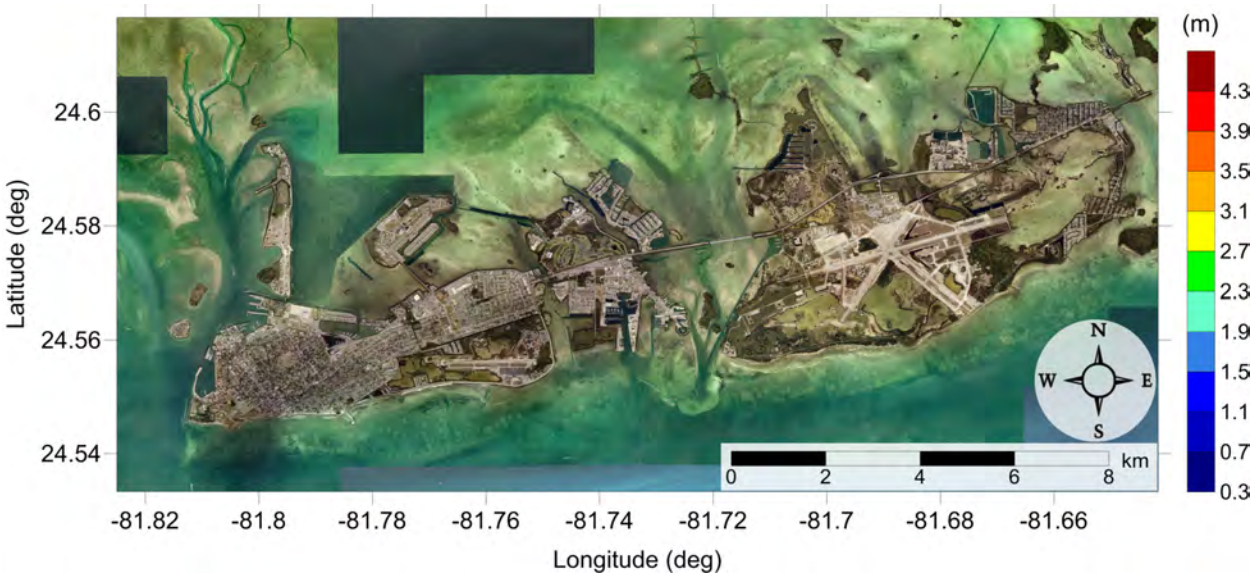


Figure 17: Maximum inundation depth (m) caused by the East Breaks submarine landslide in Key West, FL. Contour drawn is the zero-meter contour for land elevation.

## Key West, FL
## East Breaks submarine landslide
## Maximum Momentum Flux

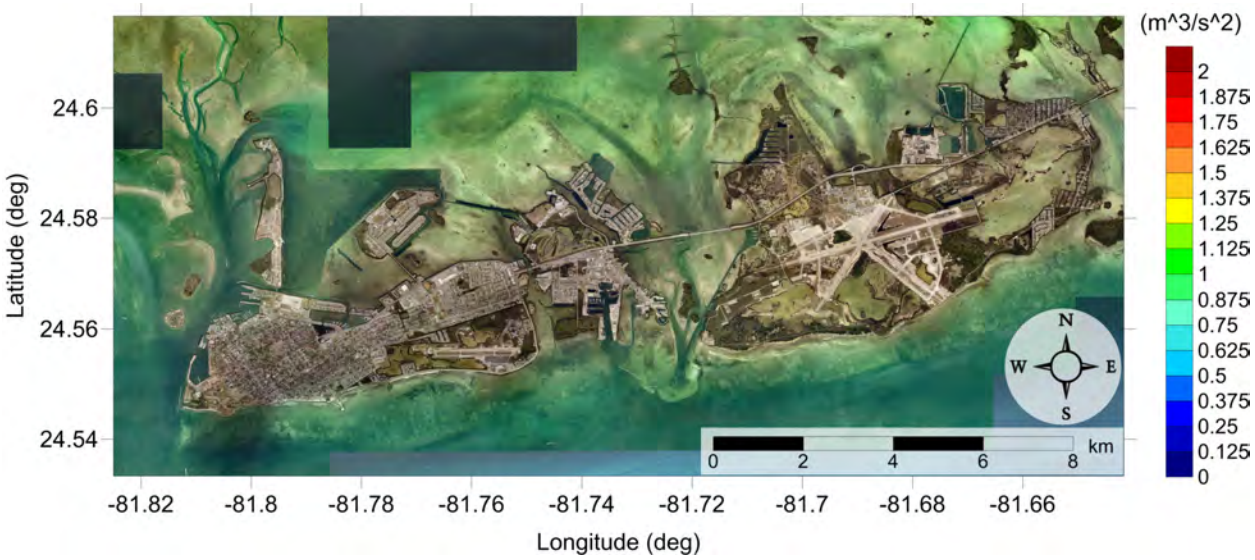


Figure 18: Maximum momentum flux ($m^3/s^2$) caused by the East Breaks submarine landslide in Key West, FL. Arrows represent direction of maximum momentum flux. Contour drawn is the zero-meter contour for land elevation.

## Key West, FL
## Probabilistic Submarine Landslide A
## Maximum Inundation Depth

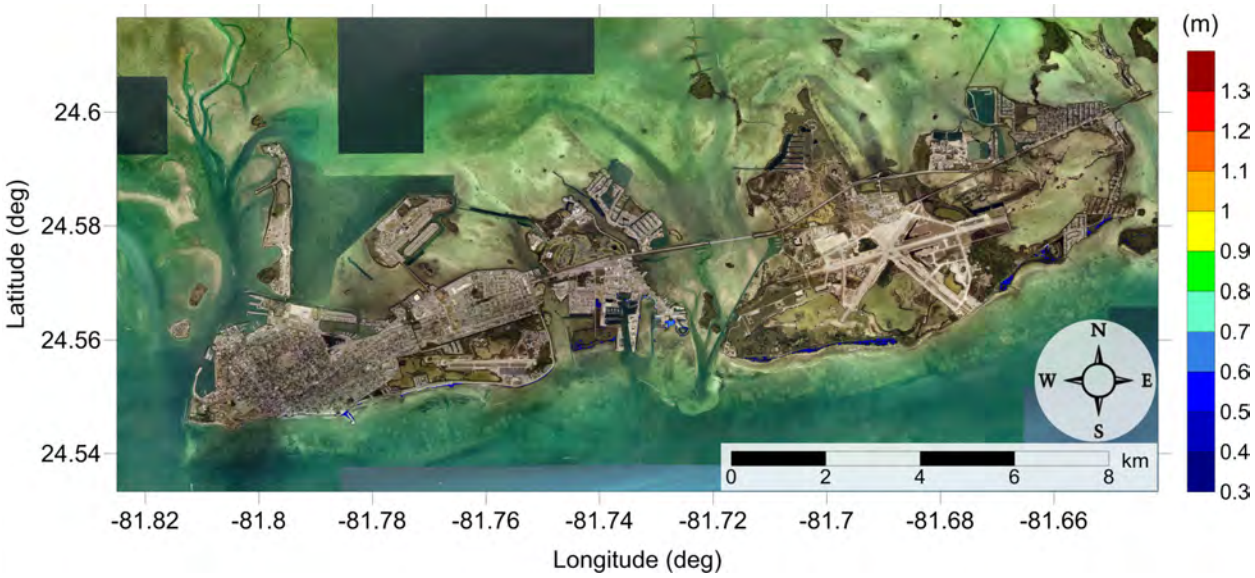


Figure 19: Maximum inundation depth (m) caused by the Probabilistic Submarine Landslide A in Key West, FL. Contour drawn is the zero-meter contour for land elevation.

## Key West, FL
## Probabilistic Submarine Landslide A
## Maximum Momentum Flux

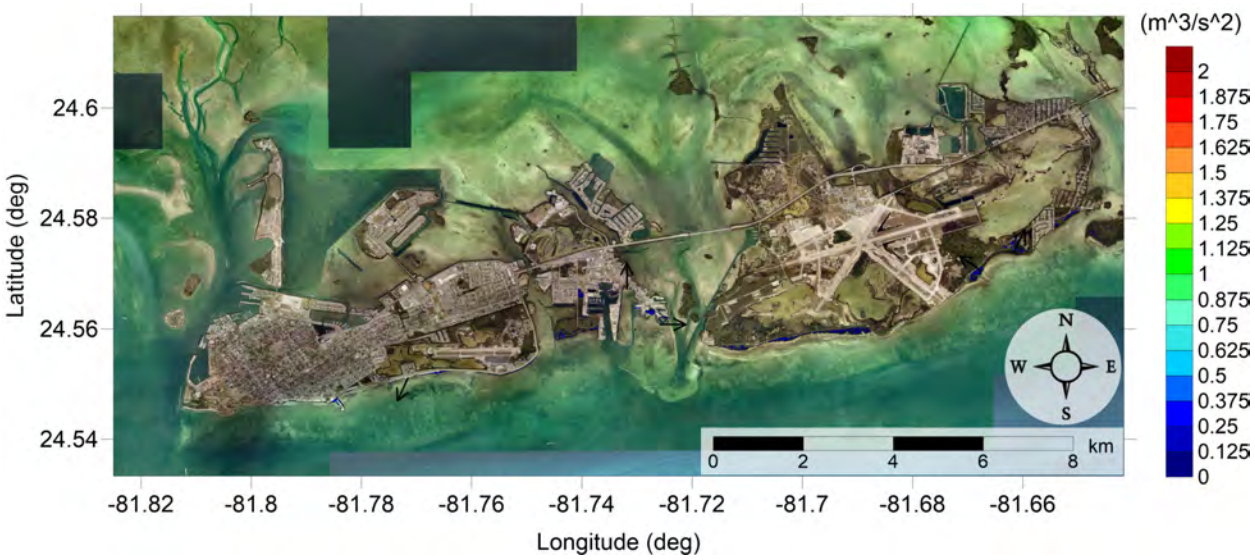


Figure 20: Maximum momentum flux ($m^3/s^2$) caused by the Probabilistic Submarine Landslide A in Key West, FL. Arrows represent direction of maximum momentum flux. Contour drawn is the zero-meter contour for land elevation.

## Key West, FL
## Probabilistic Submarine Landslide B1
## Maximum Inundation Depth

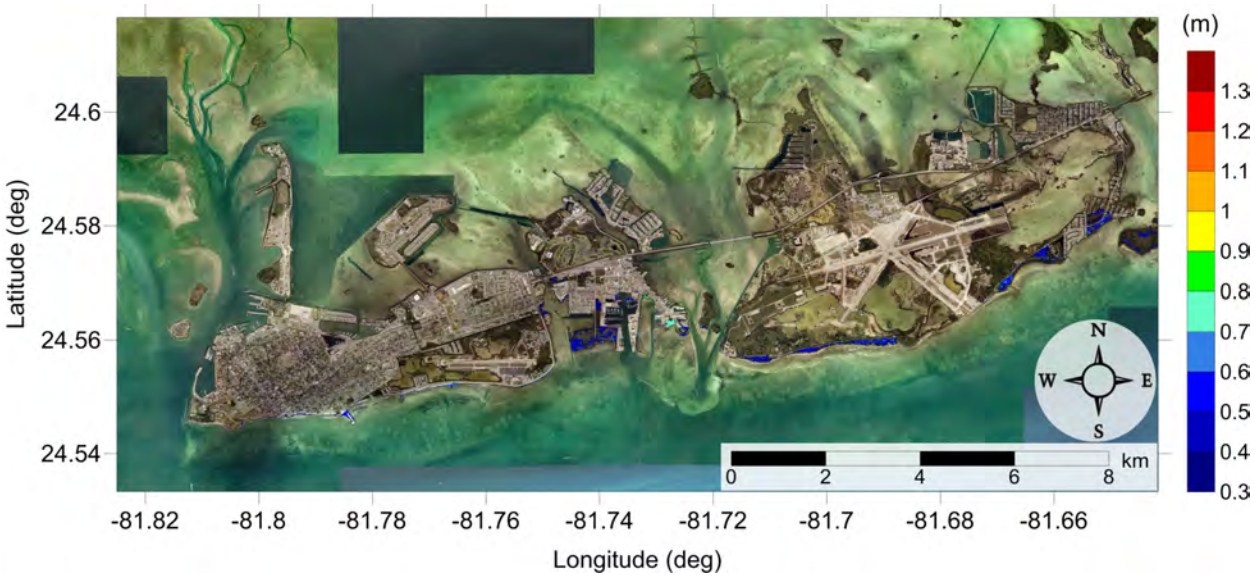


Figure 21: Maximum inundation depth (m) caused by the Probabilistic Submarine Landslide B1 in Key West, FL. Contour drawn is the zero-meter contour for land elevation.

## Key West, FL
## Probabilistic Submarine Landslide B1
## Maximum Momentum Flux

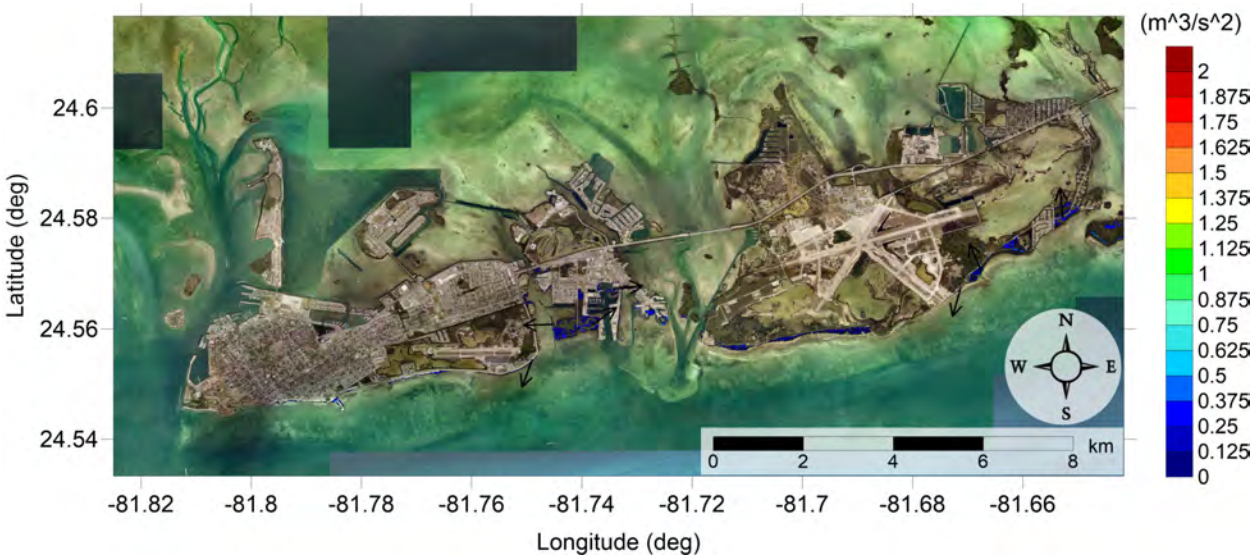


Figure 22: Maximum momentum flux ($m^3/s^2$) caused by the Probabilistic Submarine Landslide B1 in Key West, FL. Arrows represent direction of maximum momentum flux. Contour drawn is the zero-meter contour for land elevation.

## Key West, FL
## Probabilistic Submarine Landslide B2
## Maximum Inundation Depth


Figure 23: Maximum inundation depth (m) caused by the Probabilistic Submarine Landslide B2 in Key West, FL. Contour drawn is the zero-meter contour for land elevation.

## Key West, FL
## Probabilistic Submarine Landslide B2
## Maximum Momentum Flux

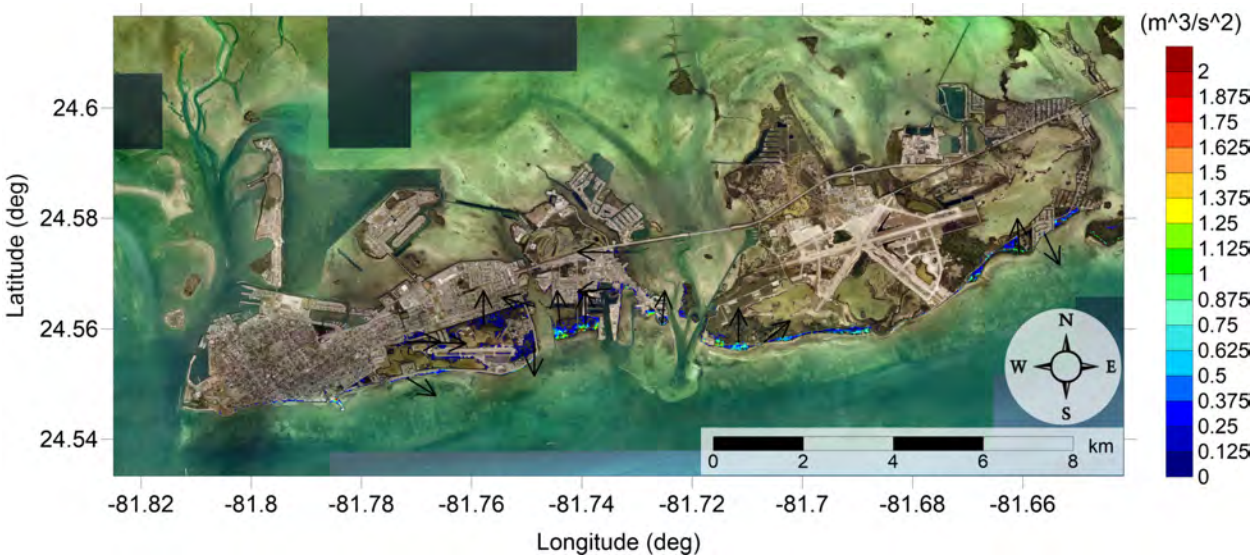


Figure 24: Maximum momentum flux ($m^3/s^2$) caused by the Probabilistic Submarine Landslide B2 in Key West, FL. Arrows represent direction of maximum momentum flux. Contour drawn is the zero-meter contour for land elevation.

## Key West, FL
## Mississippi Canyon submarine landslide
## Maximum Inundation Depth

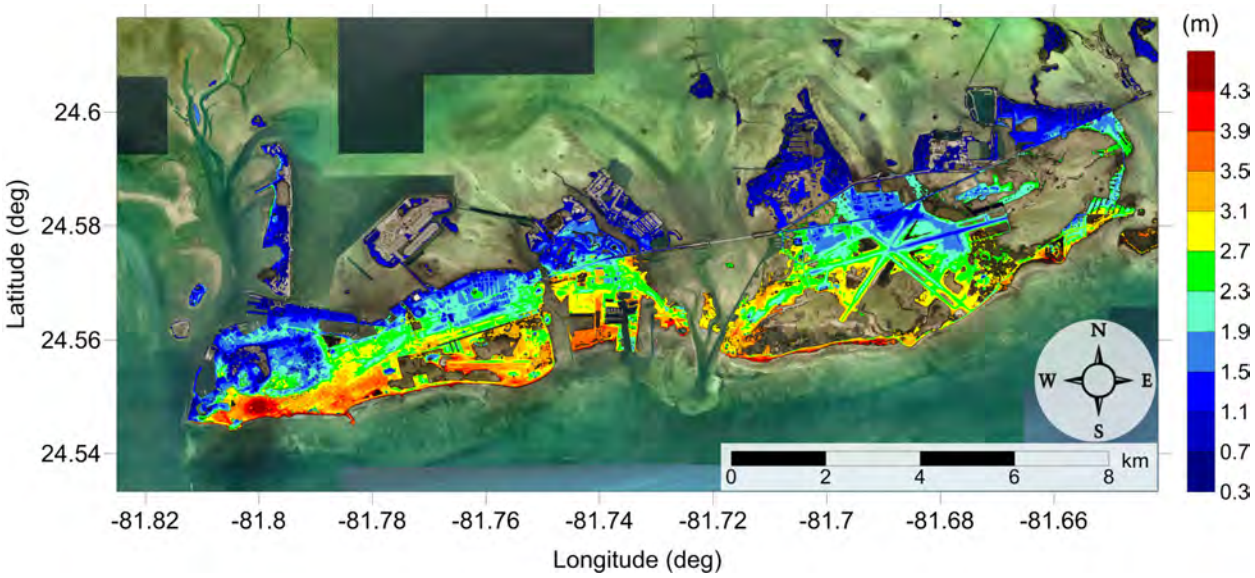


Figure 25: Maximum inundation depth (m) caused by the Mississippi Canyon submarine landslide in Key West, FL. Contour drawn is the zero-meter contour for land elevation.

## Key West, FL
## Mississippi Canyon submarine landslide
## Maximum Momentum Flux

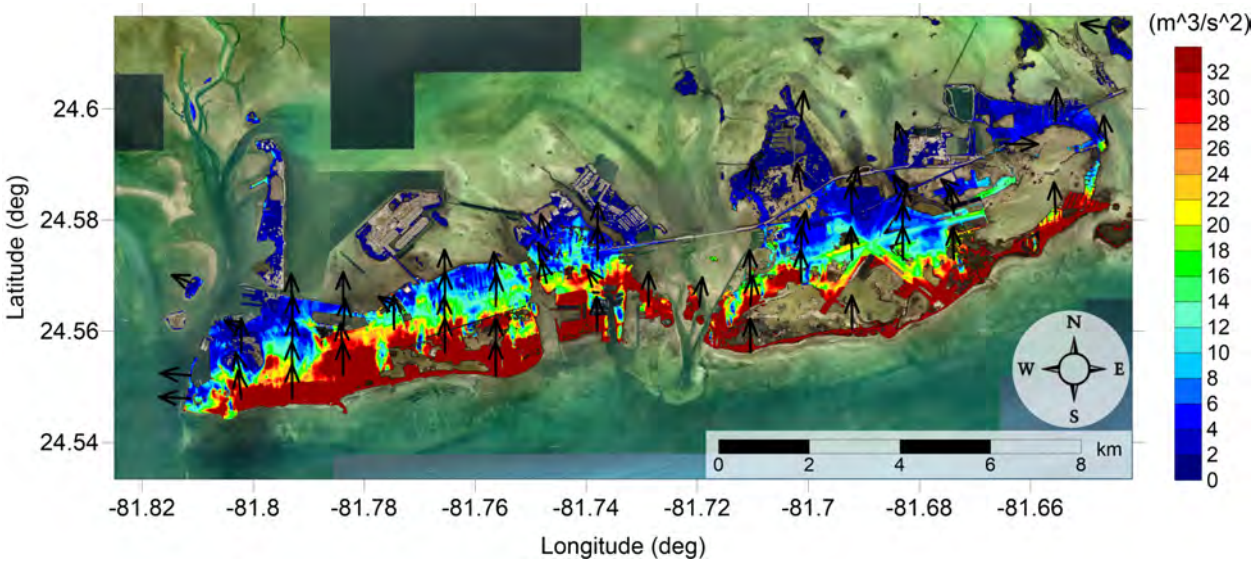


Figure 26: Maximum momentum flux ($m^3/s^2$) caused by the Mississippi Canyon submarine landslide in Key West, FL. Arrows represent direction of maximum momentum flux. Contour drawn is the zero-meter contour for land elevation.

## Key West, FL
## Probabilistic Submarine Landslide C
## Maximum Inundation Depth

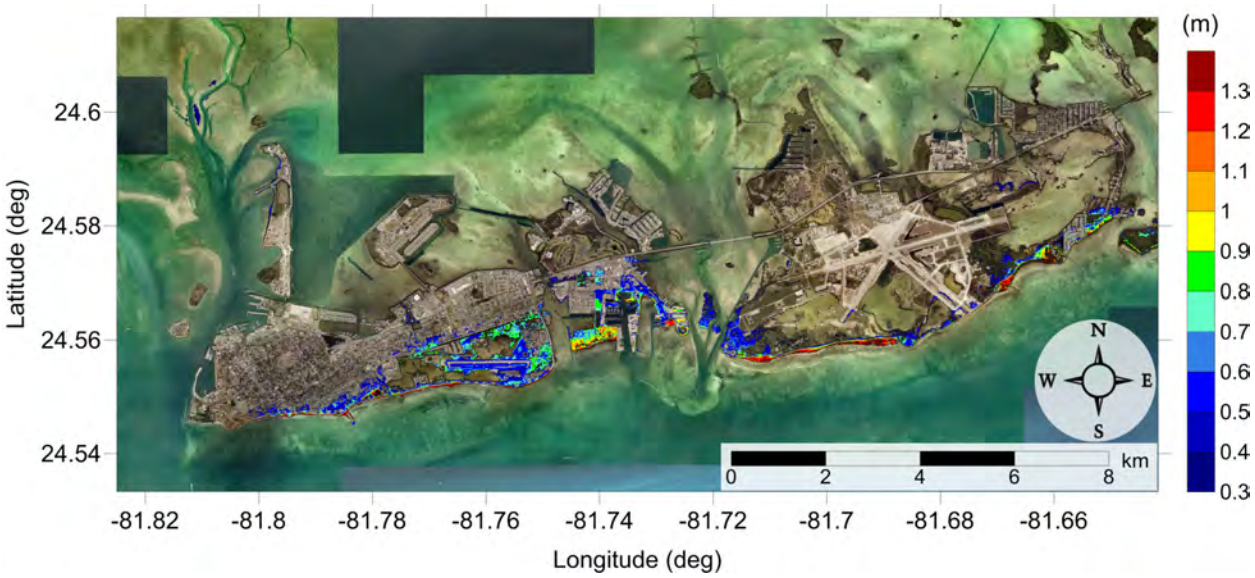


Figure 27: Maximum inundation depth (m) caused by the Probabilistic Submarine Landslide C in Key West, FL. Contour drawn is the zero-meter contour for land elevation.

## Key West, FL
## Probabilistic Submarine Landslide C
## Maximum Momentum Flux

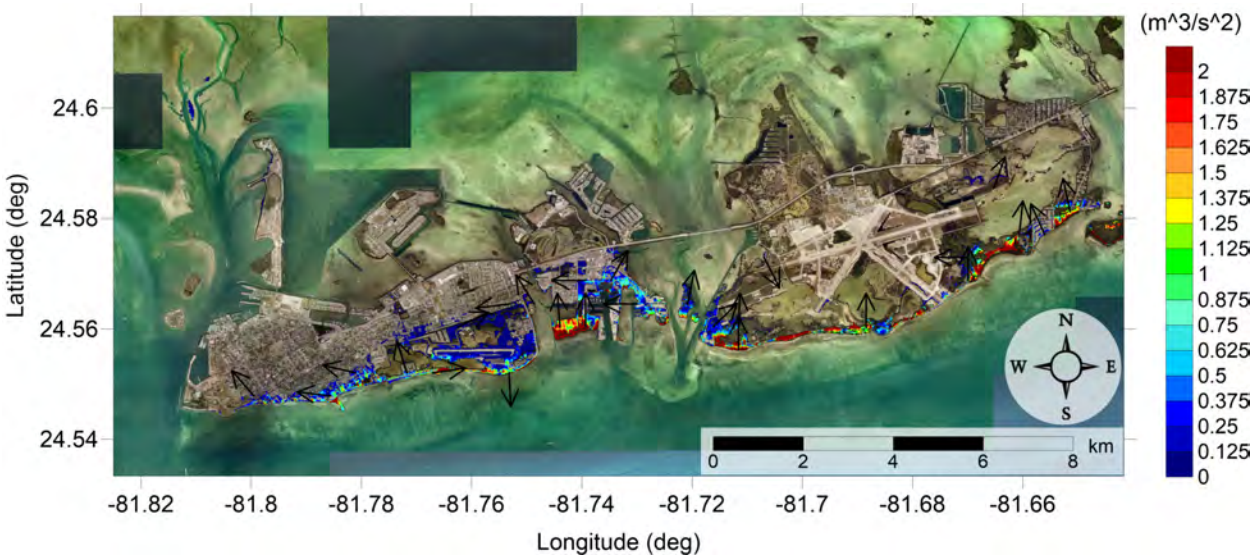


Figure 28: Maximum momentum flux ($m^3/s^2$) caused by the Probabilistic Submarine Landslide C in Key West, FL. Arrows represent direction of maximum momentum flux. Contour drawn is the zero-meter contour for land elevation.

## Key West, FL
## West Florida submarine landslide
## Maximum Inundation Depth

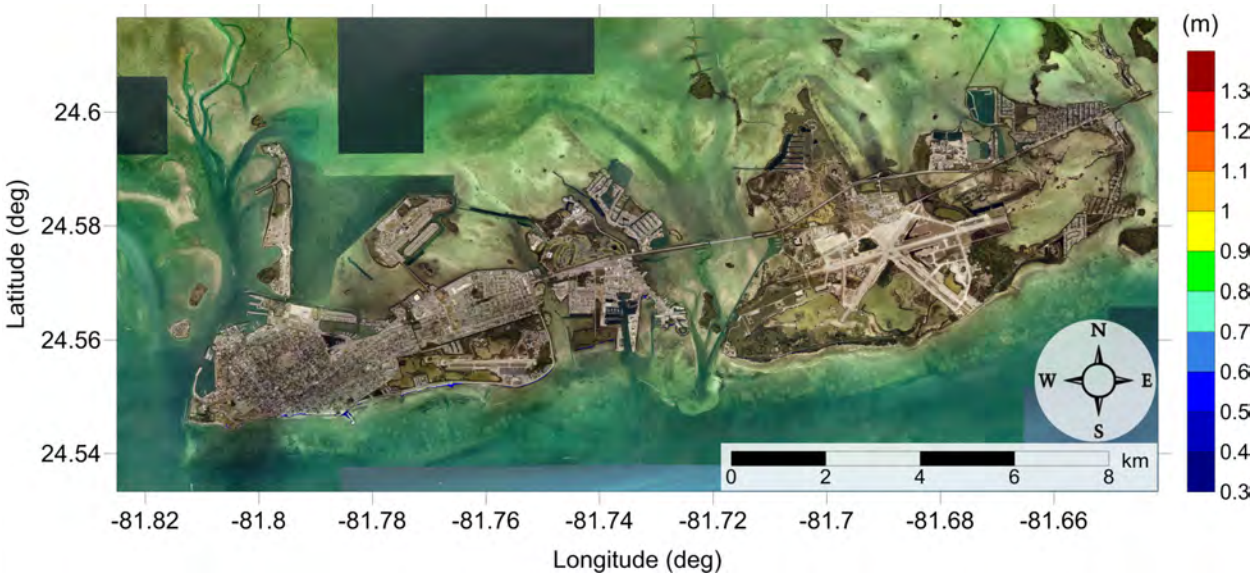


Figure 29: Maximum inundation depth (m) caused by the West Florida submarine landslide in Key West, FL. Contour drawn is the zero-meter contour for land elevation.

## Key West, FL
## West Florida submarine landslide
## Maximum Momentum Flux

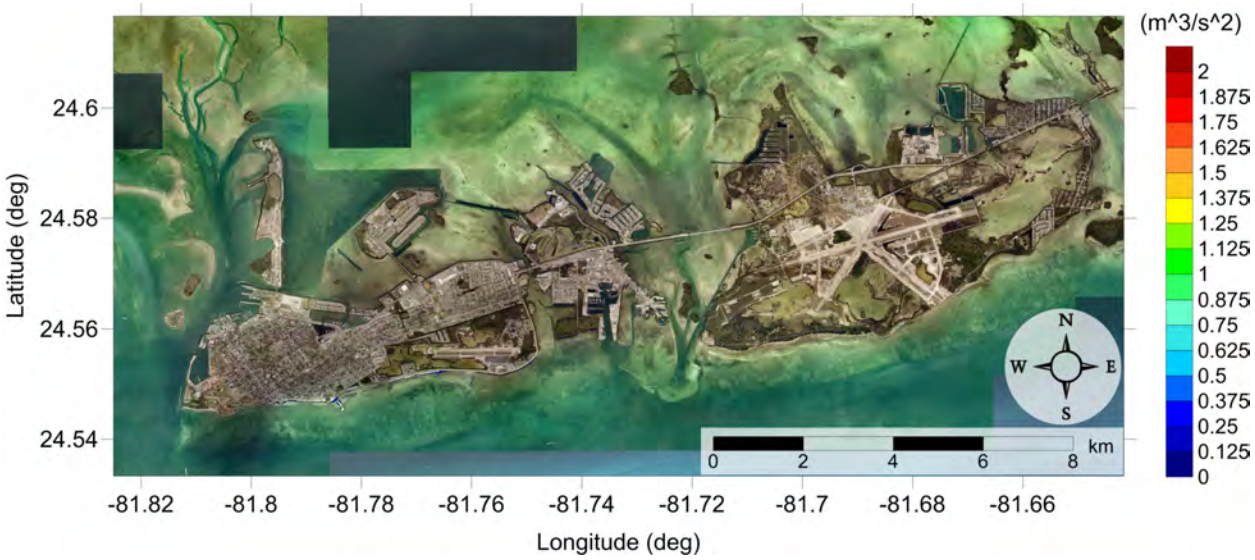


Figure 30: Maximum momentum flux ($m^3/s^2$) caused by the West Florida submarine landslide in Key West, FL. Arrows represent direction of maximum momentum flux. Contour drawn is the zero-meter contour for land elevation.

## Key West, FL
## All Sources
## Maximum of Maximum Inundation Depth

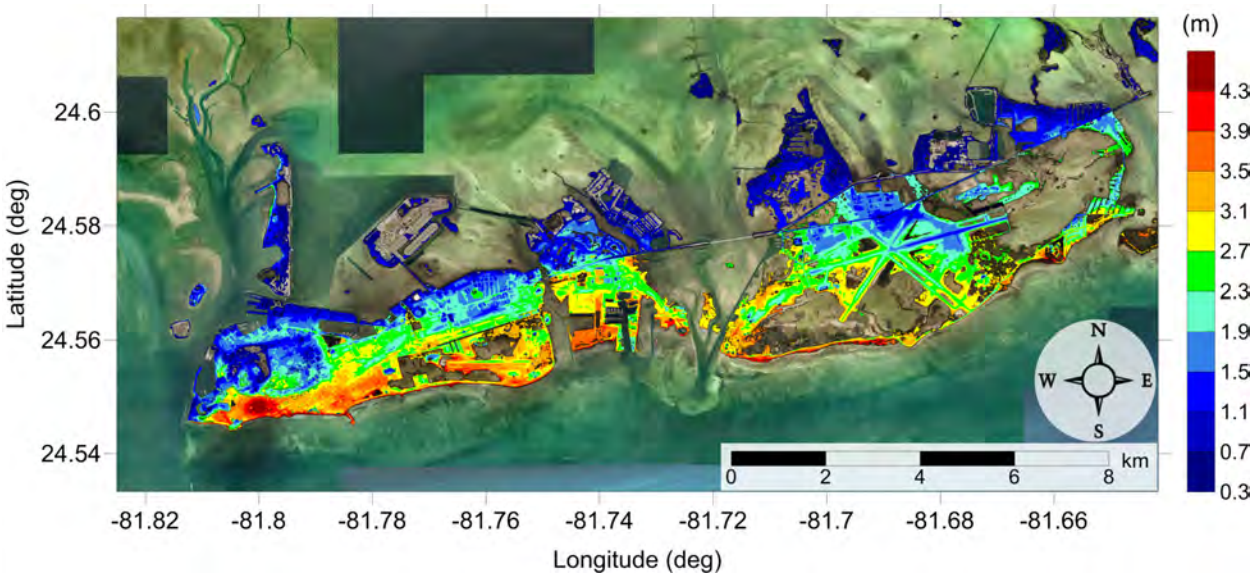


Figure 31: Maximum of maximums inundation depth (m) in Key West, FL, calculated as the maximum inundation depth in each grid cell from an ensemble of all tsunami sources considered. Contour drawn is the zero-meter contour for land elevation.

## Key West, FL
## All Sources
## Maximum Inundation Depth by Source

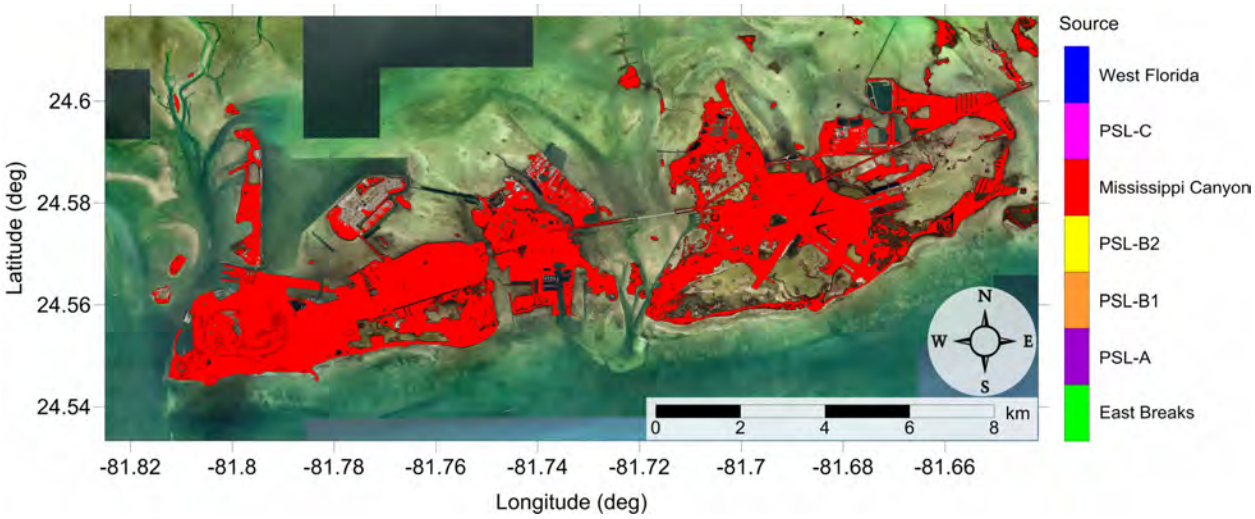


Figure 32: Indication of the tsunami source which causes the maximum of maximums inundation depth (m) in each grid cell from an ensemble of all tsunami sources in Key West, FL. Contour drawn is the zero-meter contour for land elevation.

## 3.3 Okaloosa County, FL

Table 3: Maximum tsunami wave amplitude and corresponding arrival time after landslide failure at Okaloosa County, FL numerical wave gauge: 30°20'18.50"N, 86°30'50.00"W (Fig. 1), approximate water depth 22 m.

| Tsunami Source | Maximum Wave Amplitude (m) | Arrival Time After Landslide Failure (hr) |
|---|---|---|
| East Breaks | 0.28 | 2.9 |
| PSL-A | 0.41 | 2.5 |
| PSL-B1 | 0.44 | 1.7 |
| PSL-B2 | 0.37 | 1.9 |
| Mississippi Canyon | 4.09 | 1.2 |
| PSL-C | 1.71 | 1.7 |
| West Florida | 0.43 | 1.8 |

## Okaloosa County, FL
## East Breaks submarine landslide
## Maximum Momentum Flux

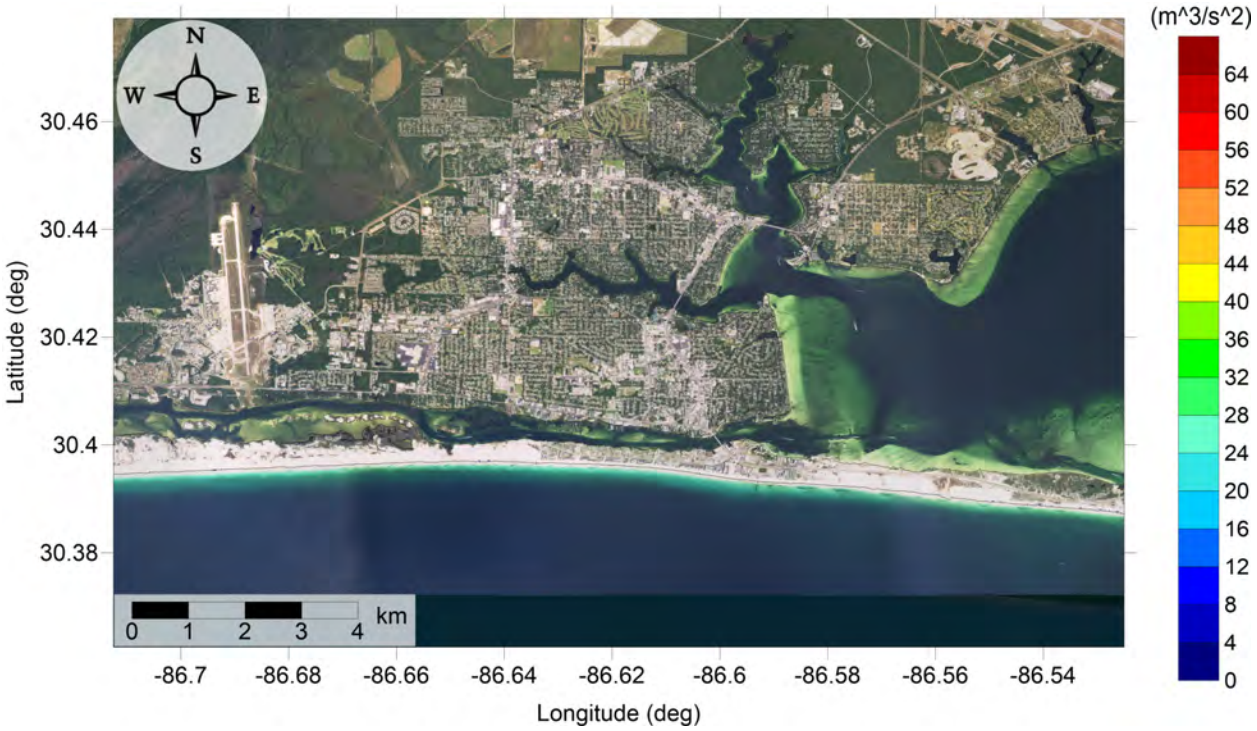


Figure 33: Maximum momentum flux ($m^3/s^2$) caused by the East Breaks submarine landslide in Okaloosa Island, FL. Arrows represent direction of maximum momentum flux. Contour drawn is the zero-meter contour for land elevation.

**Okaloosa County, FL**
**East Breaks submarine landslide**
**Maximum Momentum Flux**

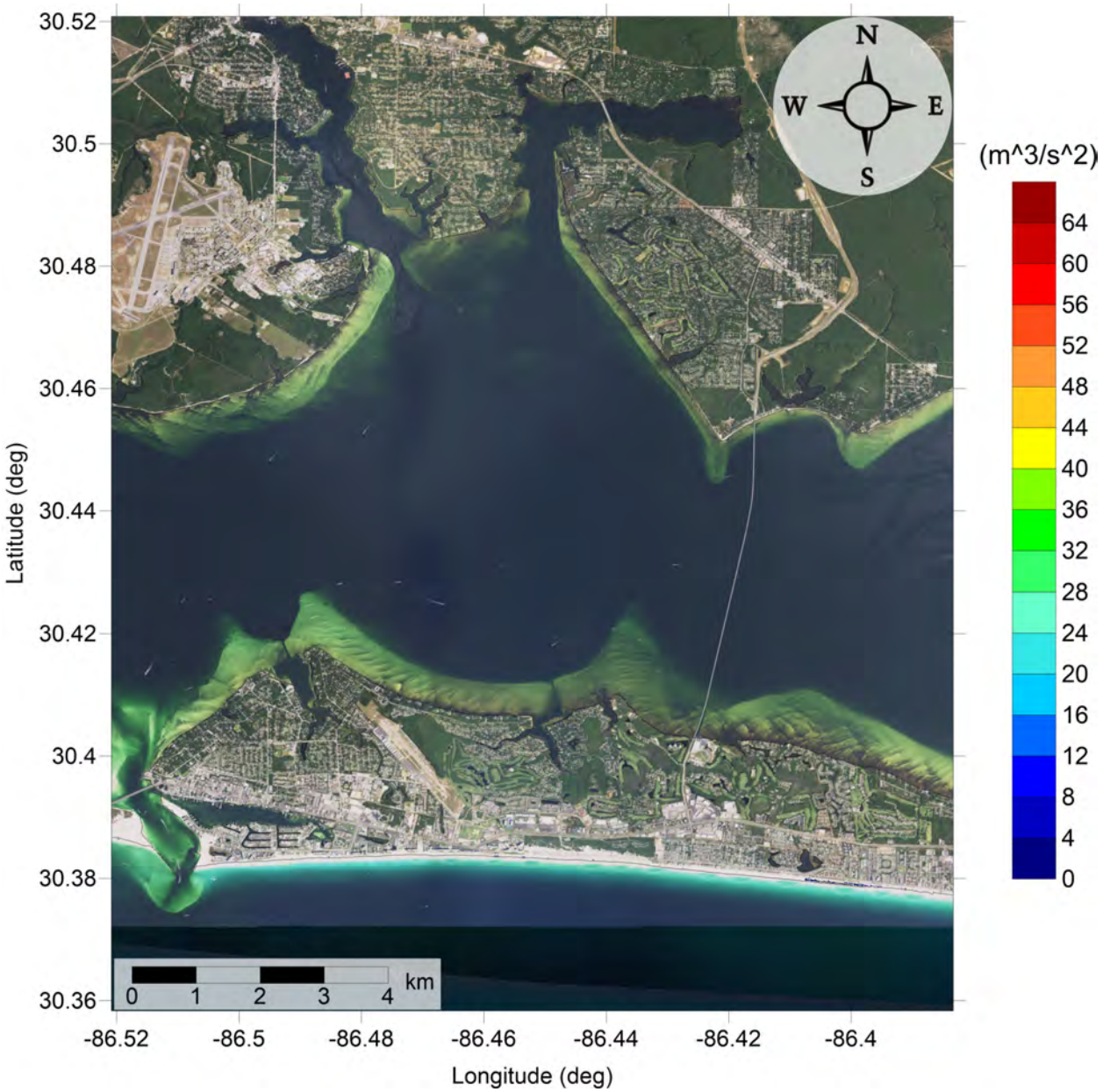


Figure 34: Maximum momentum flux ($m^3/s^2$) caused by the East Breaks submarine landslide in Destin, FL. Arrows represent direction of maximum momentum flux. Contour drawn is the zero-meter contour for land elevation.

**Okaloosa County, FL**
**East Breaks submarine landslide**
**Maximum Inundation Depth**


Figure 35: Maximum inundation depth (m) caused by the East Breaks submarine landslide in Okaloosa Island, FL. Contour drawn is the zero-meter contour for land elevation.

**Okaloosa County, FL**
**East Breaks submarine landslide**
**Maximum Inundation Depth**

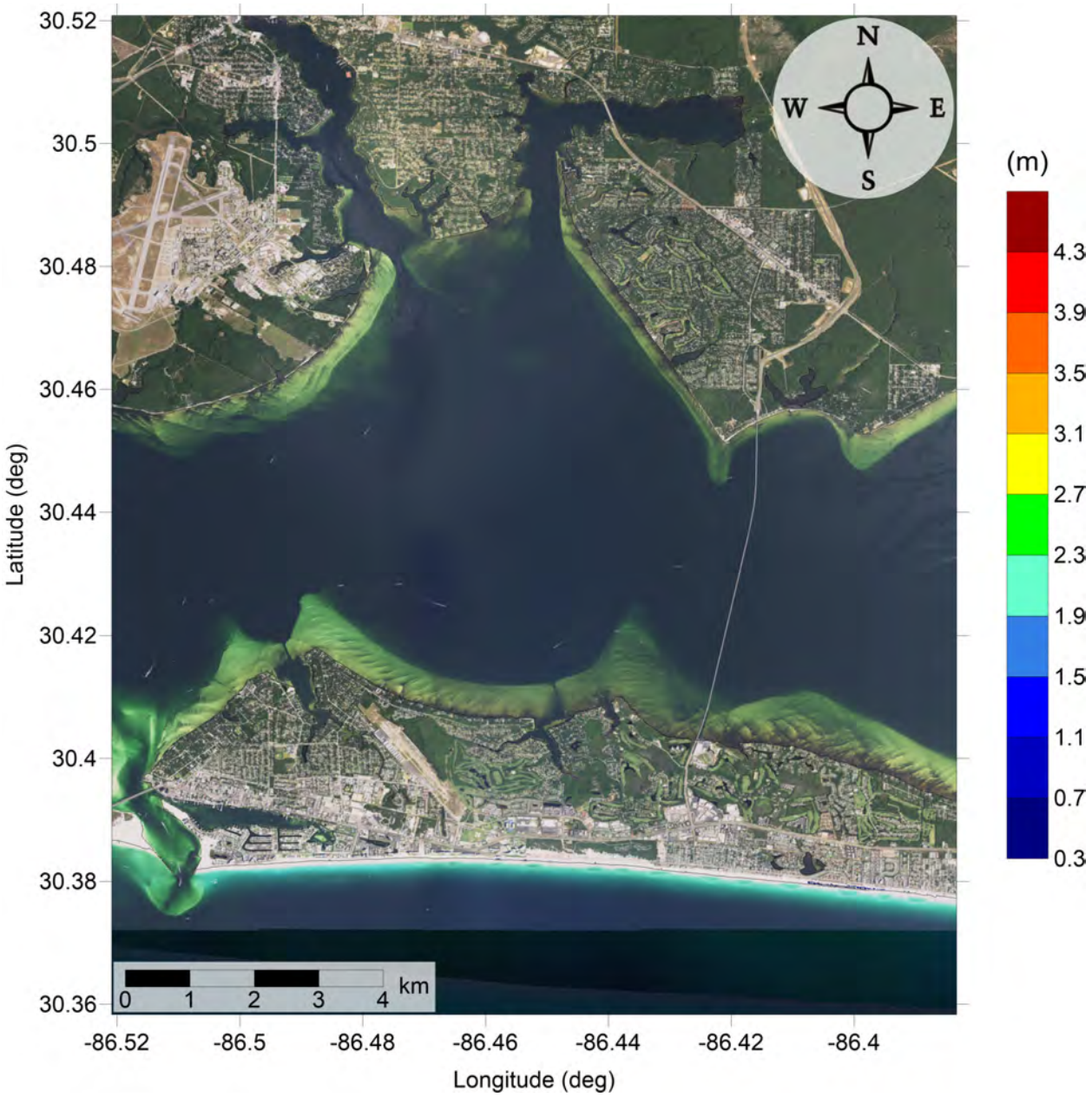


Figure 36: Maximum inundation depth (m) caused by the East Breaks submarine landslide in Destin, FL. Contour drawn is the zero-meter contour for land elevation.

## Okaloosa County, FL
## Probabilistic Submarine Landslide A
## Maximum Momentum Flux

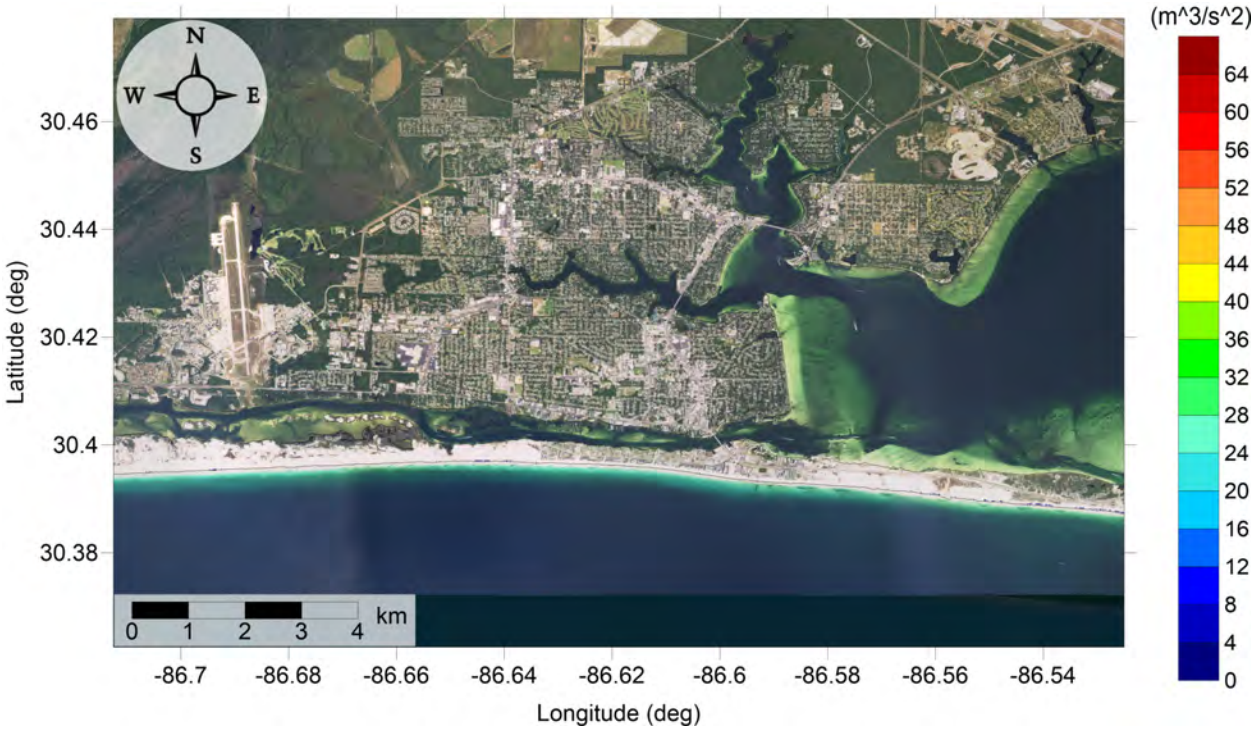


Figure 37: Maximum momentum flux ($m^3/s^2$) caused by the Probabilistic Submarine Landslide A in Okaloosa Island, FL. Arrows represent direction of maximum momentum flux. Contour drawn is the zero-meter contour for land elevation.

**Okaloosa County, FL**
**Probabilistic Submarine Landslide A**
**Maximum Momentum Flux**

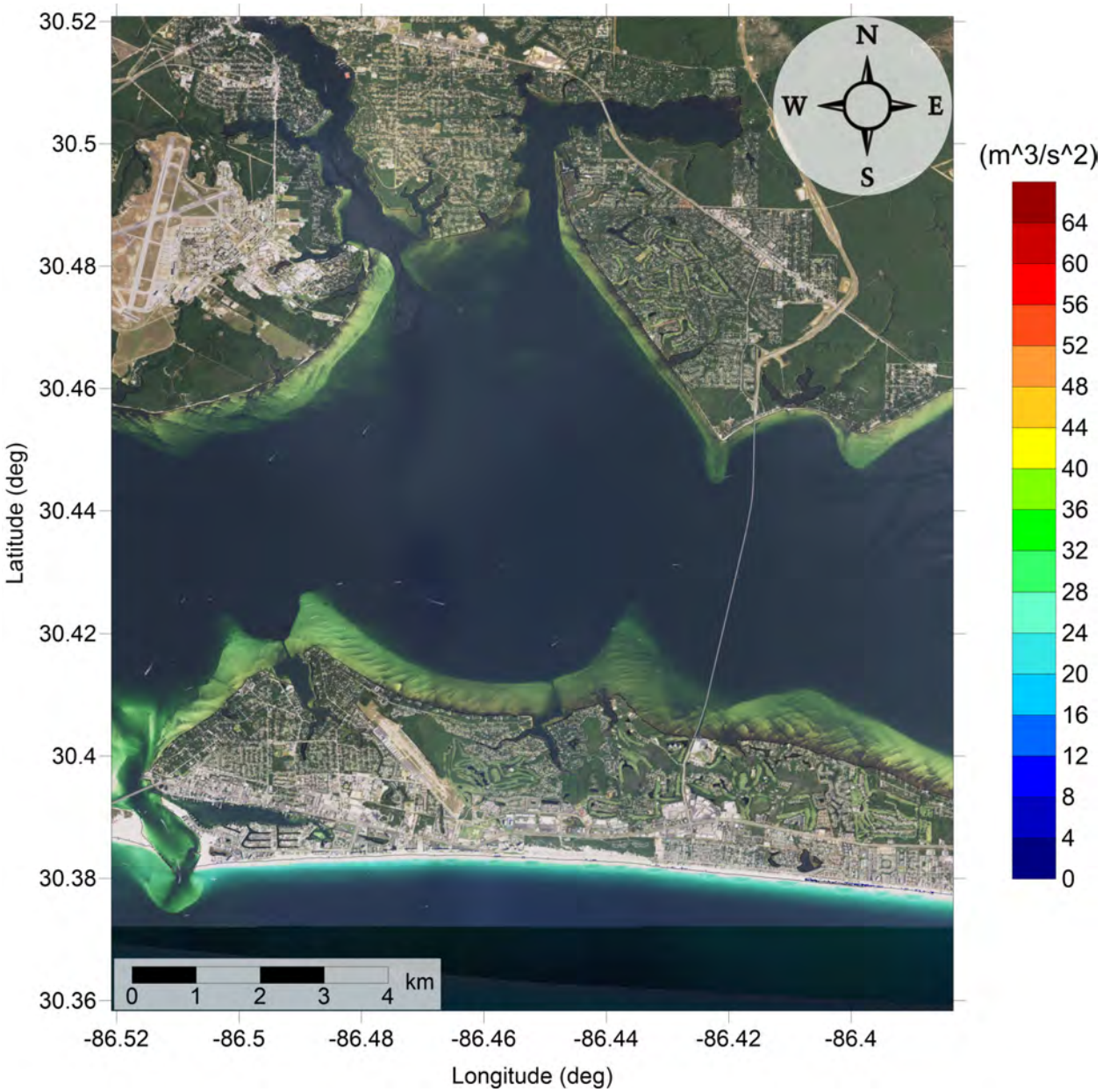


Figure 38: Maximum momentum flux ($m^3/s^2$) caused by the Probabilistic Submarine Landslide A in Destin, FL. Arrows represent direction of maximum momentum flux. Contour drawn is the zero-meter contour for land elevation.

## Okaloosa County, FL
## Probabilistic Submarine Landslide A
## Maximum Inundation Depth

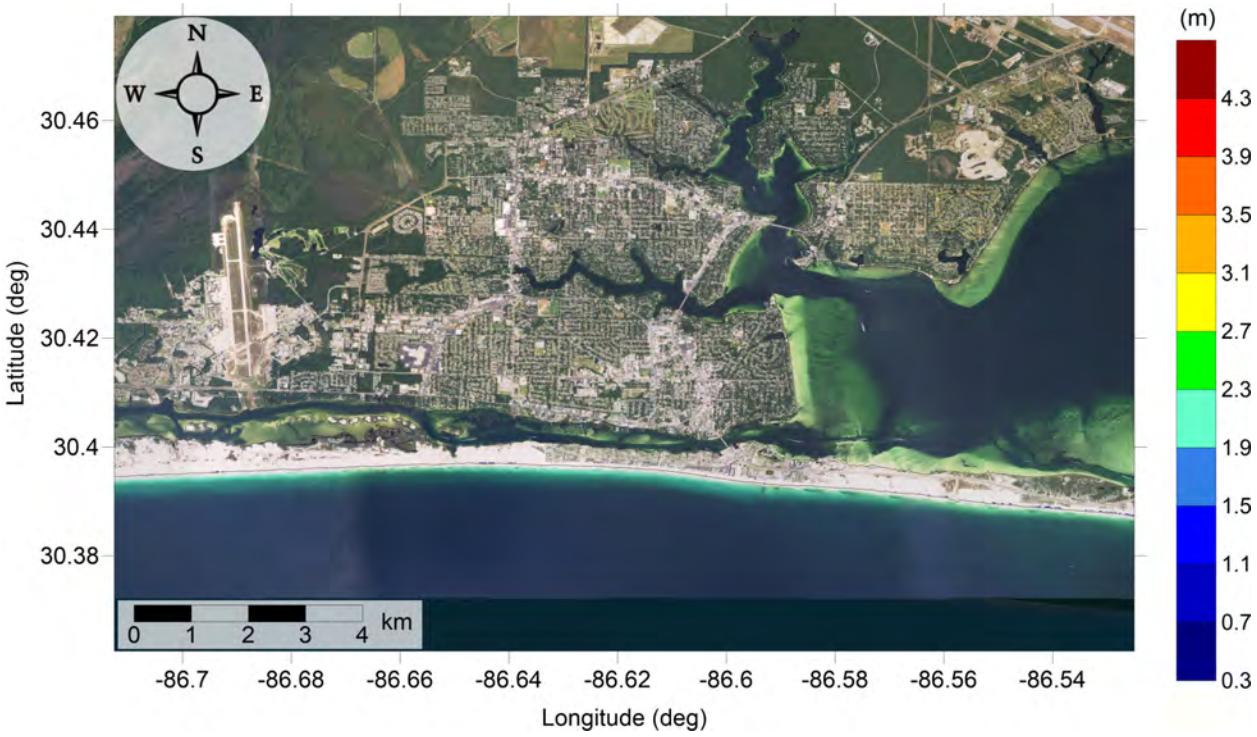


Figure 39: Maximum inundation depth (m) caused by the Probabilistic Submarine Landslide A in Okaloosa Island, FL. Contour drawn is the zero-meter contour for land elevation.

**Okaloosa County, FL**
**Probabilistic Submarine Landslide A**
**Maximum Inundation Depth**

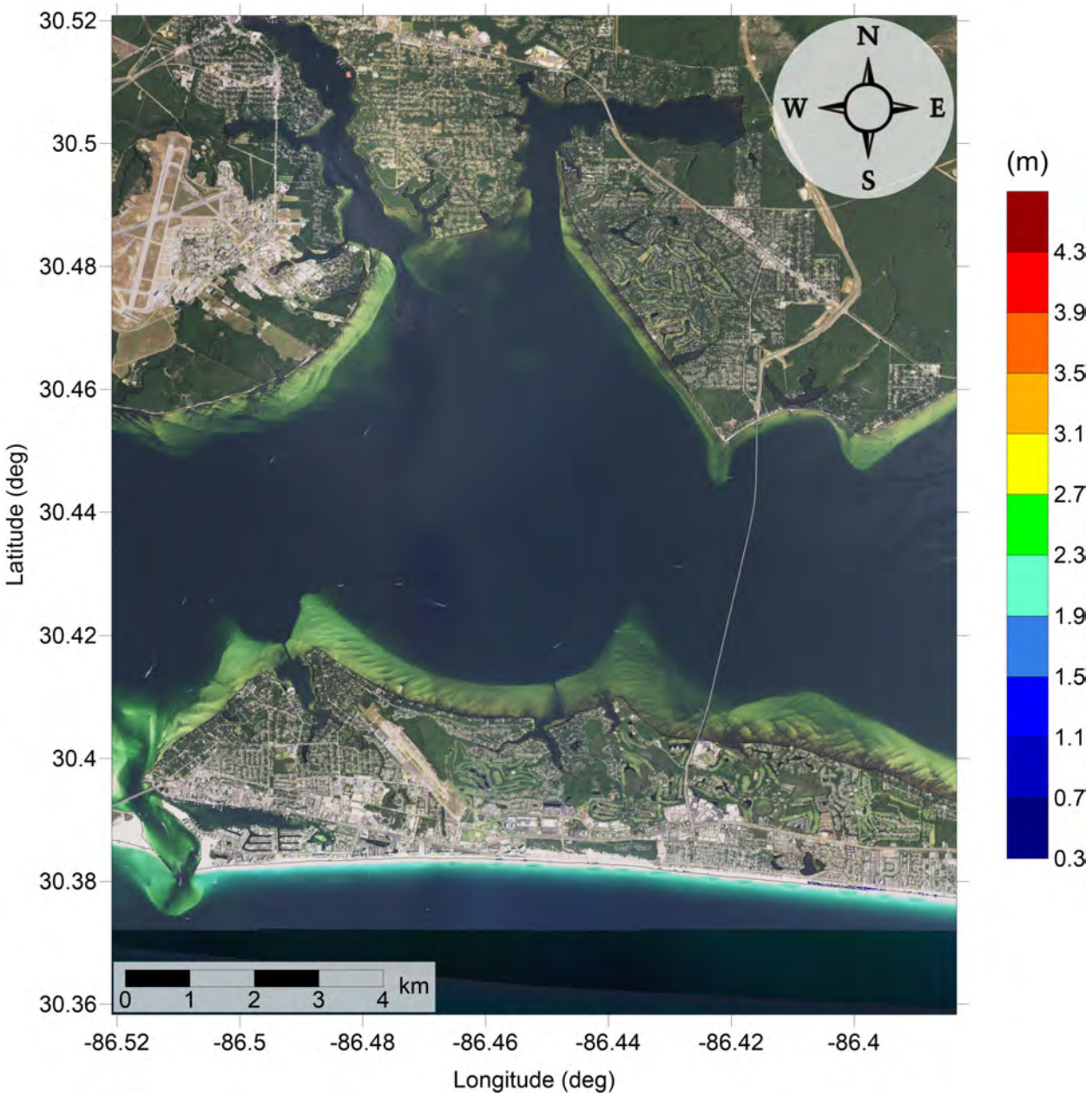


Figure 40: Maximum inundation depth (m) caused by the Probabilistic Submarine Landslide A in Destin, FL. Contour drawn is the zero-meter contour for land elevation.

## Okaloosa County, FL
## Probabilistic Submarine Landslide B1
## Maximum Momentum Flux

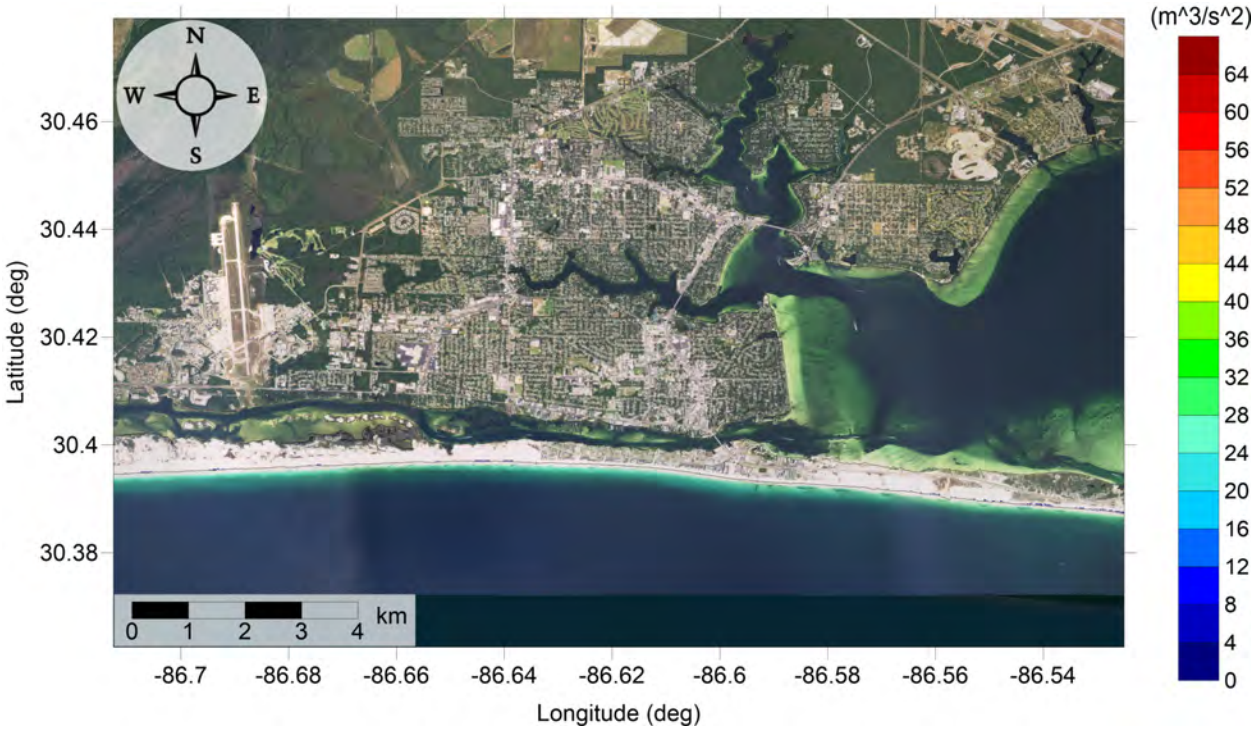


Figure 41: Maximum momentum flux ($m^3/s^2$) caused by the Probabilistic Submarine Landslide B1 in Okaloosa Island, FL. Arrows represent direction of maximum momentum flux. Contour drawn is the zero-meter contour for land elevation.

**Okaloosa County, FL**
**Probabilistic Submarine Landslide B1**
**Maximum Momentum Flux**

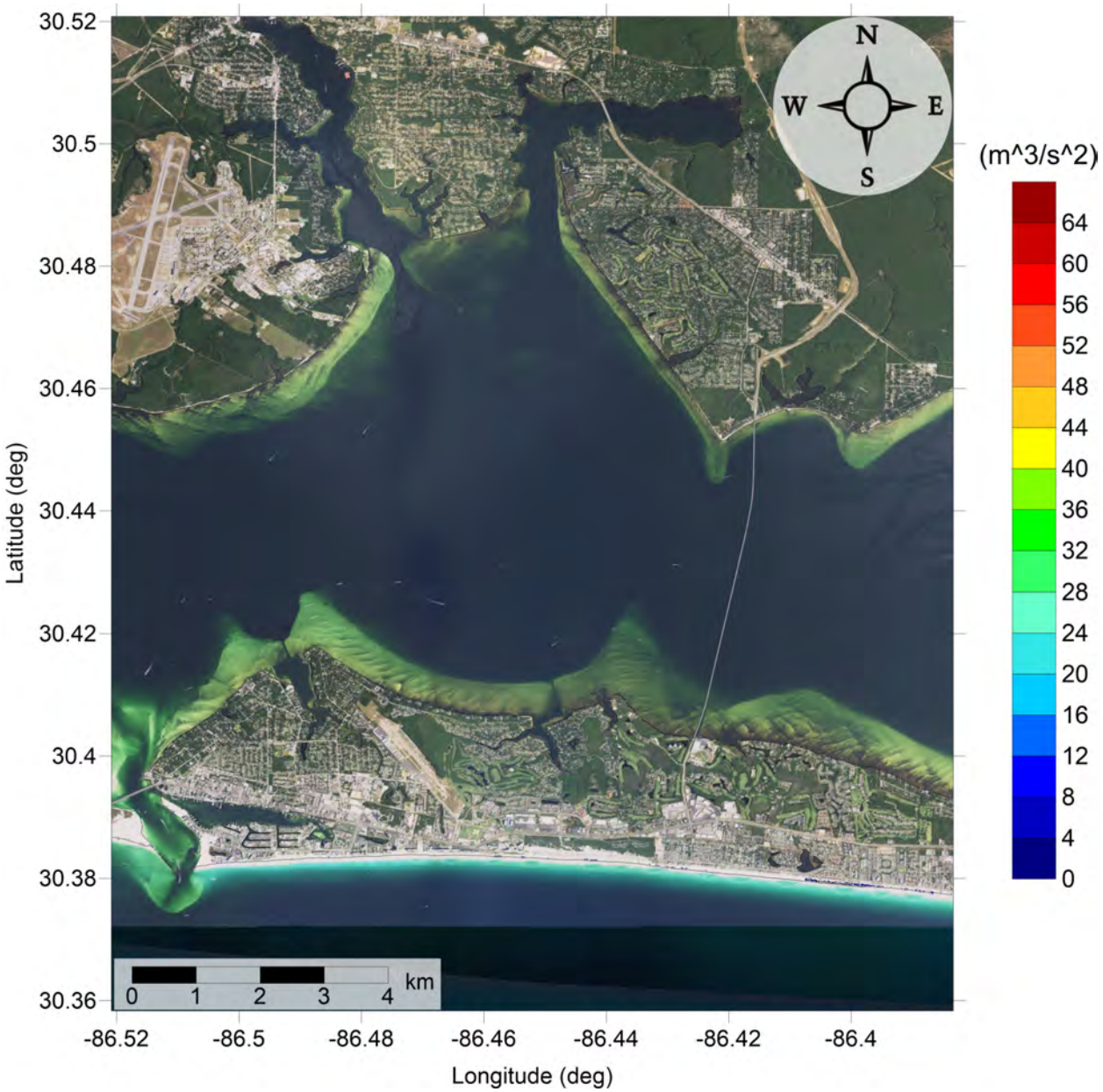


Figure 42: Maximum momentum flux ($m^3/s^2$) caused by the Probabilistic Submarine Landslide B1 in Destin, FL. Arrows represent direction of maximum momentum flux. Contour drawn is the zero-meter contour for land elevation.

## Okaloosa County, FL
## Probabilistic Submarine Landslide B1
## Maximum Inundation Depth

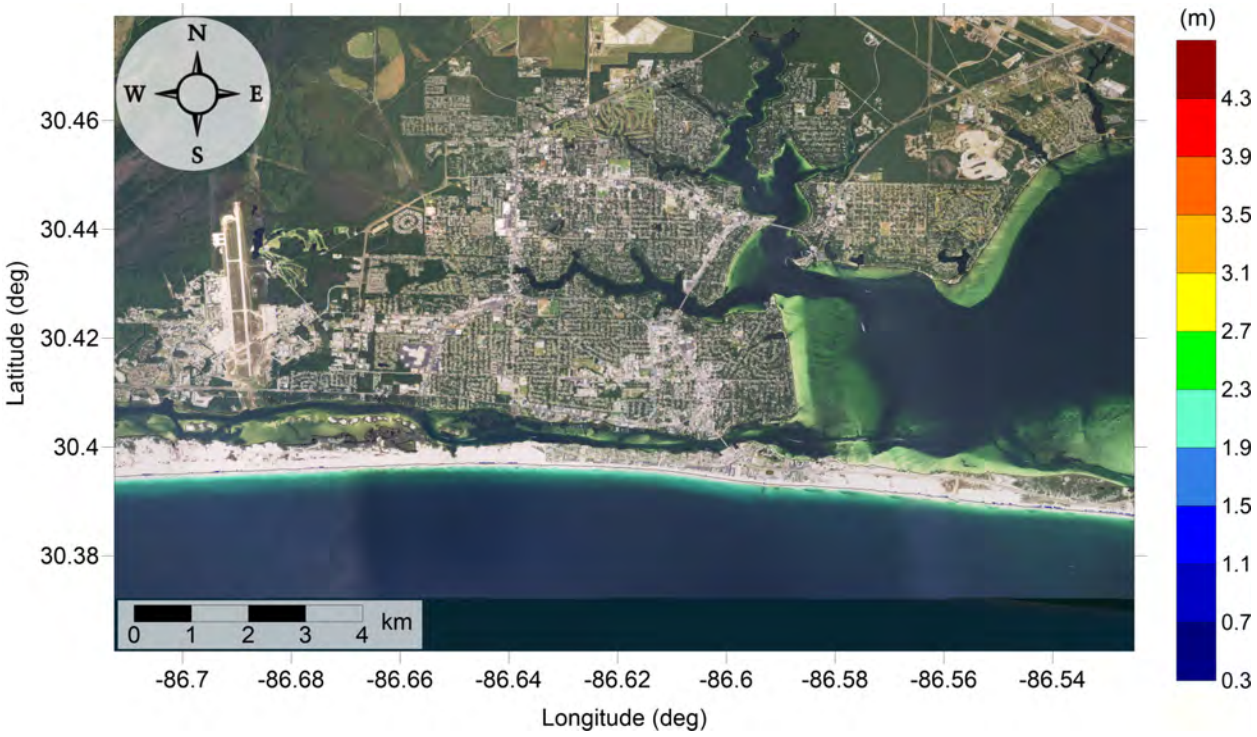


Figure 43: Maximum inundation depth (m) caused by the Probabilistic Submarine Landslide B1 in Okaloosa Island, FL. Contour drawn is the zero-meter contour for land elevation.

**Okaloosa County, FL**
**Probabilistic Submarine Landslide B1**
**Maximum Inundation Depth**

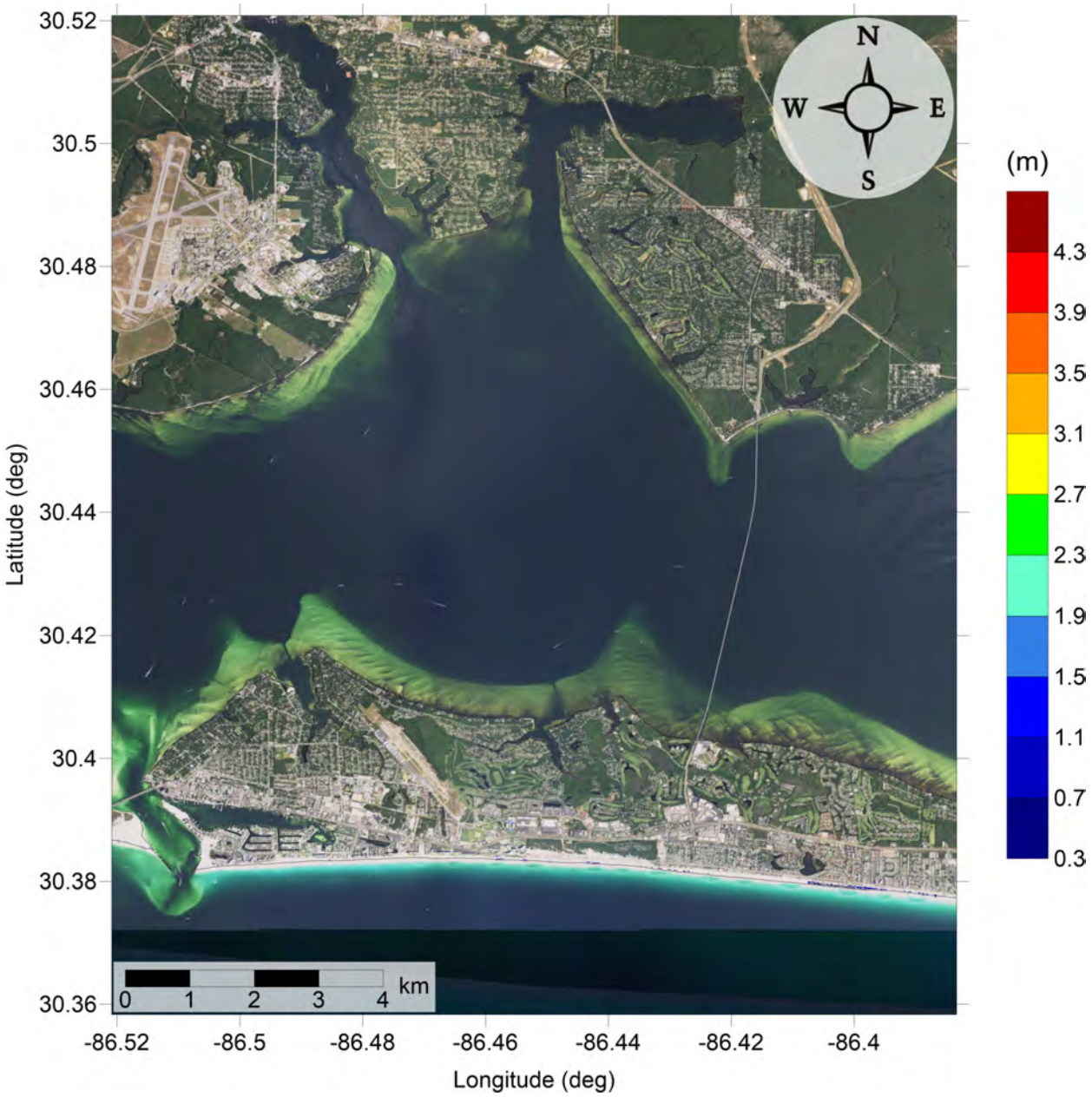


Figure 44: Maximum inundation depth (m) caused by the Probabilistic Submarine Landslide B1 in Destin, FL. Contour drawn is the zero-meter contour for land elevation.

## Okaloosa County, FL
## Probabilistic Submarine Landslide B2
## Maximum Momentum Flux

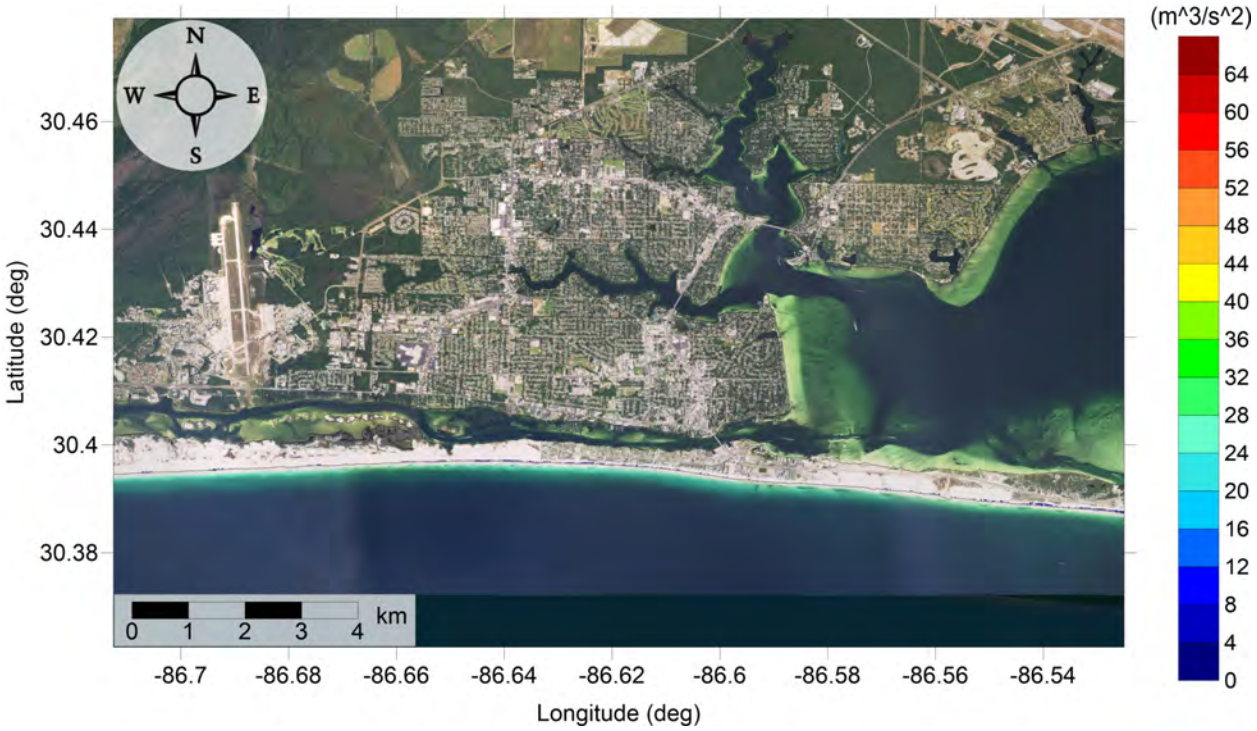


Figure 45: Maximum momentum flux ($m^3/s^2$) caused by the Probabilistic Submarine Landslide B2 in Okaloosa Island, FL. Arrows represent direction of maximum momentum flux. Contour drawn is the zero-meter contour for land elevation.

**Okaloosa County, FL**
**Probabilistic Submarine Landslide B2**
**Maximum Momentum Flux**

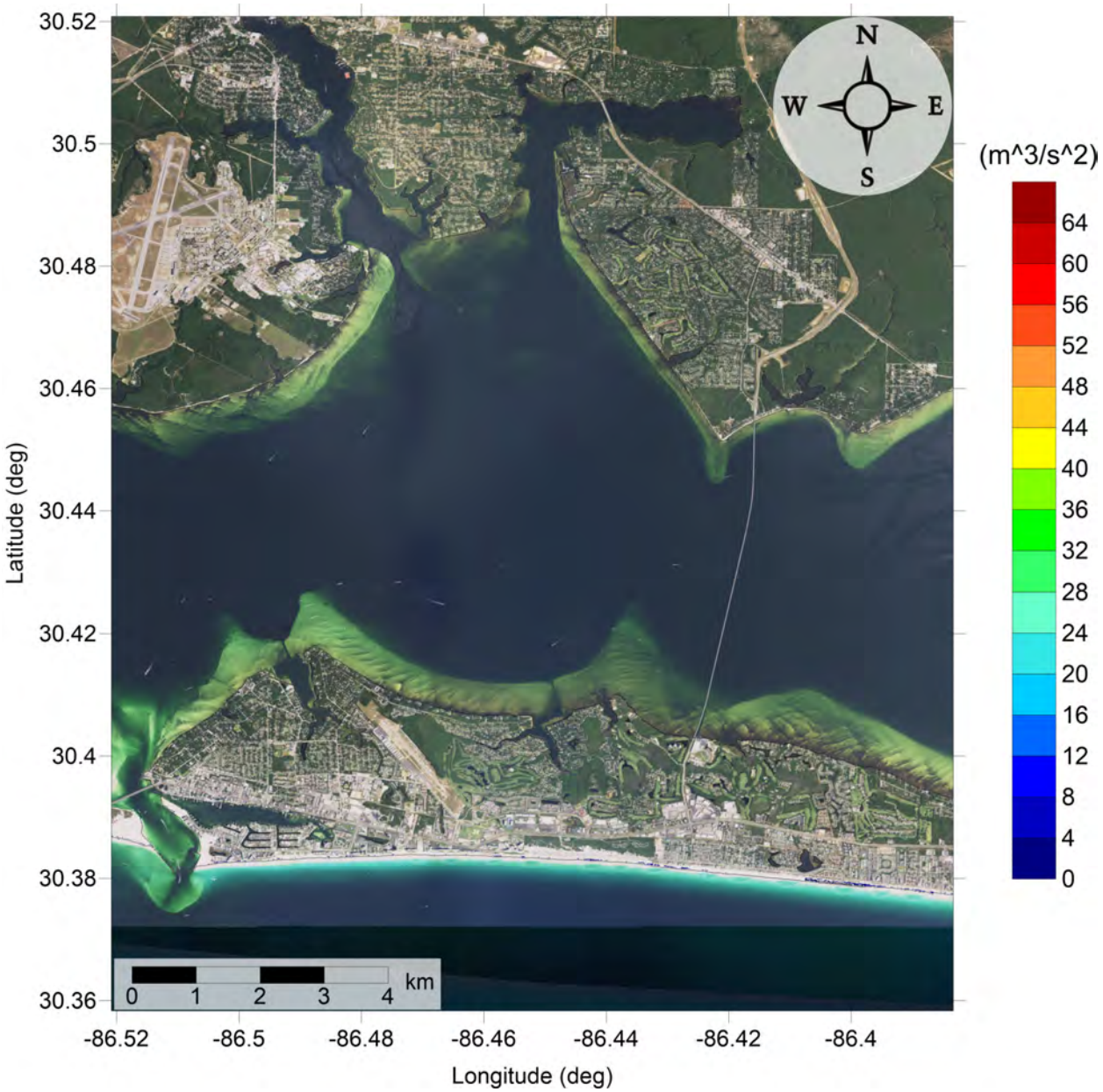


Figure 46: Maximum momentum flux ($m^3/s^2$) caused by the Probabilistic Submarine Landslide B2 in Destin, FL. Arrows represent direction of maximum momentum flux. Contour drawn is the zero-meter contour for land elevation.

## Okaloosa County, FL
## Probabilistic Submarine Landslide B2
## Maximum Inundation Depth


Figure 47: Maximum inundation depth (m) caused by the Probabilistic Submarine Landslide B2 in Okaloosa Island, FL. Contour drawn is the zero-meter contour for land elevation.

**Okaloosa County, FL**
**Probabilistic Submarine Landslide B2**
**Maximum Inundation Depth**

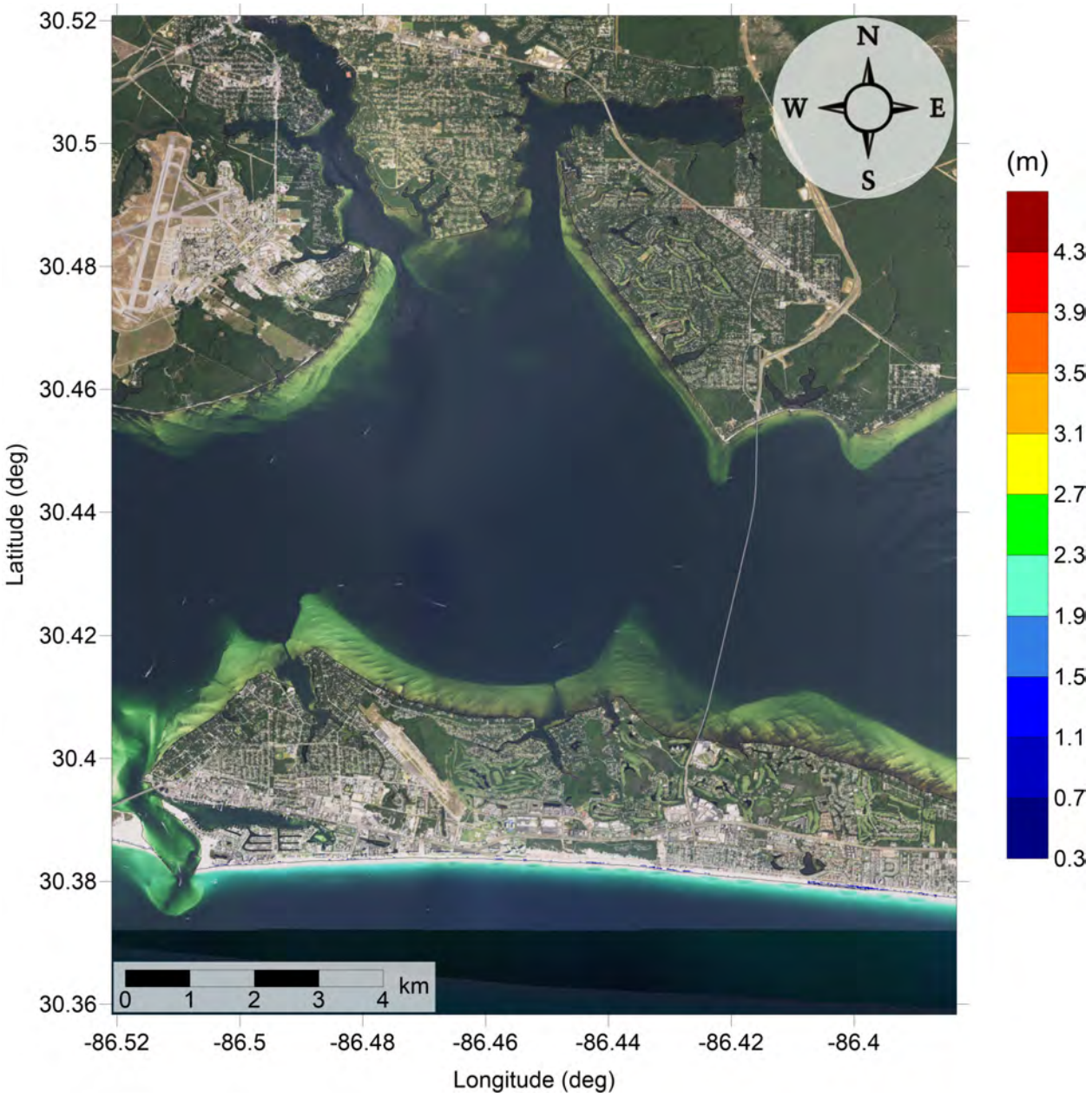


Figure 48: Maximum inundation depth (m) caused by the Probabilistic Submarine Landslide B2 in Destin, FL. Contour drawn is the zero-meter contour for land elevation.

## Okaloosa County, FL
## Mississippi Canyon submarine landslide
## Maximum Momentum Flux

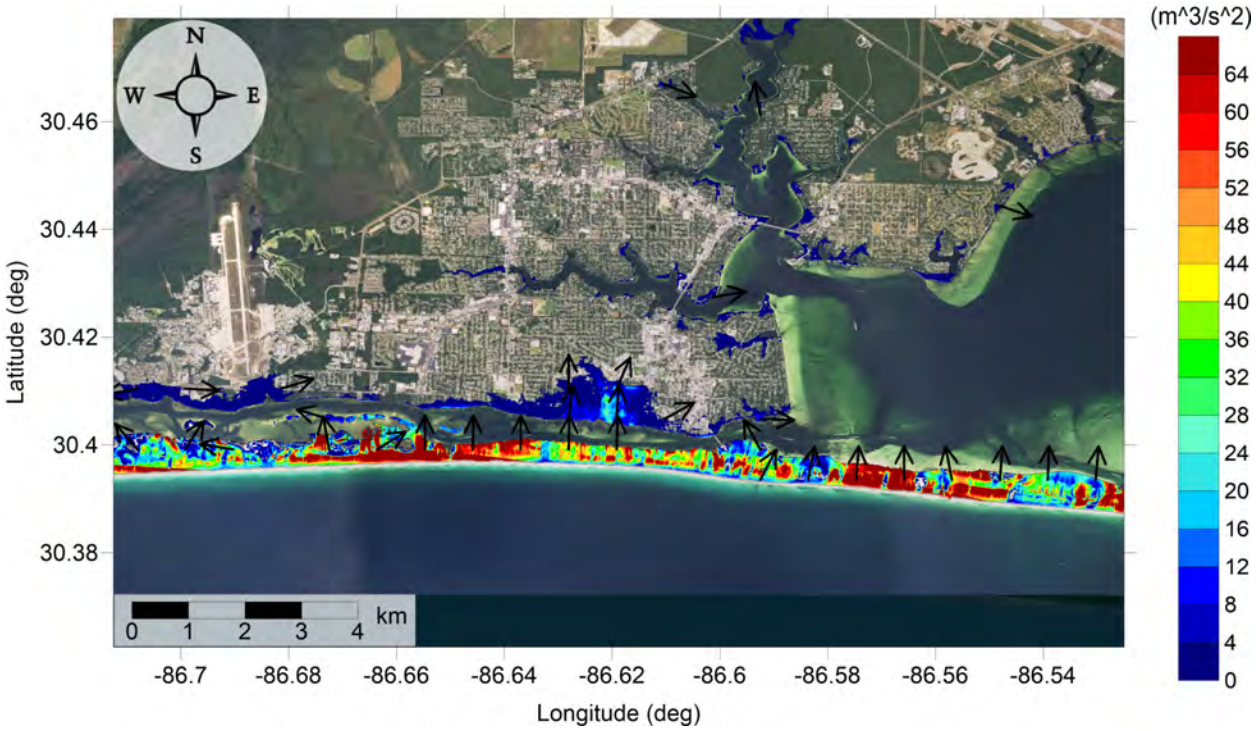


Figure 49: Maximum momentum flux ($m^3/s^2$) caused by the Mississippi Canyon submarine landslide in Okaloosa Island, FL. Arrows represent direction of maximum momentum flux. Contour drawn is the zero-meter contour for land elevation.

**Okaloosa County, FL**
**Mississippi Canyon submarine landslide**
**Maximum Momentum Flux**

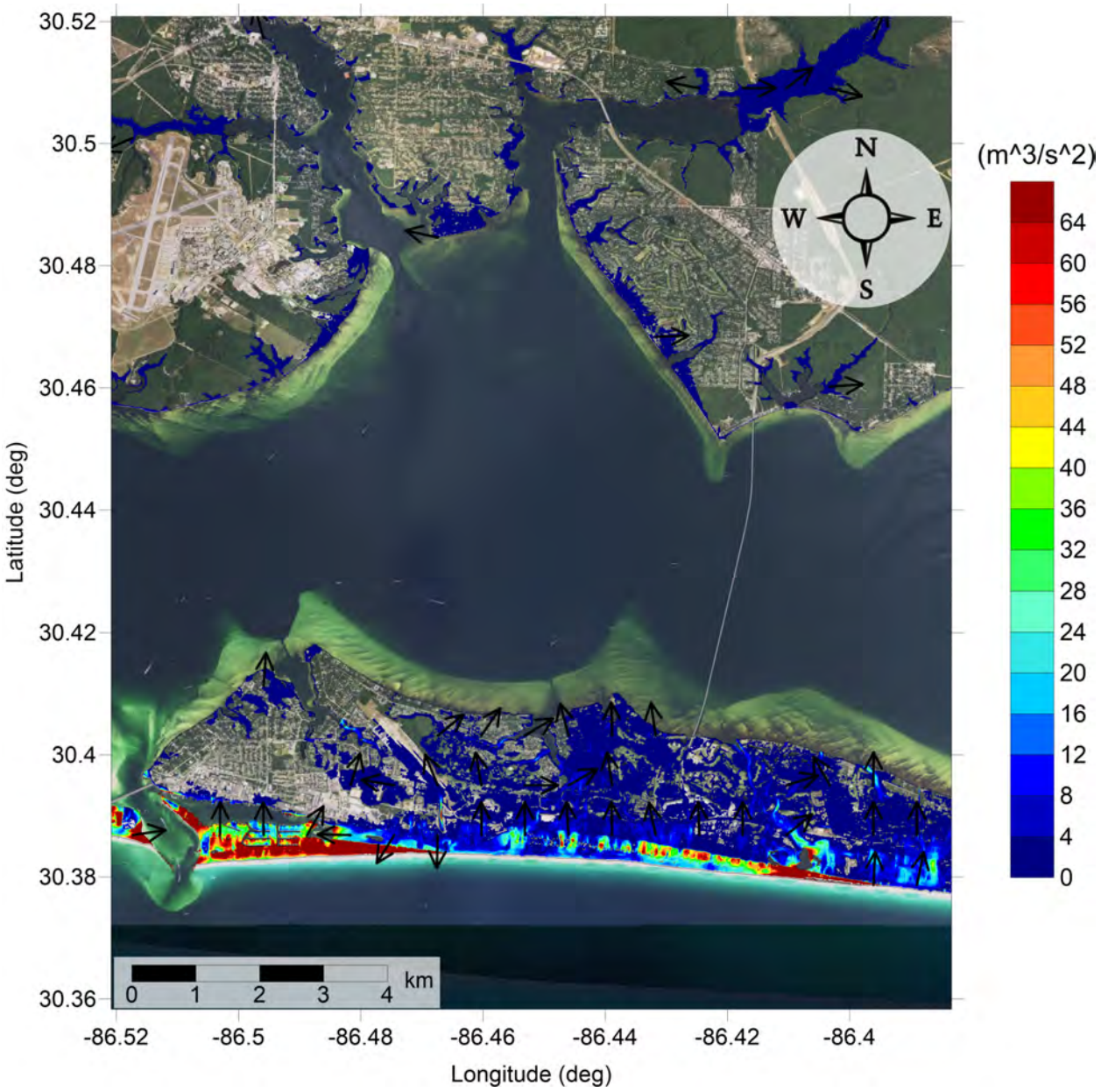


Figure 50: Maximum momentum flux ($m^3/s^2$) caused by the Mississippi Canyon submarine landslide in Destin, FL. Arrows represent direction of maximum momentum flux. Contour drawn is the zero-meter contour for land elevation.

## Okaloosa County, FL
## Mississippi Canyon submarine landslide
## Maximum Inundation Depth

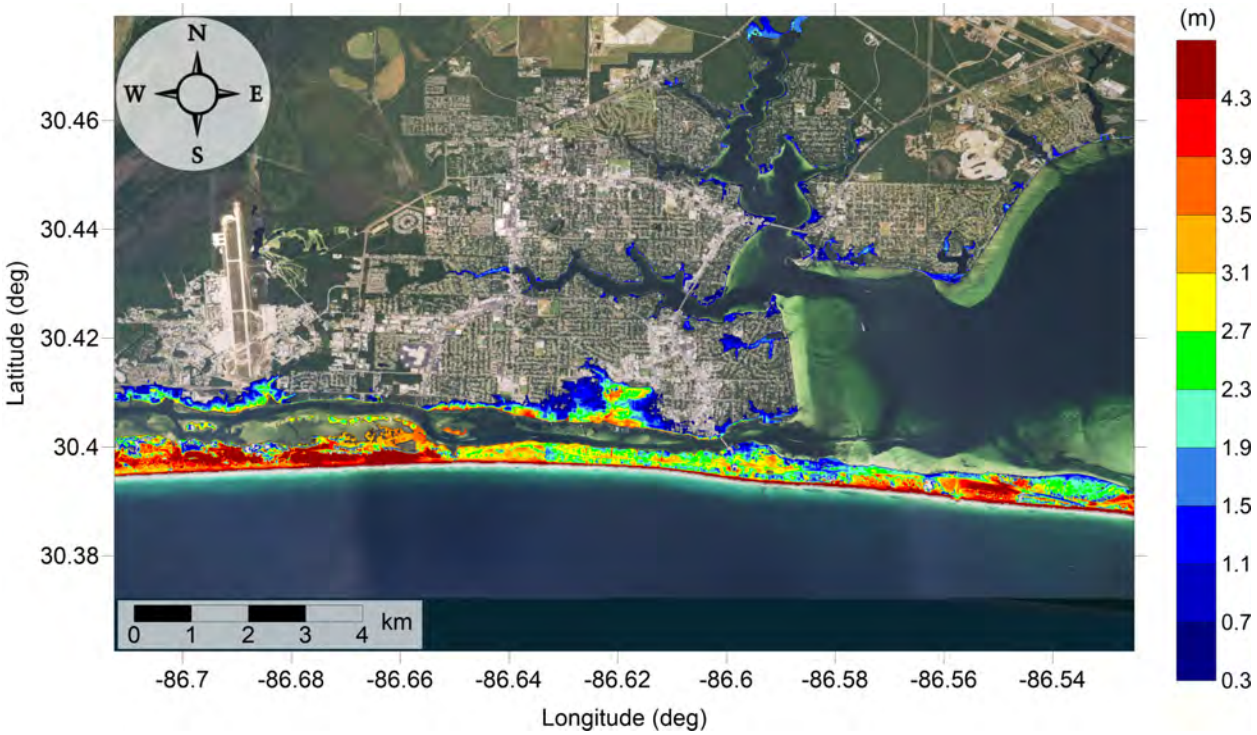


Figure 51: Maximum inundation depth (m) caused by the Mississippi Canyon submarine landslide in Okaloosa Island, FL. Contour drawn is the zero-meter contour for land elevation.

**Okaloosa County, FL**
**Mississippi Canyon submarine landslide**
**Maximum Inundation Depth**

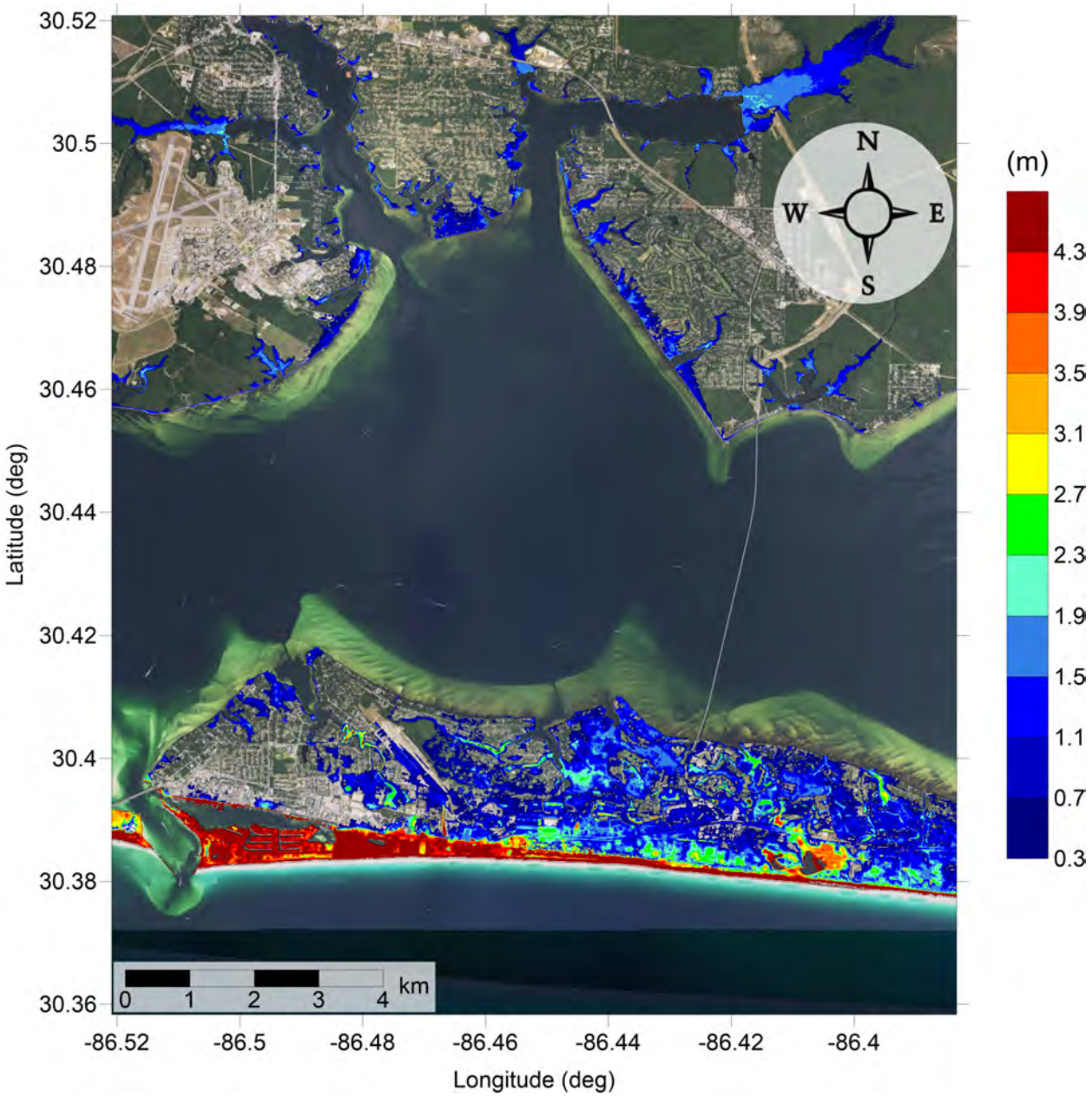


Figure 52: Maximum inundation depth (m) caused by the Mississippi Canyon submarine landslide in Destin, FL. Contour drawn is the zero-meter contour for land elevation.

## Okaloosa County, FL
## Probabilistic Submarine Landslide C
## Maximum Momentum Flux

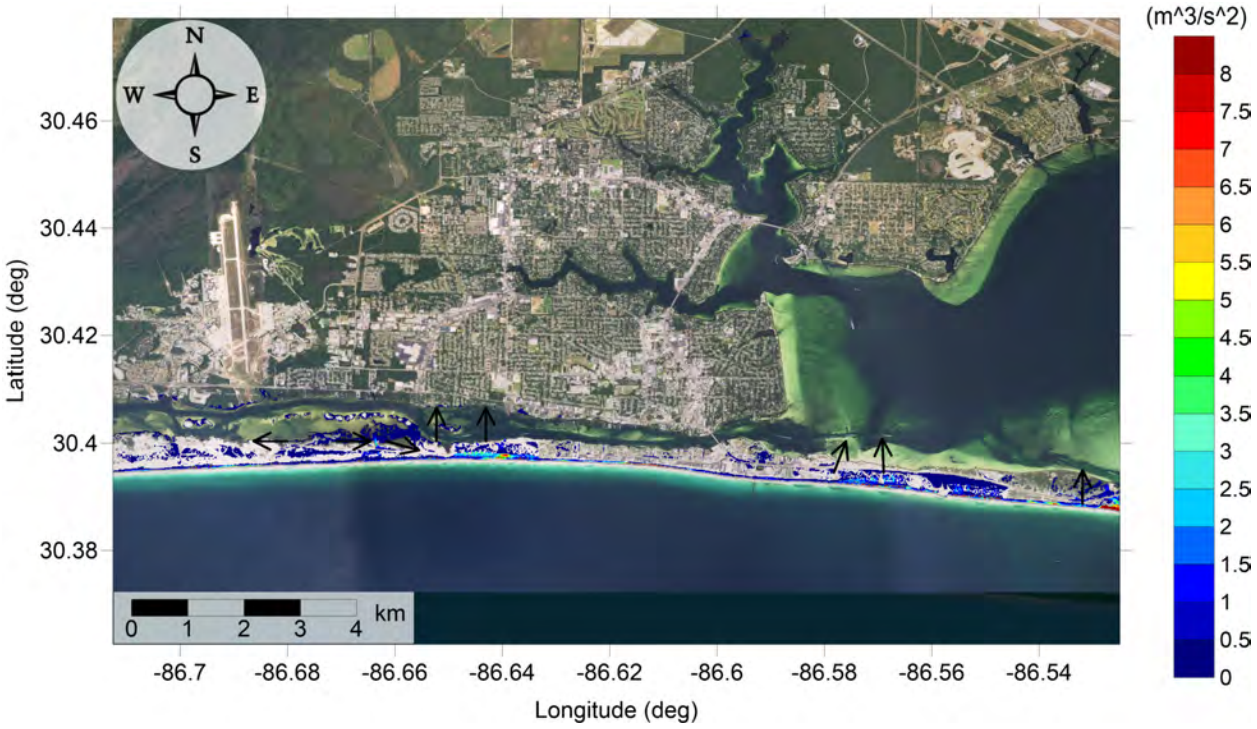


Figure 53: Maximum momentum flux ($m^3/s^2$) caused by the Probabilistic Submarine Landslide C in Okaloosa Island, FL. Arrows represent direction of maximum momentum flux. Contour drawn is the zero-meter contour for land elevation.

**Okaloosa County, FL**
**Probabilistic Submarine Landslide C**
**Maximum Momentum Flux**

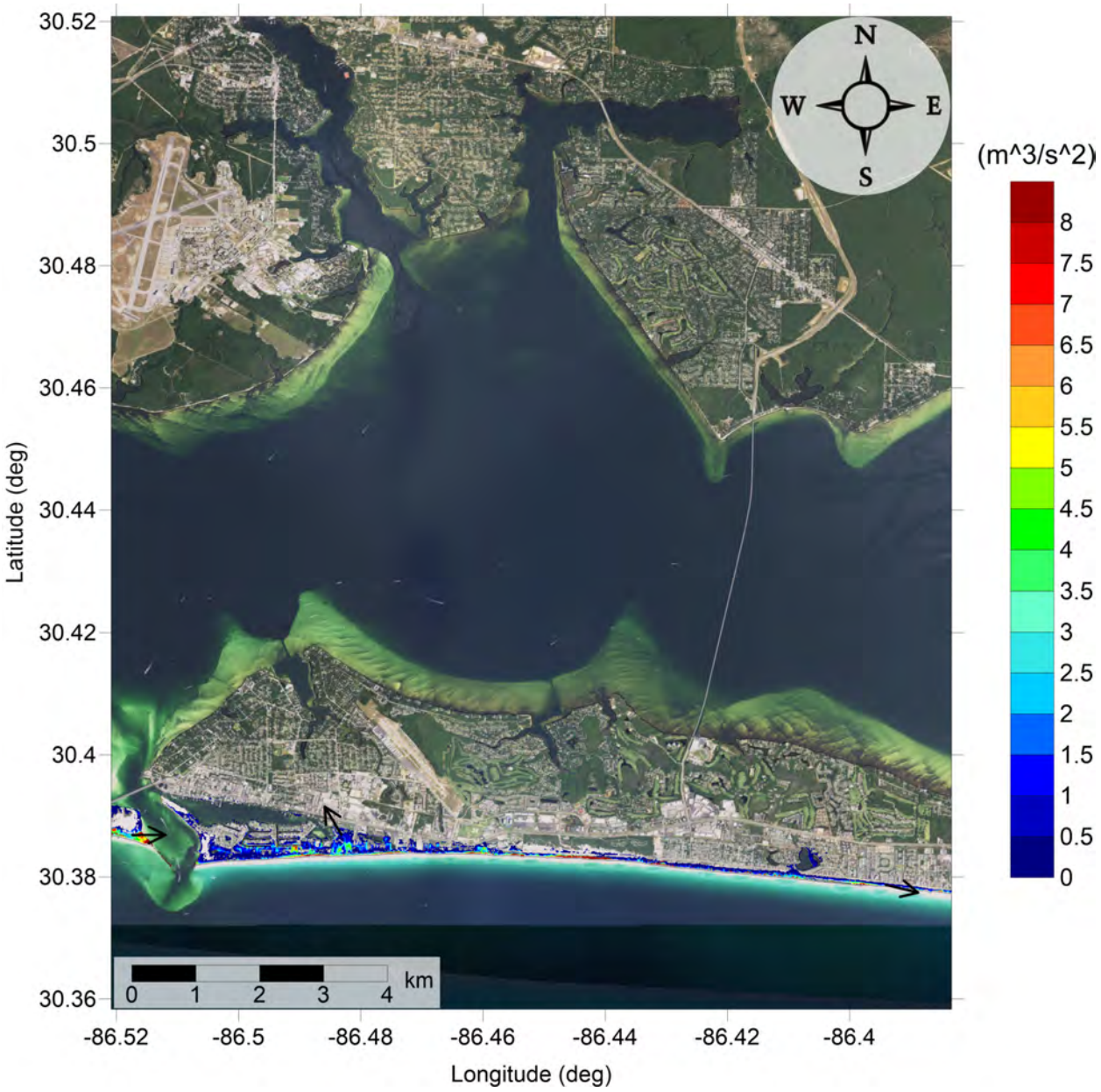


Figure 54: Maximum momentum flux ($m^3/s^2$) caused by the Probabilistic Submarine Landslide C in Destin, FL. Arrows represent direction of maximum momentum flux. Contour drawn is the zero-meter contour for land elevation.

## Okaloosa County, FL
## Probabilistic Submarine Landslide C
## Maximum Inundation Depth

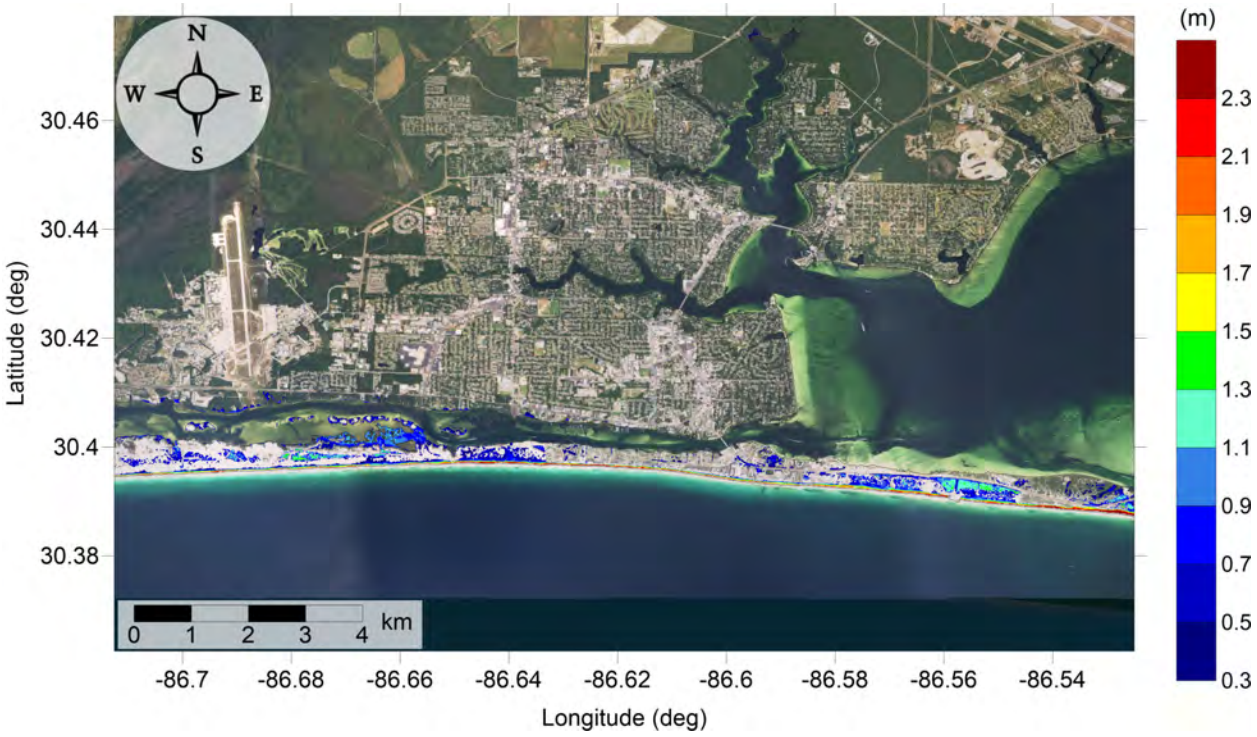


Figure 55: Maximum inundation depth (m) caused by the Probabilistic Submarine Landslide C in Okaloosa Island, FL. Contour drawn is the zero-meter contour for land elevation.

**Okaloosa County, FL**
**Probabilistic Submarine Landslide C**
**Maximum Inundation Depth**

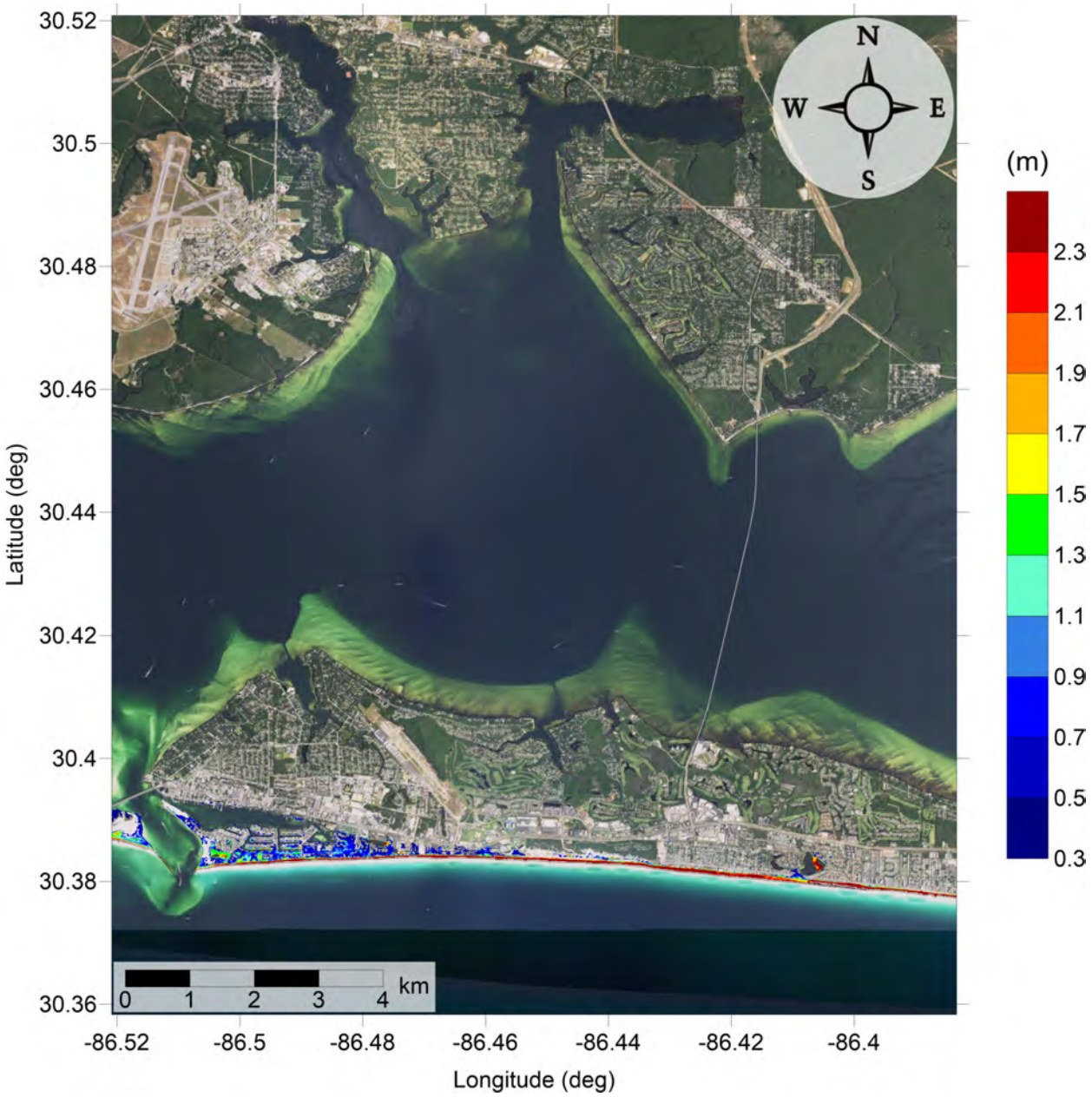


Figure 56: Maximum inundation depth (m) caused by the Probabilistic Submarine Landslide C in Destin, FL. Contour drawn is the zero-meter contour for land elevation.

## Okaloosa County, FL
## West Florida submarine landslide
## Maximum Momentum Flux

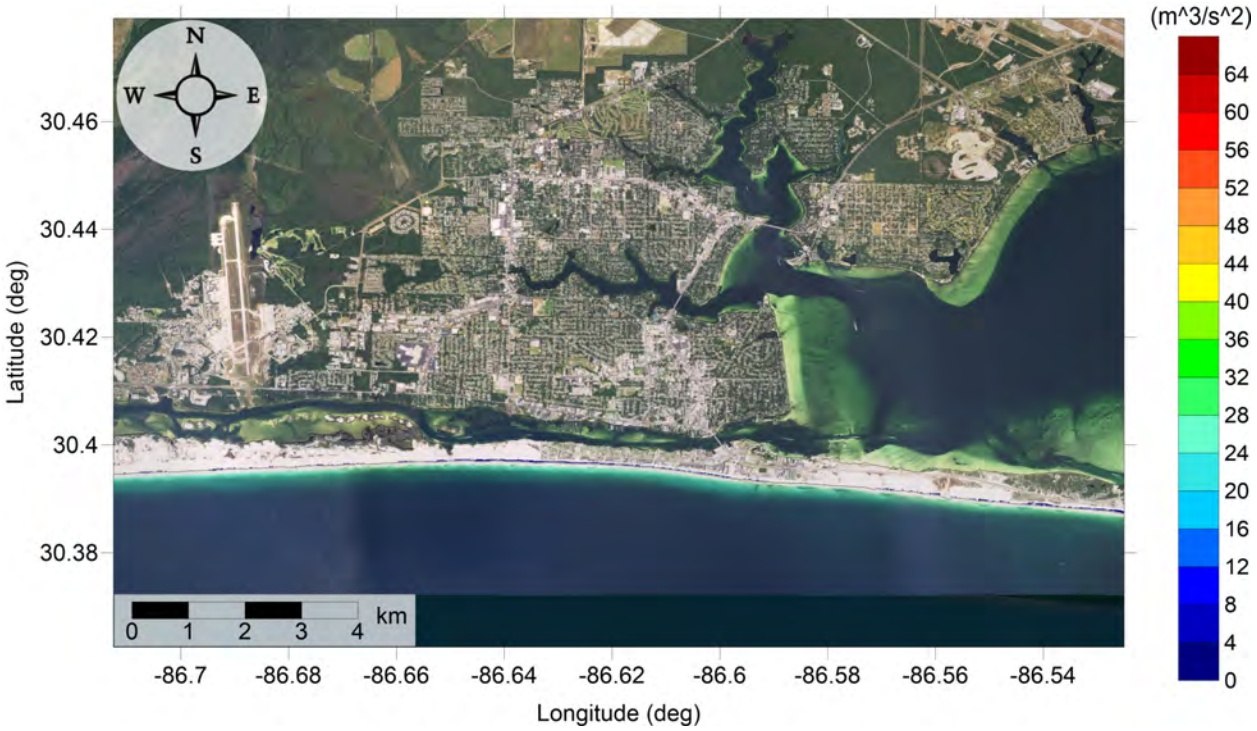


Figure 57: Maximum momentum flux ($m^3/s^2$) caused by the West Florida submarine landslide in Okaloosa Island, FL. Arrows represent direction of maximum momentum flux. Contour drawn is the zero-meter contour for land elevation.

**Okaloosa County, FL**
**West Florida submarine landslide**
**Maximum Momentum Flux**

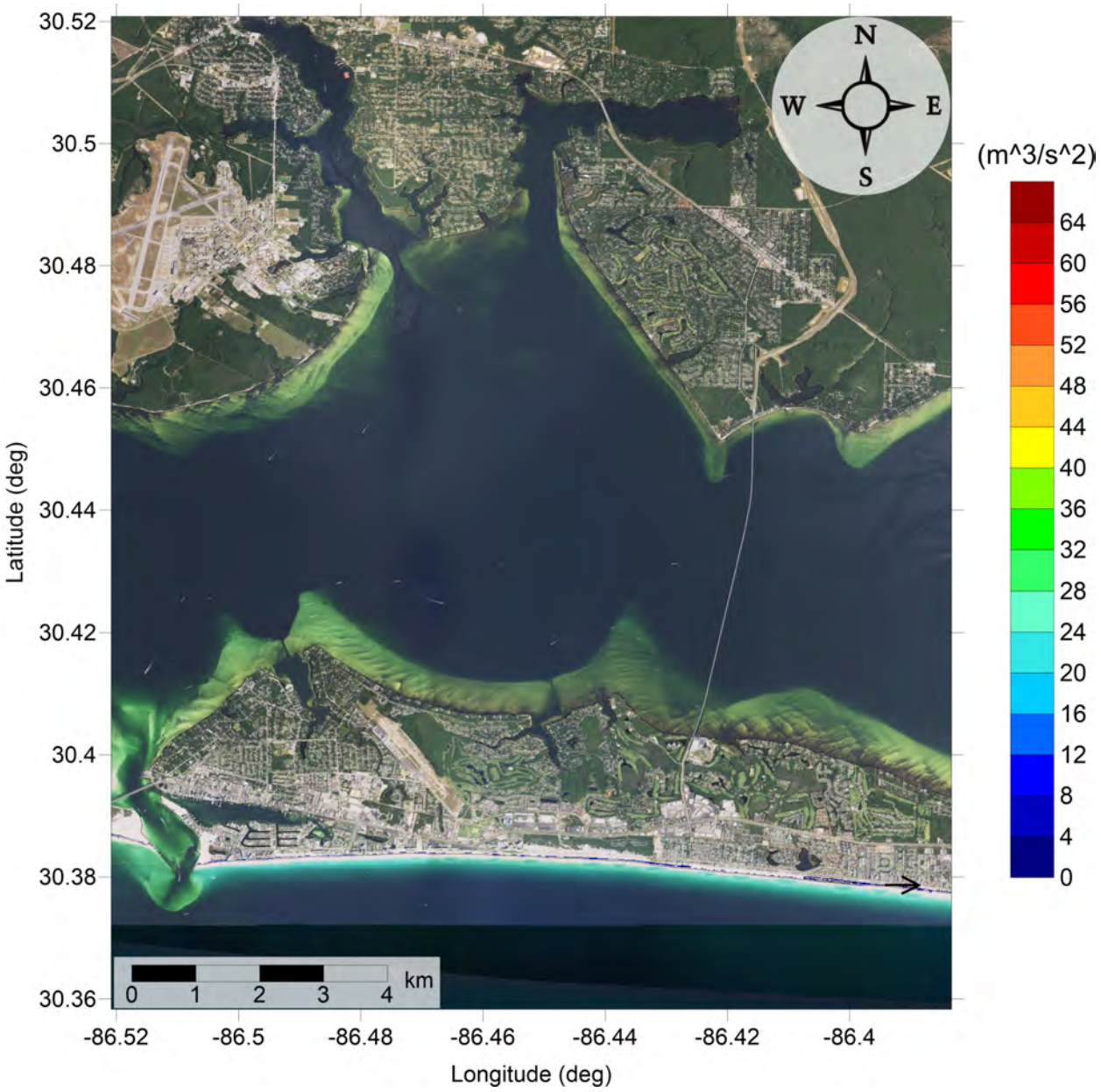


Figure 58: Maximum momentum flux ($m^3/s^2$) caused by the West Florida submarine landslide in Destin, FL. Arrows represent direction of maximum momentum flux. Contour drawn is the zero-meter contour for land elevation.

## Okaloosa County, FL
## West Florida submarine landslide
## Maximum Inundation Depth


Figure 59: Maximum inundation depth (m) caused by the West Florida submarine landslide in Okaloosa Island, FL. Contour drawn is the zero-meter contour for land elevation.

**Okaloosa County, FL**
**West Florida submarine landslide**
**Maximum Inundation Depth**

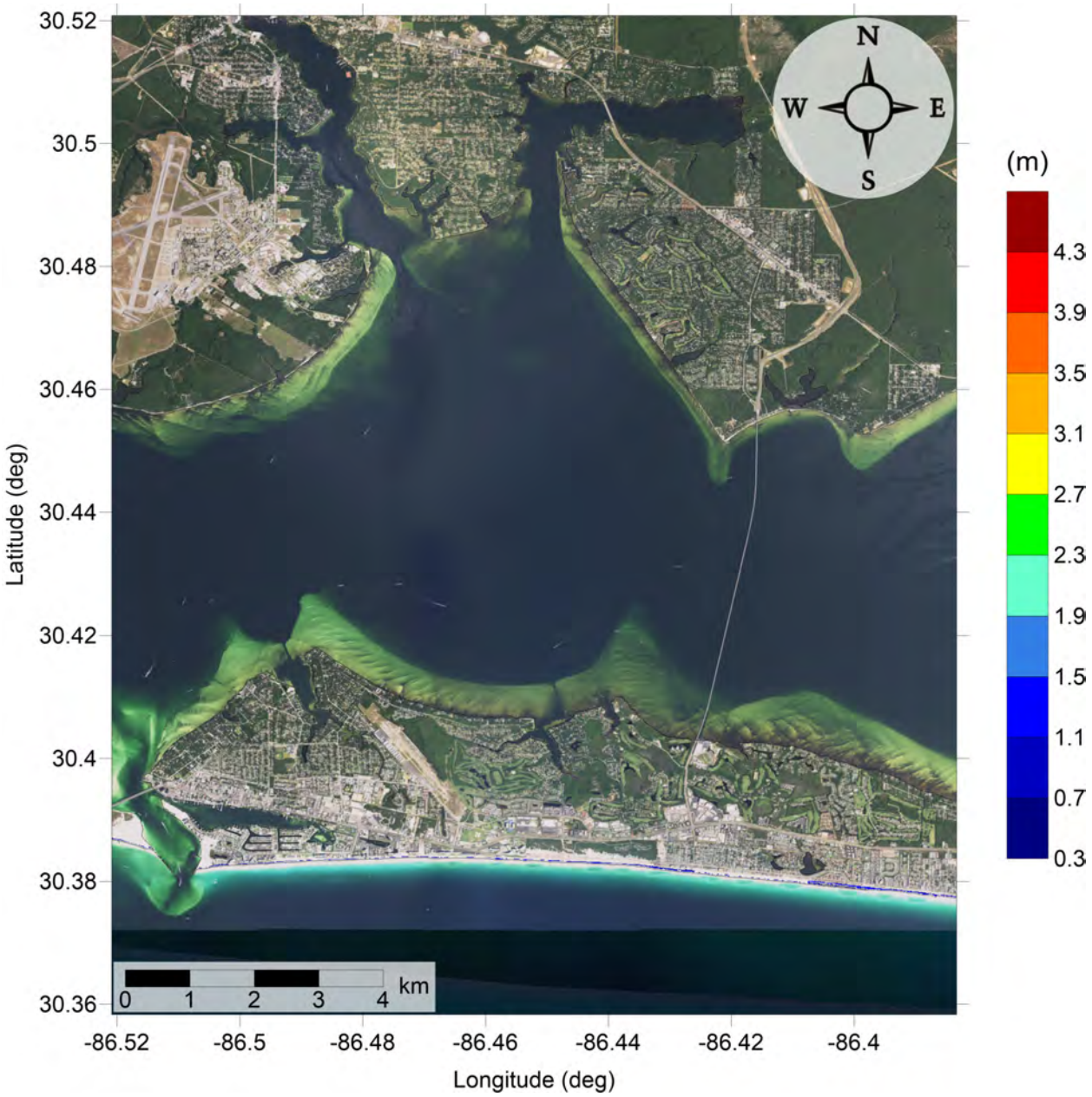


Figure 60: Maximum inundation depth (m) caused by the West Florida submarine landslide in Destin, FL. Contour drawn is the zero-meter contour for land elevation.

## Okaloosa County, FL
## All Sources
## Maximum of Maximum Inundation Depth

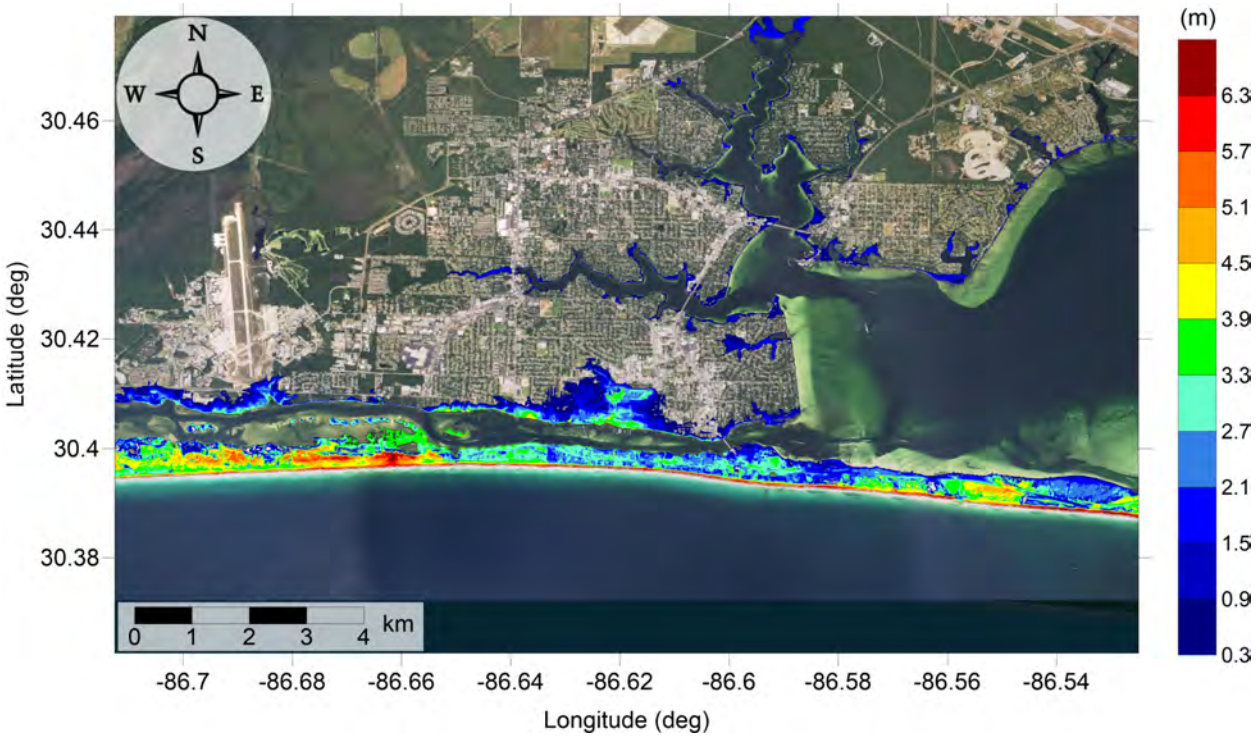


Figure 61: Maximum of maximums inundation depth (m) in Okaloosa Island, calculated as the maximum inundation depth in each grid cell from an ensemble of all tsunami sources considered. Contour drawn is the zero-meter contour for land elevation.

## Okaloosa County, FL
## All Sources
## Maximum Inundation Depth by Source

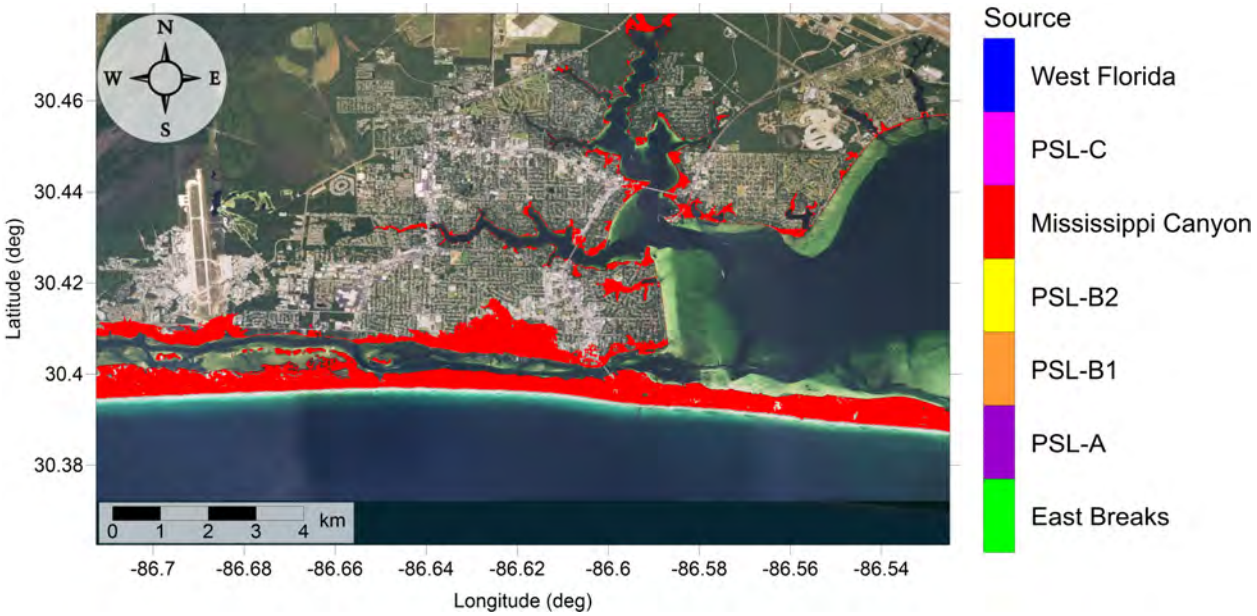


Figure 62: Indication of the tsunami source which causes the maximum of maximums inundation depth (m) in each grid cell from an ensemble of all tsunami sources in Okaloosa Island, FL. Contour drawn is the zero-meter contour for land elevation.

**Okaloosa County, FL**
**All Sources**
**Maximum of Maximum Inundation Depth**

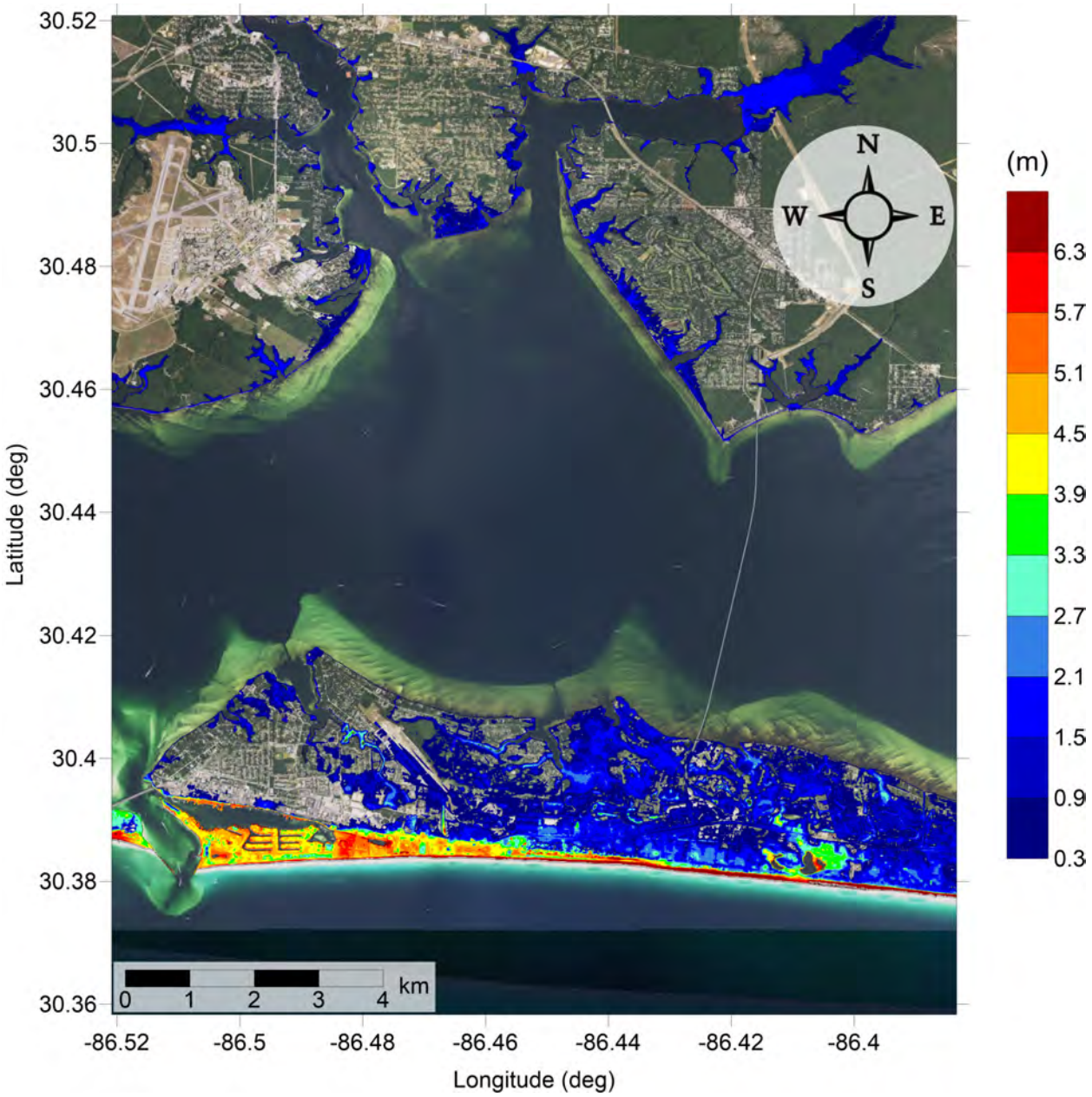


Figure 63: Maximum of maximums inundation depth (m) in Destin, FL, calculated as the maximum inundation depth in each grid cell from an ensemble of all tsunami sources considered. Contour drawn is the zero-meter contour for land elevation.

## Okaloosa County, FL
## All Sources
## Maximum Inundation Depth by Source

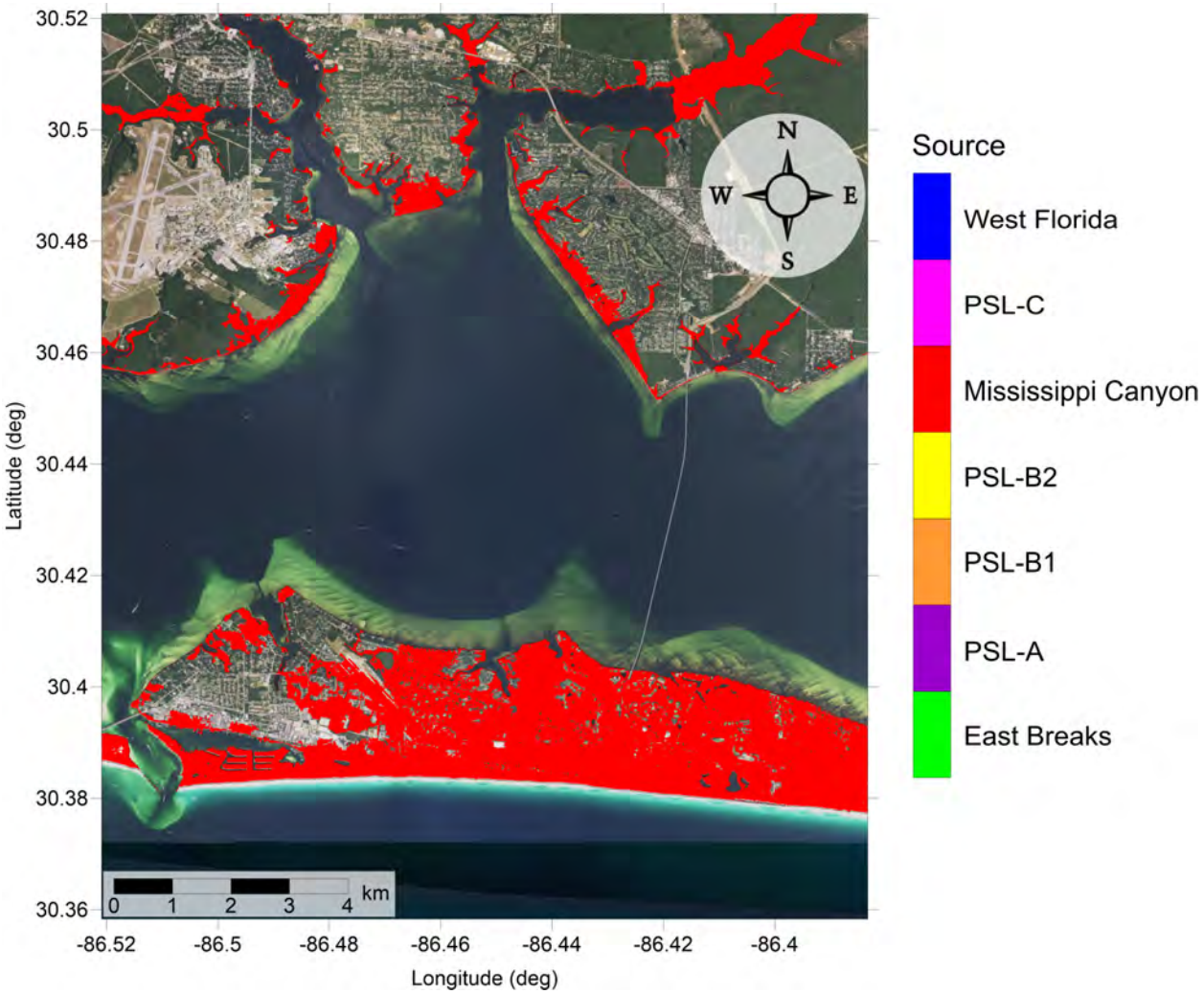


Figure 64: Indication of the tsunami source which causes the maximum of maximums inundation depth (m) in each grid cell from an ensemble of all tsunami sources in Destin, FL. Contour drawn is the zero-meter contour for land elevation.

## 3.4 Santa Rosa County, FL

Table 4: Maximum tsunami wave amplitude and corresponding arrival time after landslide failure at Santa Rosa County, FL numerical wave gauge: 30°14'45.00"N, 87°12'30.00"W (the same as the Pensacola gauge, Fig. 1), approximate water depth 21 m.

| Tsunami Source | Maximum Wave Amplitude (m) | Arrival Time After Landslide Failure (hr) |
|---|---|---|
| East Breaks | 0.28 | 2.9 |
| PSL-A | 0.41 | 2.5 |
| PSL-B1 | 0.44 | 1.7 |
| PSL-B2 | 0.37 | 1.9 |
| Mississippi Canyon | 4.09 | 1.2 |
| PSL-C | 1.71 | 1.7 |
| West Florida | 0.43 | 1.8 |

## Santa Rosa County, FL
## East Breaks submarine landslide
## Maximum Momentum Flux

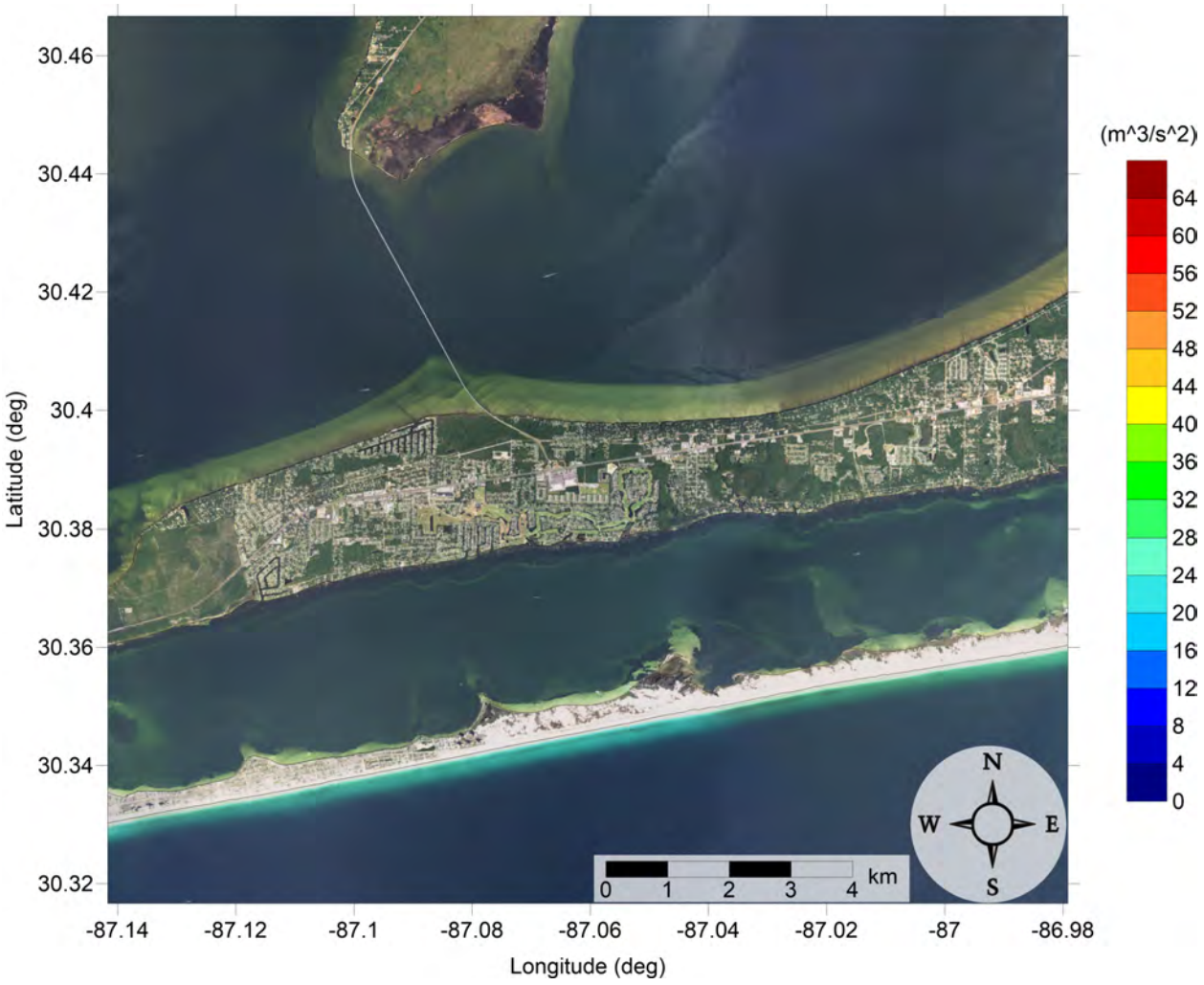


Figure 65: Maximum momentum flux ($m^3/s^2$) caused by the East Breaks submarine landslide in East Gulf Breeze, FL. Arrows represent direction of maximum momentum flux. Contour drawn is the zero-meter contour for land elevation.

**Santa Rosa County, FL**
**East Breaks submarine landslide**
**Maximum Momentum Flux**

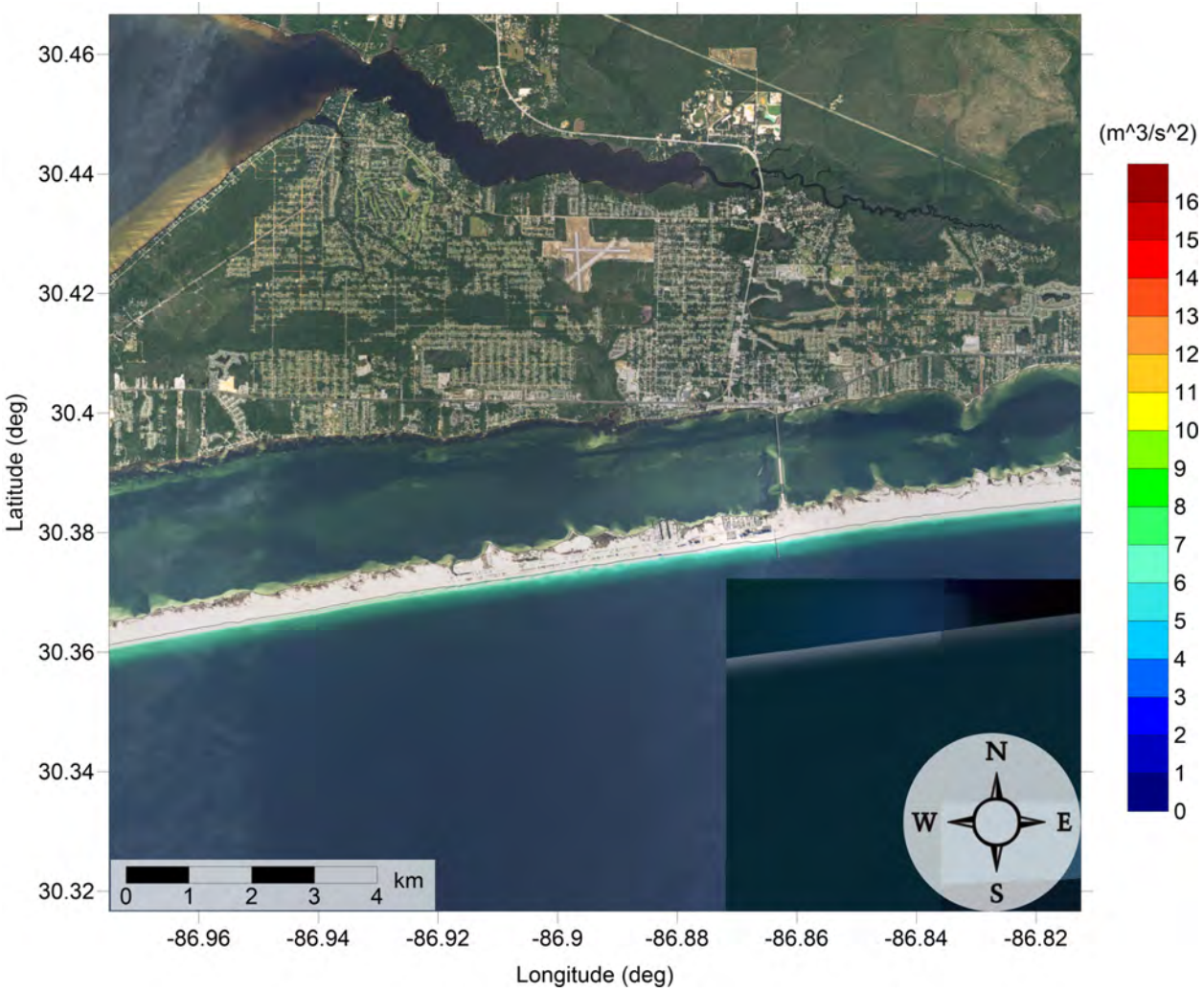


Figure 66: Maximum momentum flux ($m^3/s^2$) caused by the East Breaks submarine landslide in Navarre, FL. Arrows represent direction of maximum momentum flux. Contour drawn is the zero-meter contour for land elevation.

**Santa Rosa County, FL**
**East Breaks submarine landslide**
**Maximum Inundation Depth**


Figure 67: Maximum inundation depth (m) caused by the East Breaks submarine landslide in East Gulf Breeze, FL. Contour drawn is the zero-meter contour for land elevation.

## Santa Rosa County, FL
## East Breaks submarine landslide
## Maximum Inundation Depth

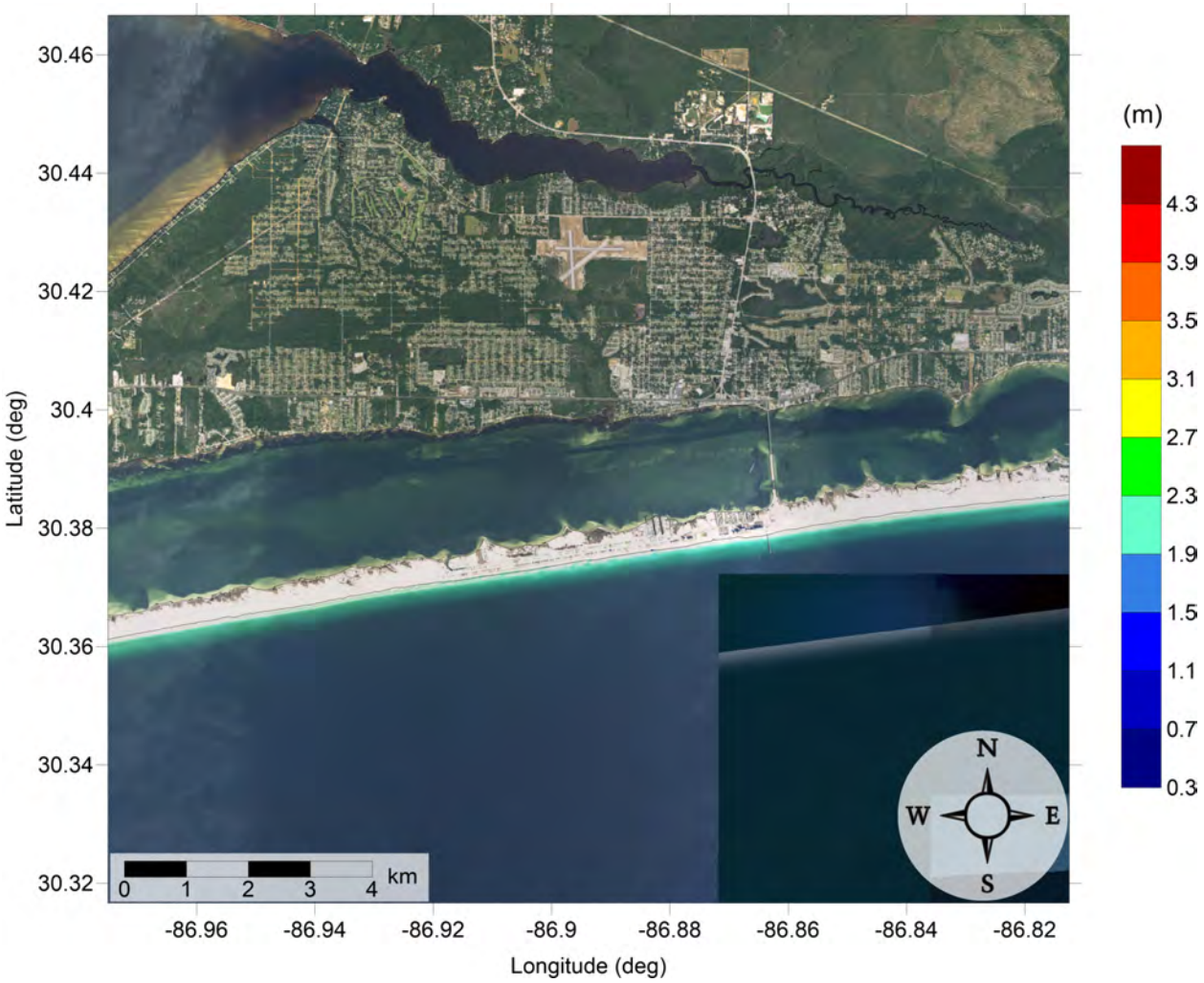


Figure 68: Maximum inundation depth (m) caused by the East Breaks submarine landslide in Navarre, FL. Contour drawn is the zero-meter contour for land elevation.

## Santa Rosa County, FL
## Probabilistic Submarine Landslide A
## Maximum Momentum Flux

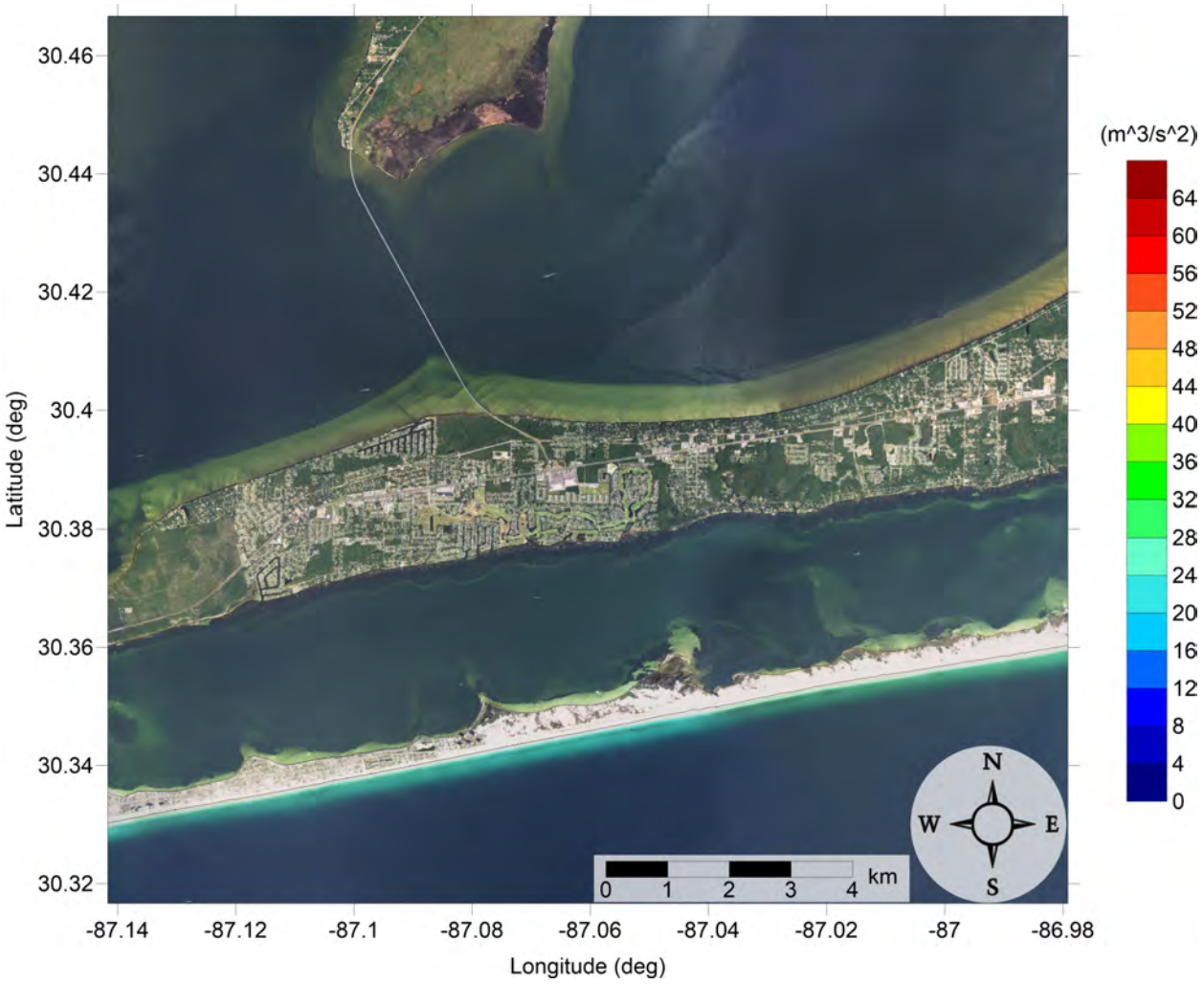


Figure 69: Maximum momentum flux ($m^3/s^2$) caused by the Probabilistic Submarine Landslide A in East Gulf Breeze, FL. Arrows represent direction of maximum momentum flux. Contour drawn is the zero-meter contour for land elevation.

## Santa Rosa County, FL
## Probabilistic Submarine Landslide A
## Maximum Momentum Flux

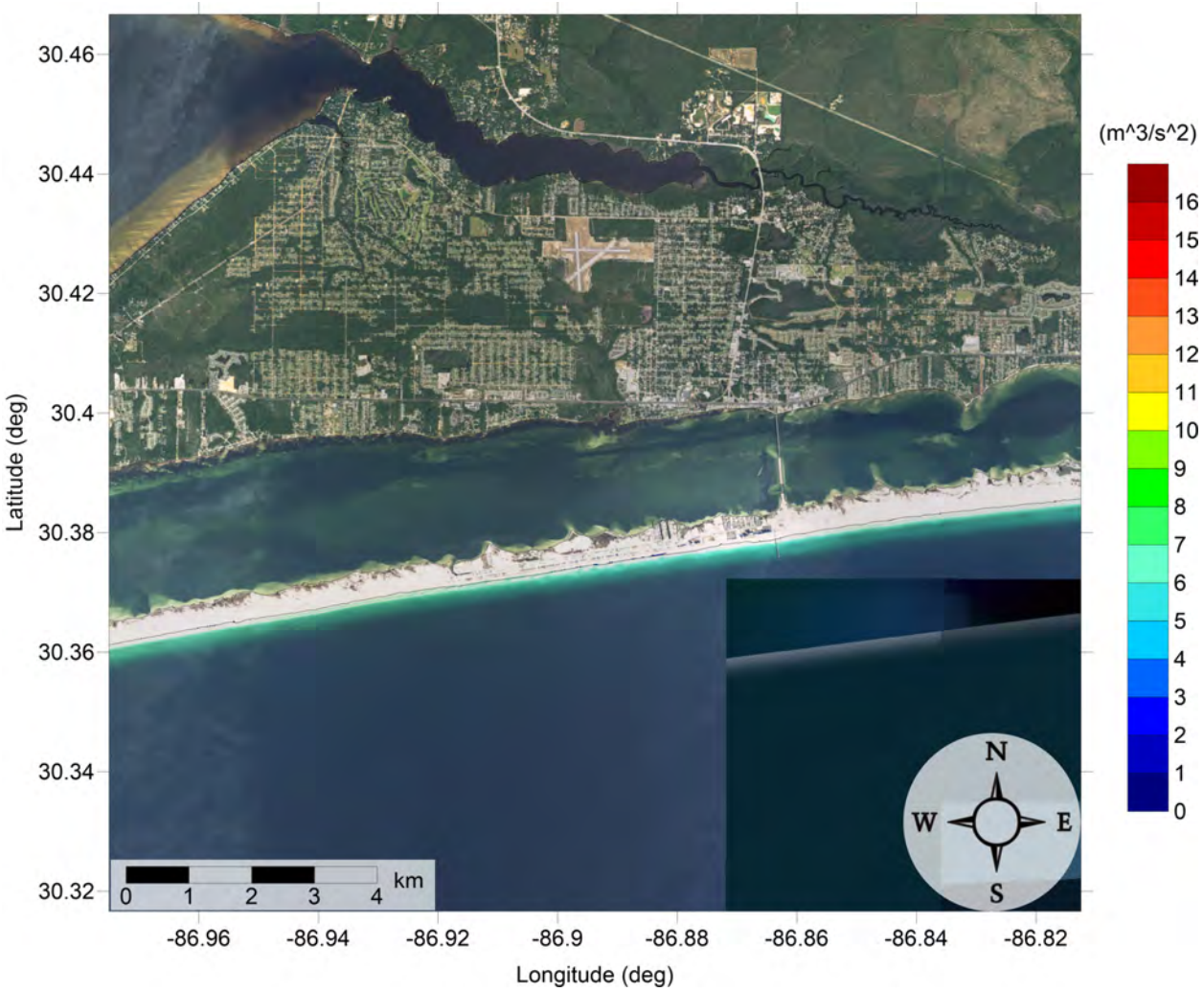


Figure 70: Maximum momentum flux ($m^3/s^2$) caused by the Probabilistic Submarine Landslide A in Navarre, FL. Arrows represent direction of maximum momentum flux. Contour drawn is the zero-meter contour for land elevation.

## Santa Rosa County, FL
## Probabilistic Submarine Landslide A
## Maximum Inundation Depth


Figure 71: Maximum inundation depth (m) caused by the Probabilistic Submarine Landslide A in East Gulf Breeze, FL. Contour drawn is the zero-meter contour for land elevation.

## Santa Rosa County, FL
## Probabilistic Submarine Landslide A
## Maximum Inundation Depth

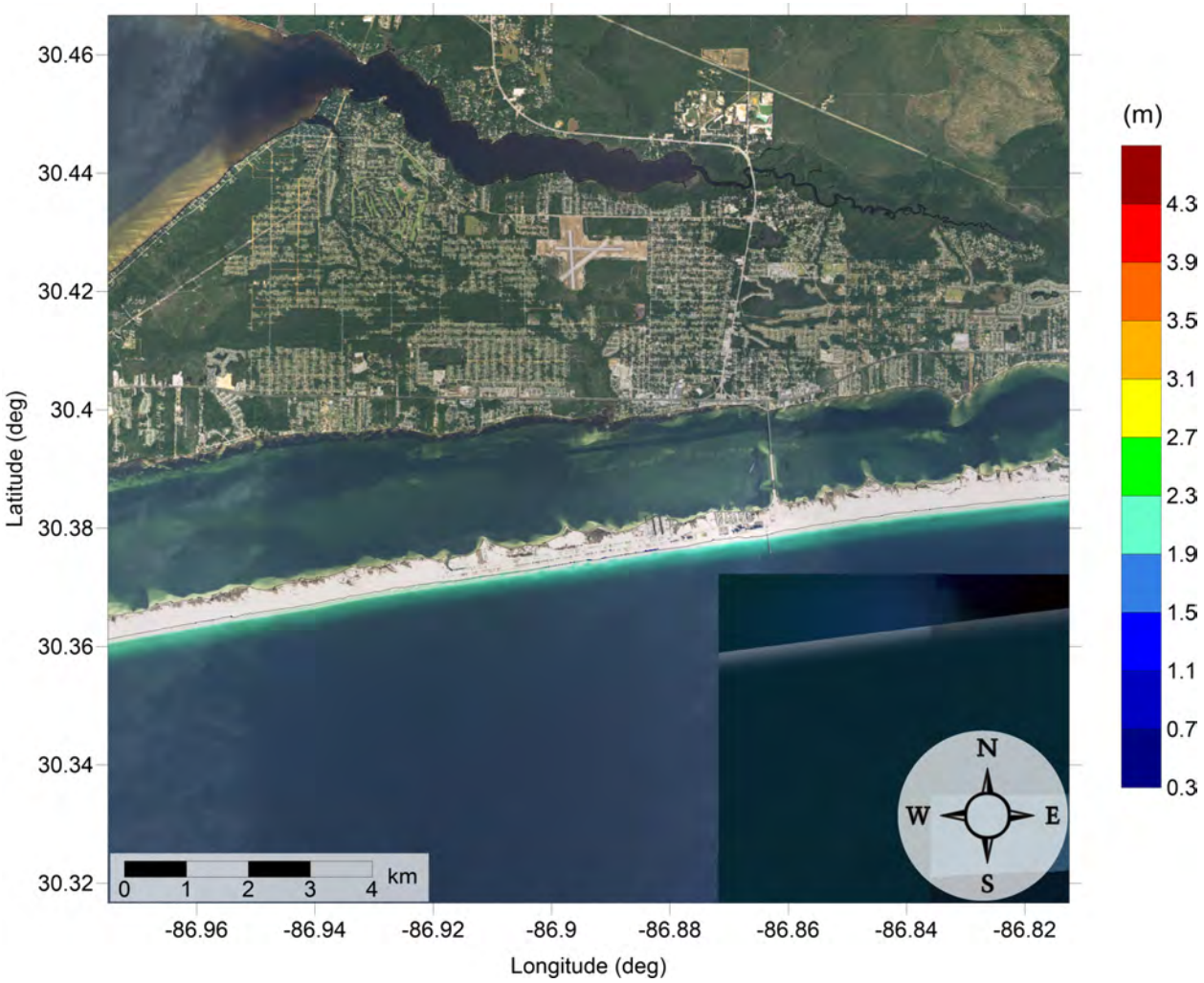


Figure 72: Maximum inundation depth (m) caused by the Probabilistic Submarine Landslide A in Navarre, FL. Contour drawn is the zero-meter contour for land elevation.

## Santa Rosa County, FL
## Probabilistic Submarine Landslide B1
## Maximum Momentum Flux


Figure 73: Maximum momentum flux ($m^3/s^2$) caused by the Probabilistic Submarine Landslide B1 in East Gulf Breeze, FL. Arrows represent direction of maximum momentum flux. Contour drawn is the zero-meter contour for land elevation.

## Santa Rosa County, FL
## Probabilistic Submarine Landslide B1
## Maximum Momentum Flux

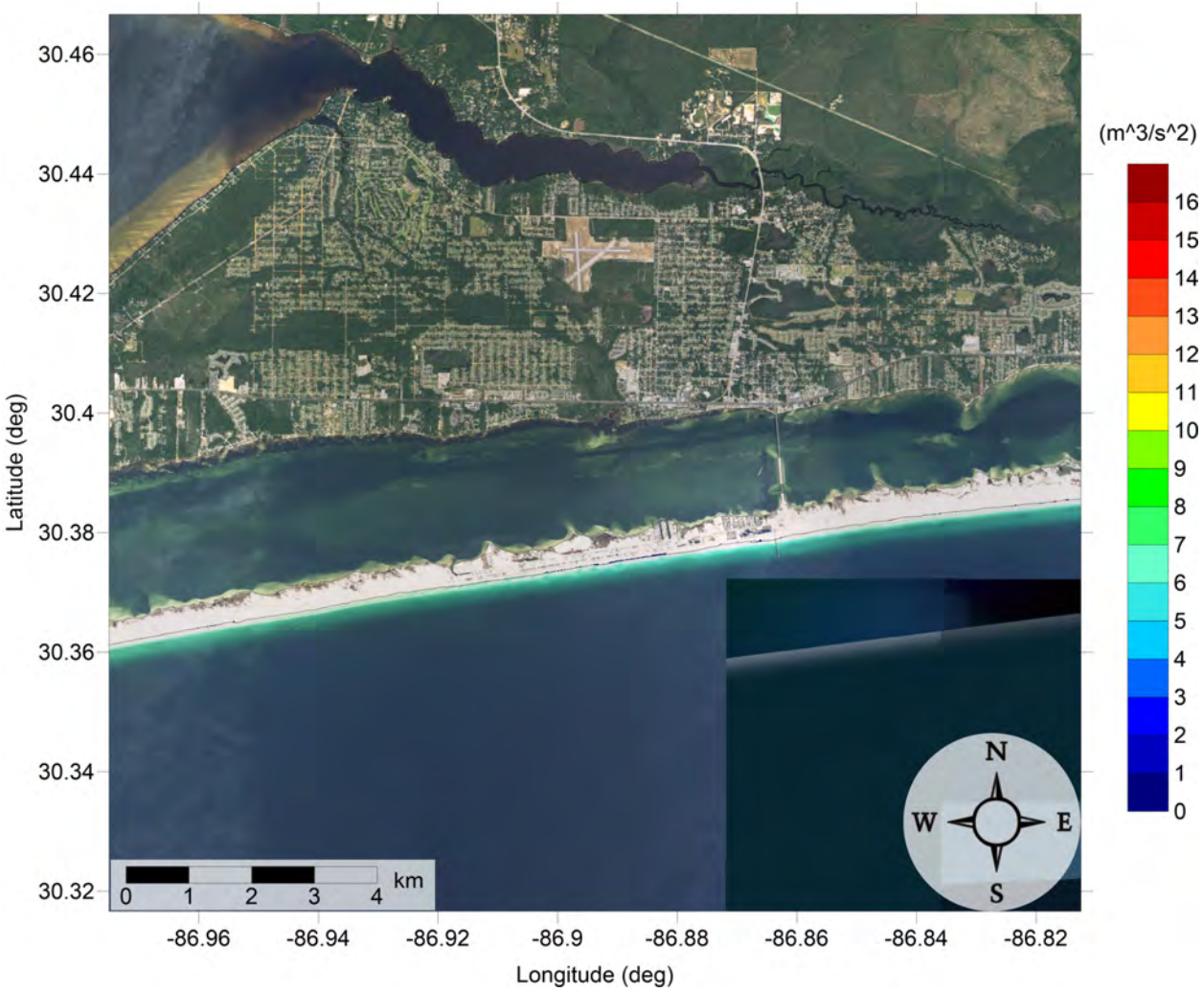


Figure 74: Maximum momentum flux ($m^3/s^2$) caused by the Probabilistic Submarine Landslide B1 in Navarre, FL. Arrows represent direction of maximum momentum flux. Contour drawn is the zero-meter contour for land elevation.

## Santa Rosa County, FL
## Probabilistic Submarine Landslide B1
## Maximum Inundation Depth


Figure 75: Maximum inundation depth (m) caused by the Probabilistic Submarine Landslide B1 in East Gulf Breeze, FL. Contour drawn is the zero-meter contour for land elevation.

**Santa Rosa County, FL**
**Probabilistic Submarine Landslide B1**
**Maximum Inundation Depth**

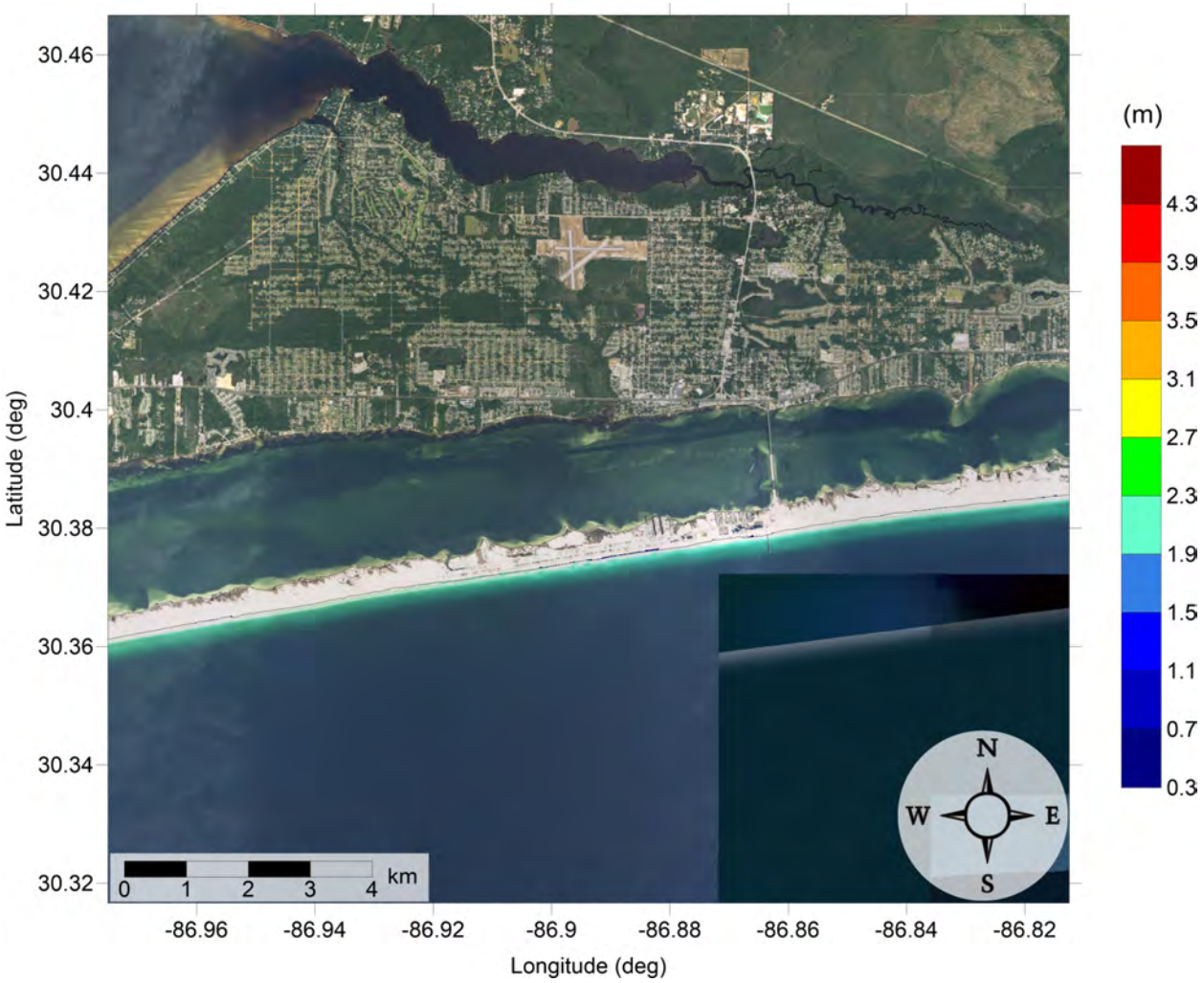


Figure 76: Maximum inundation depth (m) caused by the Probabilistic Submarine Landslide B1 in Navarre, FL. Contour drawn is the zero-meter contour for land elevation.

## Santa Rosa County, FL
## Probabilistic Submarine Landslide B2
## Maximum Momentum Flux

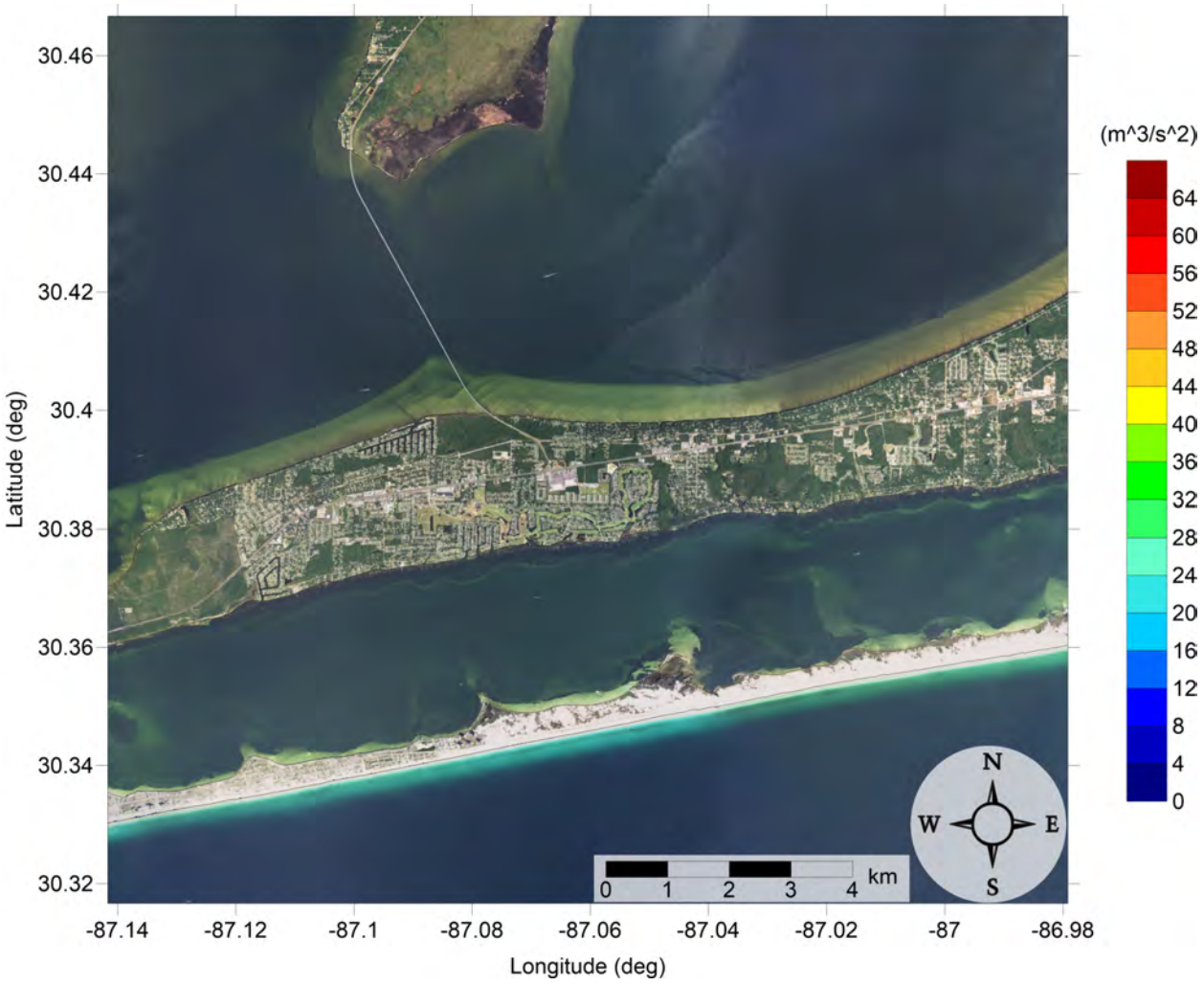


Figure 77: Maximum momentum flux ($m^3/s^2$) caused by the Probabilistic Submarine Landslide B2 in East Gulf Breeze, FL. Arrows represent direction of maximum momentum flux. Contour drawn is the zero-meter contour for land elevation.

## Santa Rosa County, FL
## Probabilistic Submarine Landslide B2
## Maximum Momentum Flux

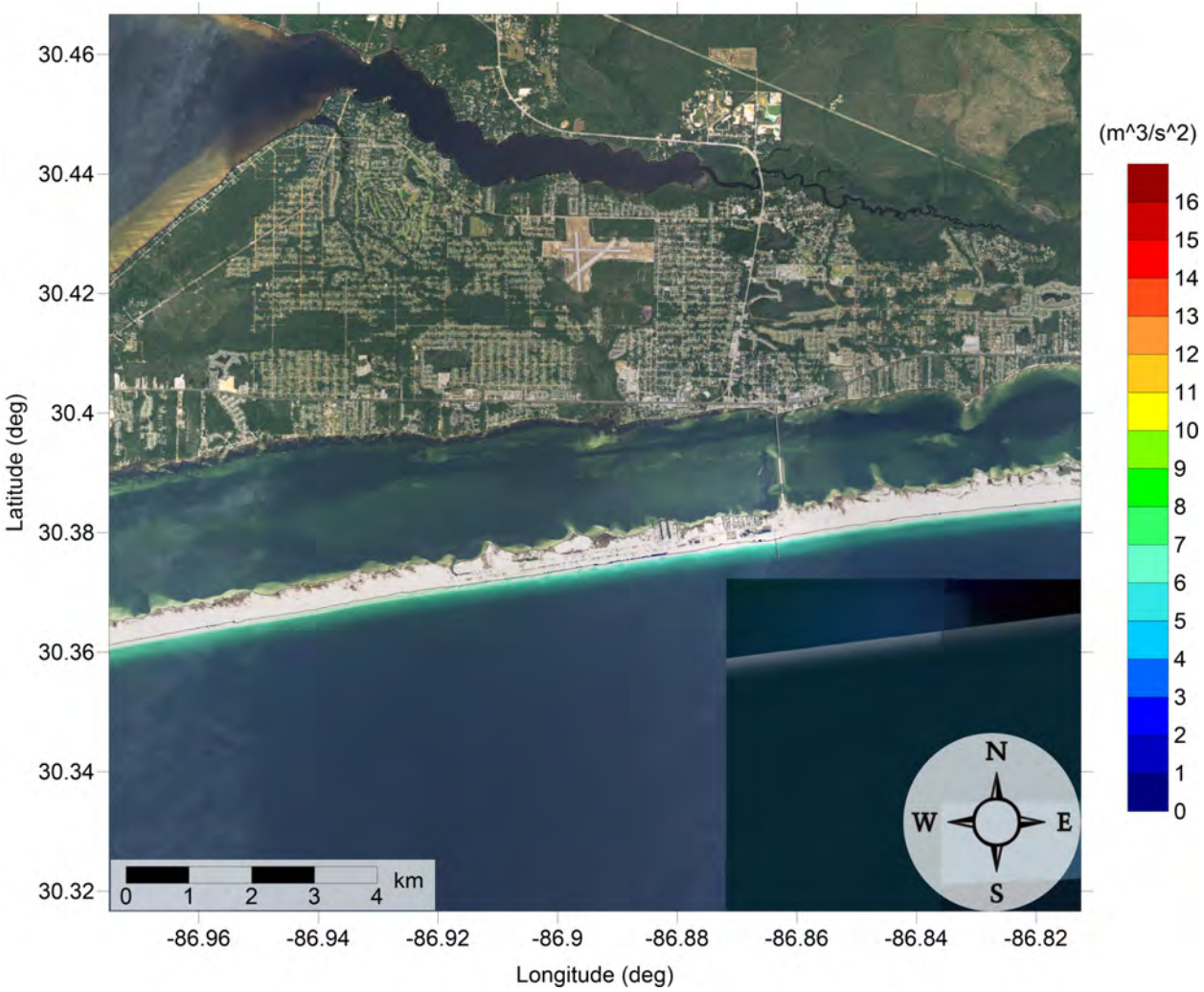


Figure 78: Maximum momentum flux ($m^3/s^2$) caused by the Probabilistic Submarine Landslide B2 in Navarre, FL. Arrows represent direction of maximum momentum flux. Contour drawn is the zero-meter contour for land elevation.

## Santa Rosa County, FL
## Probabilistic Submarine Landslide B2
## Maximum Inundation Depth


Figure 79: Maximum inundation depth (m) caused by the Probabilistic Submarine Landslide B2 in East Gulf Breeze, FL. Contour drawn is the zero-meter contour for land elevation.

**Santa Rosa County, FL**
**Probabilistic Submarine Landslide B2**
**Maximum Inundation Depth**

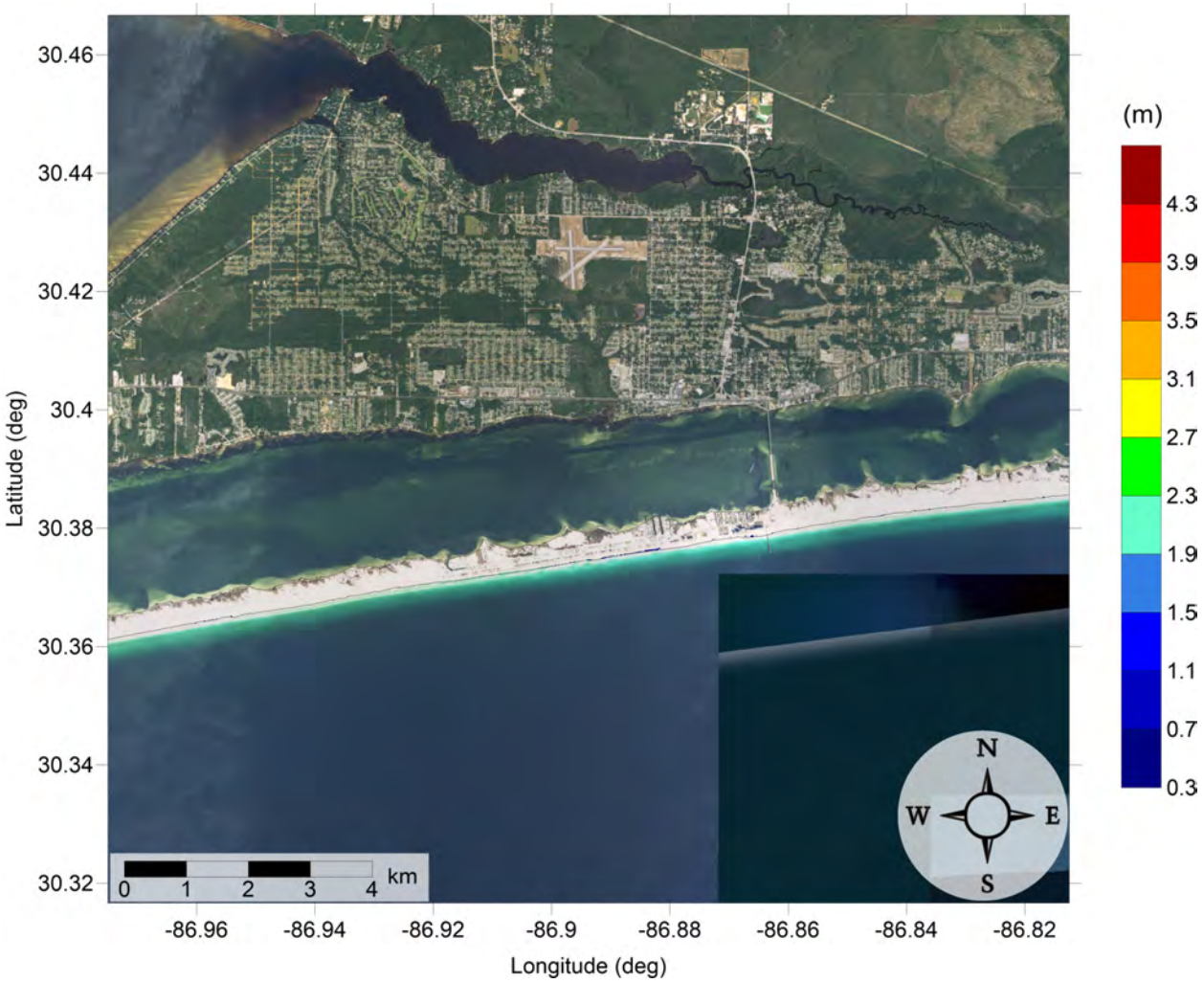


Figure 80: Maximum inundation depth (m) caused by the Probabilistic Submarine Landslide B2 in Navarre, FL. Contour drawn is the zero-meter contour for land elevation.

## Santa Rosa County, FL
## Mississippi Canyon submarine landslide
## Maximum Momentum Flux

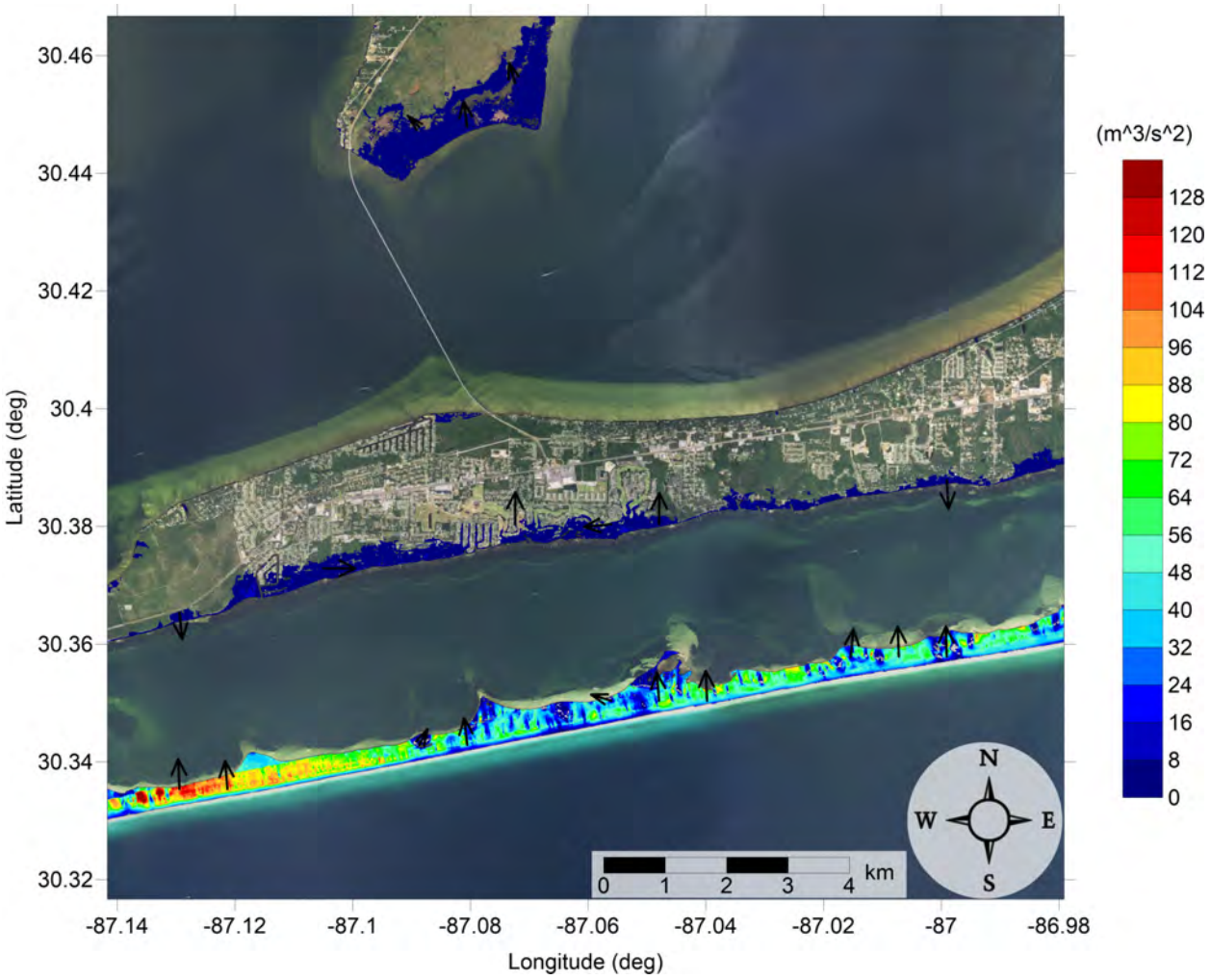


Figure 81: Maximum momentum flux ($m^3/s^2$) caused by the Mississippi Canyon submarine landslide in East Gulf Breeze, FL. Arrows represent direction of maximum momentum flux. Contour drawn is the zero-meter contour for land elevation.

## Santa Rosa County, FL
## Mississippi Canyon submarine landslide
## Maximum Momentum Flux

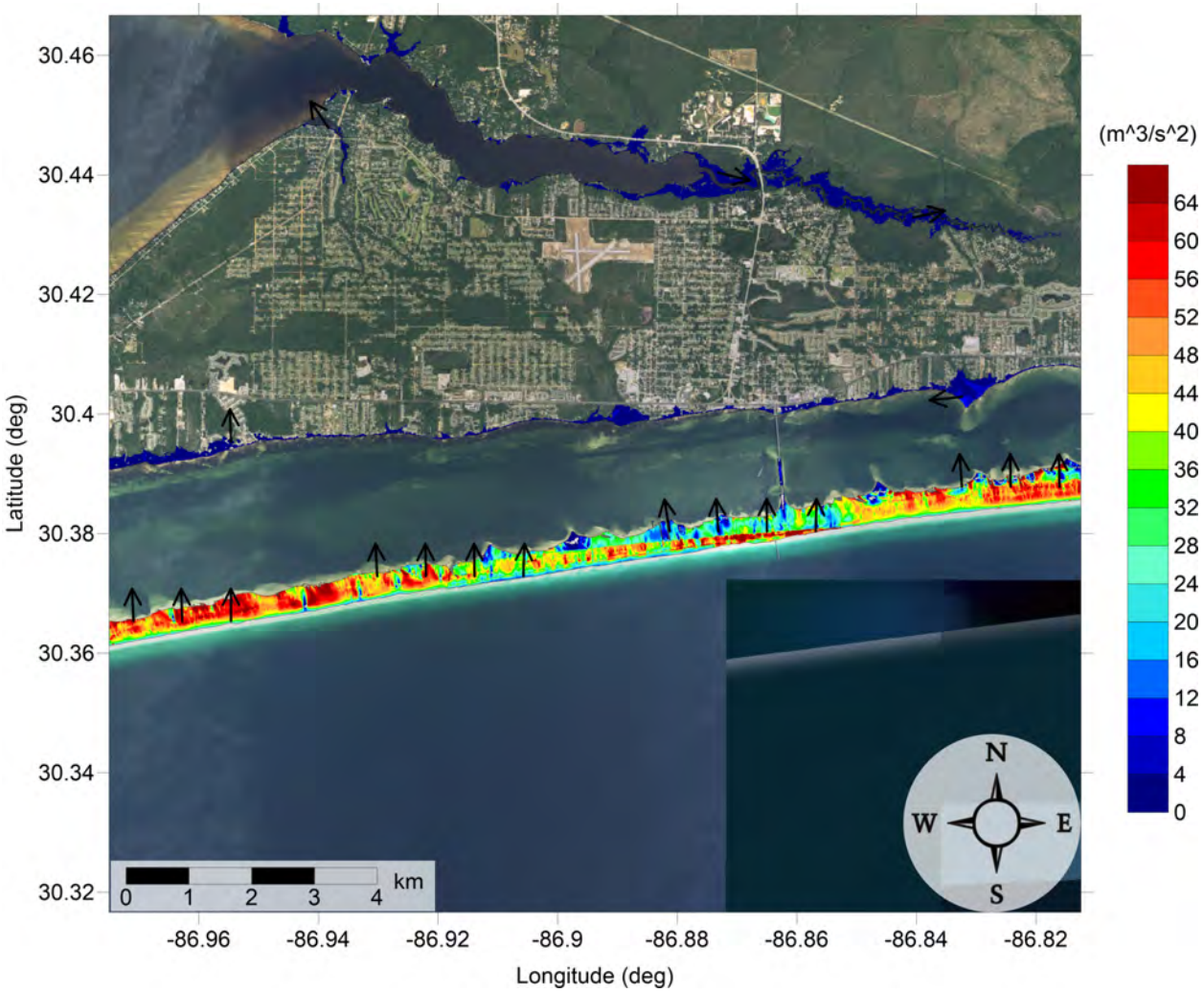


Figure 82: Maximum momentum flux ($m^3/s^2$) caused by the Mississippi Canyon submarine landslide in Navarre, FL. Arrows represent direction of maximum momentum flux. Contour drawn is the zero-meter contour for land elevation.

## Santa Rosa County, FL
## Mississippi Canyon submarine landslide
## Maximum Inundation Depth

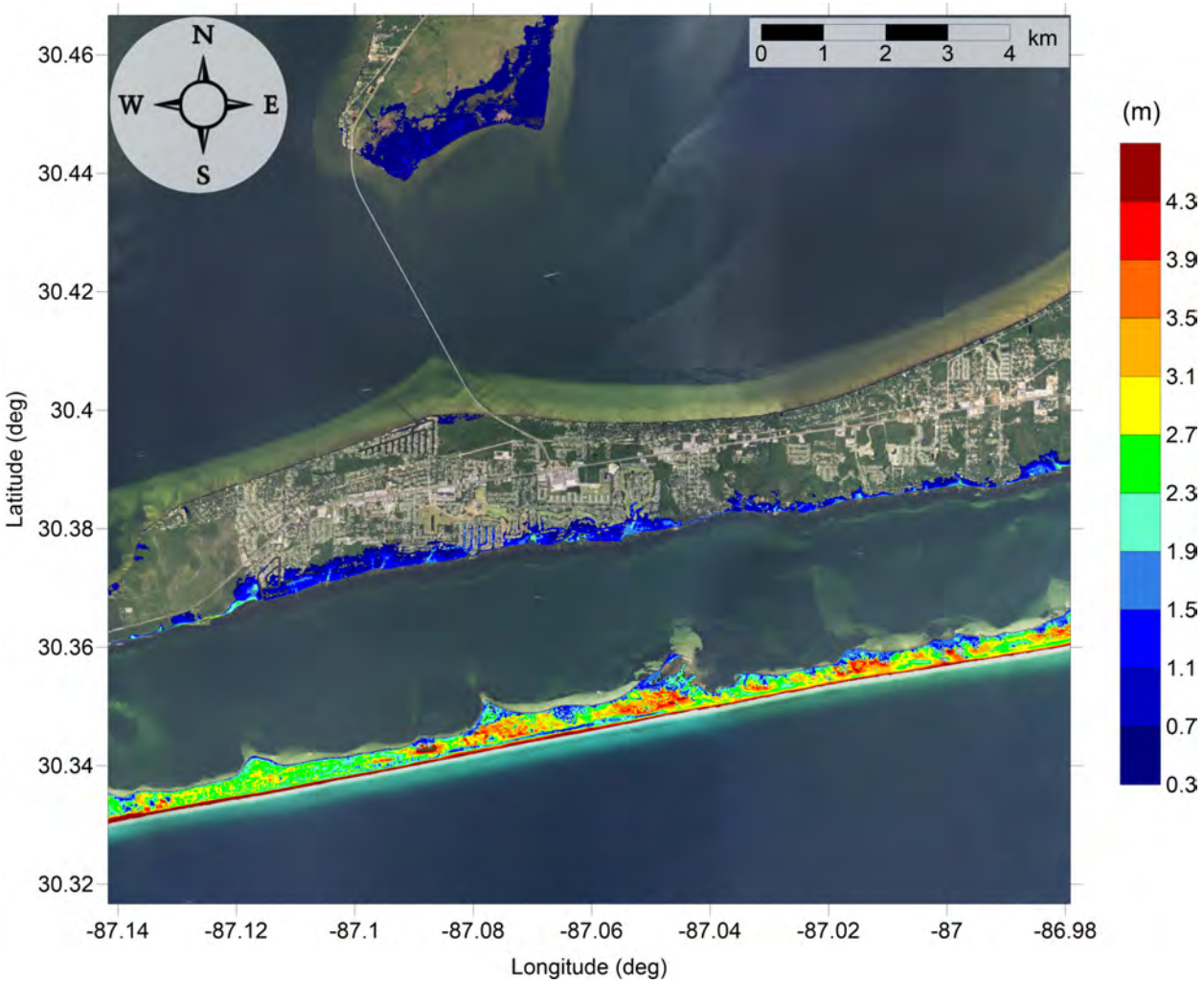


Figure 83: Maximum inundation depth (m) caused by the Mississippi Canyon submarine landslide in East Gulf Breeze, FL. Contour drawn is the zero-meter contour for land elevation.

## Santa Rosa County, FL
## Mississippi Canyon submarine landslide
## Maximum Inundation Depth

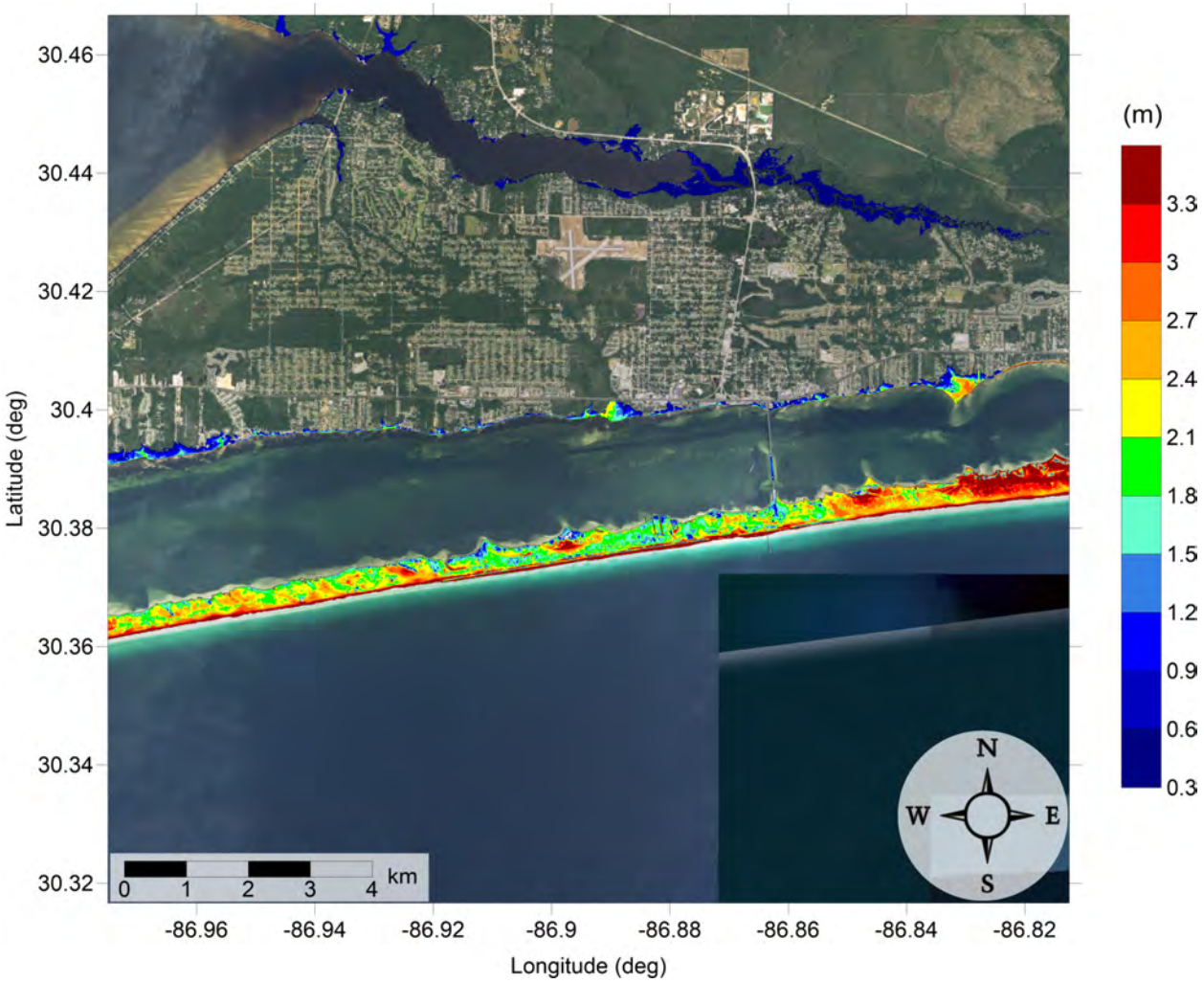


Figure 84: Maximum inundation depth (m) caused by the Mississippi Canyon submarine landslide in Navarre, FL. Contour drawn is the zero-meter contour for land elevation.

## Santa Rosa County, FL
## Probabilistic Submarine Landslide C
## Maximum Momentum Flux

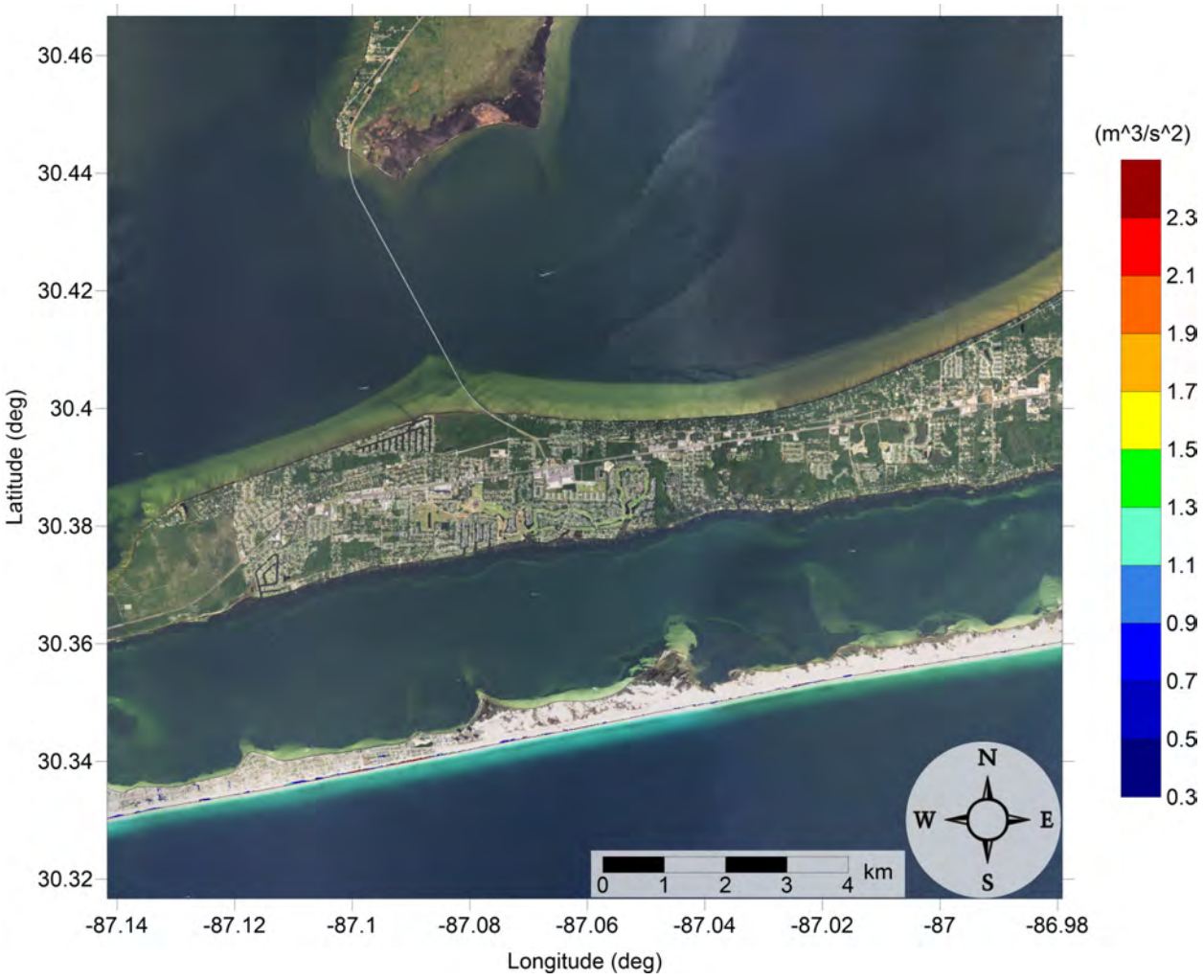


Figure 85: Maximum momentum flux ($m^3/s^2$) caused by the Probabilistic Submarine Landslide C in East Gulf Breeze, FL. Arrows represent direction of maximum momentum flux. Contour drawn is the zero-meter contour for land elevation.

## Santa Rosa County, FL
## Probabilistic Submarine Landslide C
## Maximum Momentum Flux

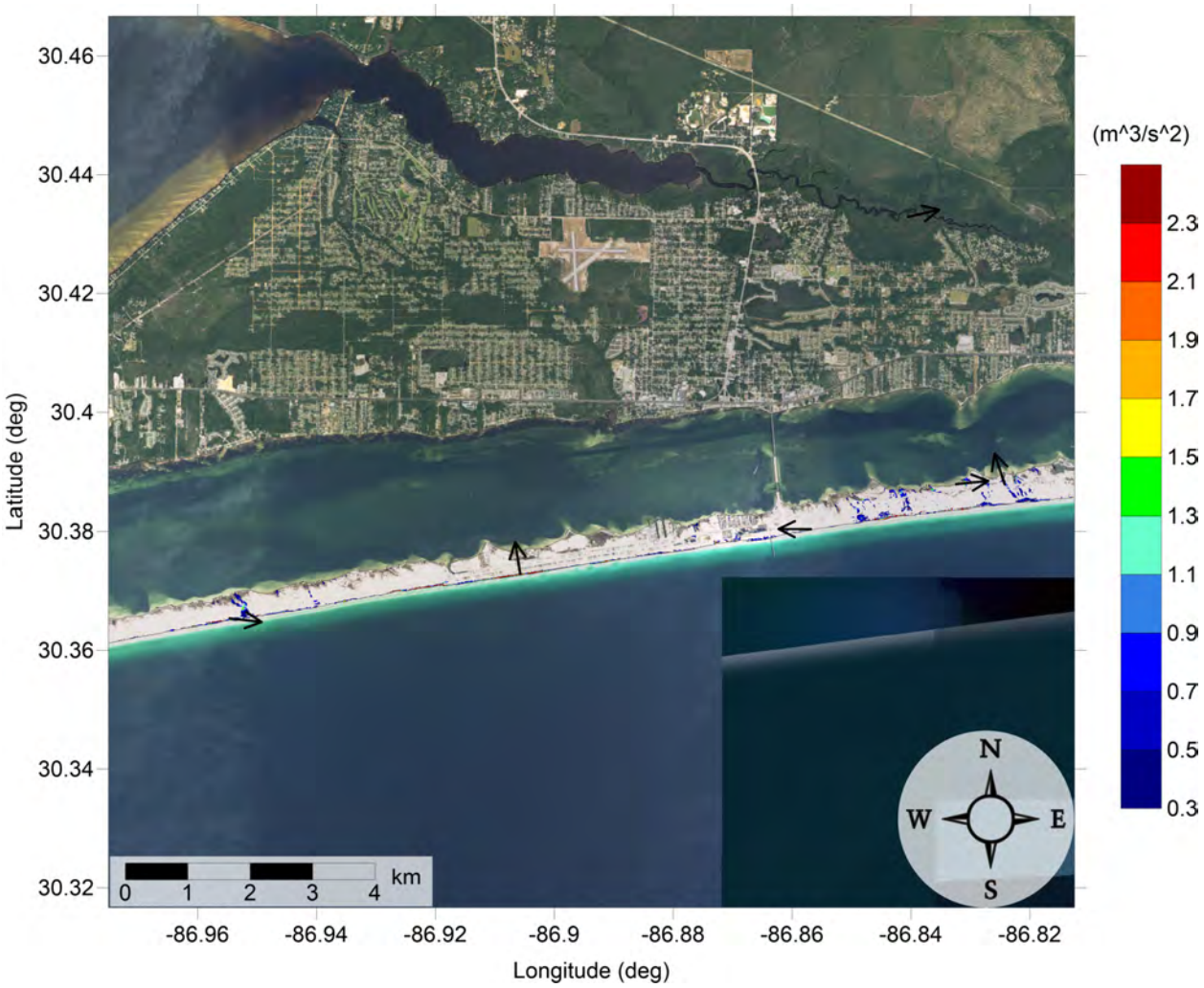


Figure 86: Maximum momentum flux ($m^3/s^2$) caused by the Probabilistic Submarine Landslide C in Navarre, FL. Arrows represent direction of maximum momentum flux. Contour drawn is the zero-meter contour for land elevation.

## Santa Rosa County, FL
## Probabilistic Submarine Landslide C
## Maximum Inundation Depth


Figure 87: Maximum inundation depth (m) caused by the Probabilistic Submarine Landslide C in East Gulf Breeze, FL. Contour drawn is the zero-meter contour for land elevation.

## Santa Rosa County, FL
## Probabilistic Submarine Landslide C
## Maximum Inundation Depth

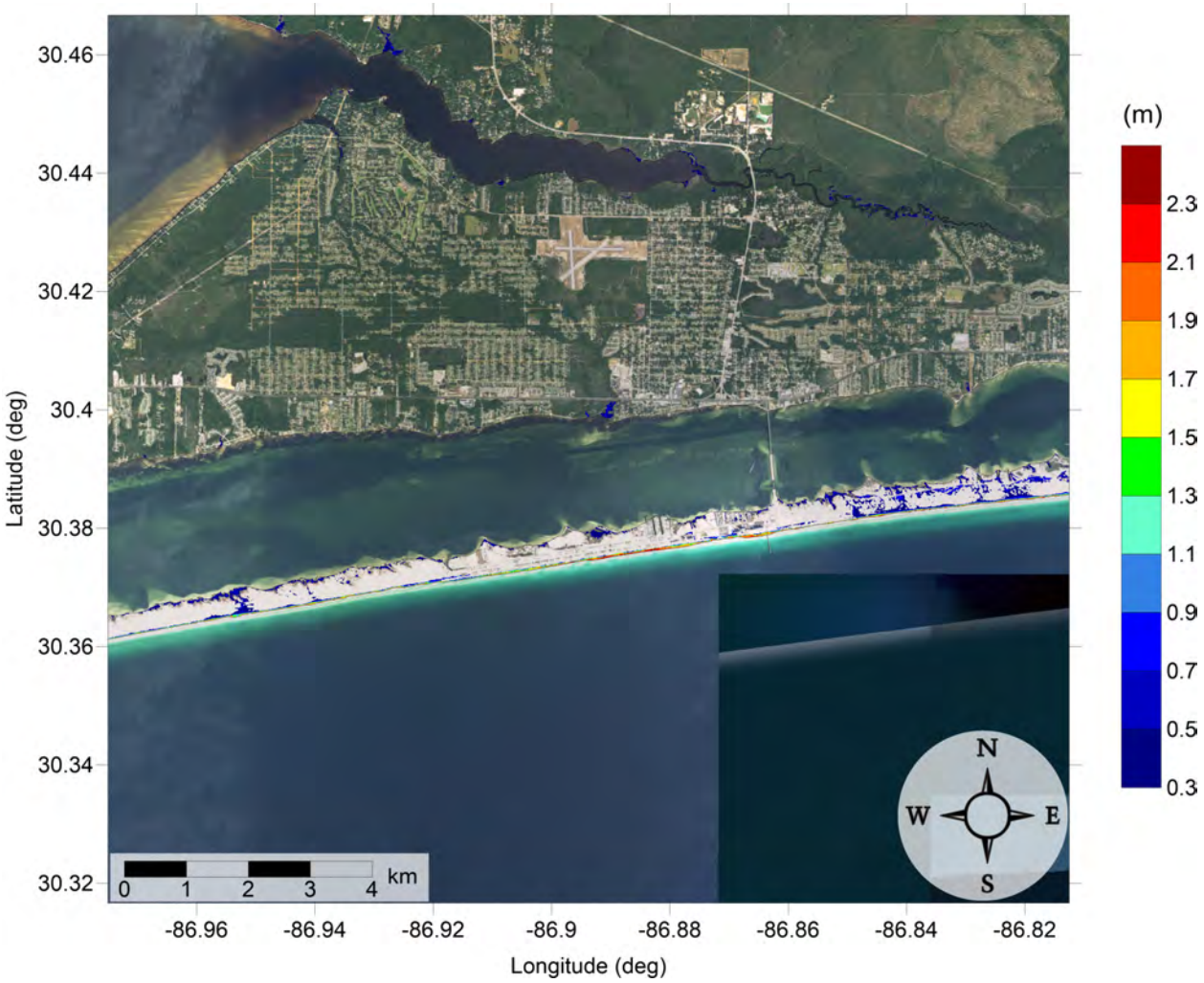


Figure 88: Maximum inundation depth (m) caused by the Probabilistic Submarine Landslide C in Navarre, FL. Contour drawn is the zero-meter contour for land elevation.

## Santa Rosa County, FL
## West Florida submarine landslide
## Maximum Momentum Flux

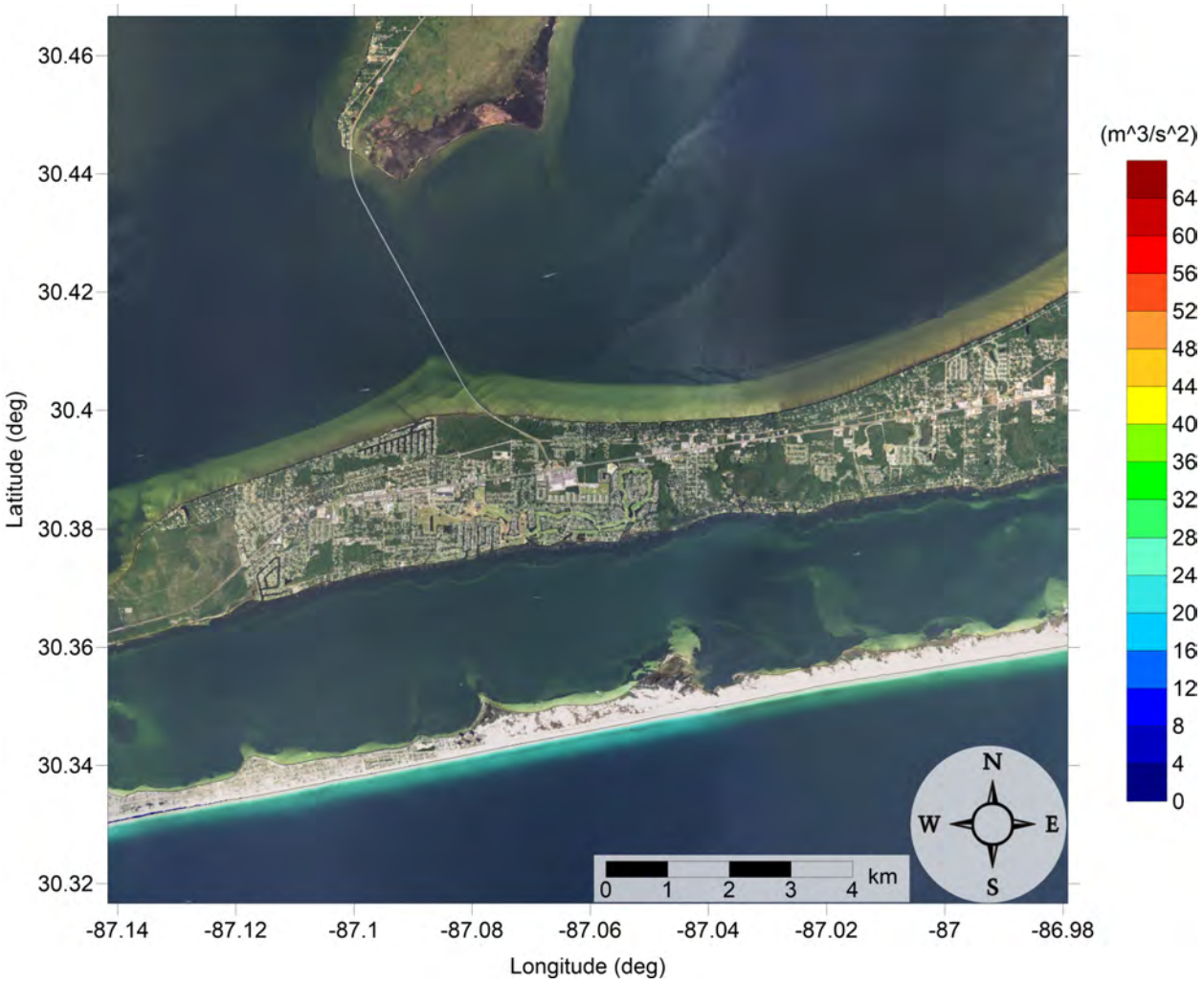


Figure 89: Maximum momentum flux ($m^3/s^2$) caused by the West Florida submarine landslide in East Gulf Breeze, FL. Arrows represent direction of maximum momentum flux. Contour drawn is the zero-meter contour for land elevation.

**Santa Rosa County, FL**
**West Florida submarine landslide**
**Maximum Momentum Flux**

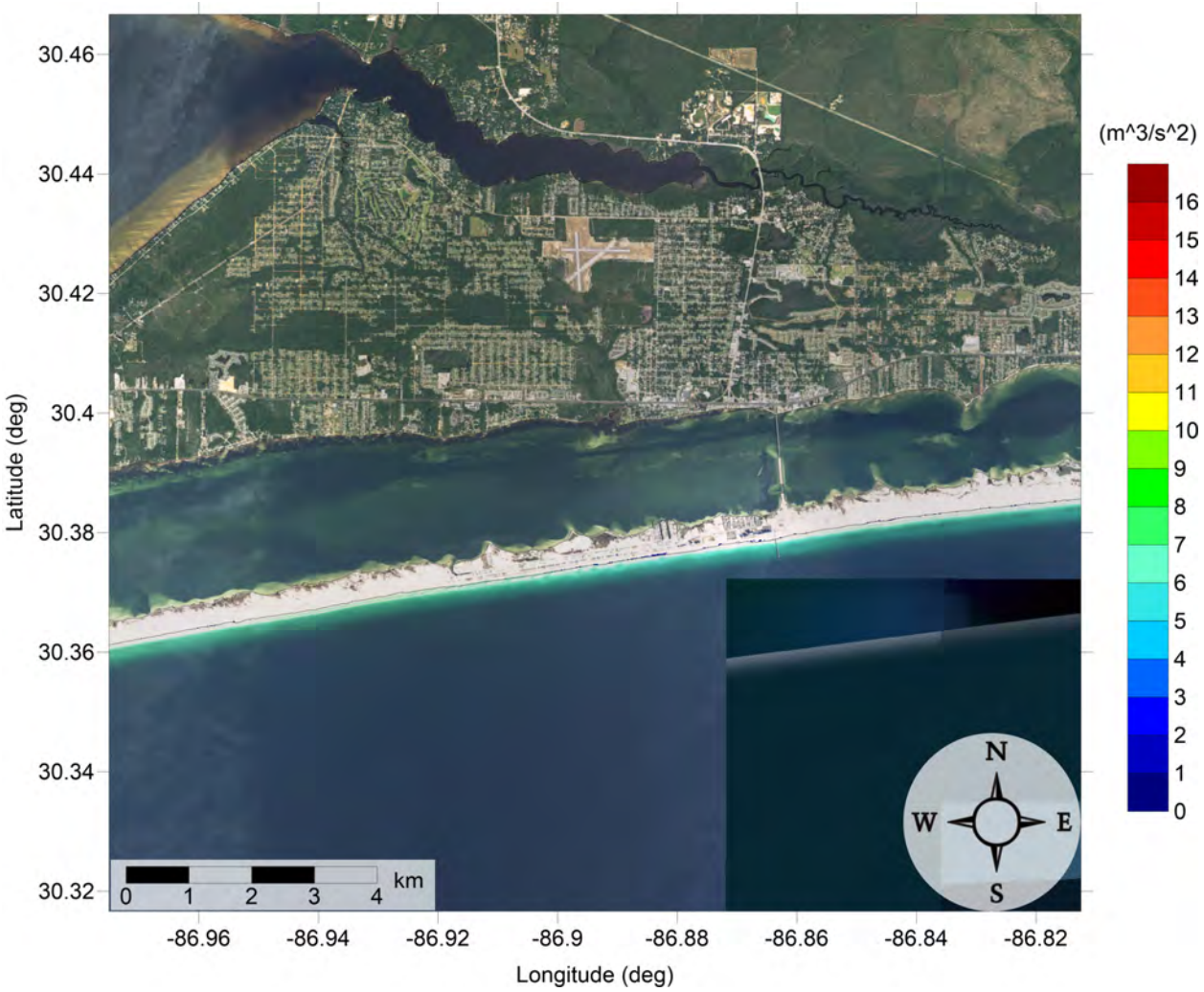


Figure 90: Maximum momentum flux ($m^3/s^2$) caused by the West Florida submarine landslide in Navarre, FL. Arrows represent direction of maximum momentum flux. Contour drawn is the zero-meter contour for land elevation.

## Santa Rosa County, FL
## West Florida submarine landslide
## Maximum Inundation Depth


Figure 91: Maximum inundation depth (m) caused by the West Florida submarine landslide in East Gulf Breeze, FL. Contour drawn is the zero-meter contour for land elevation.

## Santa Rosa County, FL
## West Florida submarine landslide
## Maximum Inundation Depth

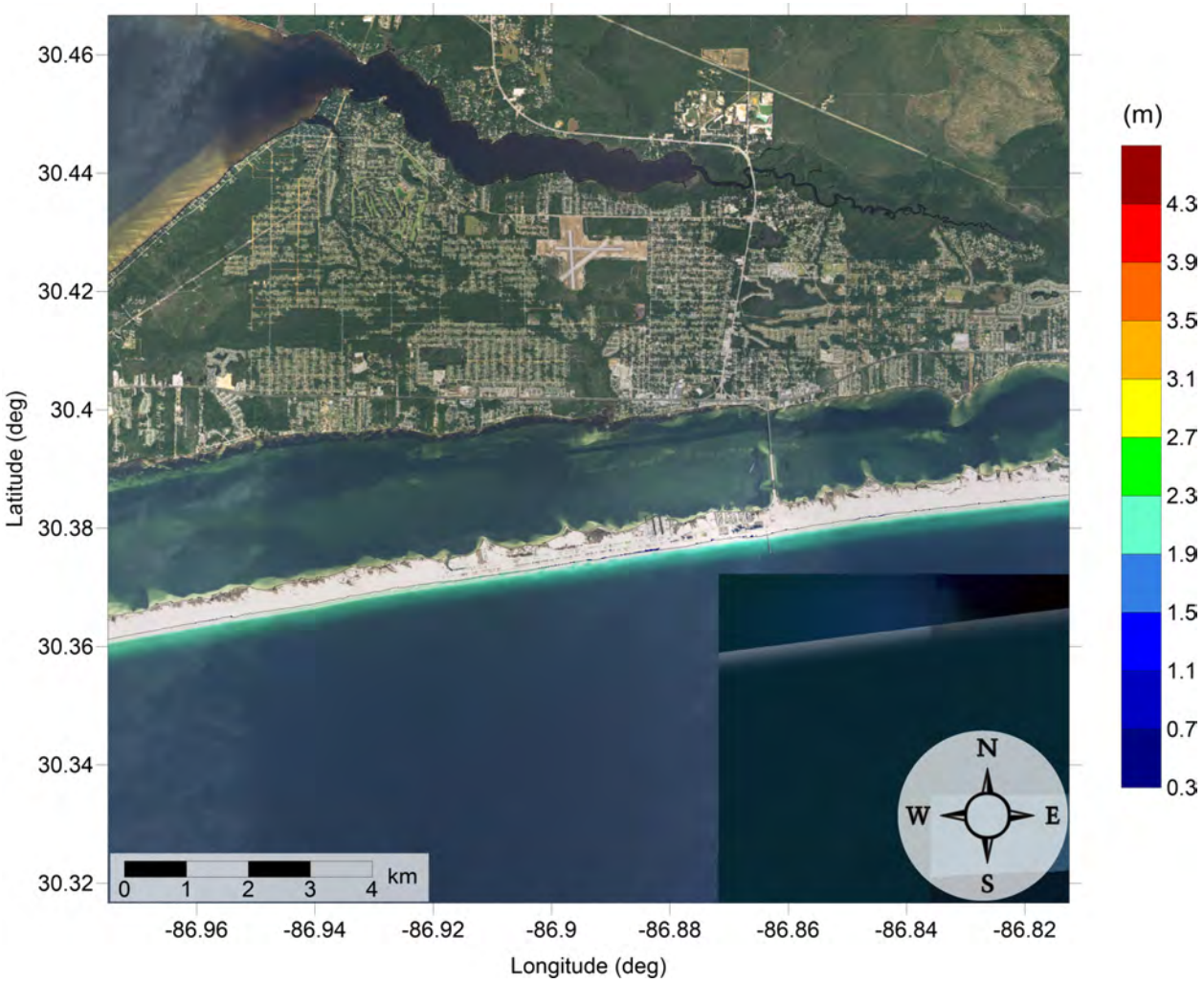


Figure 92: Maximum inundation depth (m) caused by the West Florida submarine landslide in Navarre, FL. Contour drawn is the zero-meter contour for land elevation.

## Santa Rosa County, FL
## All Sources
## Maximum of Maximum Inundation Depth

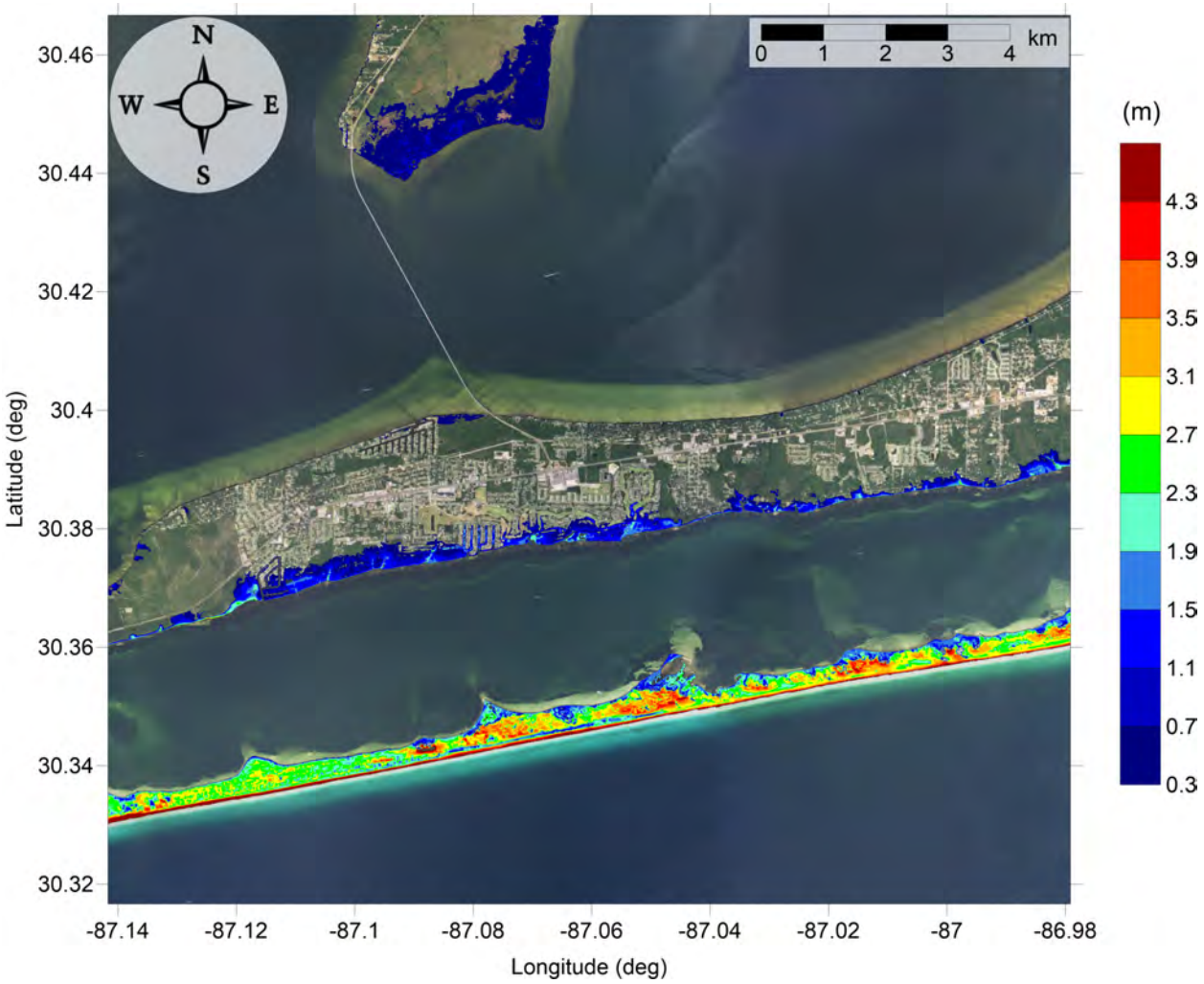


Figure 93: Maximum of maximums inundation depth (m) in East Gulf Breeze, FL, calculated as the maximum inundation depth in each grid cell from an ensemble of all tsunami sources considered. Contour drawn is the zero-meter contour for land elevation.

## Santa Rosa County, FL
## All Sources
## Maximum Inundation Depth by Source

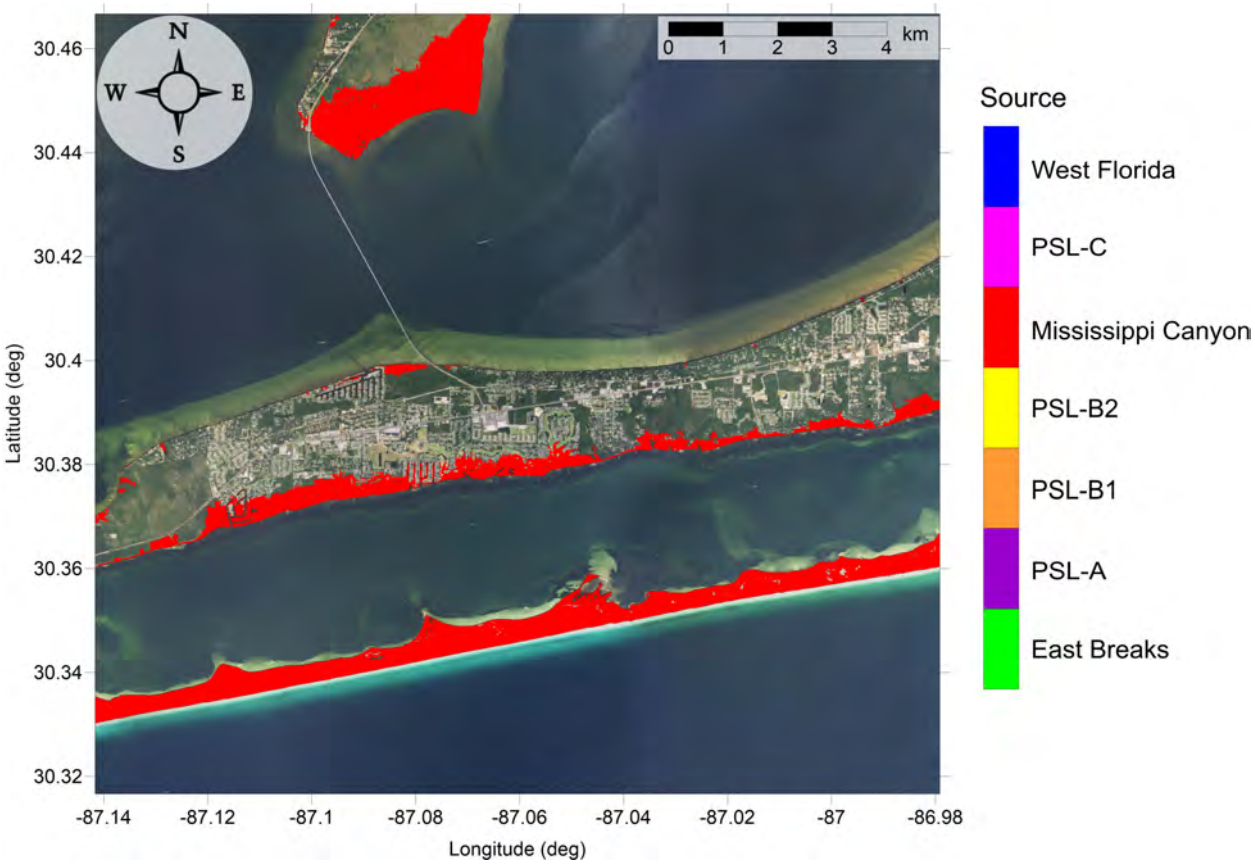


Figure 94: Indication of the tsunami source which causes the maximum of maximums inundation depth (m) in each grid cell from an ensemble of all tsunami sources in East Gulf Breeze, FL. Contour drawn is the zero-meter contour for land elevation.

## Santa Rosa County, FL
## All Sources
## Maximum of Maximum Inundation Depth

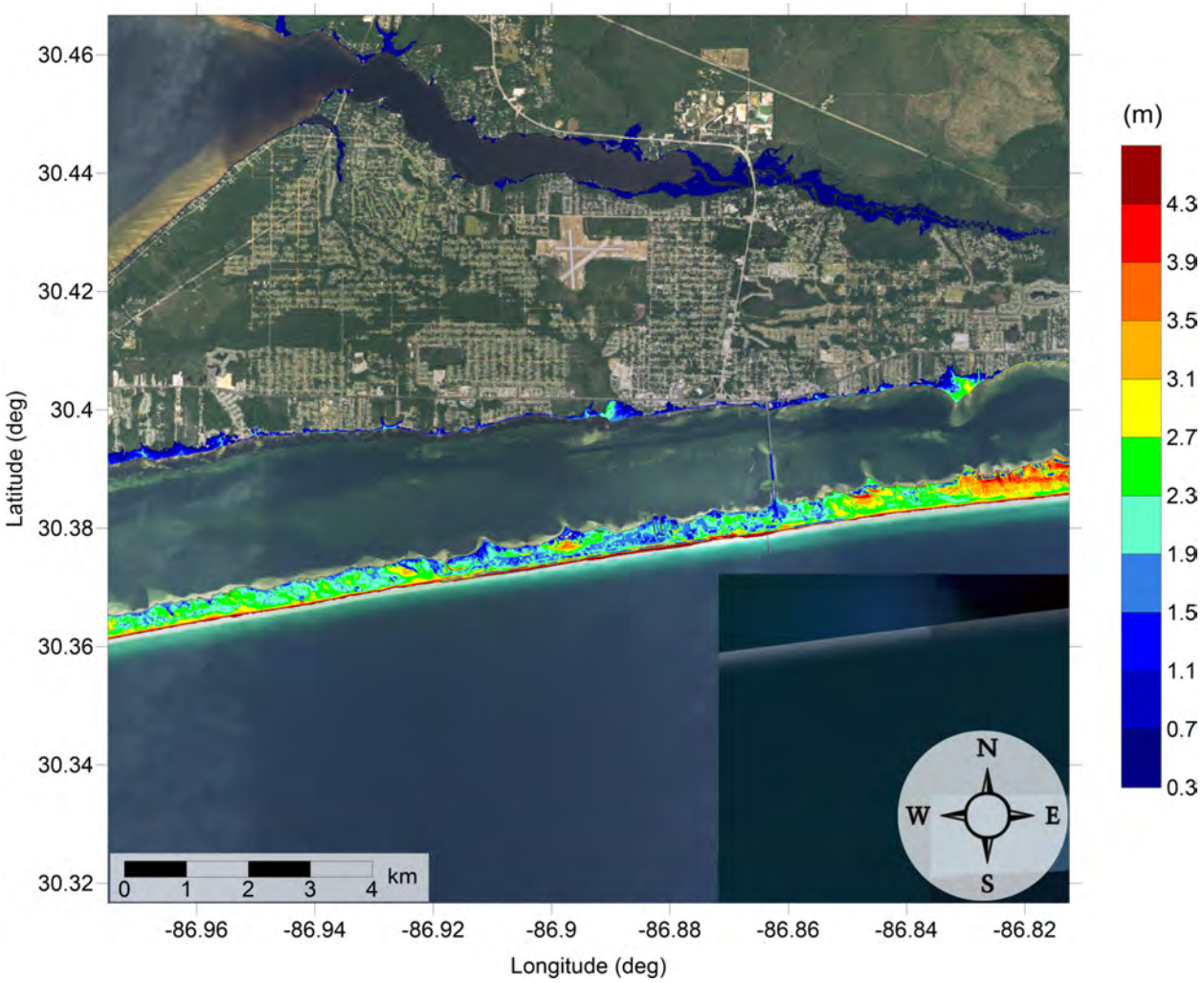


Figure 95: Maximum of maximums inundation depth (m) in Navarre, FL, calculated as the maximum inundation depth in each grid cell from an ensemble of all tsunami sources considered. Contour drawn is the zero-meter contour for land elevation.

## Santa Rosa County, FL
## All Sources
## Maximum Inundation Depth by Source

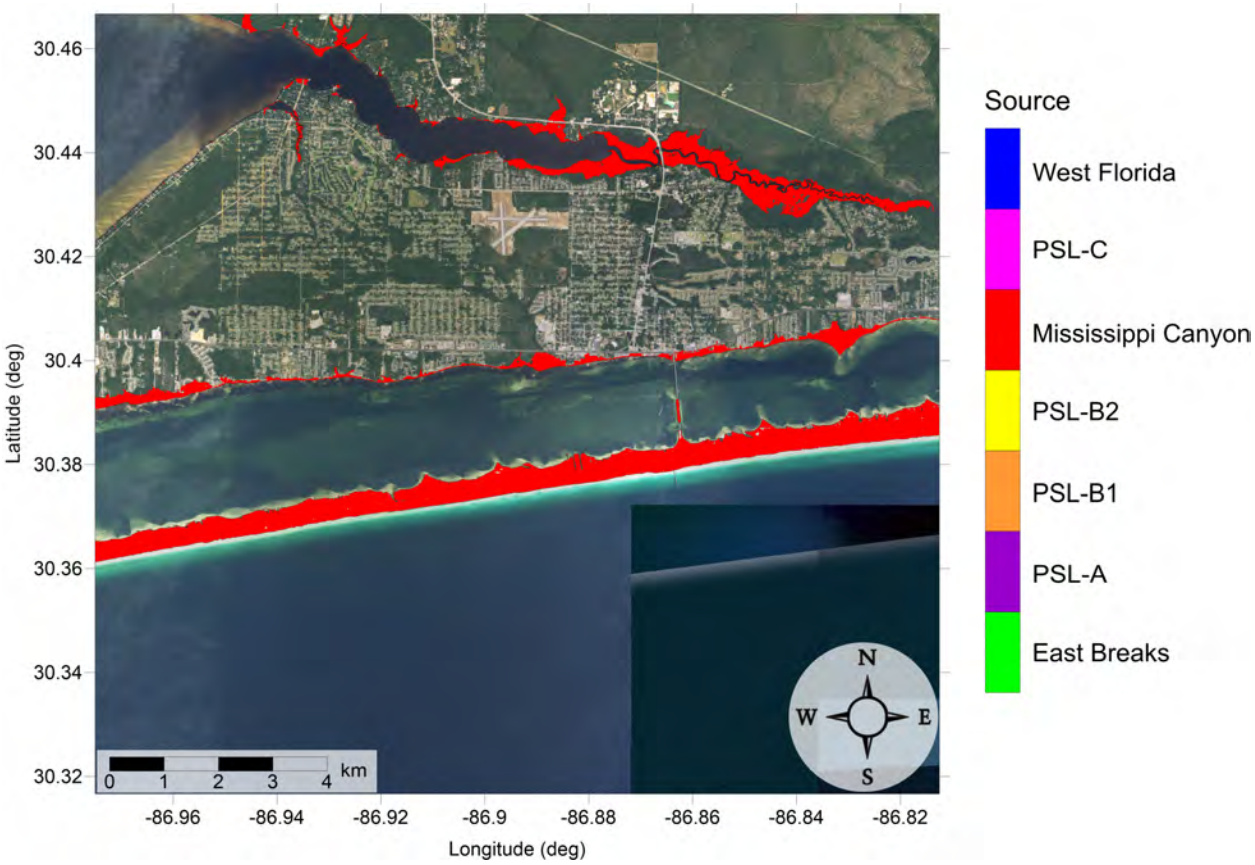


Figure 96: Indication of the tsunami source which causes the maximum of maximums inundation depth (m) in each grid cell from an ensemble of all tsunami sources in Navarre, FL. Contour drawn is the zero-meter contour for land elevation.

## 3.5 Mustang Island, TX

Table 5: Maximum tsunami wave amplitude and corresponding arrival time after landslide failure at Mustang Island, TX numerical wave gauge: 27°47'9.77"N, 96°56'32.22"W (Fig. 1), approximate water depth 20 m.

| Tsunami Source | Maximum Wave Amplitude (m) | Arrival Time After Landslide Failure (hr) |
|---|---|---|
| East Breaks | 3.1 | 1.0 |
| PSL-A | 2.16 | 1.2 |
| PSL-B1 | 1.26 | 1.8 |
| PSL-B2 | 0.64 | 2.0 |
| Mississippi Canyon | 5.15 | 2.2 |
| PSL-C | 2.87 | 2.7 |
| West Florida | 0.21 | 3.0 |

**Mustang Island, TX**
**East Breaks submarine landslide**
**Maximum Momentum Flux**

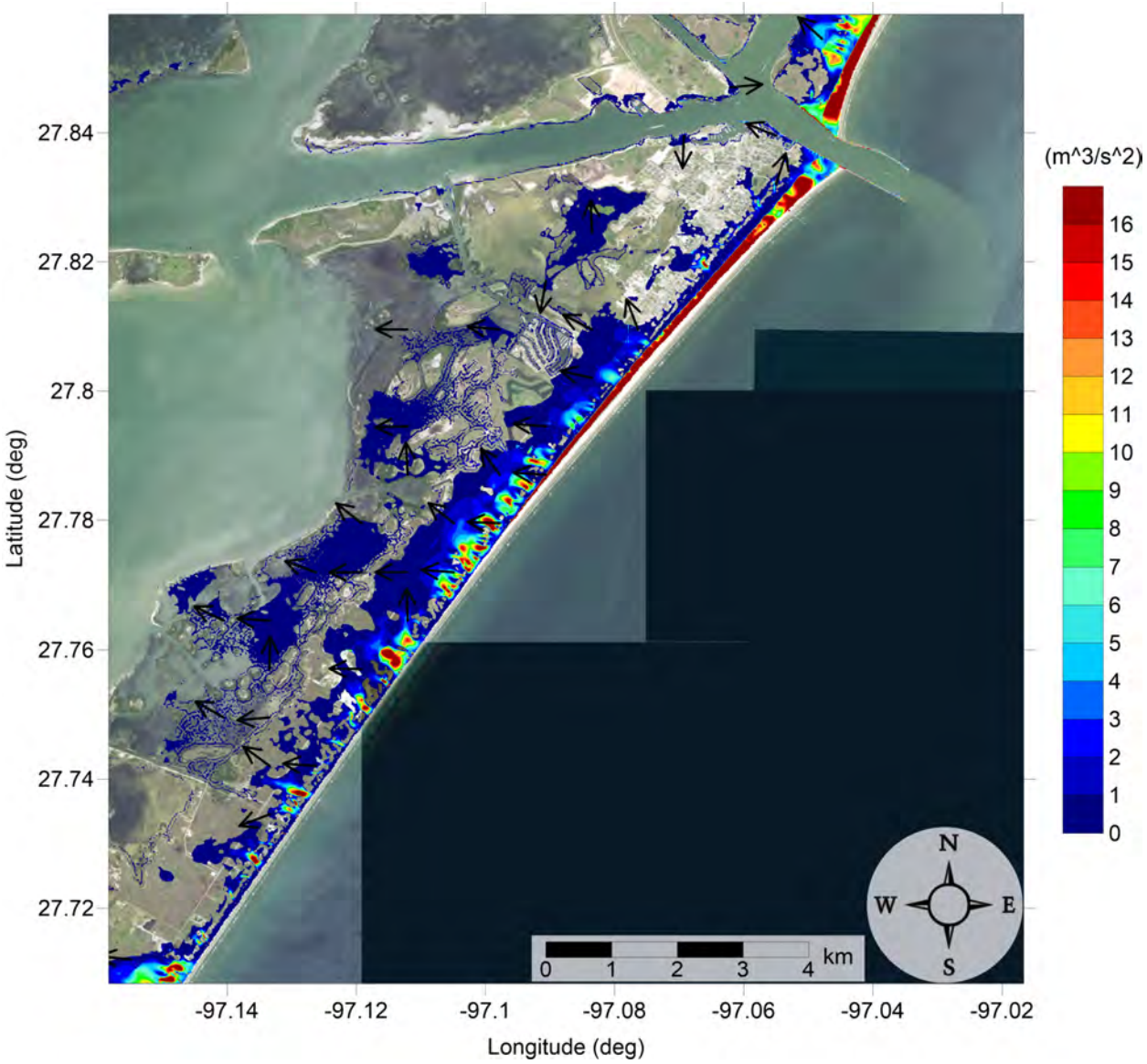


Figure 97: Maximum momentum flux ($m^3/s^2$) caused by the East Breaks submarine landslide in Port Aransas, TX. Arrows represent direction of maximum momentum flux. Contour drawn is the zero-meter contour for land elevation.

**Mustang Island, TX**
**East Breaks submarine landslide**
**Maximum Momentum Flux**

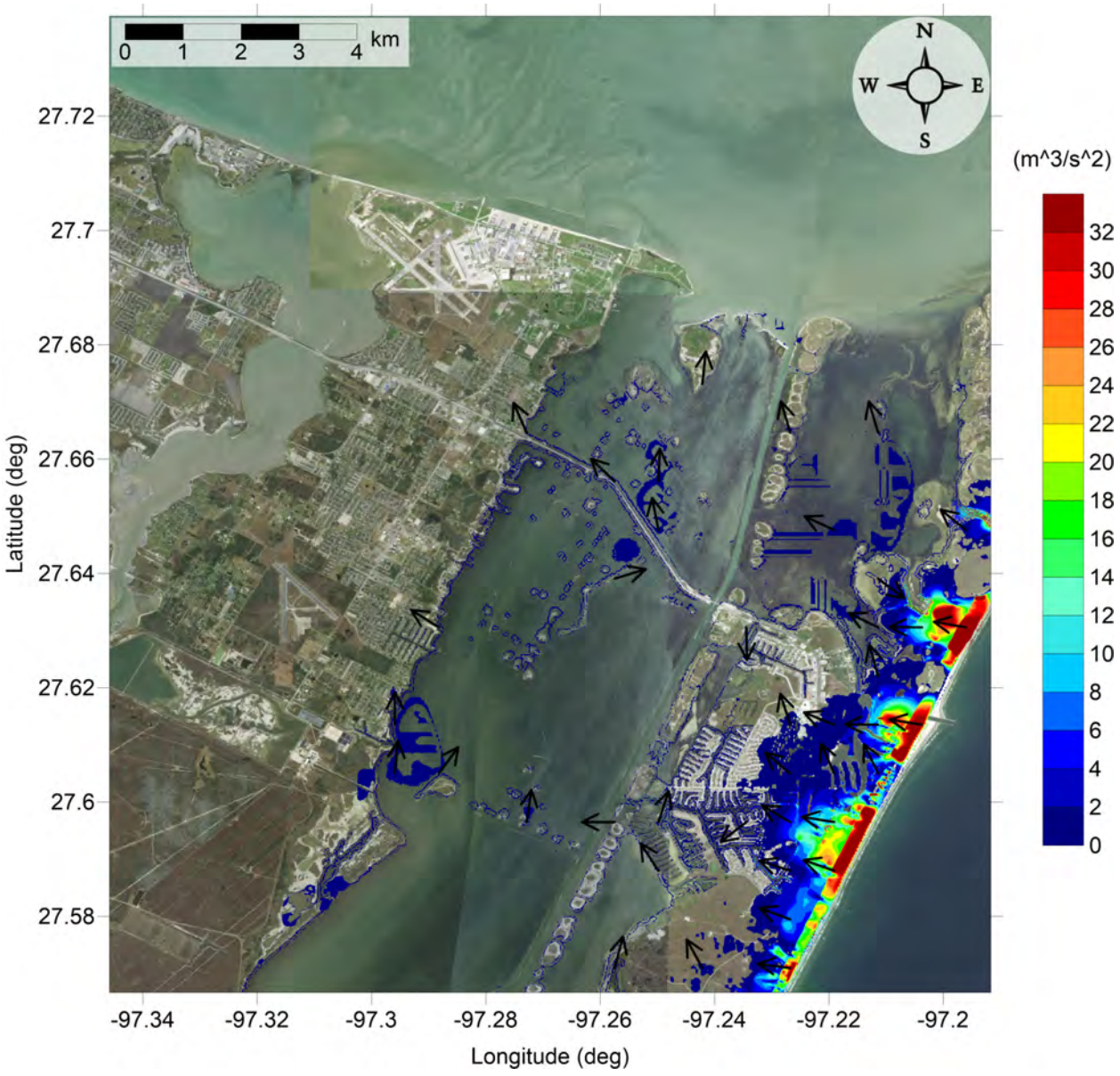


Figure 98: Maximum momentum flux ($m^3/s^2$) caused by the East Breaks submarine landslide in South-East Corpus Christi, TX. Arrows represent direction of maximum momentum flux. Contour drawn is the zero-meter contour for land elevation.

**Mustang Island, TX**
**East Breaks submarine landslide**
**Maximum Inundation Depth**

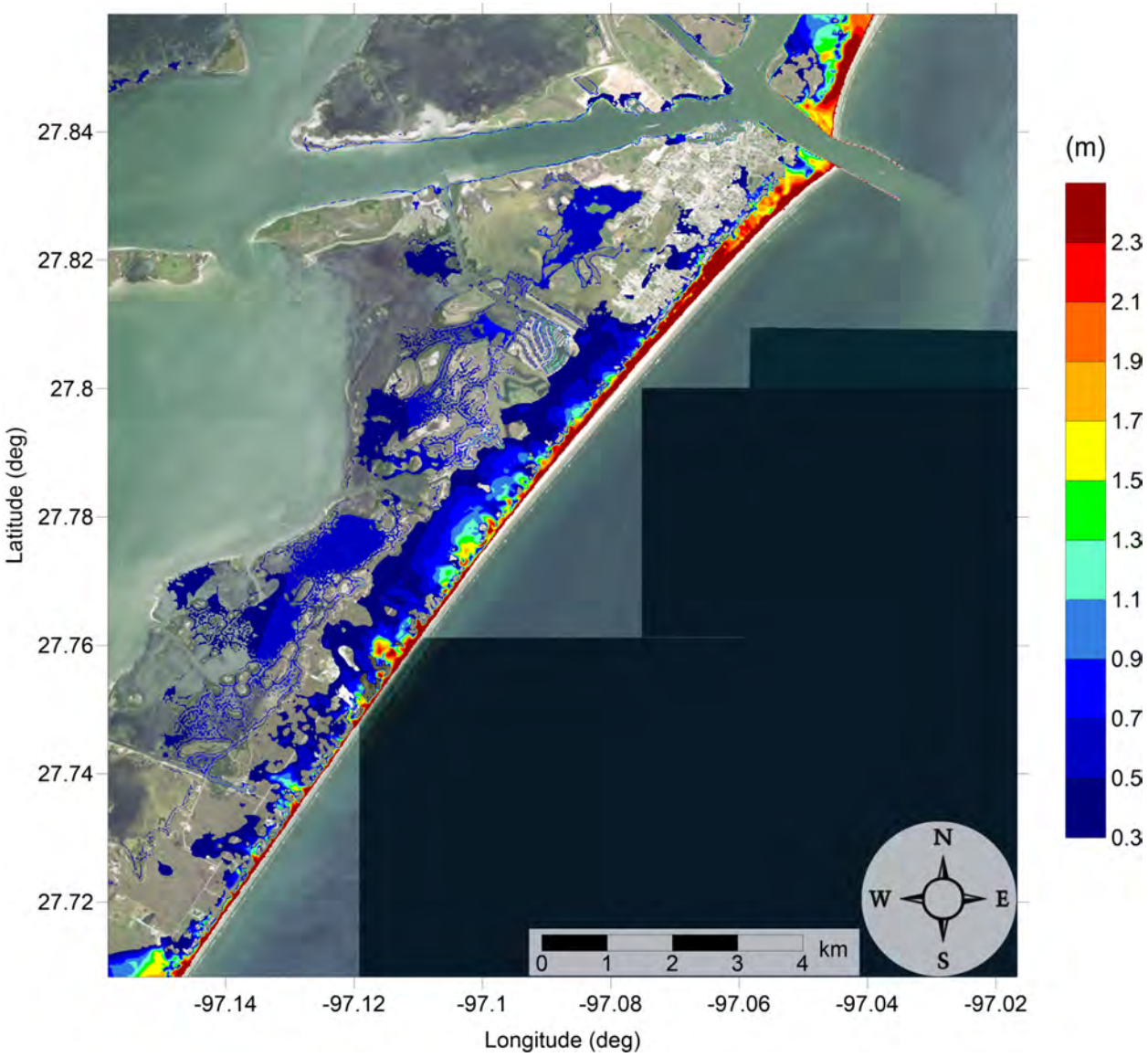


Figure 99: Maximum inundation depth (m) caused by the East Breaks submarine landslide in Port Aransas, TX. Contour drawn is the zero-meter contour for land elevation.

## Mustang Island, TX
## East Breaks submarine landslide
## Maximum Inundation Depth

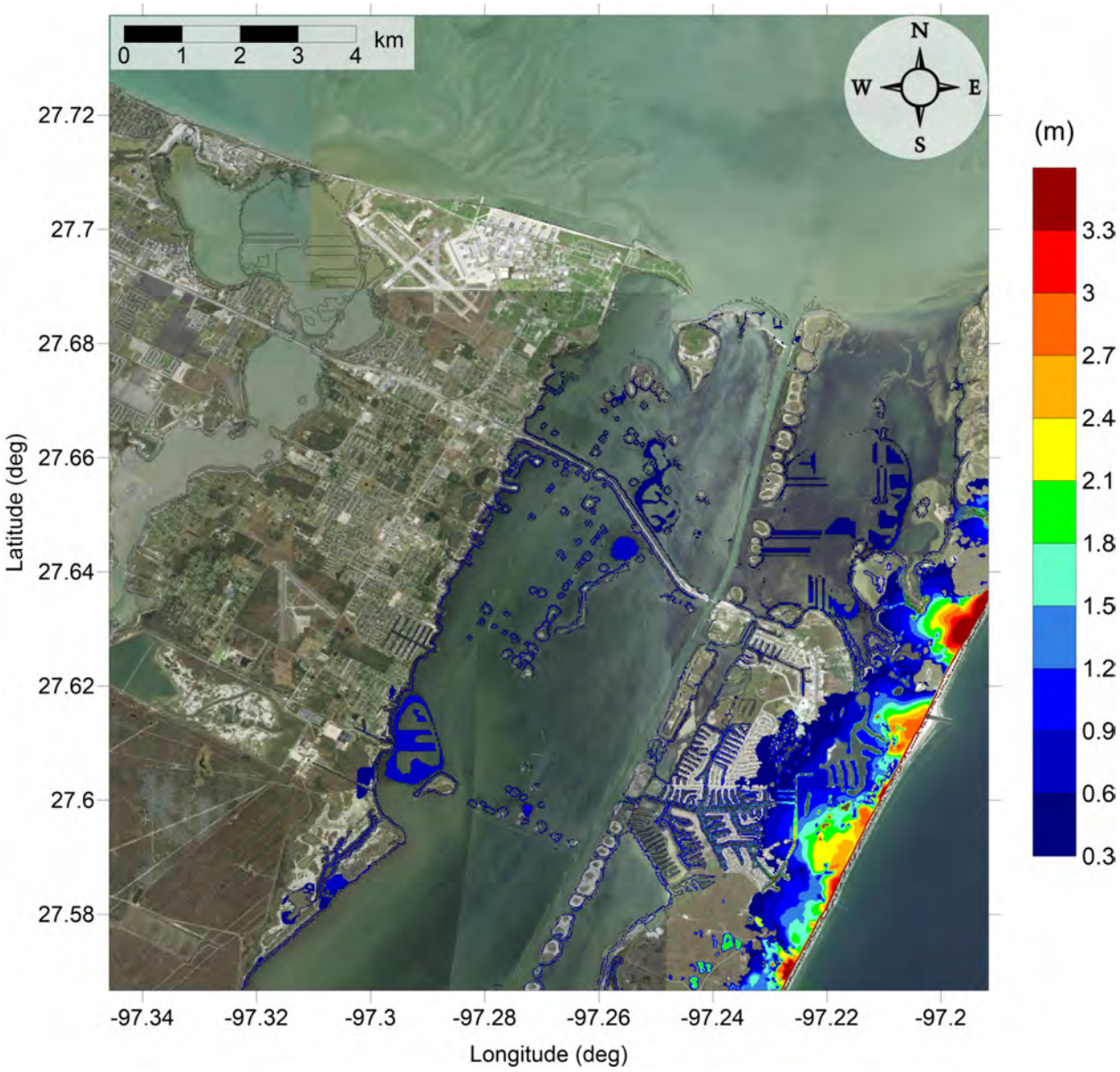


Figure 100: Maximum inundation depth (m) caused by the East Breaks submarine landslide in South-East Corpus Christi, TX. Contour drawn is the zero-meter contour for land elevation.

## Mustang Island, TX
## Probabilistic Submarine Landslide A
## Maximum Momentum Flux

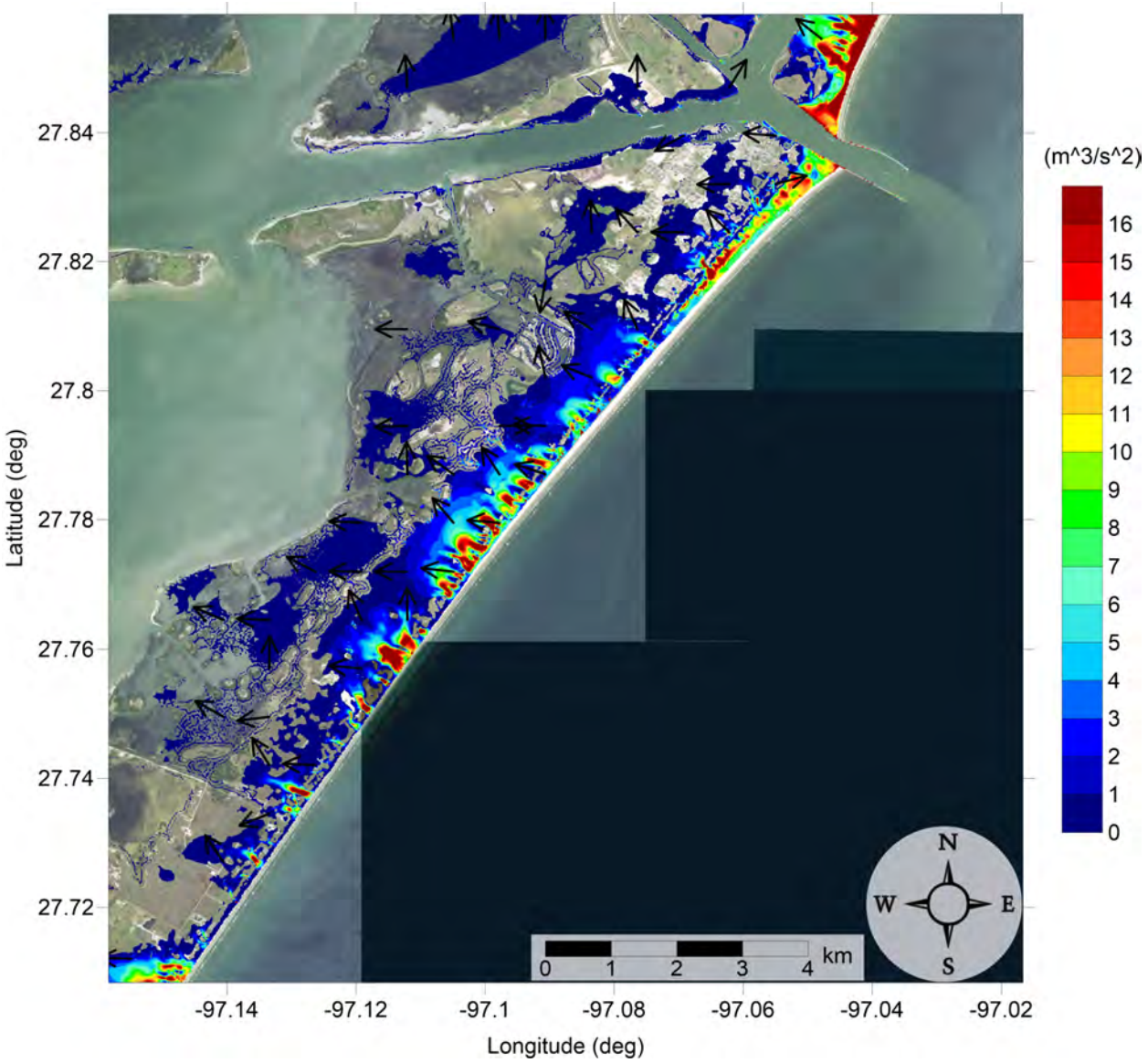


Figure 101: Maximum momentum flux ($m^3/s^2$) caused by the Probabilistic Submarine Landslide A in Port Aransas, TX. Arrows represent direction of maximum momentum flux. Contour drawn is the zero-meter contour for land elevation.

## Mustang Island, TX
## Probabilistic Submarine Landslide A
## Maximum Momentum Flux

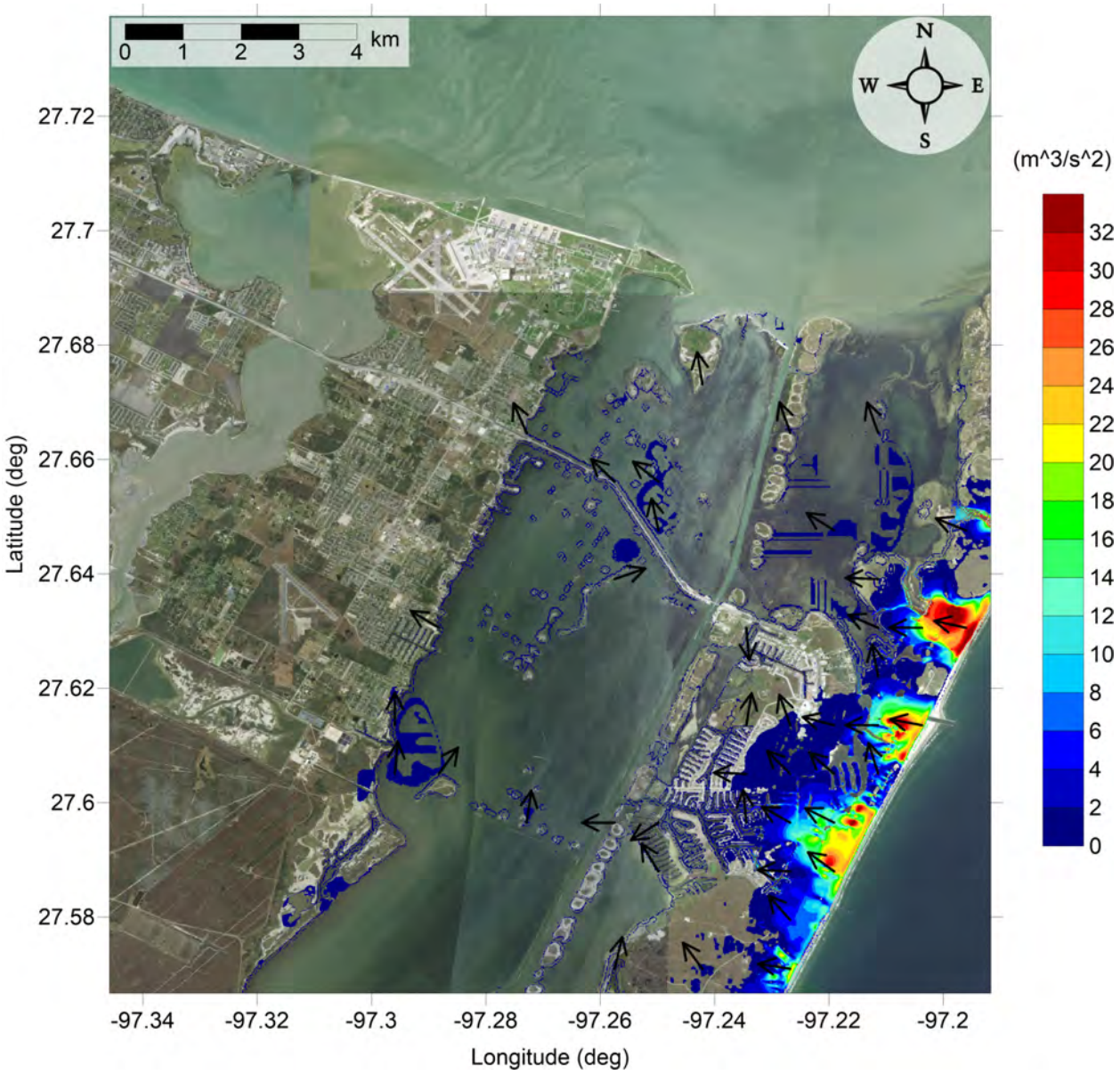


Figure 102: Maximum momentum flux ($m^3/s^2$) caused by the Probabilistic Submarine Landslide A in South-East Corpus Christi, TX. Arrows represent direction of maximum momentum flux. Contour drawn is the zero-meter contour for land elevation.

## Mustang Island, TX
## Probabilistic Submarine Landslide A
## Maximum Inundation Depth

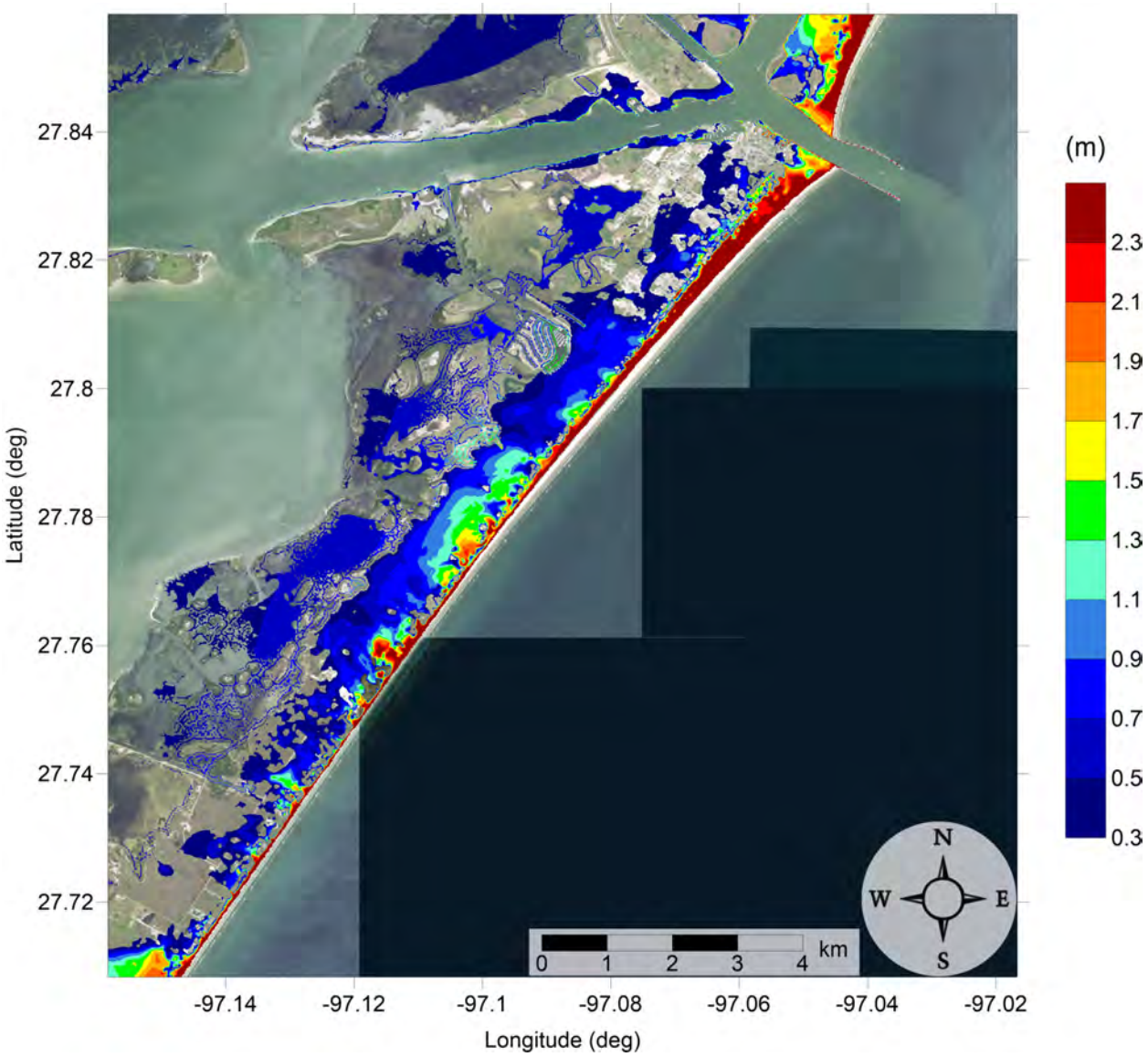


Figure 103: Maximum inundation depth (m) caused by the Probabilistic Submarine Landslide A in Port Aransas, TX. Contour drawn is the zero-meter contour for land elevation.

## Mustang Island, TX
## Probabilistic Submarine Landslide A
## Maximum Inundation Depth

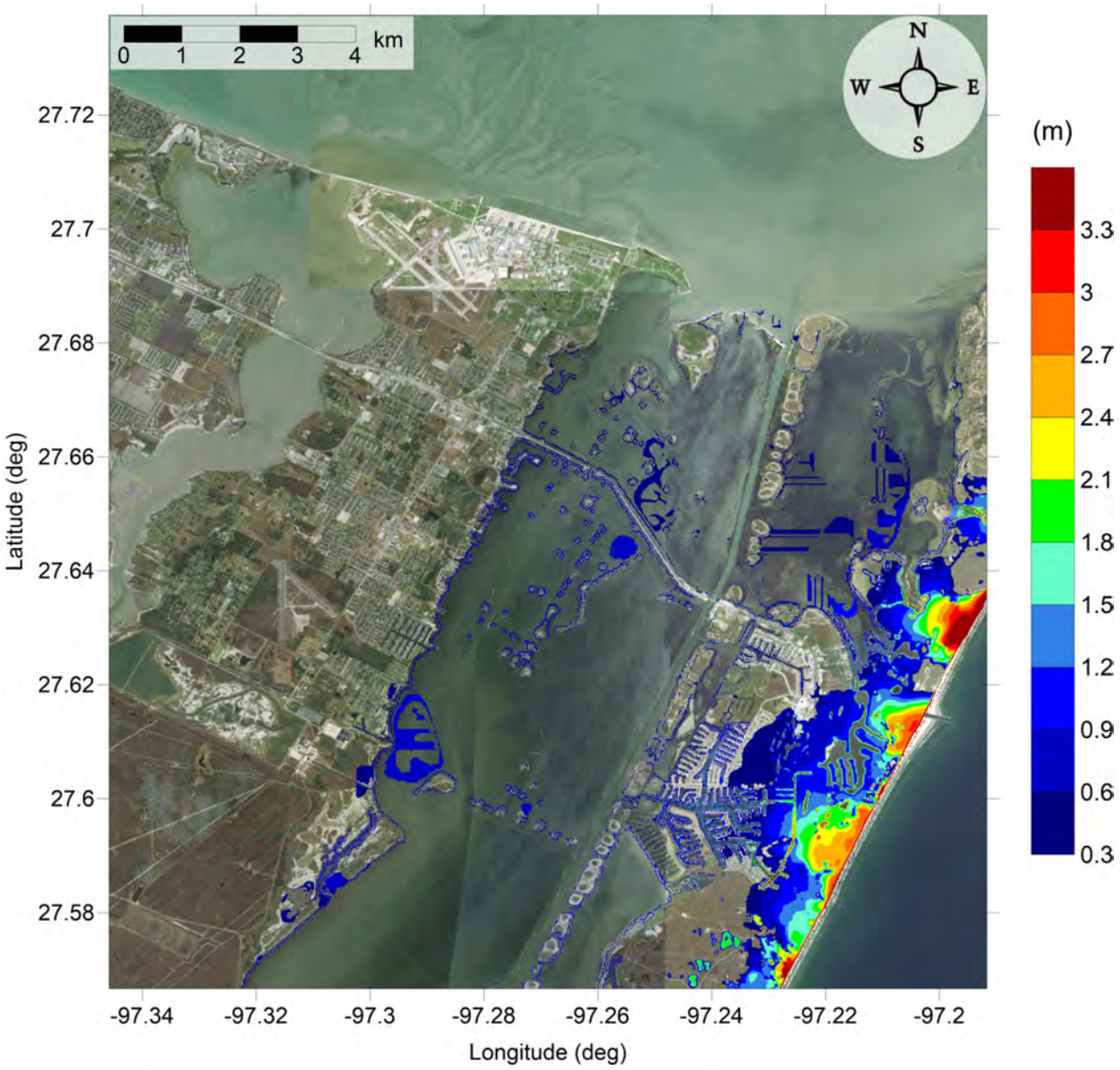


Figure 104: Maximum inundation depth (m) caused by the Probabilistic Submarine Landslide A in South-East Corpus Christi, TX. Contour drawn is the zero-meter contour for land elevation.

## Mustang Island, TX
## Probabilistic Submarine Landslide B1
## Maximum Momentum Flux

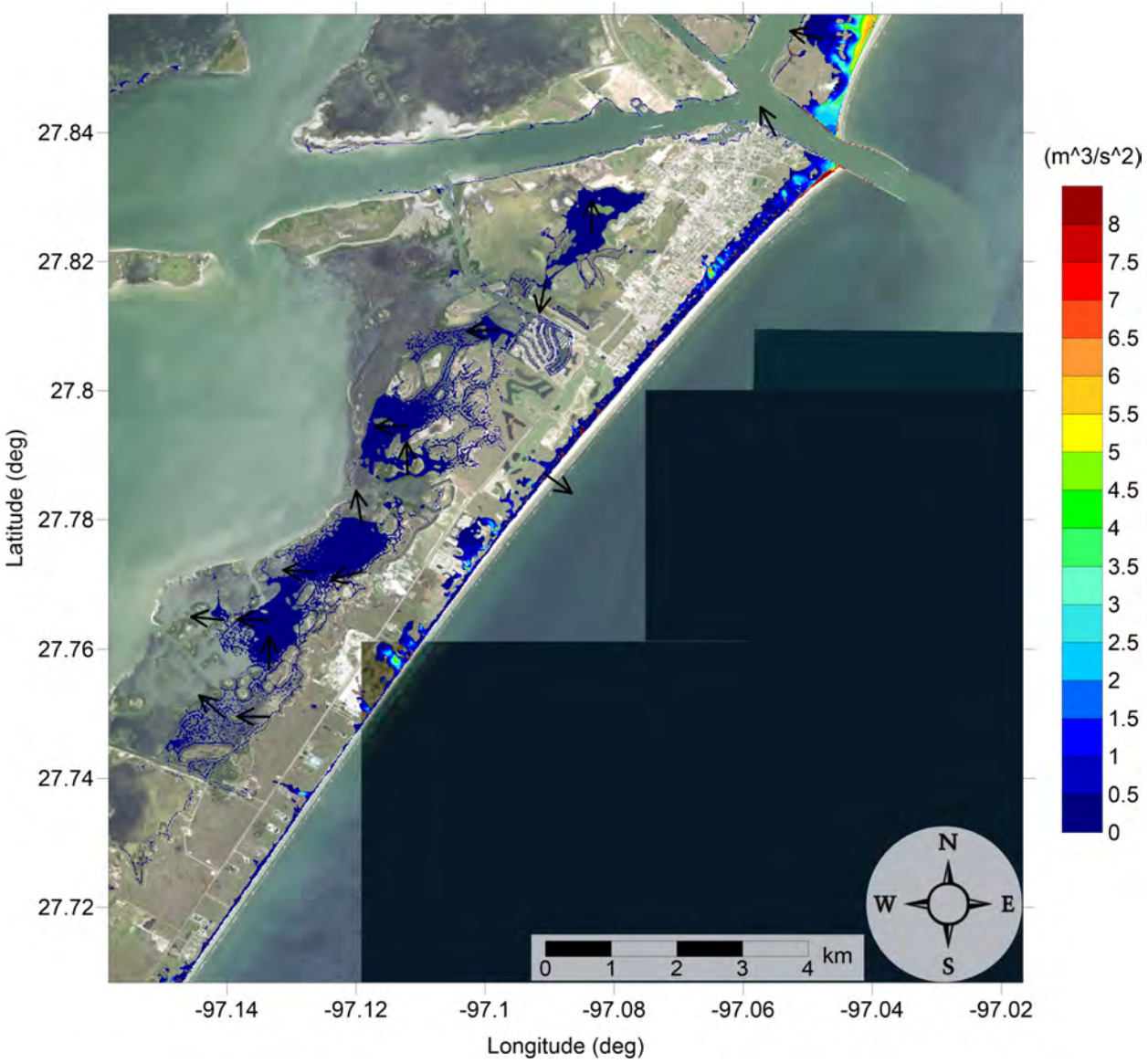


Figure 105: Maximum momentum flux ($m^3/s^2$) caused by the Probabilistic Submarine Landslide B1 in Port Aransas, TX. Arrows represent direction of maximum momentum flux. Contour drawn is the zero-meter contour for land elevation.

## Mustang Island, TX
## Probabilistic Submarine Landslide B1
## Maximum Momentum Flux

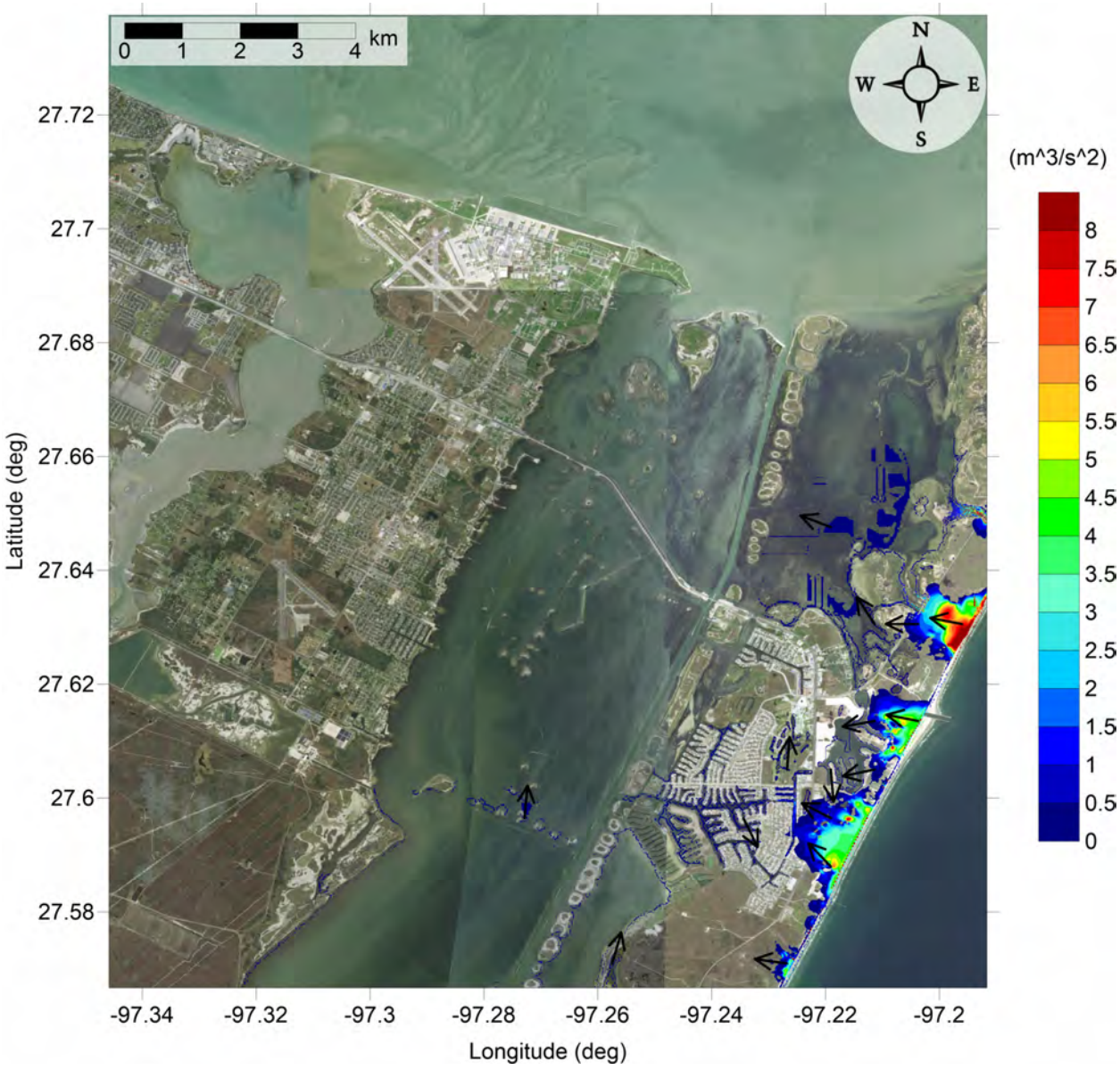


Figure 106: Maximum momentum flux ($m^3/s^2$) caused by the Probabilistic Submarine Landslide B1 in South-East Corpus Christi, TX. Arrows represent direction of maximum momentum flux. Contour drawn is the zero-meter contour for land elevation.

## Mustang Island, TX
## Probabilistic Submarine Landslide B1
## Maximum Inundation Depth

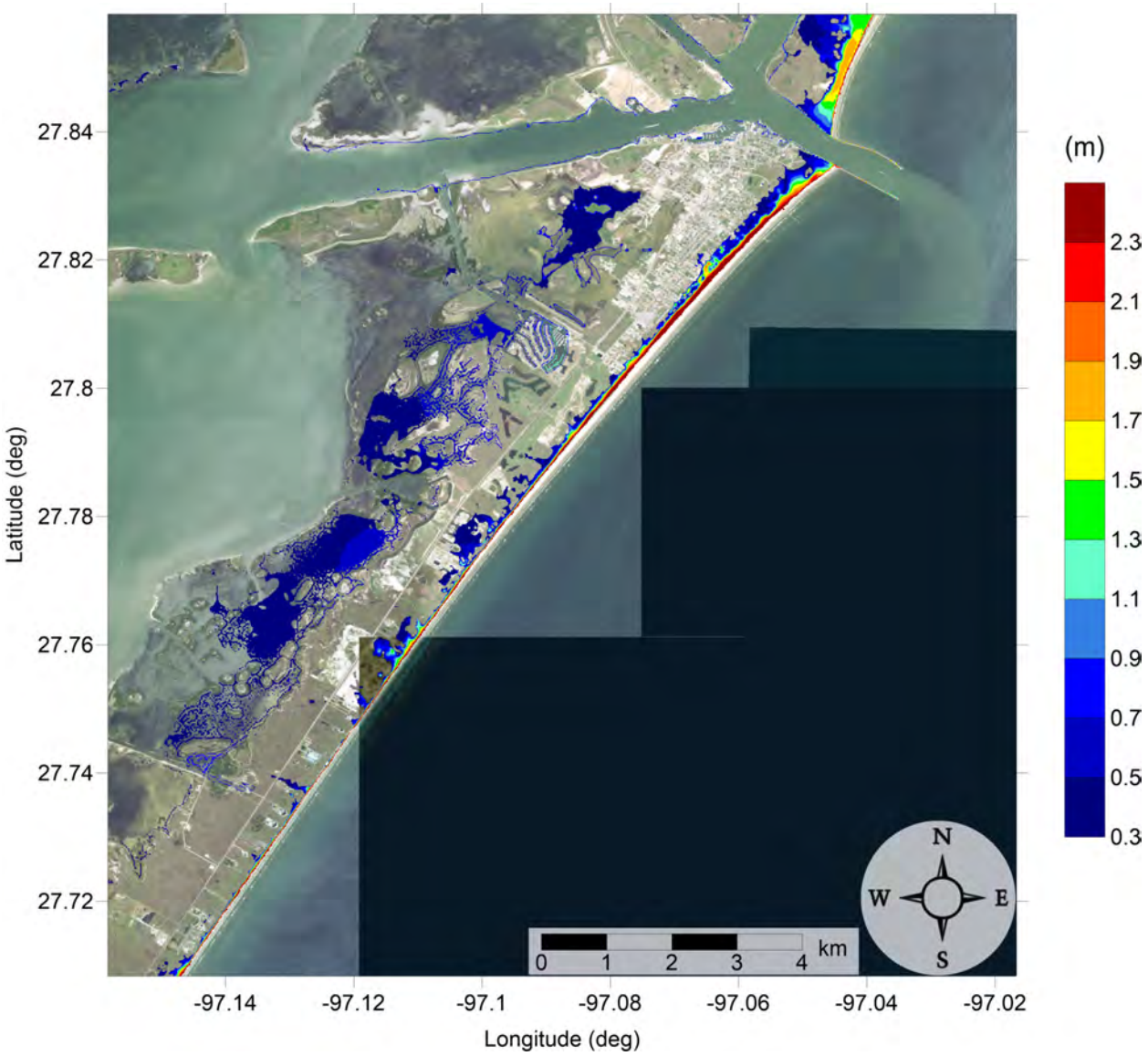


Figure 107: Maximum inundation depth (m) caused by the Probabilistic Submarine Landslide B1 in Port Aransas, TX. Contour drawn is the zero-meter contour for land elevation.

## Mustang Island, TX
## Probabilistic Submarine Landslide B1
## Maximum Inundation Depth

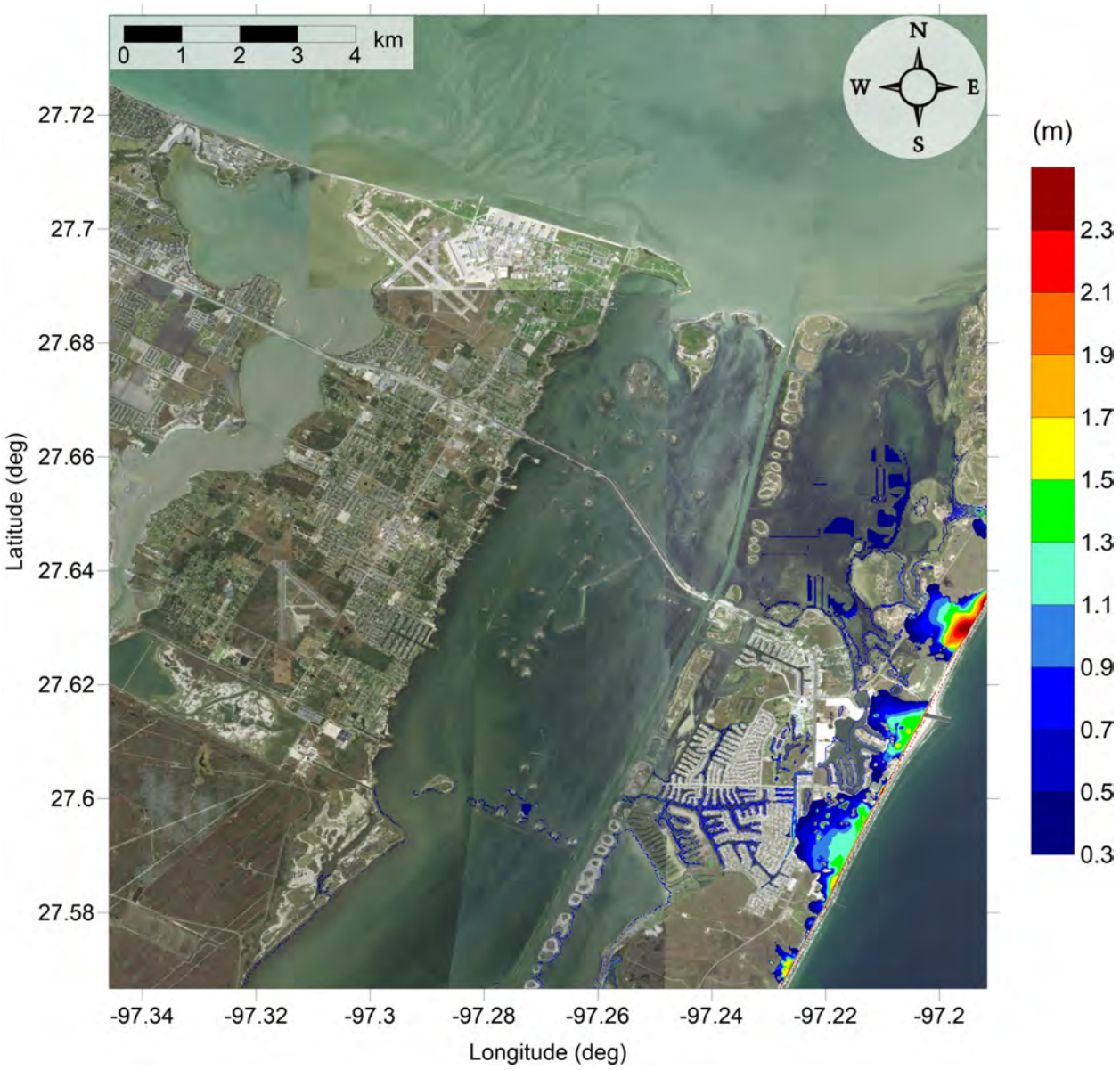


Figure 108: Maximum inundation depth (m) caused by the Probabilistic Submarine Landslide B1 in South-East Corpus Christi, TX. Contour drawn is the zero-meter contour for land elevation.

## Mustang Island, TX
## Probabilistic Submarine Landslide B2
## Maximum Momentum Flux

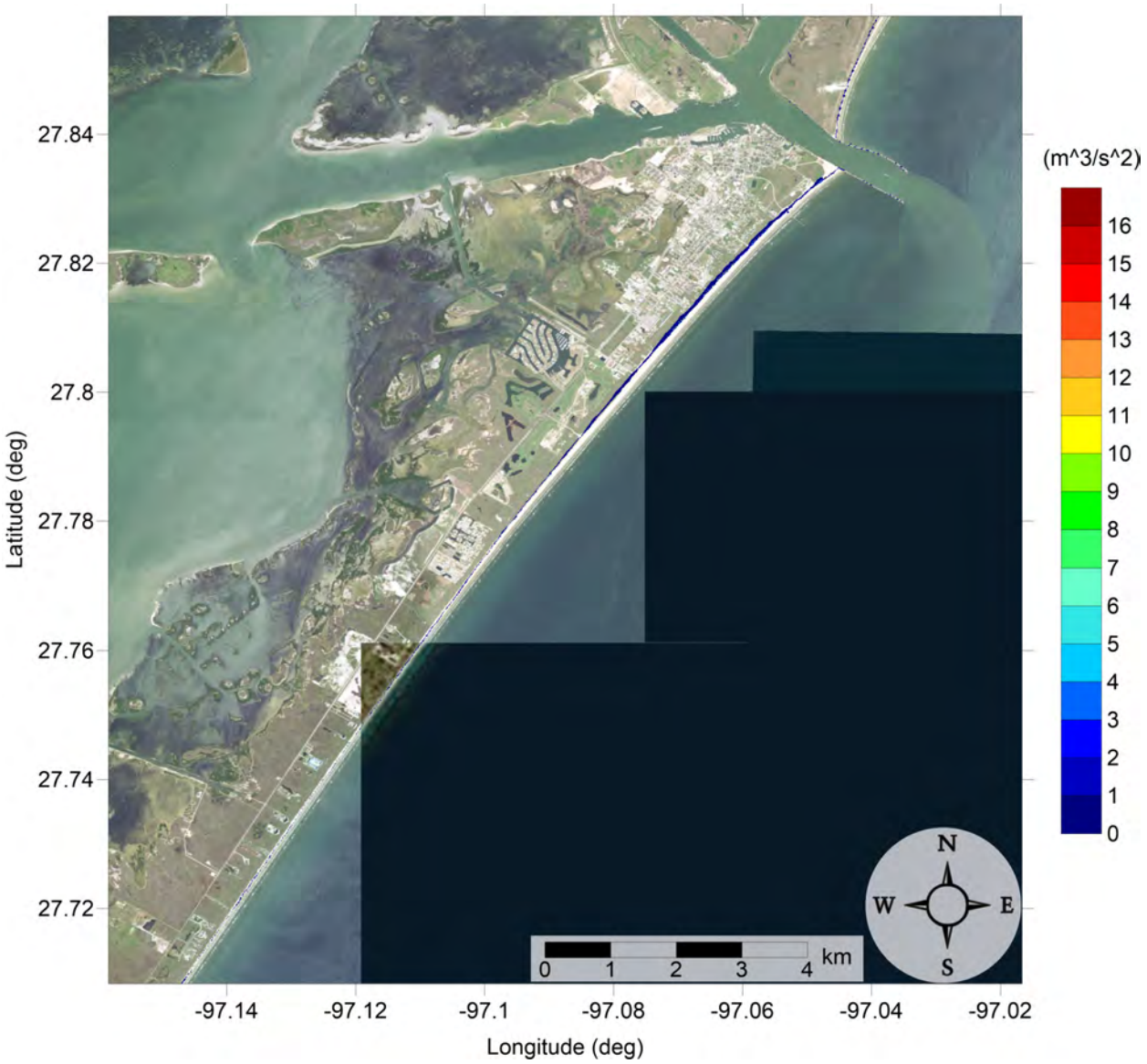


Figure 109: Maximum momentum flux ($m^3/s^2$) caused by the Probabilistic Submarine Landslide B2 in Port Aransas, TX. Arrows represent direction of maximum momentum flux. Contour drawn is the zero-meter contour for land elevation.

## Mustang Island, TX
## Probabilistic Submarine Landslide B2
## Maximum Momentum Flux

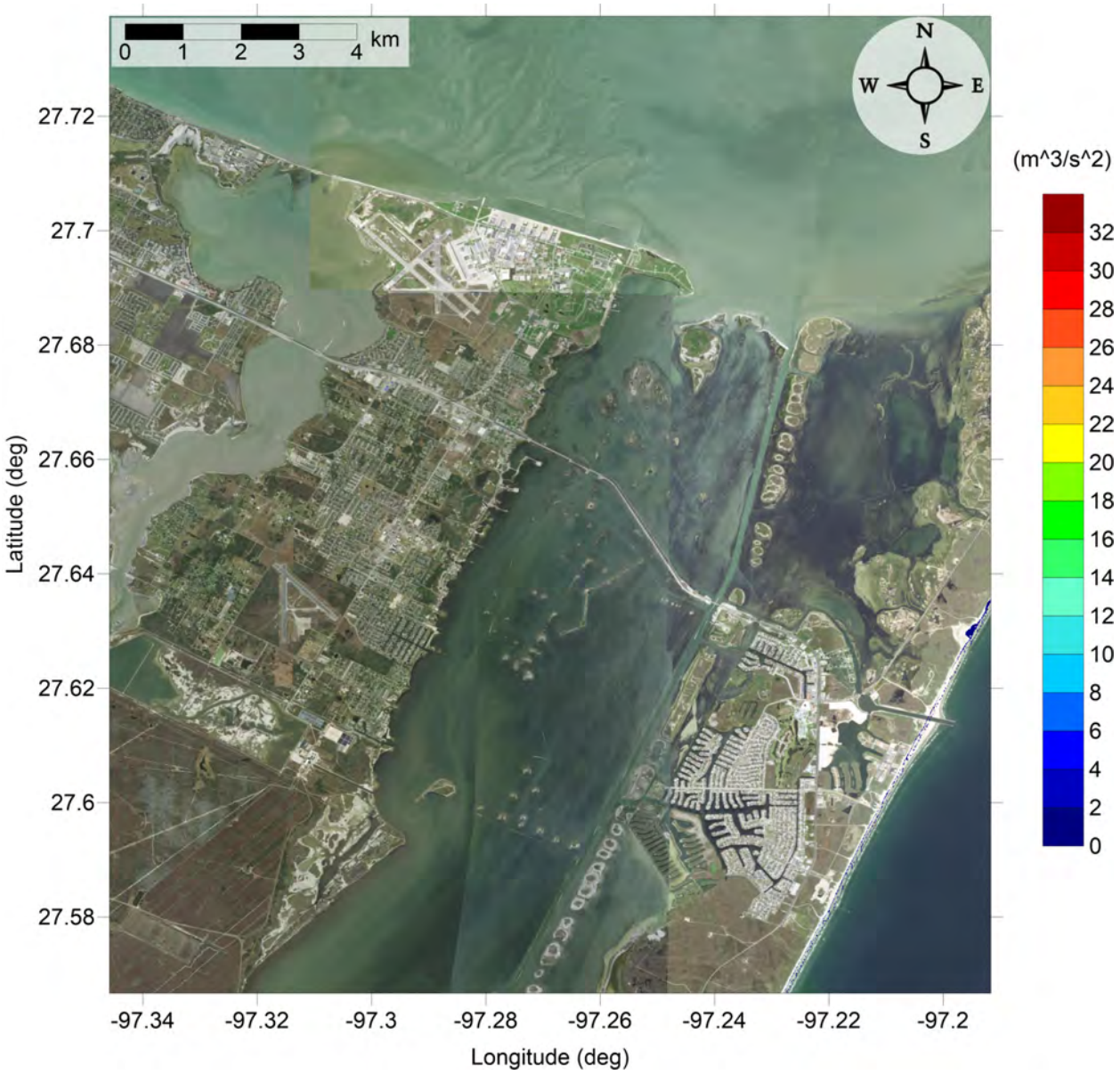


Figure 110: Maximum momentum flux ($m^3/s^2$) caused by the Probabilistic Submarine Landslide B2 in South-East Corpus Christi, TX. Arrows represent direction of maximum momentum flux. Contour drawn is the zero-meter contour for land elevation.

## Mustang Island, TX
## Probabilistic Submarine Landslide B2
## Maximum Inundation Depth

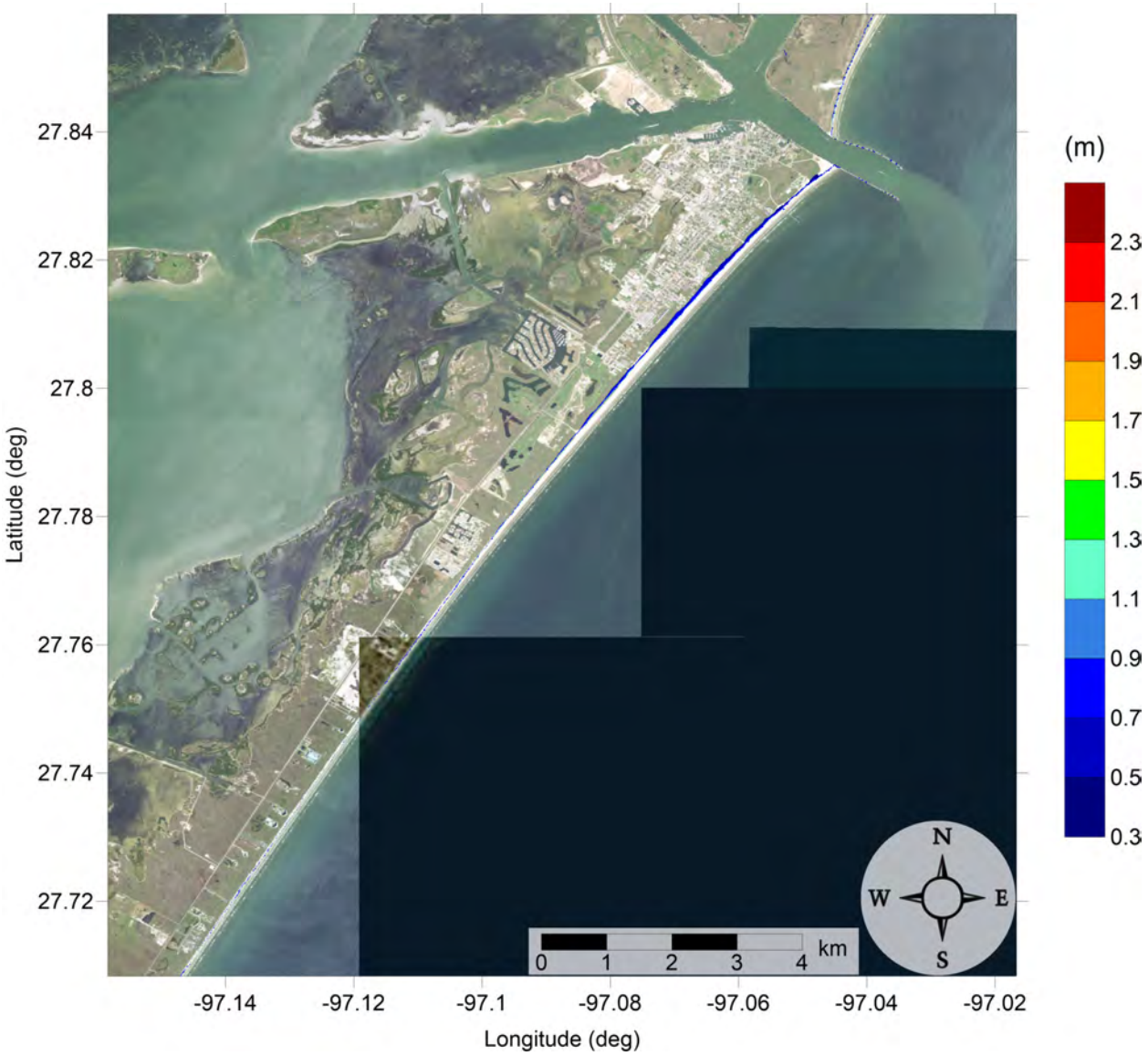


Figure 111: Maximum inundation depth (m) caused by the Probabilistic Submarine Landslide B2 in Port Aransas, TX. Contour drawn is the zero-meter contour for land elevation.

## Mustang Island, TX
## Probabilistic Submarine Landslide B2
## Maximum Inundation Depth

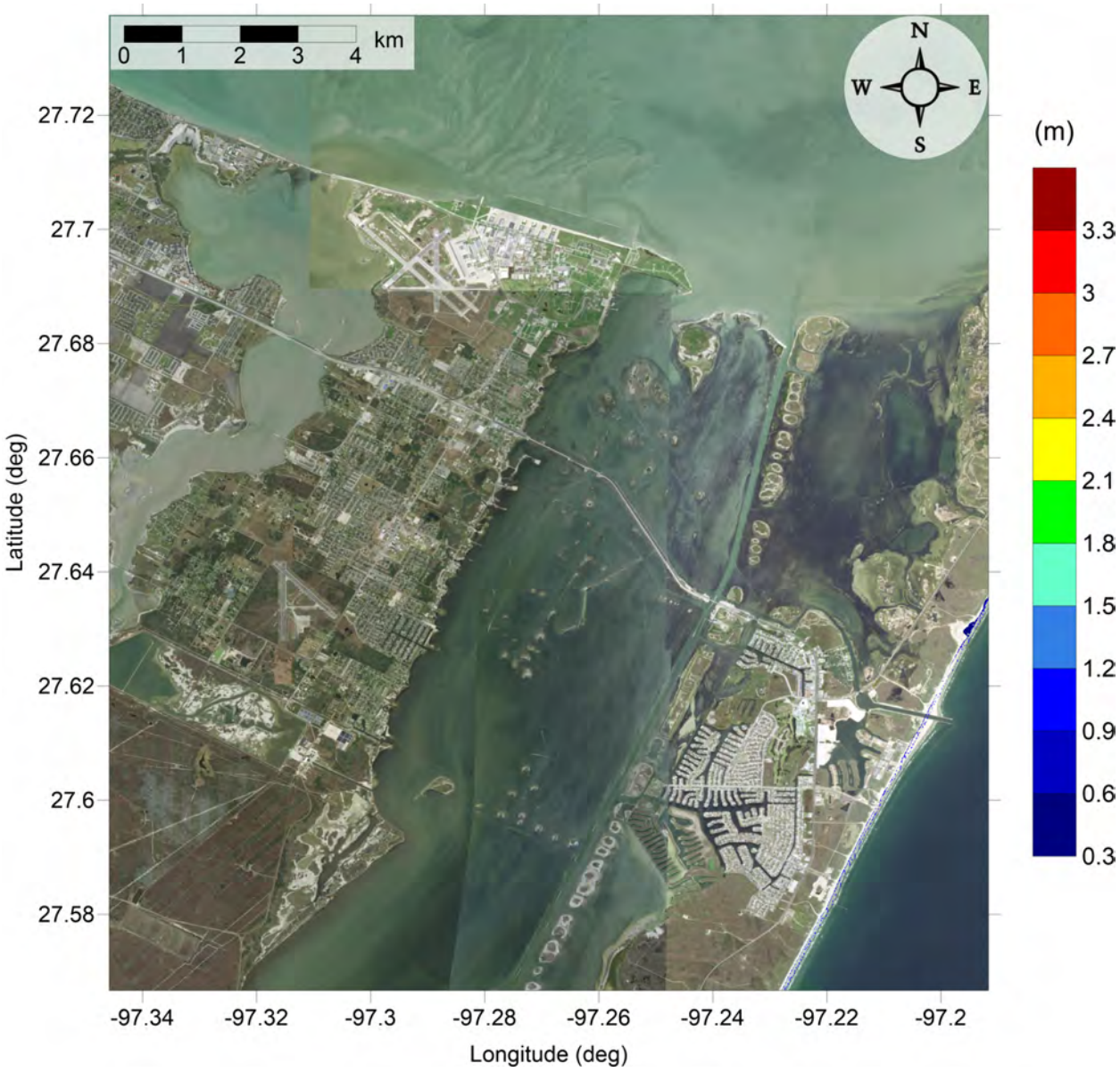


Figure 112: Maximum inundation depth (m) caused by the Probabilistic Submarine Landslide B2 in South-East Corpus Christi, TX. Contour drawn is the zero-meter contour for land elevation.

## Mustang Island, TX
## Mississippi Canyon submarine landslide
## Maximum Momentum Flux

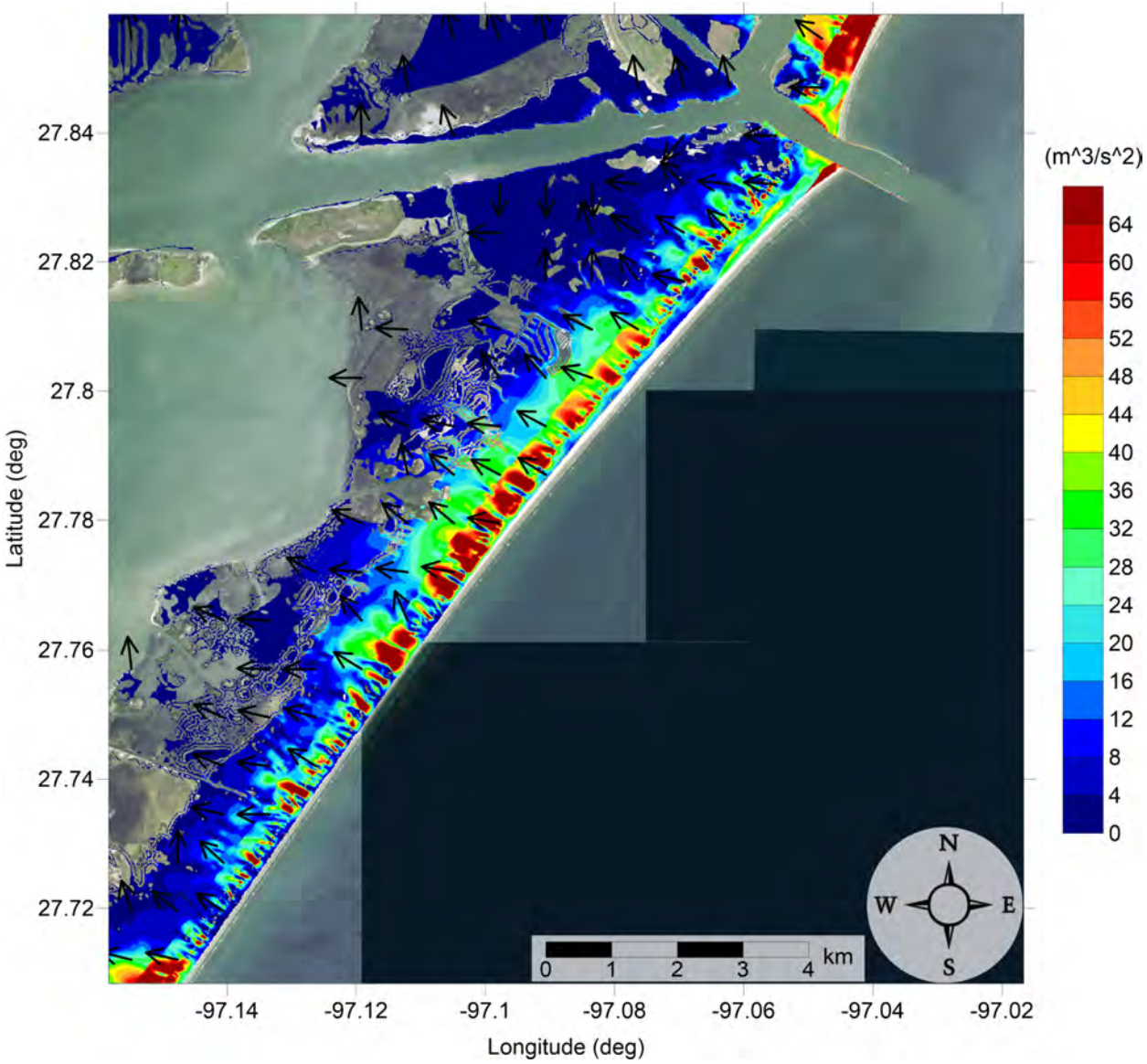


Figure 113: Maximum momentum flux ($m^3/s^2$) caused by the Mississippi Canyon submarine landslide in Port Aransas, TX. Arrows represent direction of maximum momentum flux. Contour drawn is the zero-meter contour for land elevation.

## Mustang Island, TX
## Mississippi Canyon submarine landslide
## Maximum Momentum Flux

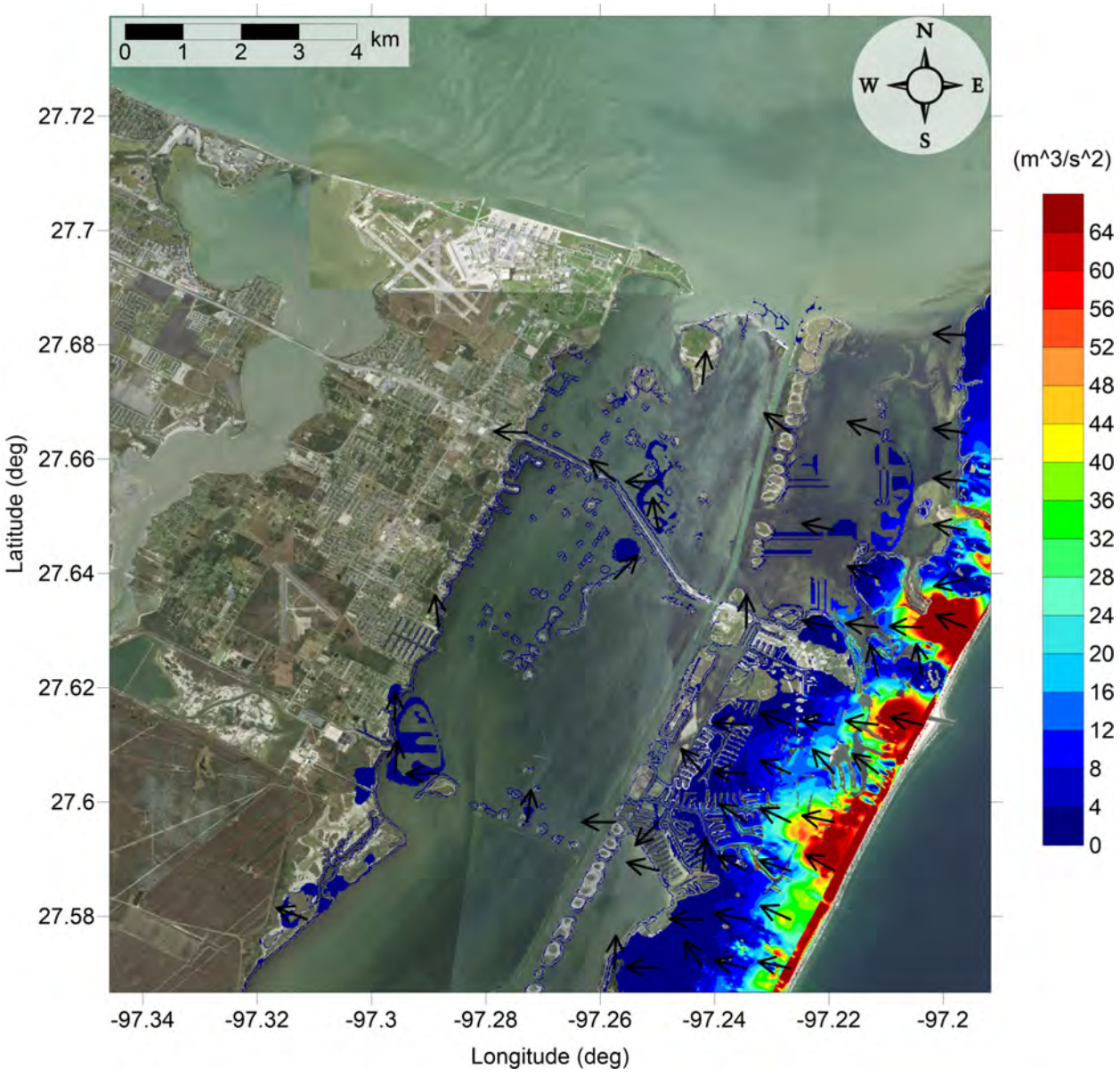


Figure 114: Maximum momentum flux ($m^3/s^2$) caused by the Mississippi Canyon submarine landslide in South-East Corpus Christi, TX. Arrows represent direction of maximum momentum flux. Contour drawn is the zero-meter contour for land elevation.

## Mustang Island, TX
## Mississippi Canyon submarine landslide
## Maximum Inundation Depth

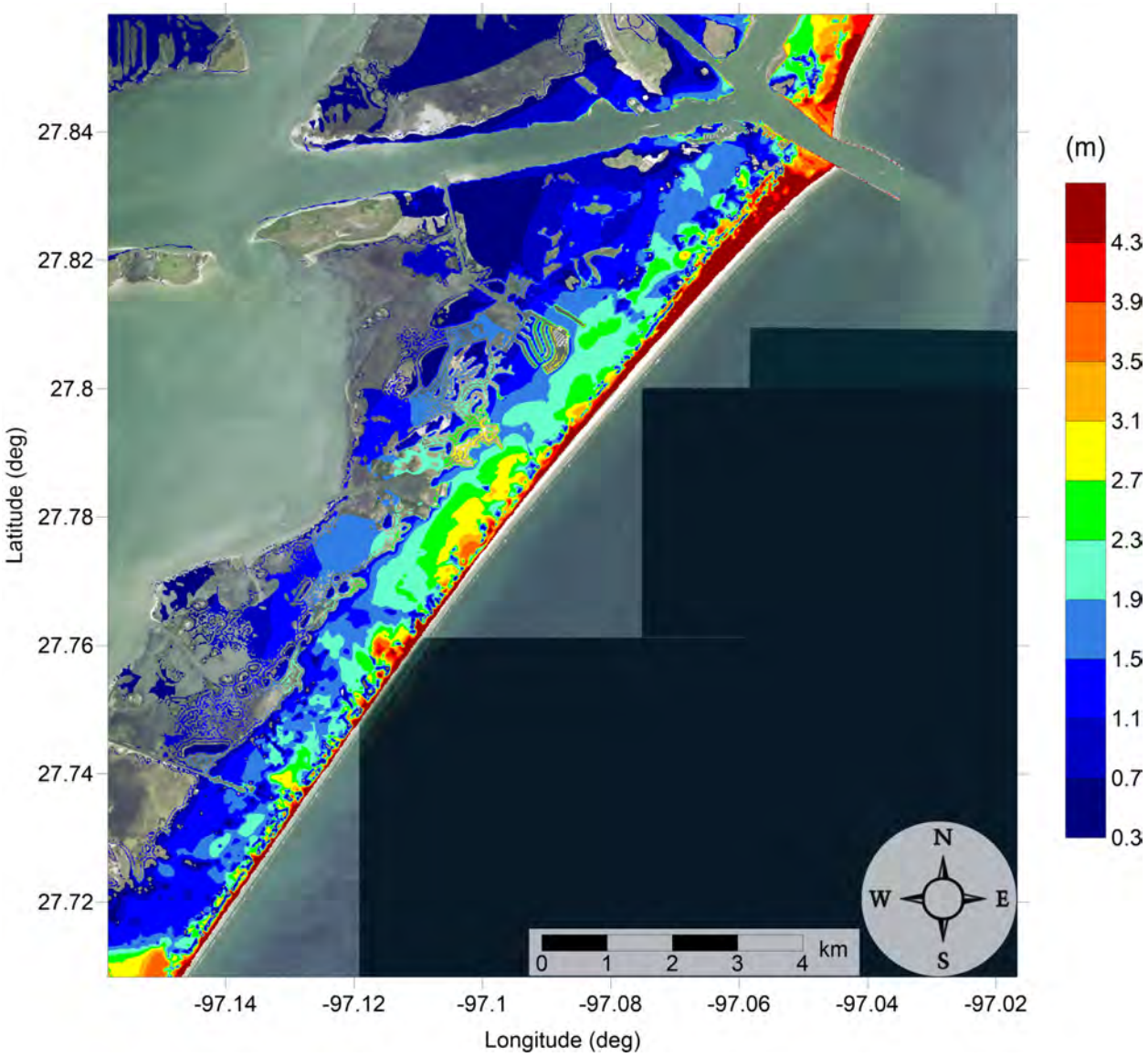


Figure 115: Maximum inundation depth (m) caused by the Mississippi Canyon submarine landslide in Port Aransas, TX. Contour drawn is the zero-meter contour for land elevation.

## Mustang Island, TX
## Mississippi Canyon submarine landslide
## Maximum Inundation Depth

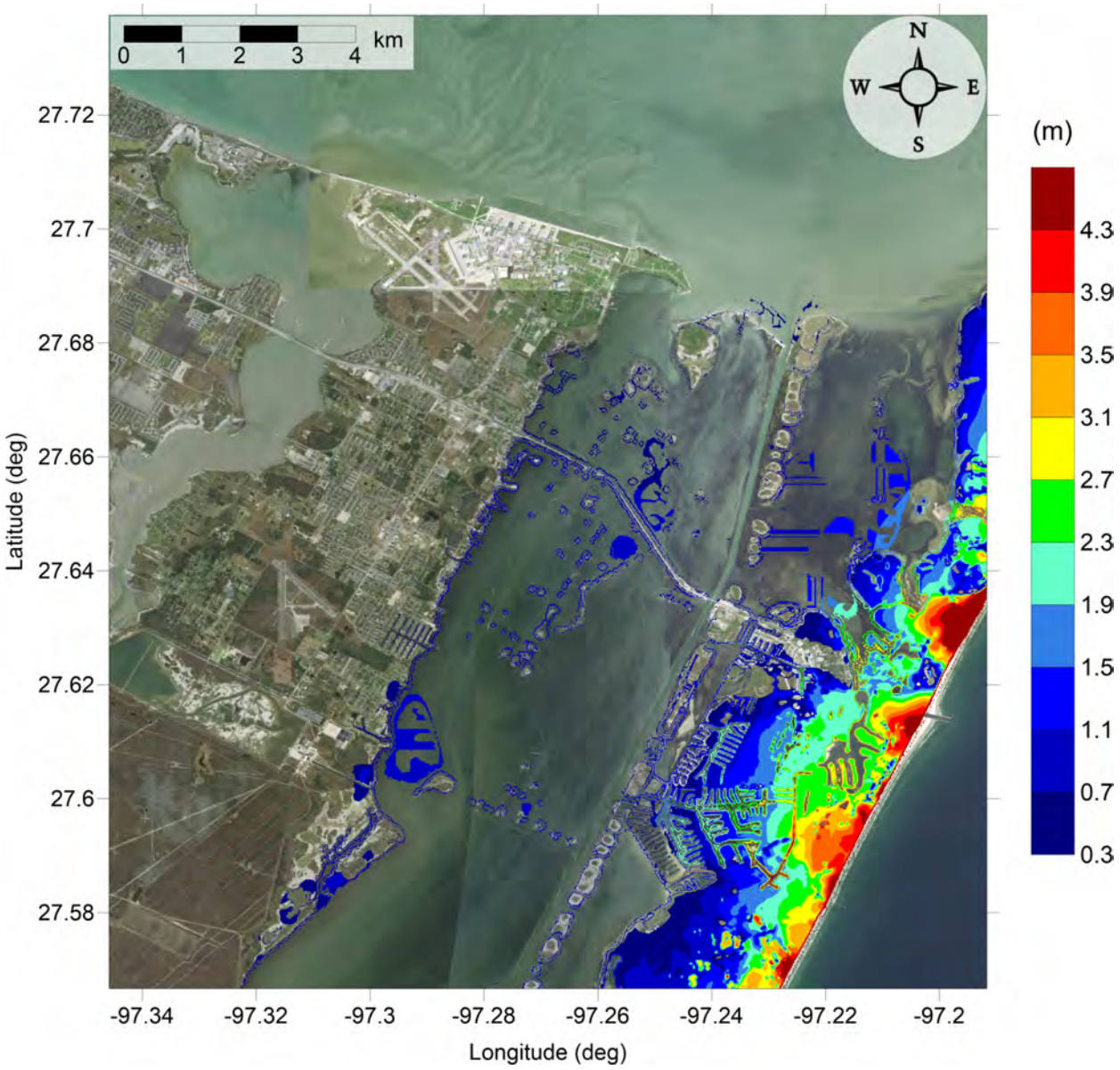


Figure 116: Maximum inundation depth (m) caused by the Mississippi Canyon submarine landslide in South-East Corpus Christi, TX. Contour drawn is the zero-meter contour for land elevation.

## Mustang Island, TX
## Probabilistic Submarine Landslide C
## Maximum Momentum Flux

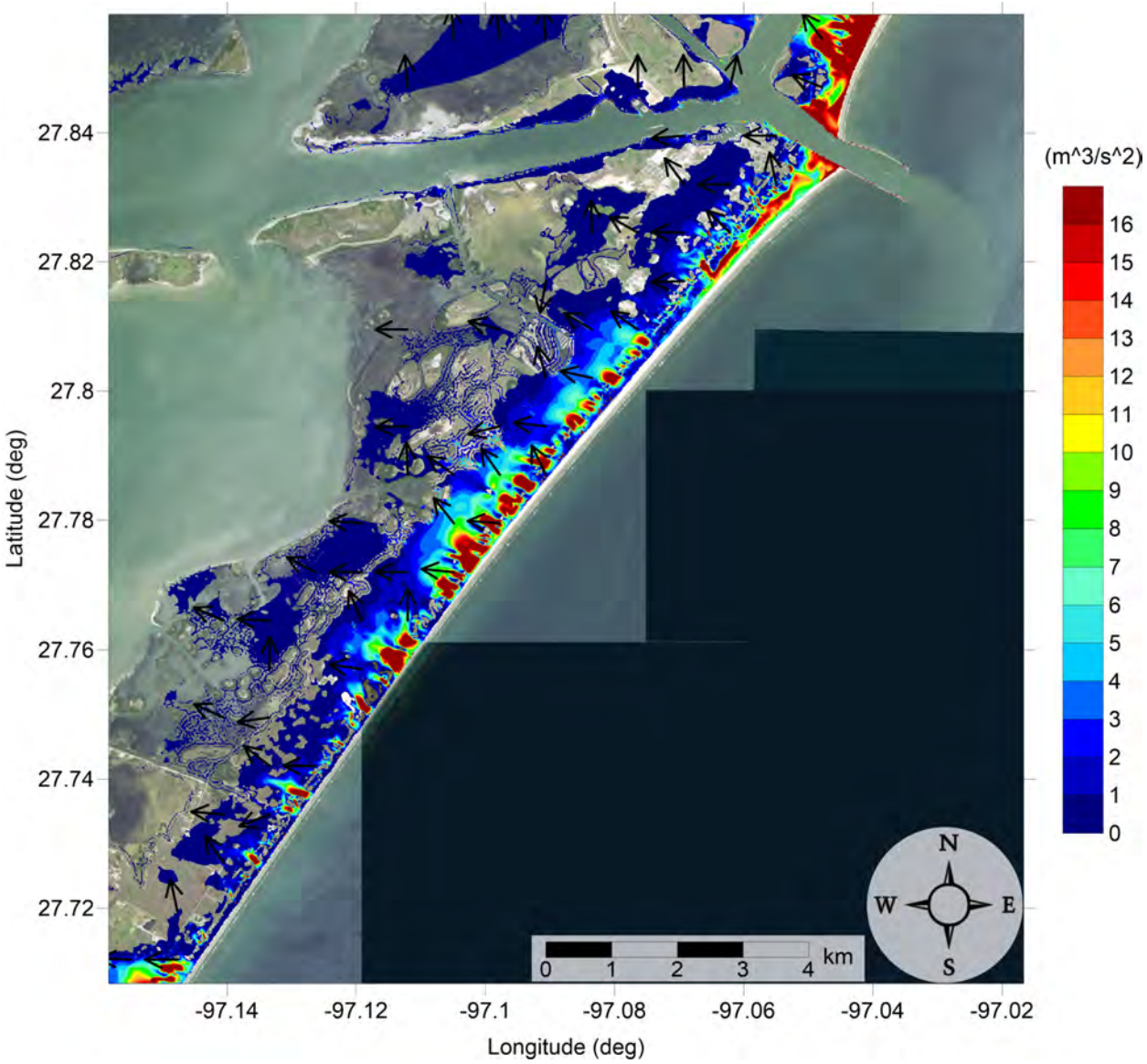


Figure 117: Maximum momentum flux ($m^3/s^2$) caused by the Probabilistic Submarine Landslide C in Port Aransas, TX. Arrows represent direction of maximum momentum flux. Contour drawn is the zero-meter contour for land elevation.

## Mustang Island, TX
## Probabilistic Submarine Landslide C
## Maximum Momentum Flux

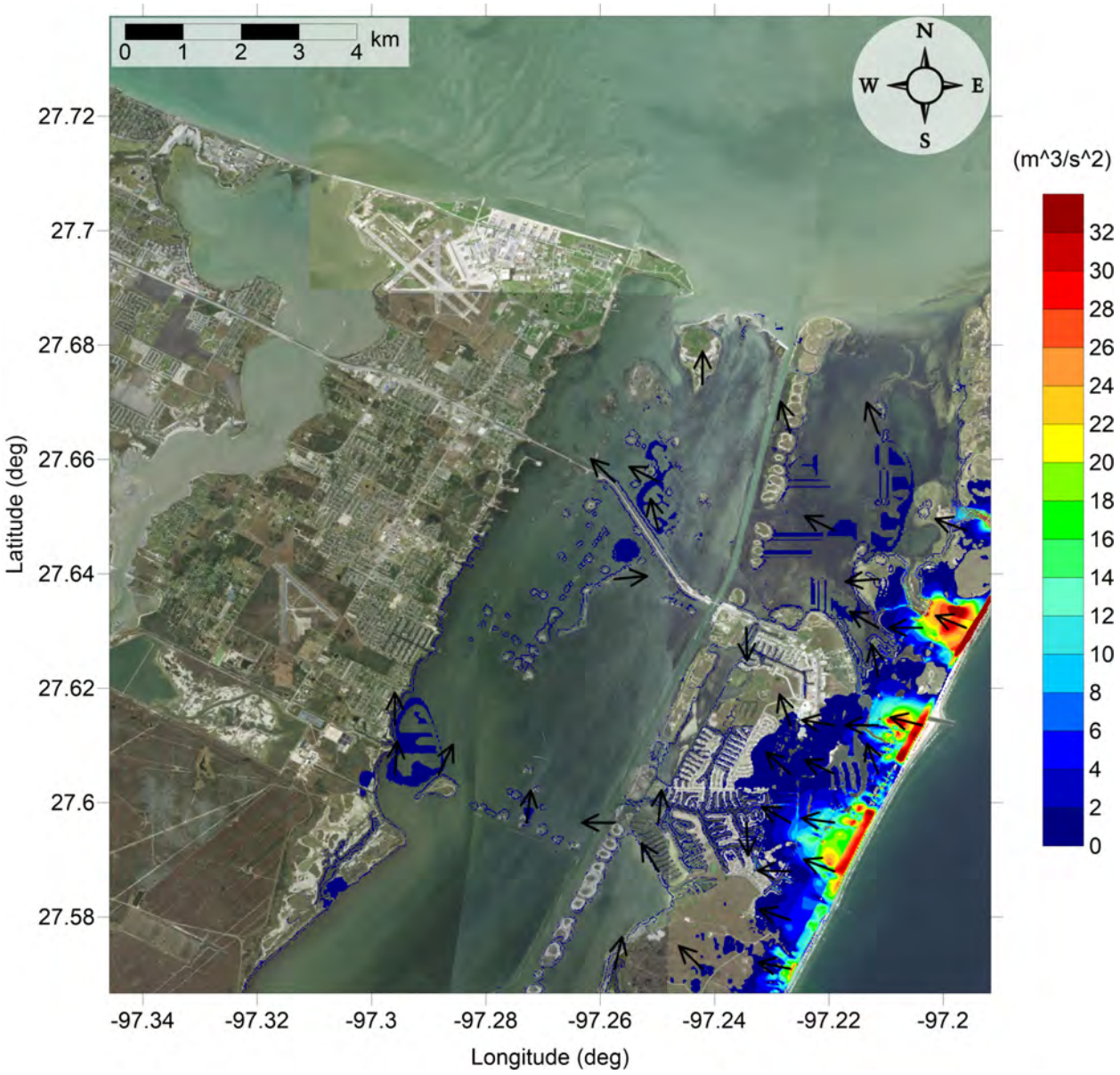


Figure 118: Maximum momentum flux ($m^3/s^2$) caused by the Probabilistic Submarine Landslide C in South-East Corpus Christi, TX. Arrows represent direction of maximum momentum flux. Contour drawn is the zero-meter contour for land elevation.

## Mustang Island, TX
## Probabilistic Submarine Landslide C
## Maximum Inundation Depth

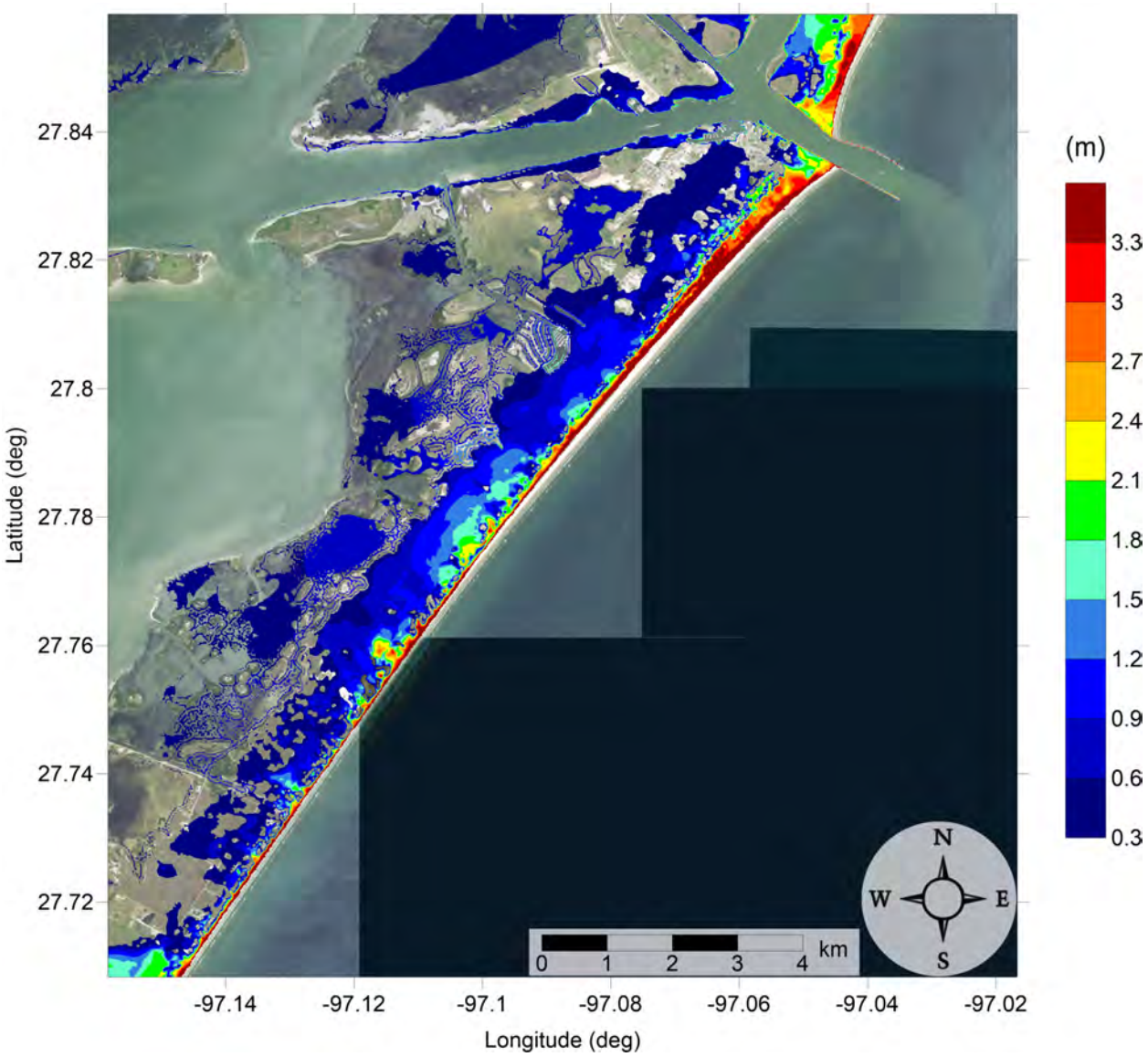


Figure 119: Maximum inundation depth (m) caused by the Probabilistic Submarine Landslide C in Port Aransas, TX. Contour drawn is the zero-meter contour for land elevation.

## Mustang Island, TX
## Probabilistic Submarine Landslide C
## Maximum Inundation Depth

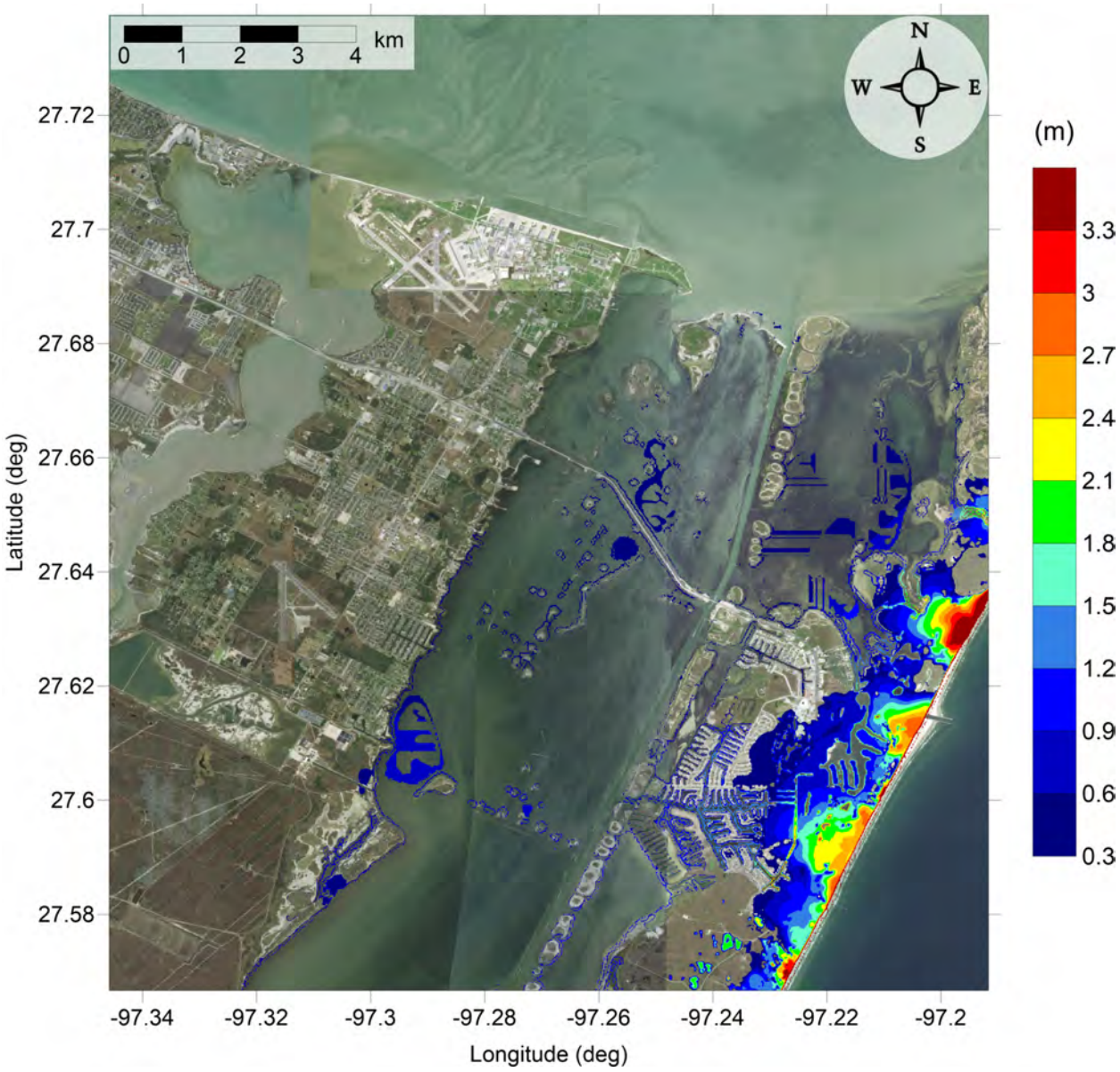


Figure 120: Maximum inundation depth (m) caused by the Probabilistic Submarine Landslide C in South-East Corpus Christi, TX. Contour drawn is the zero-meter contour for land elevation.

## Mustang Island, TX
## West Florida submarine landslide
## Maximum Momentum Flux

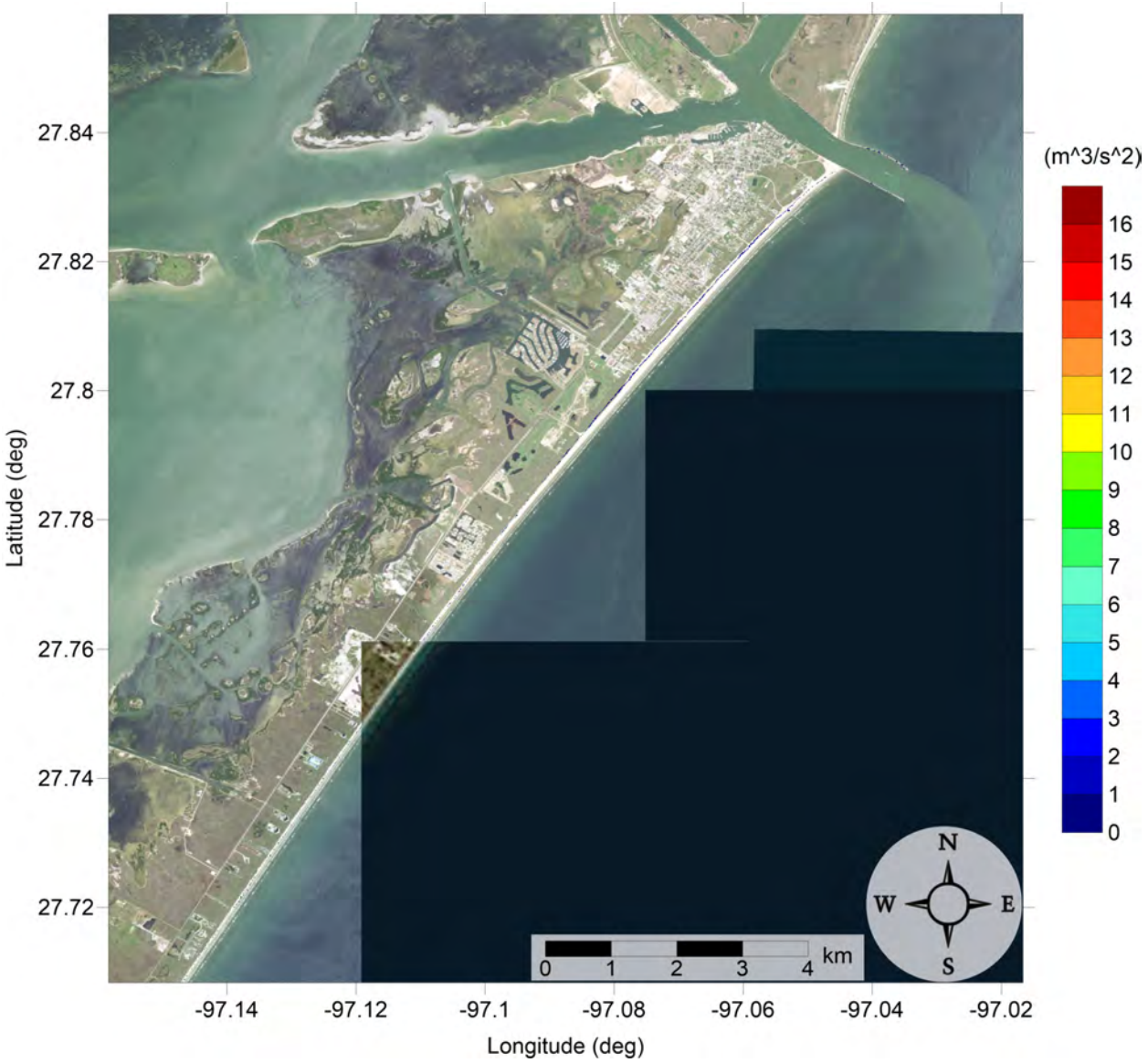


Figure 121: Maximum momentum flux ($m^3/s^2$) caused by the West Florida submarine landslide in Port Aransas, TX. Arrows represent direction of maximum momentum flux. Contour drawn is the zero-meter contour for land elevation.

**Mustang Island, TX**
**West Florida submarine landslide**
**Maximum Momentum Flux**

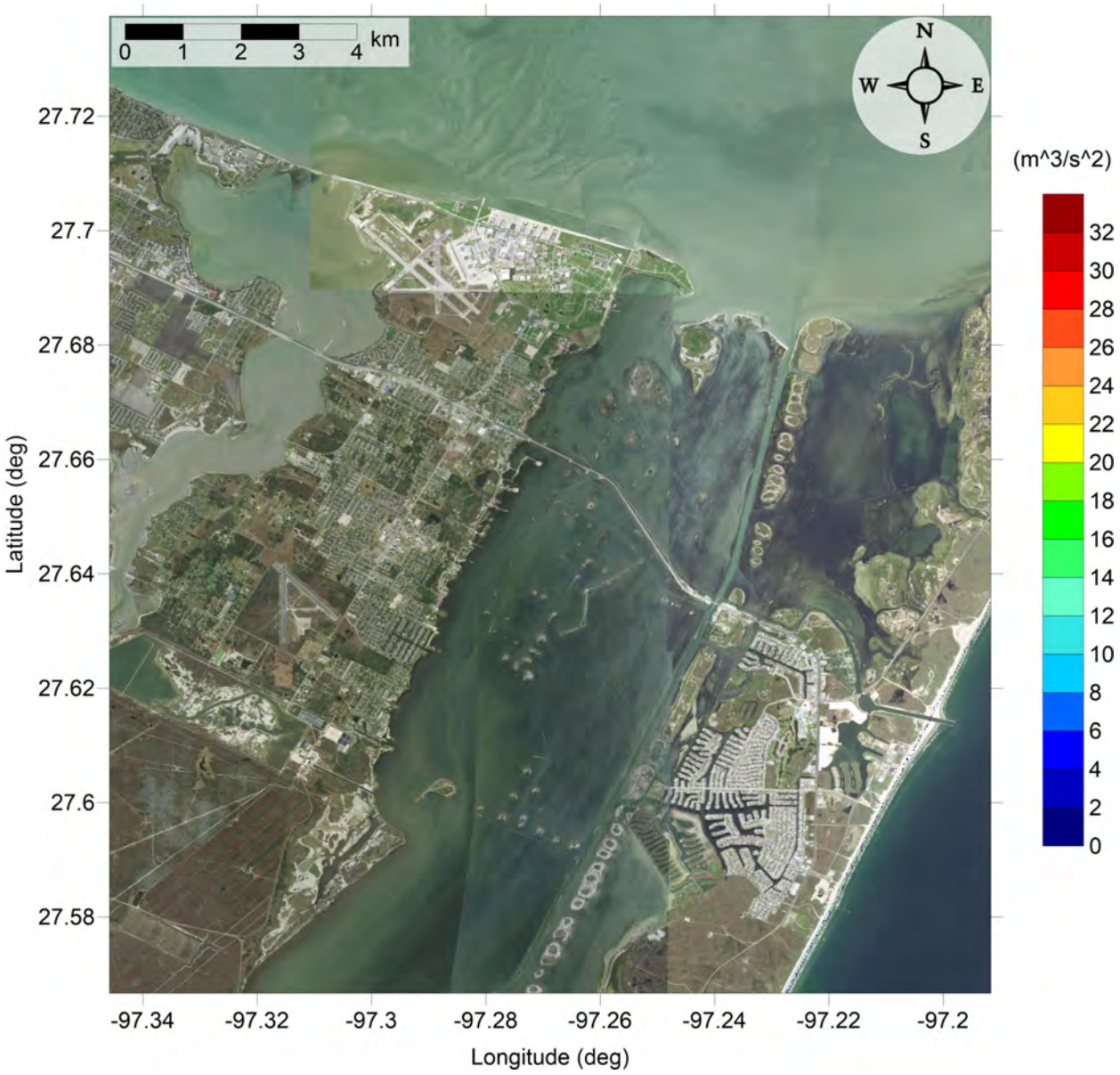


Figure 122: Maximum momentum flux ($m^3/s^2$) caused by the West Florida submarine landslide in South-East Corpus Christi, TX. Arrows represent direction of maximum momentum flux. Contour drawn is the zero-meter contour for land elevation.

**Mustang Island, TX**
**West Florida submarine landslide**
**Maximum Inundation Depth**

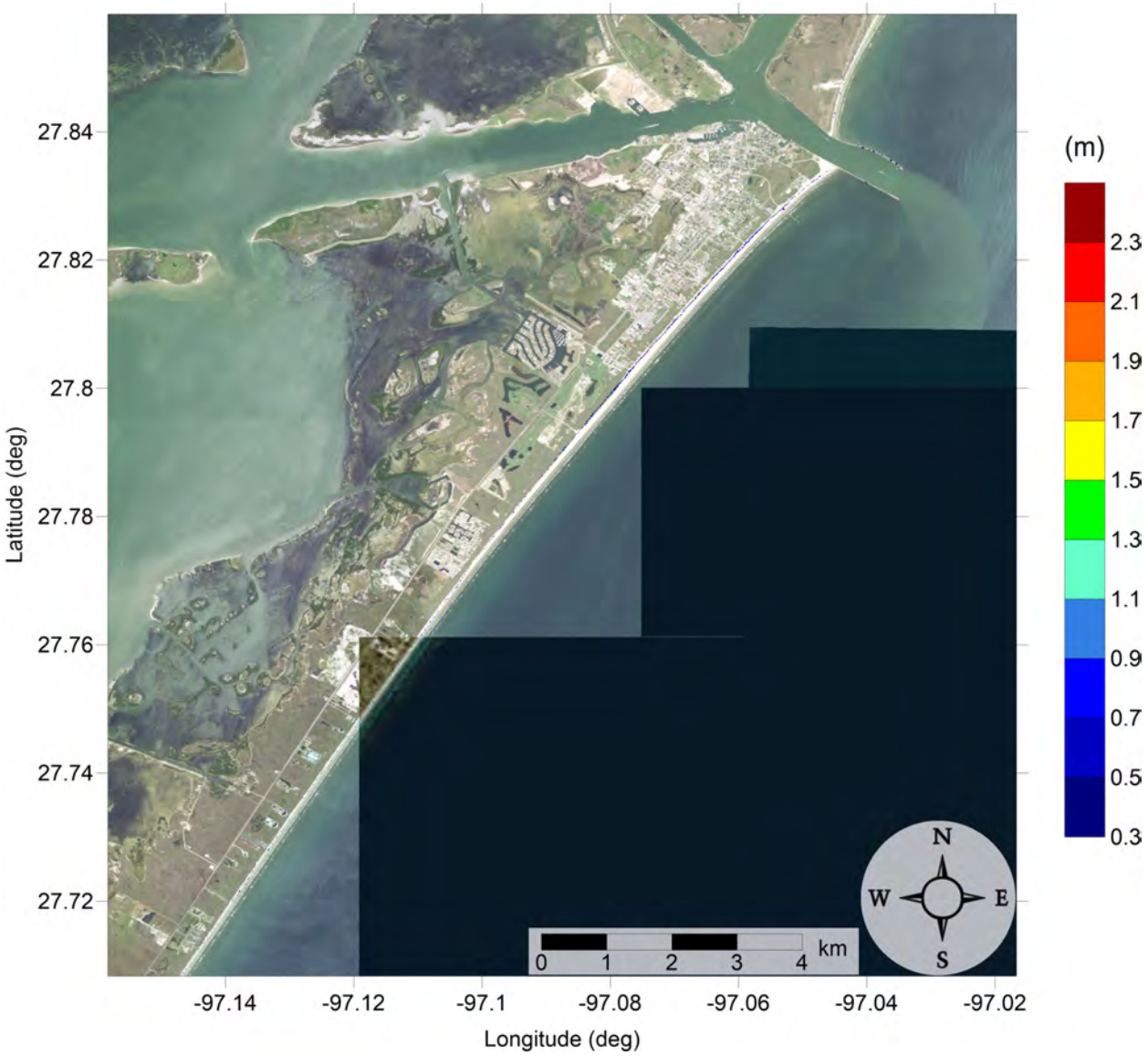


Figure 123: Maximum inundation depth (m) caused by the West Florida submarine landslide in Port Aransas, TX. Contour drawn is the zero-meter contour for land elevation.

## Mustang Island, TX
## West Florida submarine landslide
## Maximum Inundation Depth

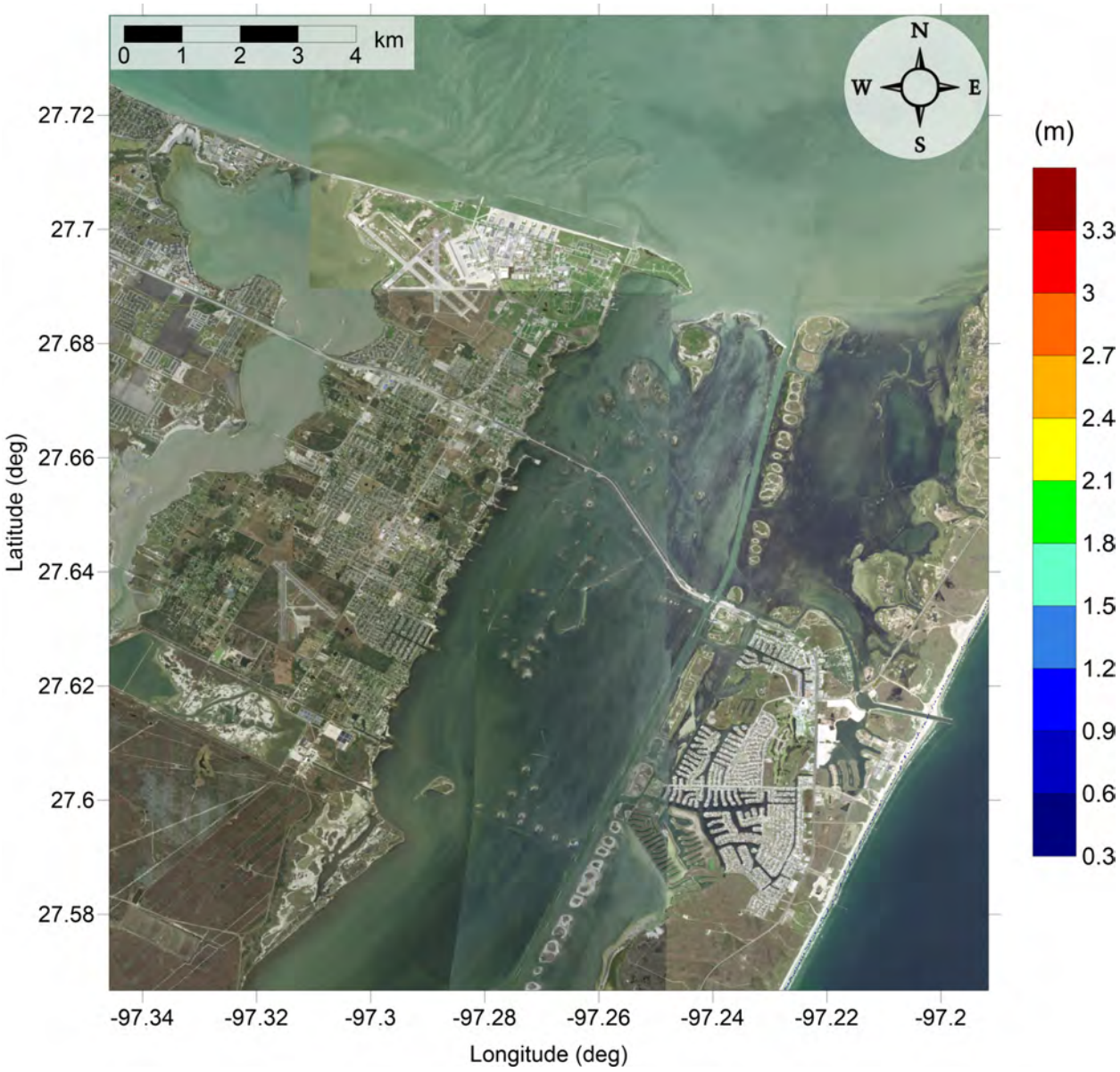


Figure 124: Maximum inundation depth (m) caused by the West Florida submarine landslide in South-East Corpus Christi, TX. Contour drawn is the zero-meter contour for land elevation.

## Mustang Island, TX
## All Sources
## Maximum of Maximum Inundation Depth

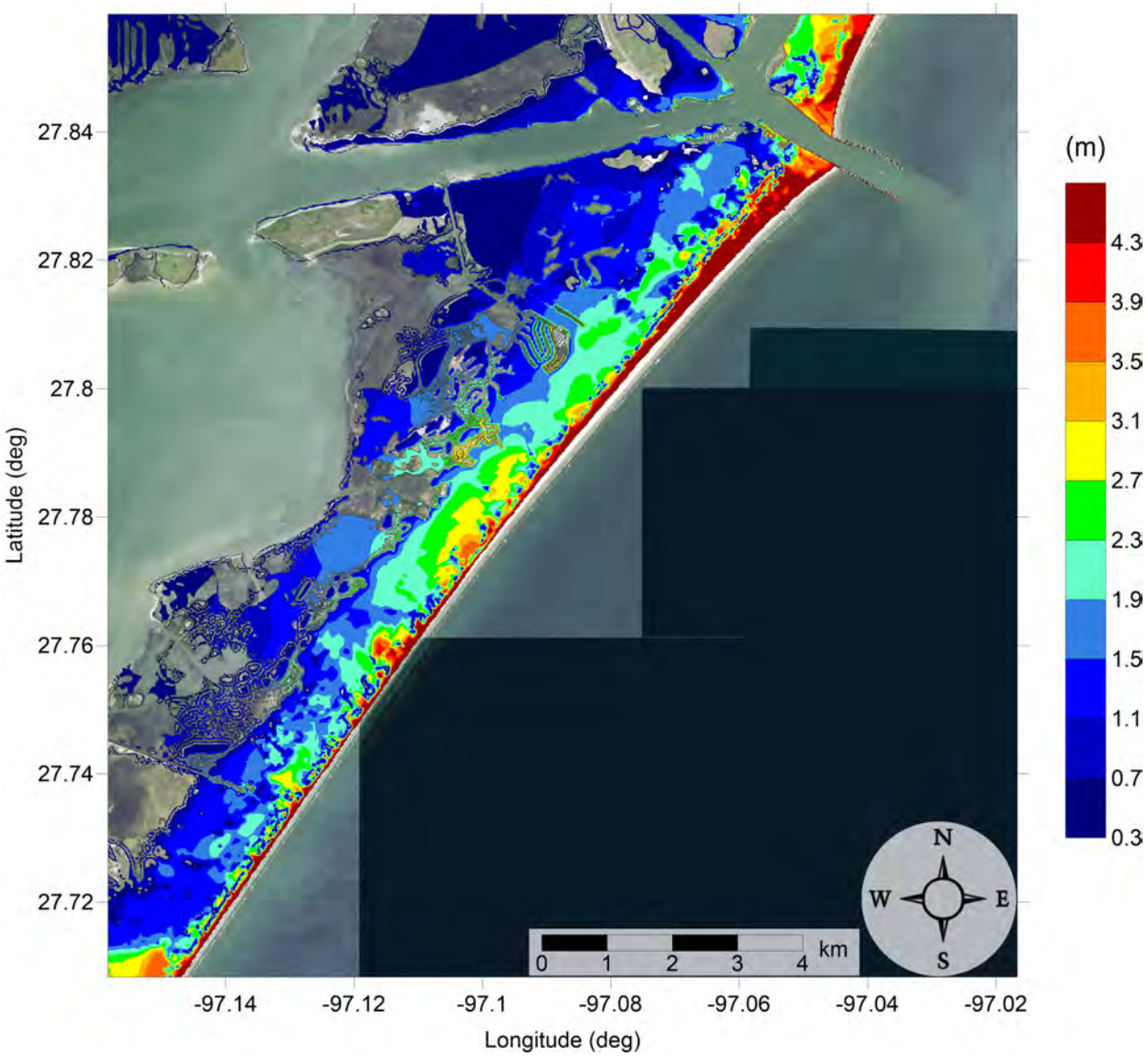


Figure 125: Maximum of maximums inundation depth (m) in Port Aransas, TX, calculated as the maximum inundation depth in each grid cell from an ensemble of all tsunami sources considered. Contour drawn is the zero-meter contour for land elevation.

## Mustang Island, TX
## All Sources
## Maximum Inundation Depth by Source

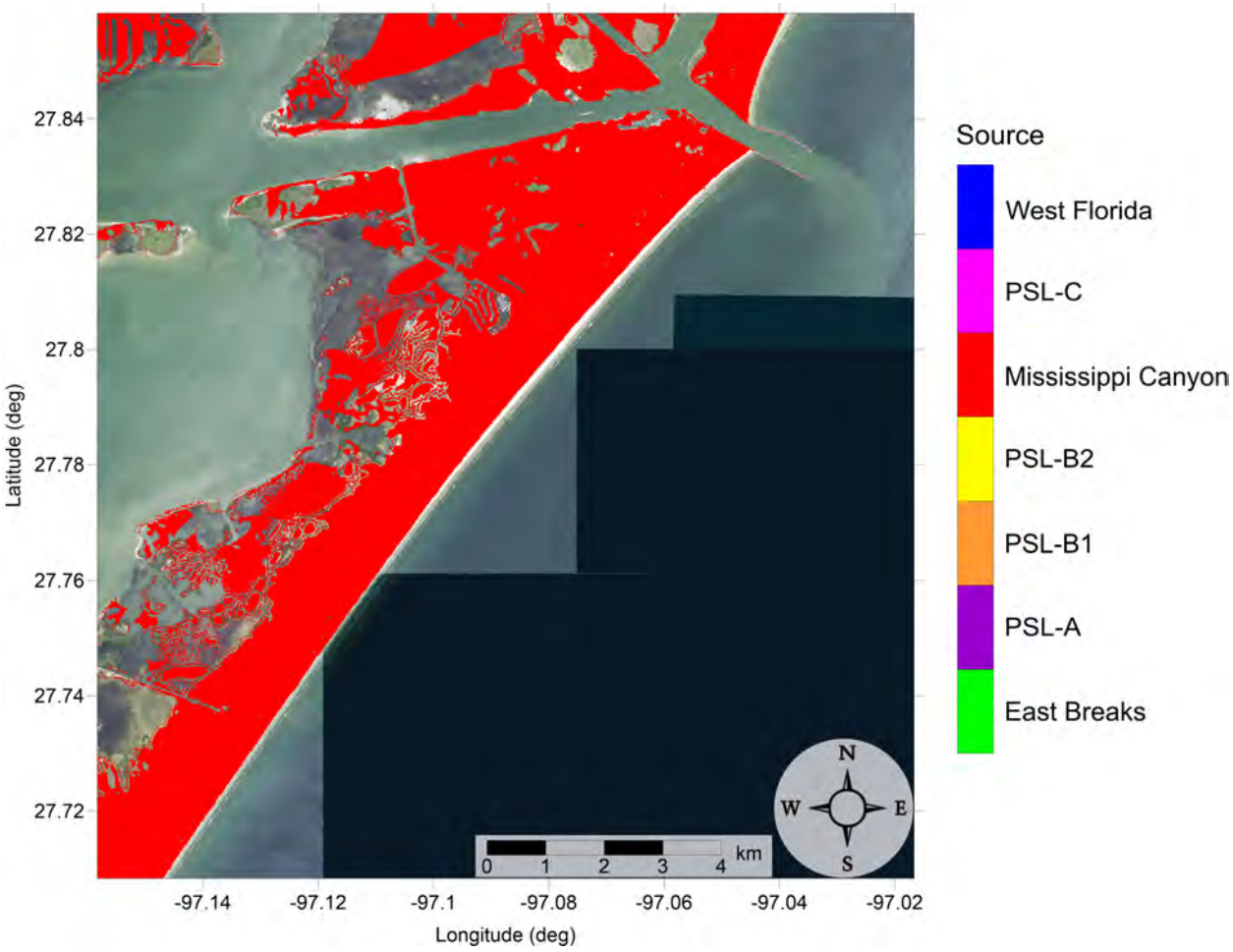


Figure 126: Indication of the tsunami source which causes the maximum of maximums inundation depth (m) in each grid cell from an ensemble of all tsunami sources in Port Aransas, TX. Contour drawn is the zero-meter contour for land elevation.

## Mustang Island, TX
## All Sources
## Maximum of Maximum Inundation Depth

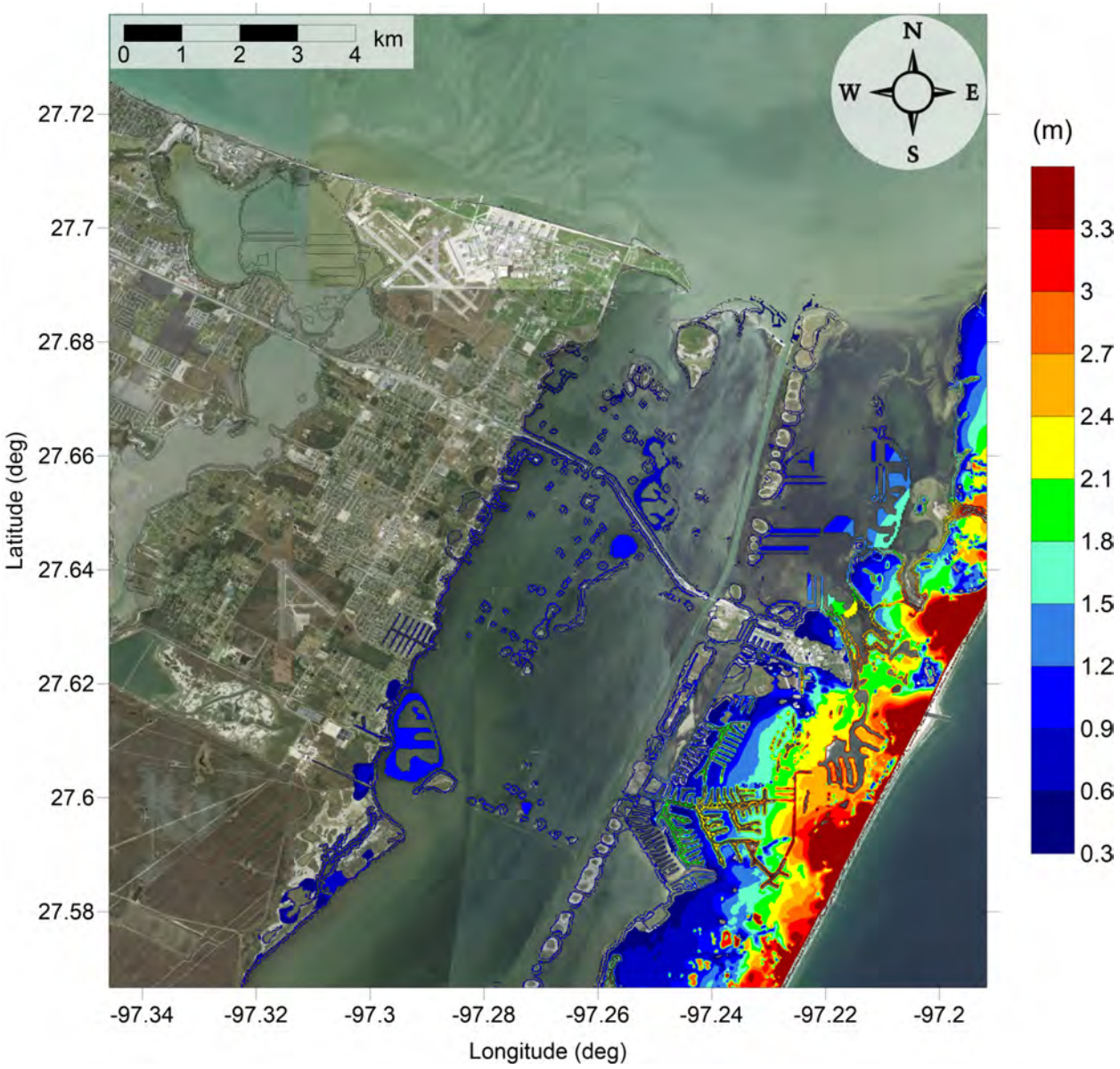


Figure 127: Maximum of maximums inundation depth (m) in South-East Corpus Christi, TX, calculated as the maximum inundation depth in each grid cell from an ensemble of all tsunami sources considered. Contour drawn is the zero-meter contour for land elevation.

## Mustang Island, TX
## All Sources
## Maximum Inundation Depth by Source

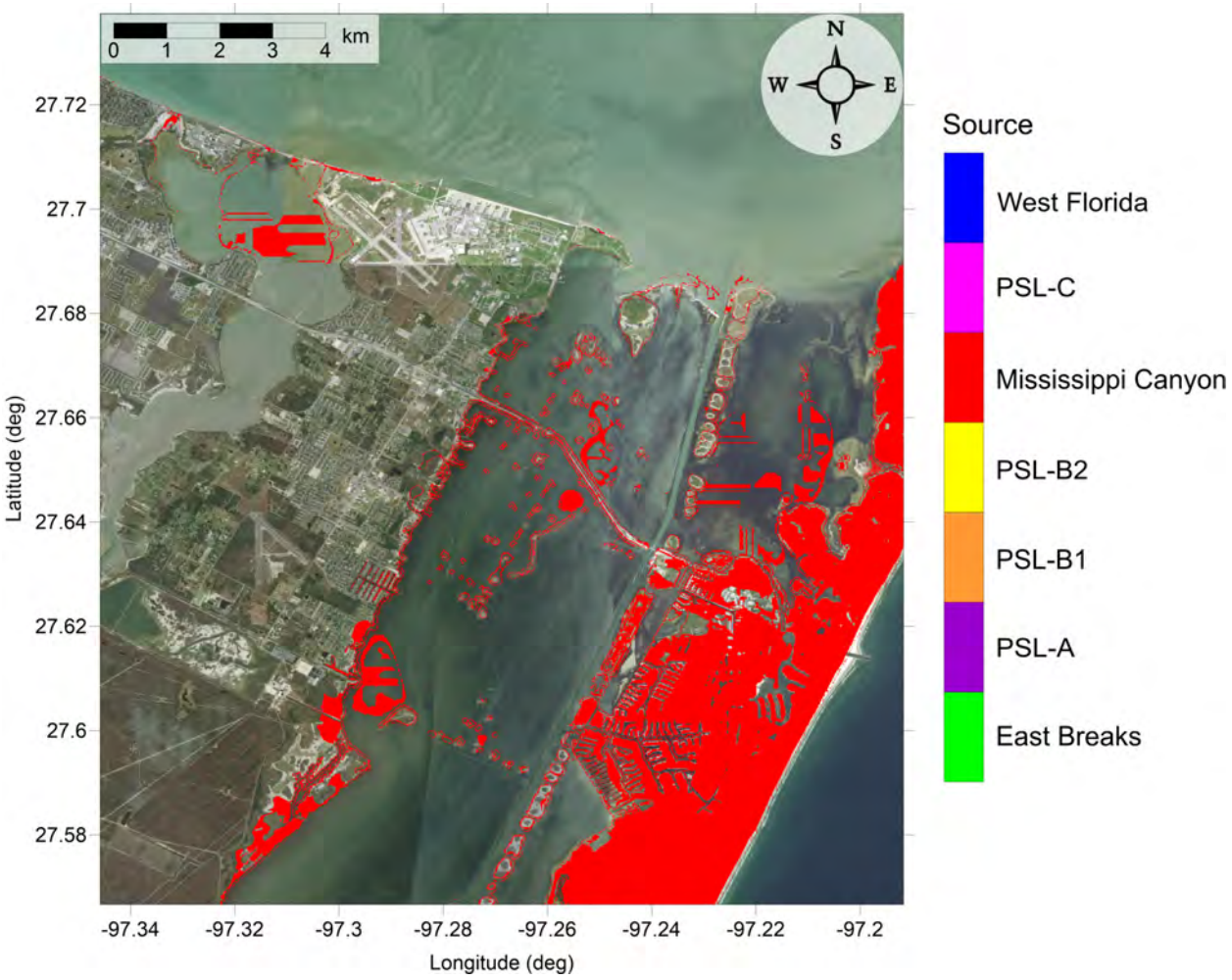


Figure 128: Indication of the tsunami source which causes the maximum of maximums inundation depth (m) in each grid cell from an ensemble of all tsunami sources in South-East Corpus Christi, TX. Contour drawn is the zero-meter contour for land elevation.

# 4 Tsunami and Hurricane Storm Surge Inundation

Tsunami inundation depth and extent has been modeled for four selected coastal communities: Pensacola, FL, Key West, FL, Okaloosa County, FL and Santa Rosa County, FL, with revision of Port Aransas, TX (Mustang Island, TX). Inundation (flooding) is determined by subtracting land elevation from water elevation, and elevations used are in reference to the Mean High Water (MHW) tidal datum. For this study, the tsunami inundation depth/extent modeled for each community is the maximum-of-maximums (MOM) inundation, which is calculated as the maximum inundation depth from an ensemble of inundation depths produced by each of the seven tsunami sources considered. That is, once inundation in a community has been modeled for each of the seven sources, the overall maximum inundation depth in each computational grid cell is taken as the MOM tsunami inundation in that cell. This approach gives a worst-case scenario perspective of estimated tsunami inundation for each coastal community. It is worth noting, however, that for all of these communities, the MOM tsunami inundation is produced solely by the Mississippi Canyon failure. That historical failure is largest in both area and volume of material removed, and therefore produces the highest amplitude wave of all sources simulated. Mustang Island is also significantly threatened by East Breaks, PSL-A and PSL-C landslide, despite Mississippi having the highest impact.

Due to the limitations on availability of high-resolution (1/3 arcsecond) DEMs, detailed inundation maps for all communities along the Gulf Coast are not yet possible. In an effort to develop a first-order estimate of potential tsunami inundation for those locations where detailed inundation maps have not yet been developed, we compare tsunami inundation modeled for the communities mentioned above to hurricane storm surge modeled data. The motivation for and implications of this approach are twofold. It provides a way to assess tsunami inundation in un-mapped communities based on existing storm surge flood data and also relates the level of tsunami hazard to that of another hazard that is better defined in this region. Tsunamis are not well-understood as a threat along the Gulf Coast, making tsunami hazard mitigation efforts somewhat difficult. However, hurricane is a relatively well-understood threat in this region, and hurricane preparedness approaches are well-developed. As a result, comparisons of tsunami and hurricane storm surge inundation levels provide a more understandable and accessible idea of the level of hazard presented by potential tsunami events and can serve as a basis for tsunami preparedness efforts.

The hurricane storm surge data used here is available from the Sea, Lake, and Overland Surges from Hurricanes (SLOSH) model (http://www.nhc.noaa.gov/surge/slosh.php). The SLOSH model was developed by the National Weather Service (NWS) to provide estimates of storm surge heights caused by historical, predicted, or hypothetical hurricanes based on different values for atmospheric pressure, hurricane size, forward speed, and track. It uses a polar, elliptical, or hyperbolic grid for computations, leading to higher resolutions near coastal areas of interest. Some limitations of the SLOSH model should be acknowledged. Resolution of the model varies from tens of meters to a kilometer or more. Near the coastal communities of interest here, resolution is on the order of 1 km. Sub-grid scale water and topographic features such as channels, rivers, levees, and roads, are parameterized instead of being explicitly modeled. Despite these limitations, the hurricane storm surge data from

the SLOSH model is currently the best data publicly available for our purposes, and efforts have been made to ensure the validity of the SLOSH data in performing comparisons with tsunami inundation.

The SLOSH MOM results provide the worst-case storm surge for a given hurricane category and initial tide level based on a set of model runs with various combinations of parameters such as forward speed, trajectory, and landfall location. To perform the storm surge and tsunami comparisons, SLOSH storm surge elevation data was first converted to meters and adjusted from the NAVD88 to the MHW vertical datum using NOAA's VDatum tool (http://vdatum.noaa.gov/). Due to the relatively low resolution of the SLOSH data as compared to the DEMs used for tsunami modeling, the SLOSH data was interpolated to 1/3 arcsecond (10 m) resolution using a kriging method. Inundation was then determined by subtracting land elevation from the storm surge elevation.

Here, an initial high tide level is used for the SLOSH MOM results in order to compare the worst-case tsunami inundation with a worst-case storm surge scenario. The high tide SLOSH MOM data includes effects of the highest predicted tide level at each location. In comparison, water elevations in the tsunami modeling are based on the MHW datum, which averages the high water levels over the National Tidal Datum Epoch (NTDE). Within the GOM, tidal ranges are relatively small, with diurnal ranges on the order of 1.5 ft (0.5 m) for most of the communities studied here, and slightly higher at around 2.5 ft (0.8 m) for the west coast of Florida. Thus, differences between highest tide levels and the mean of the highest tide levels are expected to be relatively small, though local bathymetric effects combined with tidal effects can still be significant.

It should be noted that the updated Saffir-Simpson Hurricane Wind Scale which delineates hurricane categories 1-5 does not include storm surge as a component of the measure of hurricane intensity and that other methods may capture the physics of hurricane severity and damage in a more appropriate manner (e.g. Kantha [2006], Basco and Klentzman [2006], Irish and Resio [2010]). However, the SLOSH MOM results take into account thousands of scenarios for a given hurricane category, resulting in a composite worst-case storm surge scenario for each Saffir-Simpson hurricane category. Thus, since hurricane preparedness, storm surge evacuation zones, and hazard mitigation efforts are based on hurricane category assignment, we aim to determine the hurricane category which produces MOM storm surge inundation $\zeta_h$ that is a best match to the tsunami MOM inundation $\zeta_t$. That is, we determine the hurricane category which satisfies

$$min_c(|\zeta_{h_c} - \zeta_t|), \qquad c = \text{Cat1,..,Cat5} \tag{1}$$

for each grid cell. The inundation level for the best-match category is denoted $\zeta_{h_{min}}$. The actual difference between hurricane and tsunami inundation levels $\Delta\zeta = \zeta_{h_{min}} - \zeta_t$ then indicates how close of a match the best-match category actually is. Thus, positive values of $\Delta\zeta$ indicate where hurricane storm surge inundation is higher than tsunami inundation, and negative values indicate where tsunami inundation is higher. A common local practice in tsunami modeling is to only consider inundation above a threshold of 0.3 m (1 ft) [Horrillo et al., 2011, 2015]. This is due to the extensive flat and low-lying elevation found along the Gulf Coast. All depths are calculated for tsunami inundation modeling, but inundation

less than 0.3 m (1 ft) is considered negligible here for inundation mapping purposes. Thus, comparisons are only made where either the tsunami or hurricane MOM inundation is at least 0.3 m (1 ft). Results for each of the five selected Gulf Coast communities are given in the following subsections. It is possible that tsunami inundation zone has no hurricane flooding, therefore matching with hurricane category cannot be made.

## 4.1 Pensacola, FL

The Pensacola study area covers mainland Pensacola, Gulf Breeze (west portion of the Fairpoint Peninsula) and western part of Santa Rosa Island (west of Pensacola Beach). Figure 15 shows the MOM tsunami inundation affecting Pensacola. Note that inundation less than 0.3 m (1 ft) is not shown (same for all other figures of tsunami inundation). The tsunami waves almost completely inundate the barrier island, as well as the southern part of the peninsula. On the barrier island, inundation water depth is highest (over 4 m) at the beachfront, that diminishes gradually toward the north. Tsunami also inundates the south of Escambia County, and water as high as 4 meter can be observed near the inlet. To the north, tsunami reaches as far as Pensacola, and to the east reaches the southwest portion of Gulf Breeze, with water height no more than 2.3 m. In addition, waves penetrate into the mainland through the bayous, but no significant inundation is found. The Mississippi Canyon landslide is responsible for the MOM inundation (see Fig. 16).

Fig. 129 shows the hurricane category which best matches the tsunami inundation in Pensacola. Fig. 130 shows $\Delta\zeta$ for the best-match hurricane category satisfying equation 1 and shown in Fig. 129. Note that pale colors (pale orange and yellow) in Figure 130 and subsequent figures of $\Delta\zeta$ indicate relatively good agreement between tsunami and storm surge inundation, i.e. -0.5 m $\leq \Delta\zeta \leq$ 0.5 m. The hurricane category best matching tsunami inundation in Pensacola exhibits a decreasing trend from the beach toward inland (Fig. 129), as can be expected. On the barrier island, tsunami inundation is mostly comparable to Category 4 and 5 hurricane, and Category 3 can be found as a thin strip north of the barrier island. Southern part of the Escambia County is also dominated by Category 4 and 5 where it is directly facing the inlet, with Category 3 showing up on the flanks. Toward more inland coastlines, including Pensacola and southern Gulf Breeze, Category 2 is the most common with scattered Category 3. From Fig. 130, it can be concluded that most inundated area, the hurricane categories are matching very well, because the difference stays within $\pm$ 0.5 m.

**Pensacola, FL**
**All Sources**
**SLOSH Storm Surge and MOM Tsunami Inundation Comparison**

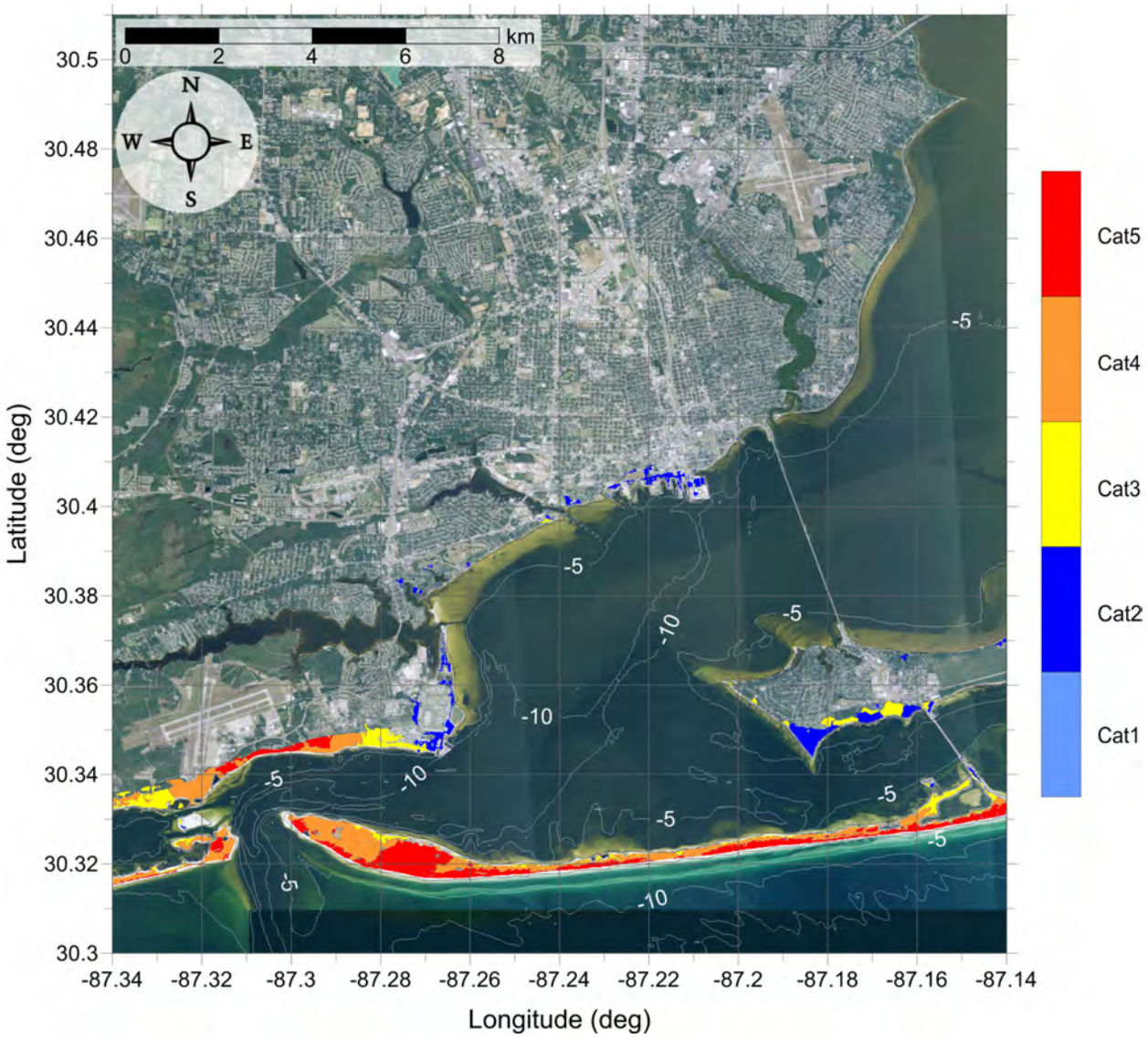


Figure 129: Hurricane category which produces inundation at high tide that best matches the MOM tsunami inundation shown in Fig. 15 for Pensacola, FL. The contours drawn and labeled are at -5 m, -10 m, and -15 m levels.

**Pensacola, FL**
**All Sources**
**SLOSH Storm Surge and MOM Tsunami Inundation Comparison**

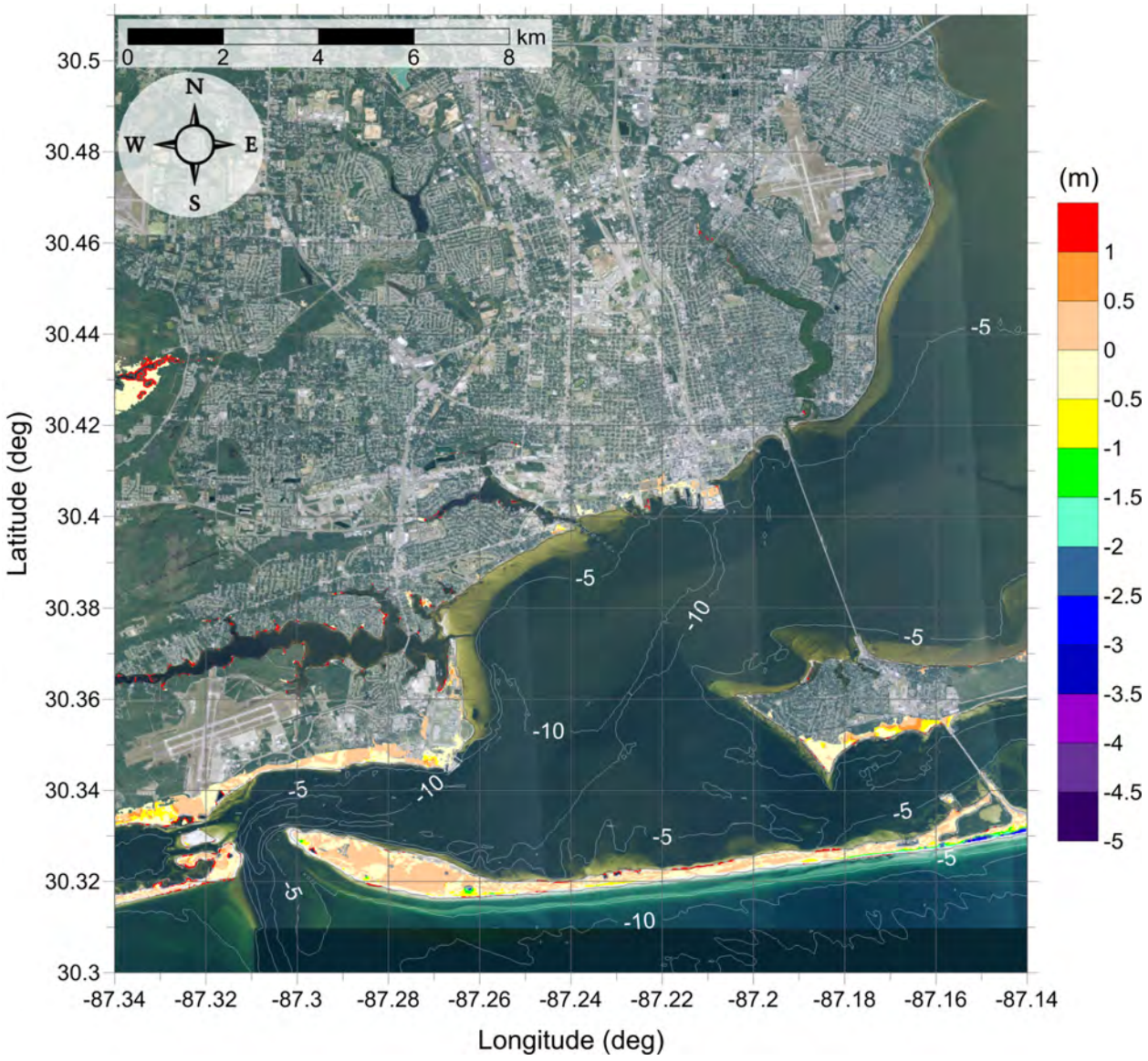


Figure 130: Actual difference $\Delta\zeta$ (in meters) between SLOSH MOM storm surge inundation and MOM tsunami inundation for the best-match hurricane category shown in Figure 129 for Pensacola, FL. Note that negative values indicate where tsunami inundation is higher than hurricane inundation, and pale colors indicate relatively good agreement between tsunami and storm surge inundation, i.e. $|\Delta\zeta| \leq 0.5$ m. The contours drawn and labeled are at -5 m, -10 m, and -15 m levels.

## 4.2 Key West, FL

Key West is an island city in the Florida Keys archipelago which extends from the southwest tip of the state of Florida. The study area covers Key West and the Stock Island to the east, as well as the Big Coppitt Key, Geiger Key, and the East Rockland Key. Fig. 31 shows the MOM tsunami inundation affecting Key West. The whole study area is completely inundated except for a few places, including, from west to east, Tank Island, Dredgers Key, Key West Naval Station. The water height is displaying a southward increasing trend because of the higher elevation toward the south. The Mississippi Canyon landslide is responsible for the MOM inundation (see Fig. 32). Key West is also slightly affected by PSL-C landslide (see Fig. 27).

Fig. 131 shows the hurricane category which best matches the tsunami inundation in Key West. Fig. 132 shows $\Delta\zeta$ for the best-match hurricane category satisfying equation 1 and shown in Fig. 131. The hurricane category that best matches tsunami inundation closely follow the MOM tsunami inundation trend. Category 5 occupies the largest area in the southern part of this region where there is maximum tsunami inundation. Category 5 though Category 1 show up progressively toward the north.

## Key West, FL
## All Sources
## SLOSH Storm Surge and MOM Tsunami Inundation Comparison

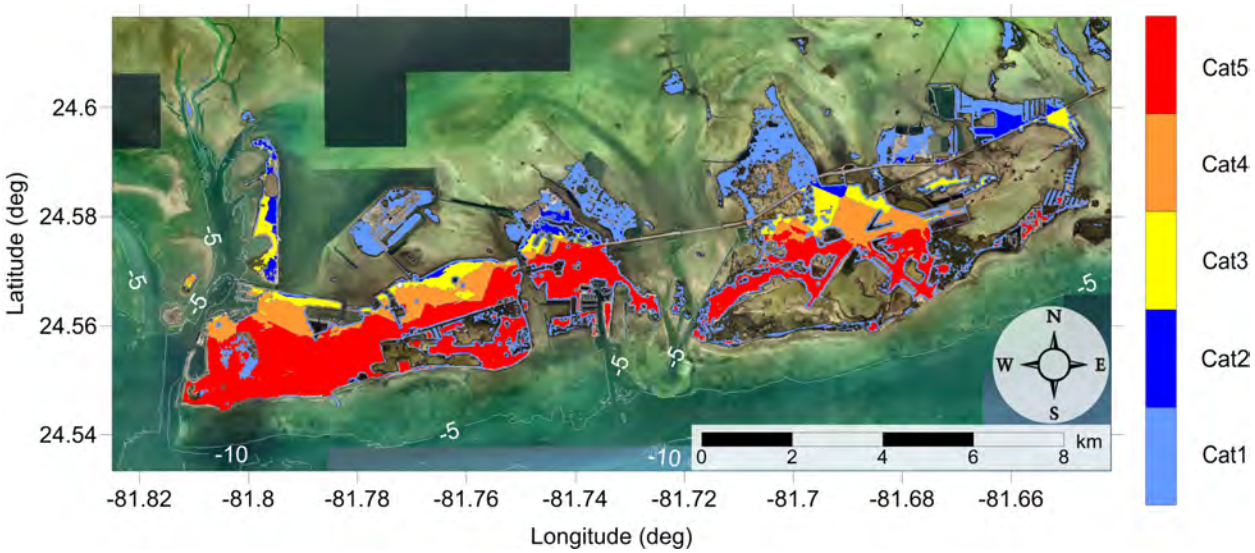


Figure 131: Hurricane category which produces inundation at high tide that best matches the MOM tsunami inundation shown in Fig. 132 for Key West, FL. The contours drawn and labeled are at -5 m, -10 m, and -15 m levels.

## Key West, FL
## All Sources
## SLOSH Storm Surge and MOM Tsunami Inundation Comparison

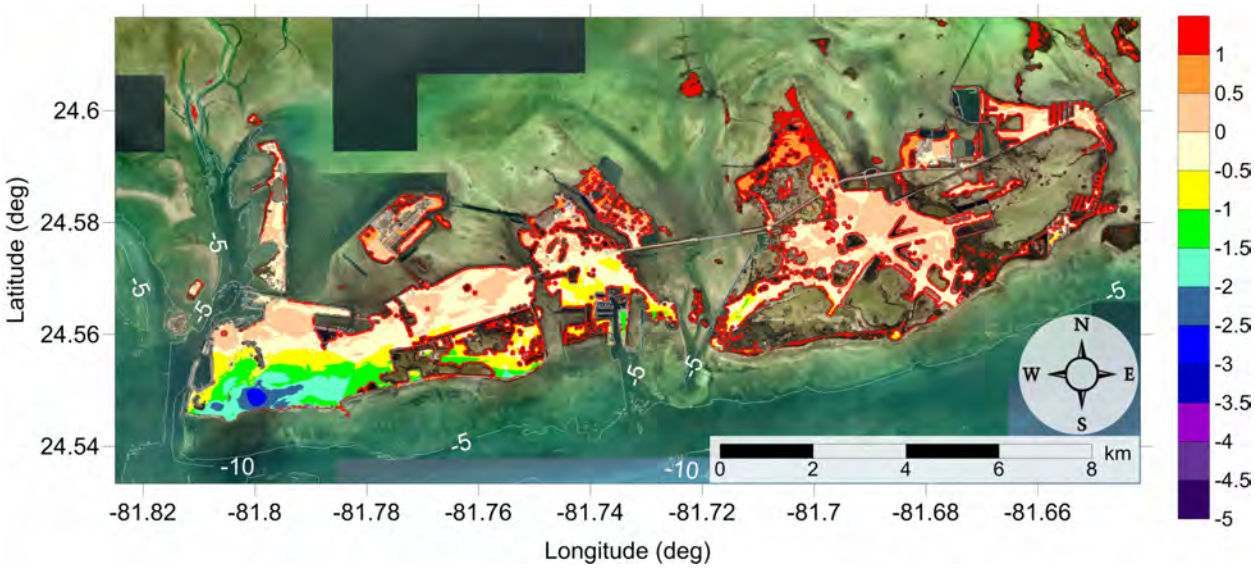


Figure 132: Actual difference $\Delta\zeta$ (in meters) between SLOSH MOM storm surge inundation and MOM tsunami inundation for the best-match hurricane category shown in Figure 131 for Key West, FL. Note that negative values indicate where tsunami inundation is higher than hurricane inundation, and pale colors indicate relatively good agreement between tsunami and storm surge inundation, i.e. $|\Delta\zeta| \leq 0.5$ m. The contours drawn and labeled are at -5 m, -10 m, and -15 m levels.

## 4.3 Okaloosa County, FL

### Okaloosa Island, FL

Fig. 61 shows the MOM tsunami inundation affecting Okaloosa Island. The whole barrier island is completely inundated, with water depth increasing from 1 m to greater than 6 m toward the GOM, and the highest water depth occurs along the beachfront. The Mississippi Canyon landslide is responsible for the MOM inundation (see Fig. 62). The water depth difference across the Okaloosa Island is mainly caused by the topography variations. In the mainland, tsunami inundation is much less severe. Fort Walton Beach is the most impacted, with inundation up to 4 m high south of Hollywood Blvd SW and west of Beal Pkwy SW.

Fig. 133 shows the hurricane category which best matches the tsunami inundation in Okaloosa Island. Fig. 134 shows $\Delta\zeta$ for the best-match hurricane category satisfying equation 1 and shown in Fig. 133. The hurricane category that best matches tsunami inundation closely follow the MOM tsunami inundation trend. Category 5 occupies most of the barrier island and Fort Walton Beach where there is maximum tsunami inundation. Category 4 and 3 appear scattered around the northern edge of the barrier island and the southern edge of the mainland, while Category 2 and 1 only appear at the banks of the bayous. The difference between tsunami inundation and hurricane flooding is mostly less than 0.5 m, however, tsunami water depth can be 4 m higher than hurricane where there is maximum tsunami inundation, especially on the beachfront.

### Destin, FL

Fig. 63 shows the MOM tsunami inundation affecting Destin. Higher tsunami inundation ($>$ 4 m) occurs south of U.S. Highway 98. North of Highway 98, water depth is mostly less than 3 m high on the east side, while the west side of the island remains dry due to high elevation. In the mainland, tsunami inundation is limited to the vicinity of the bayous, with water height no more than 2 meters. Again, the Mississippi Canyon landslide is responsible for the MOM inundation (see Fig. 64).

Fig. 135 shows the hurricane category which best matches the tsunami inundation in Destin. Fig. 136 shows $\Delta\zeta$ for the best-match hurricane category satisfying equation 1 and shown in Fig. 133. The hurricane category that best matches tsunami inundation closely follow the MOM tsunami inundation trend. Category 5, 4 and 3 appears from south to north on the barrier island, respectively. From Fig. 136, it can be seen that below Highway 98, Category 5 hurricane flooding is over 3 m lower than maximum tsunami inundation depth, which is the highest difference of all mapping locations. The difference in other inundation areas is less than 1.5 m. It is worth noting that the hached pattern denotes tsunami inundation zone not flooded by hurricane.

## Okaloosa County, FL
## All Sources
## SLOSH Storm Surge and MOM Tsunami Inundation Comparison

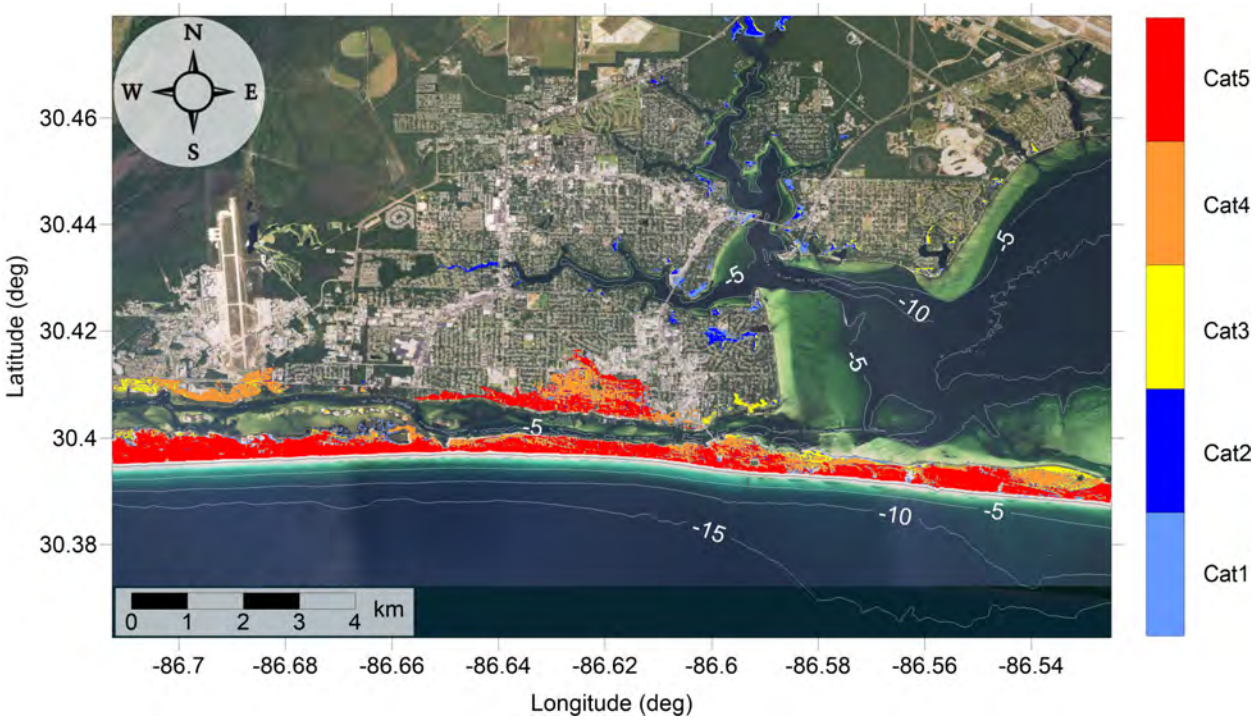


Figure 133: Hurricane category which produces inundation at high tide that best matches the MOM tsunami inundation shown in Figure 134 for Okaloosa Island, FL. The contours drawn and labeled are at -5 m, -10 m, and -15 m levels.

## Okaloosa County, FL
## All Sources
## SLOSH Storm Surge and MOM Tsunami Inundation Comparison

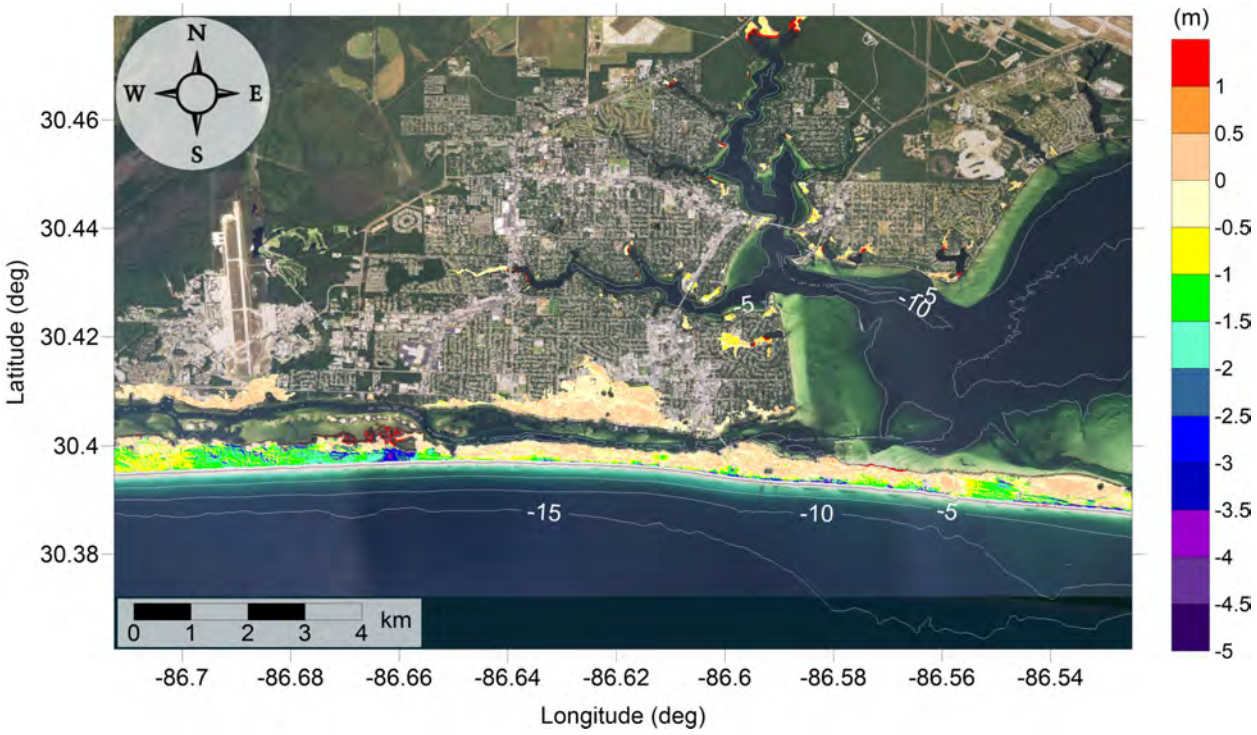


Figure 134: Actual difference $\Delta\zeta$ (in meters) between SLOSH MOM storm surge inundation and MOM tsunami inundation for the best-match hurricane category shown in Figure 133 for Okaloosa Island, FL. Note that negative values indicate where tsunami inundation is higher than hurricane inundation, and pale colors indicate relatively good agreement between tsunami and storm surge inundation, i.e. $|\Delta\zeta| \leq 0.5$ m. The contours drawn and labeled are at -5 m, -10 m, and -15 m levels.

**Okaloosa County, FL**
**All Sources**
**SLOSH Storm Surge and MOM Tsunami Inundation Comparison**

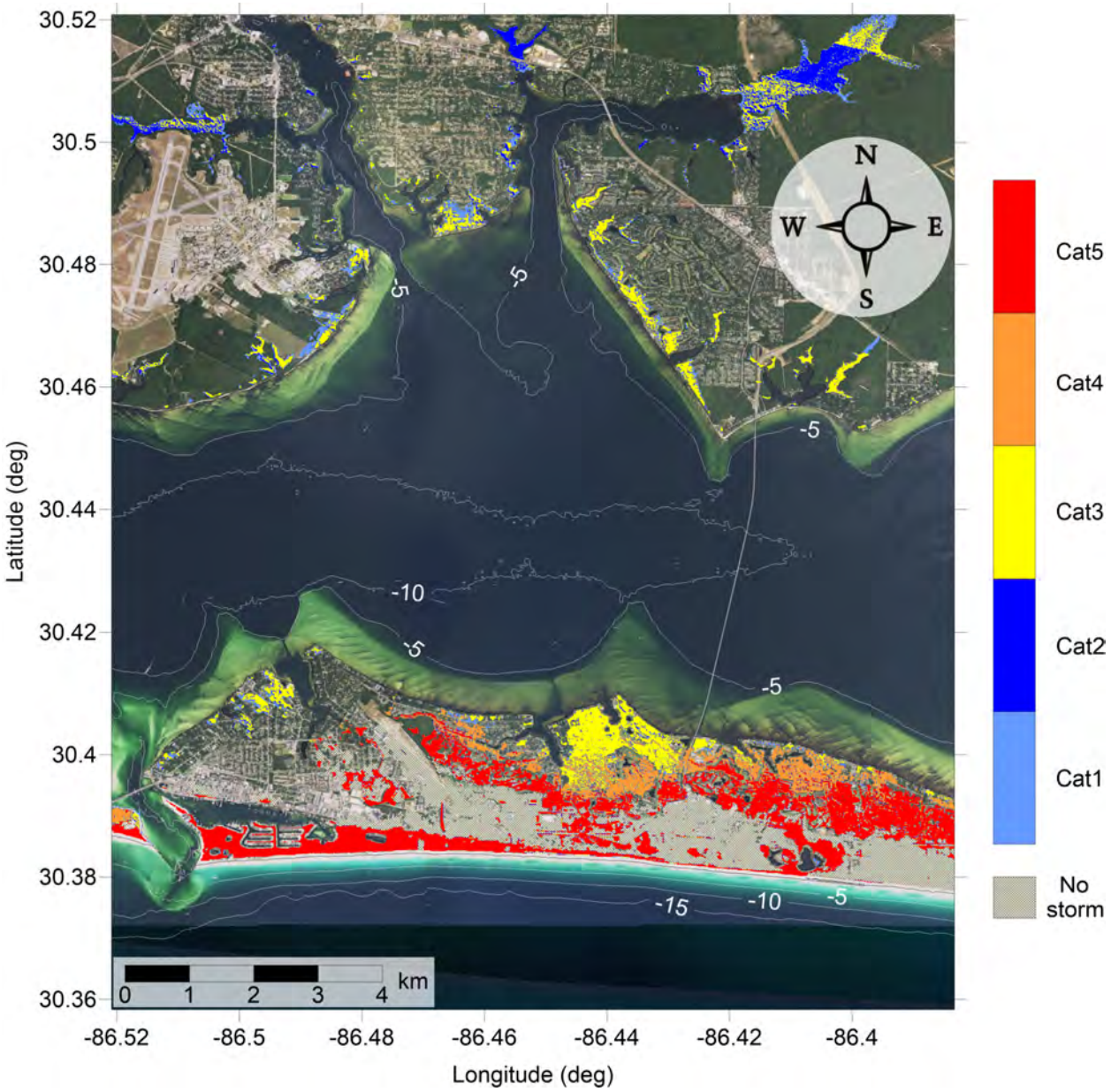


Figure 135: Hurricane category which produces inundation at high tide that best matches the MOM tsunami inundation shown in Figure 136 for Destin, FL. The contours drawn and labeled are at -5 m, -10 m, and -15 m levels. Hached area denotes tsunami inundation zone not flooded by hurricane.

**Okaloosa County, FL**
**All Sources**
**SLOSH Storm Surge and MOM Tsunami Inundation Comparison**

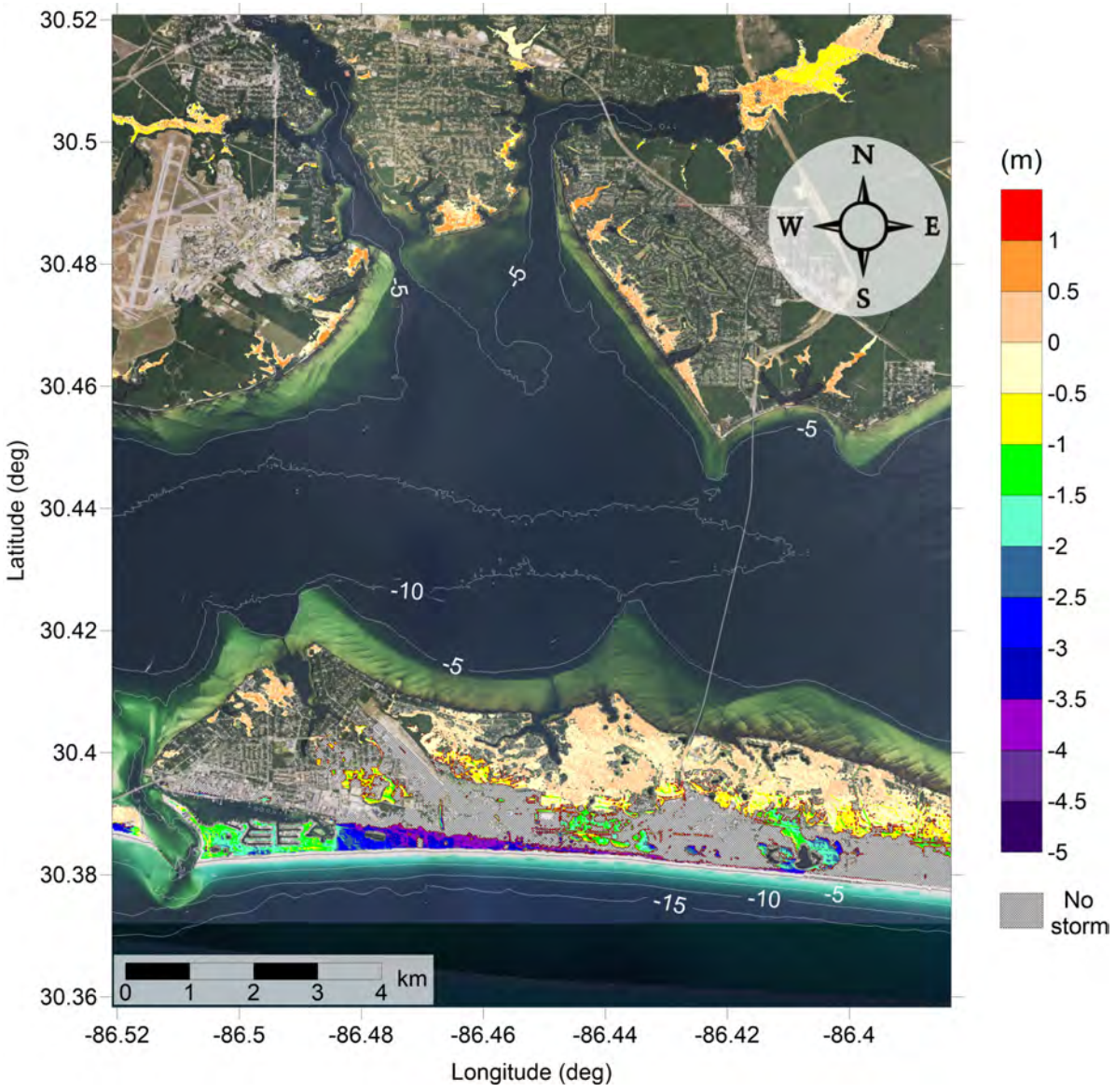


Figure 136: Actual difference $\Delta\zeta$ (in meters) between SLOSH MOM storm surge inundation and MOM tsunami inundation for the best-match hurricane category shown in Figure 135 for Destin, FL. Note that negative values indicate where tsunami inundation is higher than hurricane inundation, and pale colors indicate relatively good agreement between tsunami and storm surge inundation, i.e. $|\Delta\zeta| \leq 0.5$ m. The contours drawn and labeled are at -5 m, -10 m, and -15 m levels. Hached area denotes tsunami inundation zone not flooded by hurricane.

## 4.4 Santa Rosa County, FL

### East Gulf Breeze, FL

Fig. 93 shows the MOM tsunami inundation affecting East Gulf Breeze. The whole barrier island is completely inundated, with water depth increasing from 1 m to greater than 4 m toward the GOM. A half kilometer wide strip along the south coast of the East Gulf Breeze is also inundated by approximately 1 m water. The Mississippi Canyon landslide is responsible for the MOM inundation (see Fig. 94).

Fig. 137 shows the hurricane category which best matches the tsunami inundation in East Gulf Breeze. Fig. 138 shows $\Delta\zeta$ for the best-match hurricane category satisfying equation 1 and shown in Fig. 137. The hurricane category that best matches tsunami inundation closely follow the MOM tsunami inundation trend. Category 5 through Category 1 show up progressively toward the mainland. On the barrier island, tsunami inundation matches Category 5, 4 and 3, while on the mainland mostly Category 2 and 1. The difference between hurricane flooding and tsunami inundation is less than 0.5 m for almost all inundated areas.

### Navarre, FL

Fig. 95 shows the MOM tsunami inundation affecting Navarre. The tsunami inundation is similar to East Gulf Breeze, with the whole barrier island completely inundated with water depth increasing from 1 m to greater than 4 m toward the GOM. A thin strip along the south coast of mainland Navarre is also inundated by approximately 1 - 2 m high water. The Mississippi Canyon landslide is also responsible for the MOM inundation (see Fig. 96).

Fig. 139 shows the hurricane category which best matches the tsunami inundation in Navarre. Fig. 140 shows $\Delta\zeta$ for the best-match hurricane category satisfying equation 1 and shown in Fig. 139. The hurricane category that best matches tsunami inundation closely follow the MOM tsunami inundation trend. Similarly to East Gulf Breeze, Category 5 through Category 1 show up progressively landward. On the barrier island, tsunami inundation matches Category 5, 4 and 3, while on the mainland mostly Category 2 and 1. The difference between hurricane flooding and tsunami inundation is less than 0.5 m for all inundated areas.

## Santa Rosa County, FL
## All Sources
## SLOSH Storm Surge and MOM Tsunami Inundation Comparison

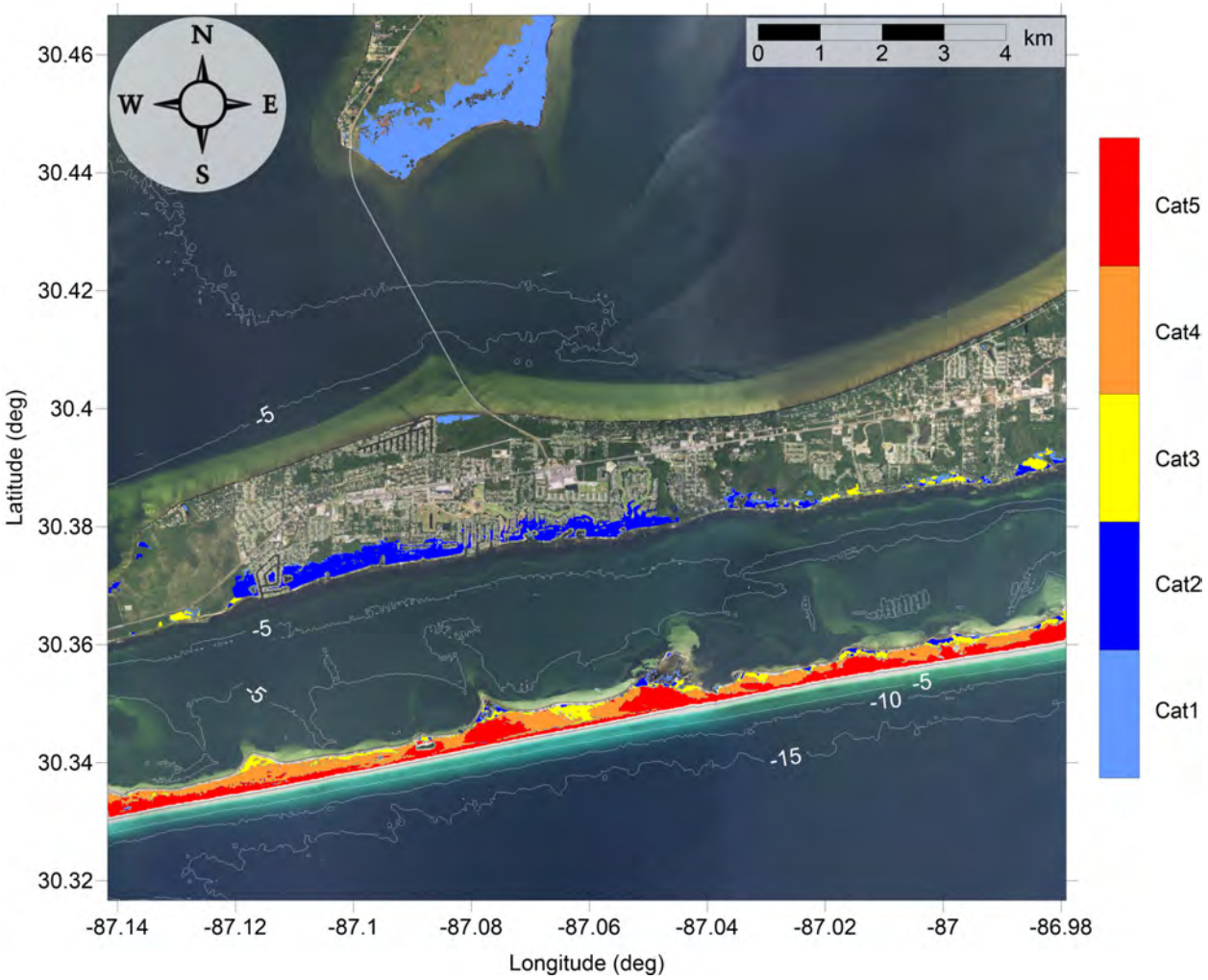


Figure 137: Hurricane category which produces inundation at high tide that best matches the MOM tsunami inundation shown in Figure 138 for East Gulf Breeze, FL. The contours drawn and labeled are at -5 m, -10 m, and -15 m levels.

## Santa Rosa County, FL
## All Sources
## SLOSH Storm Surge and MOM Tsunami Inundation Comparison

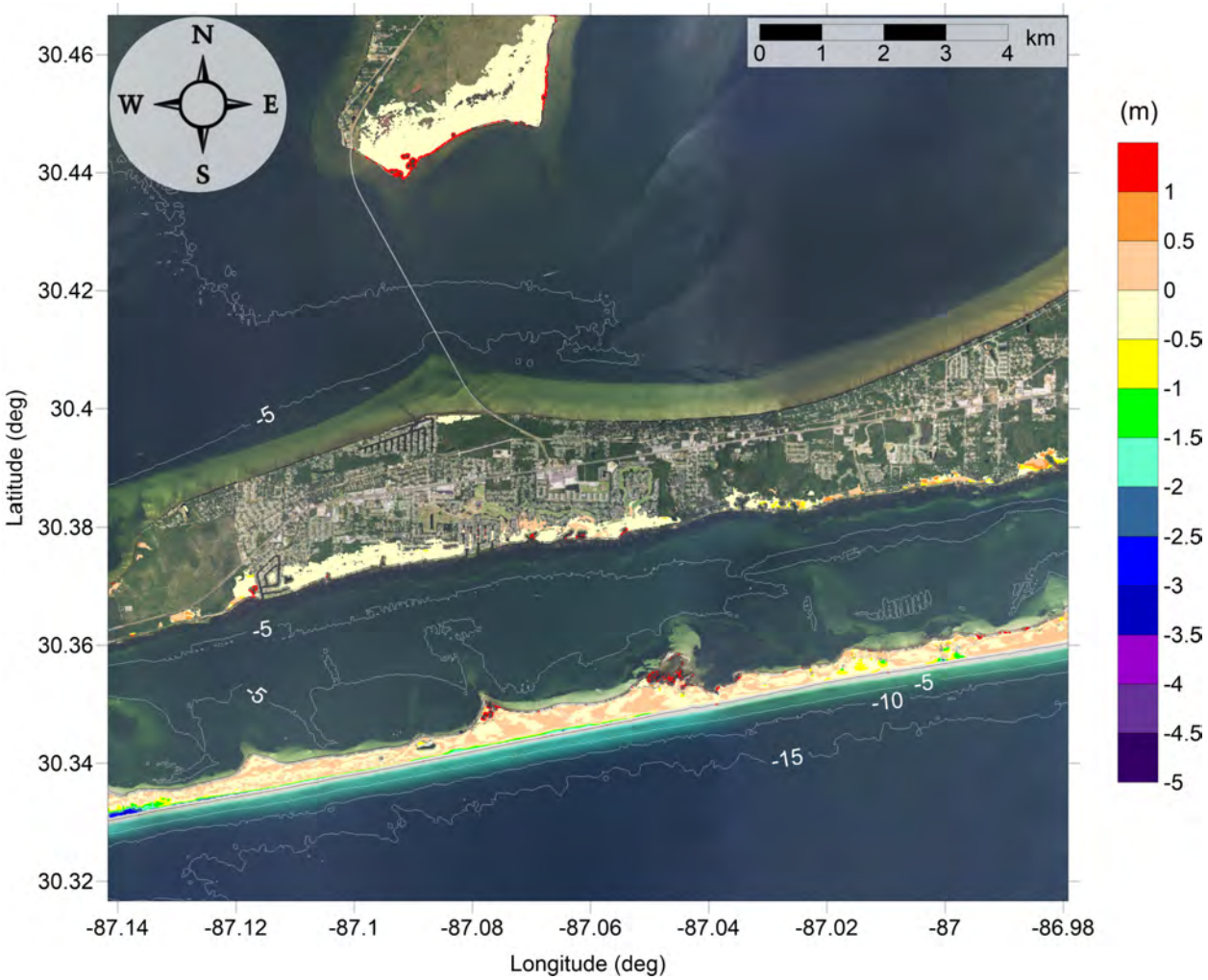


Figure 138: Actual difference $\Delta\zeta$ (in meters) between SLOSH MOM storm surge inundation and MOM tsunami inundation for the best-match hurricane category shown in Figure 137 for East Gulf Breeze, FL. Note that negative values indicate where tsunami inundation is higher than hurricane inundation, and pale colors indicate relatively good agreement between tsunami and storm surge inundation, i.e. $|\Delta\zeta| \leq 0.5$ m. The contours drawn and labeled are at -5 m, -10 m, and -15 m levels.

## Santa Rosa County, FL
## All Sources
## SLOSH Storm Surge and MOM Tsunami Inundation Comparison

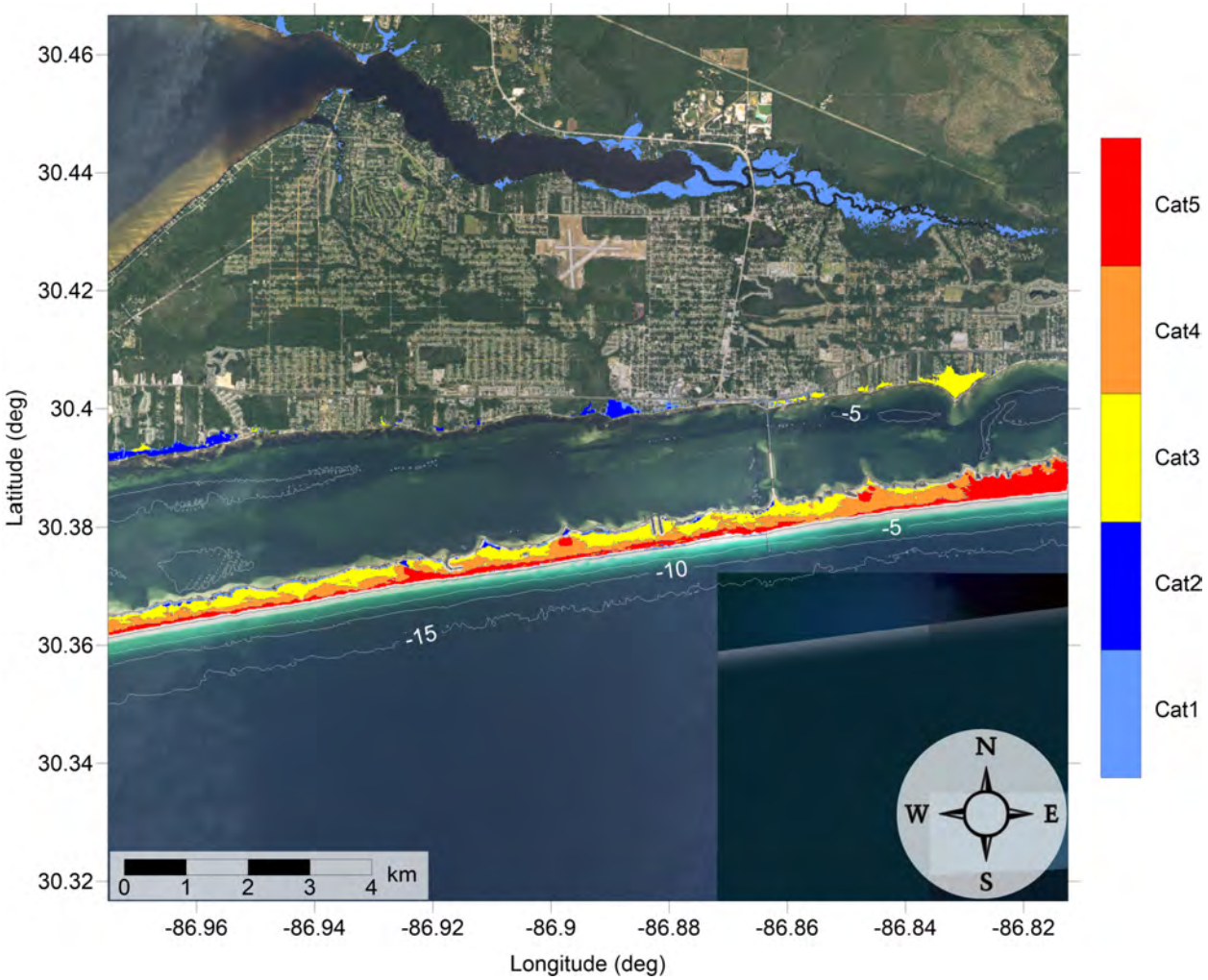


Figure 139: Hurricane category which produces inundation at high tide that best matches the MOM tsunami inundation shown in Figure 140 for Navarre, FL. The contours drawn and labeled are at -5 m, -10 m, and -15 m levels.

## Santa Rosa County, FL
## All Sources
## SLOSH Storm Surge and MOM Tsunami Inundation Comparison

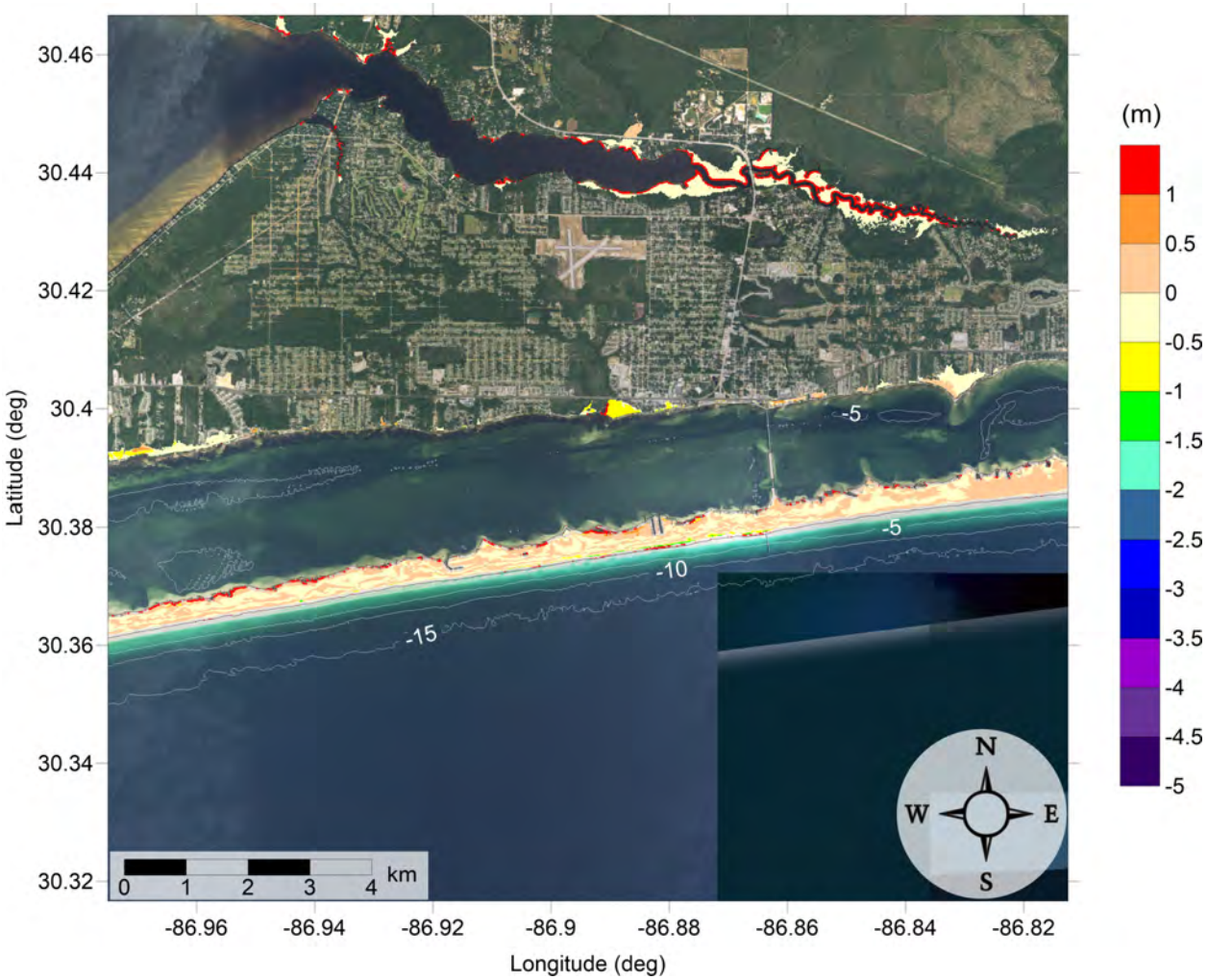


Figure 140: Actual difference $\Delta\zeta$ (in meters) between SLOSH MOM storm surge inundation and MOM tsunami inundation for the best-match hurricane category shown in Figure 139 for Navarre, FL. Note that negative values indicate where tsunami inundation is higher than hurricane inundation, and pale colors indicate relatively good agreement between tsunami and storm surge inundation, i.e. $|\Delta\zeta| \leq 0.5$ m. The contours drawn and labeled are at -5 m, -10 m, and -15 m levels.

## 4.5 Mustang Island, TX

### Port Aransas, TX

Fig. 125 shows the MOM tsunami inundation affecting Port Aransas. Tsunami inundated the whole barrier island completely with water depth up to 4 m, increasing toward the GOM. Most severe tsunami inundation ($> 4$ m) occurs at the oceanside of the natural dune system. The Mississippi Canyon landslide is responsible for the MOM inundation (see Fig. 126). Unlike the Florida communities, Port Aransas is also considerably affected by East Breaks (Fig. 99), PSL-A (Fig. 103)), and PSL-C (Fig. 119) landslides due to its proximity and tsunami energy focusing due to wave refraction by the continental shelf.

Fig. 141 shows the hurricane category which best matches the tsunami inundation in Port Aransas. Fig. 142 shows $\Delta\zeta$ for the best-match hurricane category satisfying equation 1 and shown in Fig. 141. The hurricane category that best matches tsunami inundation closely follow the MOM tsunami inundation trend. Hurricane Category decreases from 5 to 1 toward the mainland. The difference between hurricane flooding and tsunami inundation is less than 0.5 m for all inundated areas, except for oceanside of the dune, where tsunami water depth can be up to 3 m higher than hurricane flooding.

### South-East Corpus Christi, TX

Fig. 127 shows the MOM tsunami inundation affecting South-East Corpus Christi. Tsunami completely inundated the whole barrier island with water depth up to 4 m, increasing toward the GOM. Most severe tsunami inundation ($> 3$ m) occurs around three low-lying areas, first is Packery Channel, second is the channel just south of Newport Pass Road, and the third is the low elevation beach south of Whitecap Blvd. The Mississippi Canyon landslide is responsible for the MOM inundation (see Fig. 128). Unlike the Florida communities, South-East Corpus Christi is also considerably affected by East Breaks (Fig. 100), PSL-A (Fig. 104), and PSL-C (Fig. 120) landslides due to its proximity and tsunami energy focusing due to wave refraction by the continental shelf.

Fig. 143 shows the hurricane category which best matches the tsunami inundation in South-East Corpus Christi. Fig. 144 shows $\Delta\zeta$ for the best-match hurricane category satisfying equation 1 and shown in Fig. 143. The hurricane category that best matches tsunami inundation closely follow the MOM tsunami inundation trend. Hurricane Category 5 only appears around the three major tsunami inundation areas, and Category 4 3 and 2 occupy the rest of the barrier island. Category 1 areas are scattered around the fringe of mainland Corpus Christi. The difference between hurricane flooding and tsunami inundation is less than 1.5 m for all inundated areas.

## Mustang Island, TX
## All Sources
## SLOSH Storm Surge and MOM Tsunami Inundation Comparison

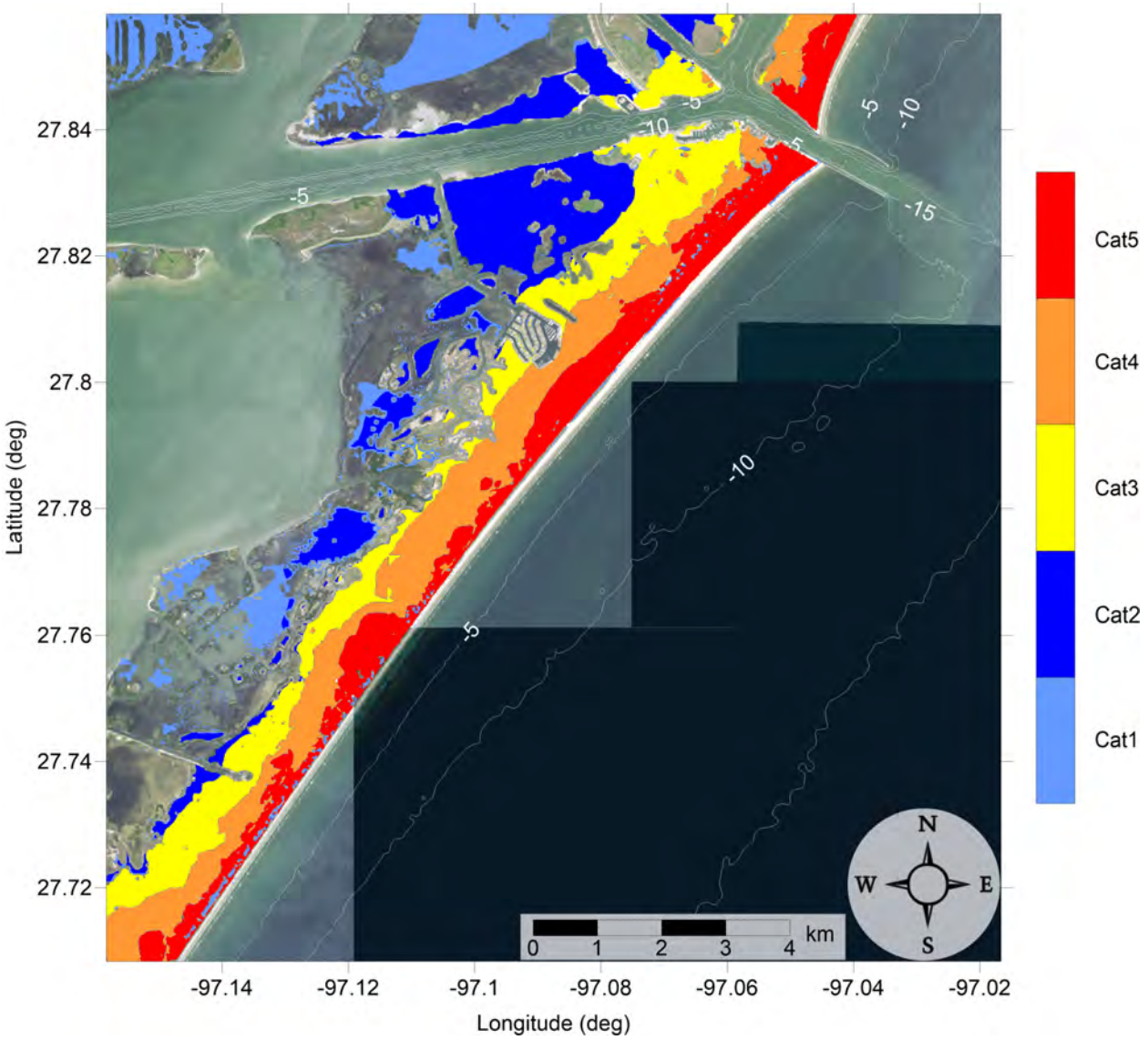


Figure 141: Actual difference $\Delta\zeta$ (in meters) between SLOSH MOM storm surge inundation and MOM tsunami inundation for the best-match hurricane category shown in Figure 142 for Port Aransas, TX. Note that negative values indicate where tsunami inundation is higher than hurricane inundation, and pale colors indicate relatively good agreement between tsunami and storm surge inundation, i.e. $|\Delta\zeta| \leq 0.5$ m. The contours drawn and labeled are at -5 m, -10 m, and -15 m levels.

## Mustang Island, TX
## All Sources
## SLOSH Storm Surge and MOM Tsunami Inundation Comparison

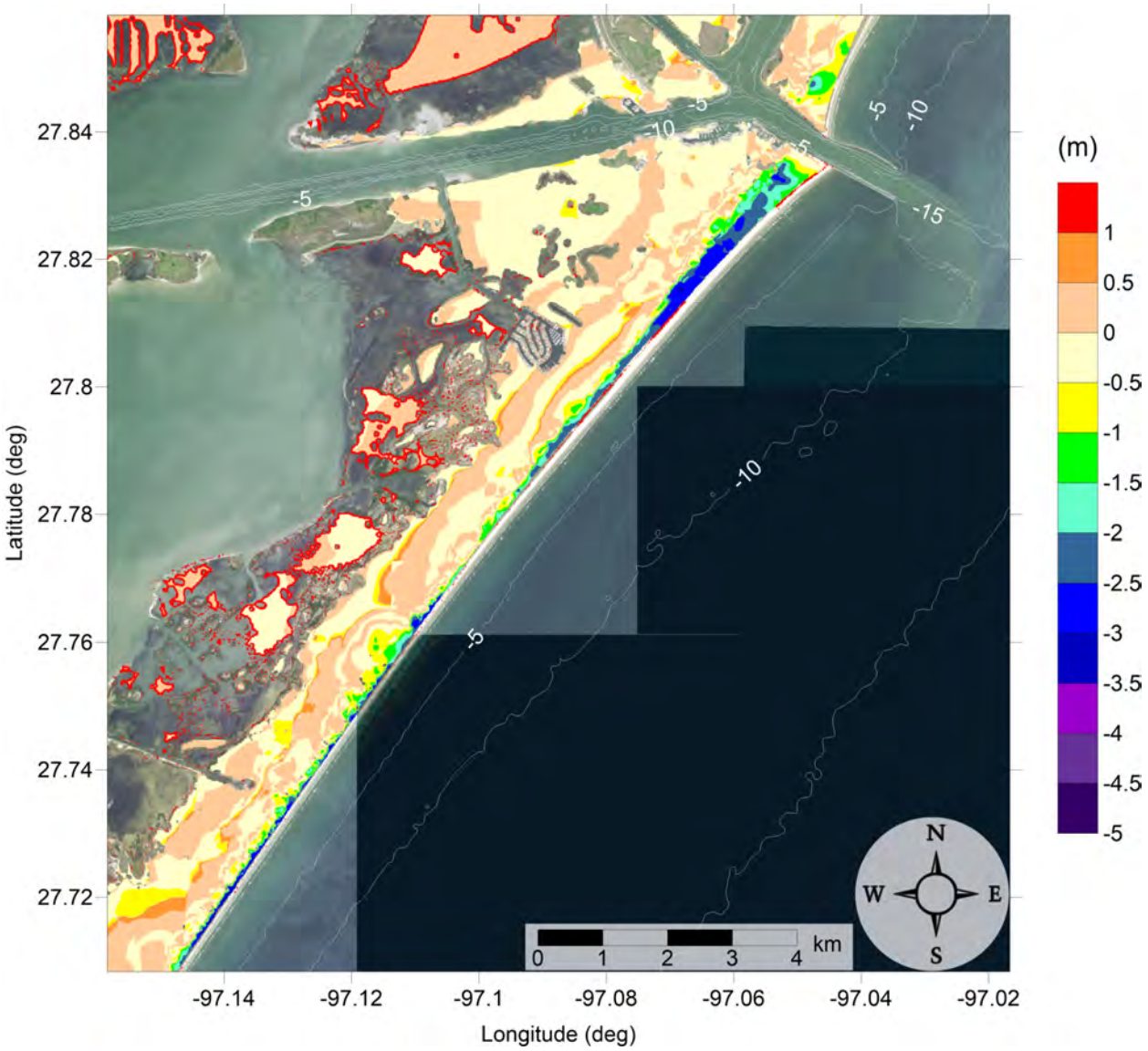


Figure 142: Actual difference $\Delta\zeta$ (in meters) between SLOSH MOM storm surge inundation and MOM tsunami inundation for the best-match hurricane category shown in Figure 141 for Port Aransas, TX. Note that negative values indicate where tsunami inundation is higher than hurricane inundation, and pale colors indicate relatively good agreement between tsunami and storm surge inundation, i.e. $|\Delta\zeta| \leq 0.5$ m. The contours drawn and labeled are at -5 m, -10 m, and -15 m levels.

## Mustang Island, TX
## All Sources
## SLOSH Storm Surge and MOM Tsunami Inundation Comparison

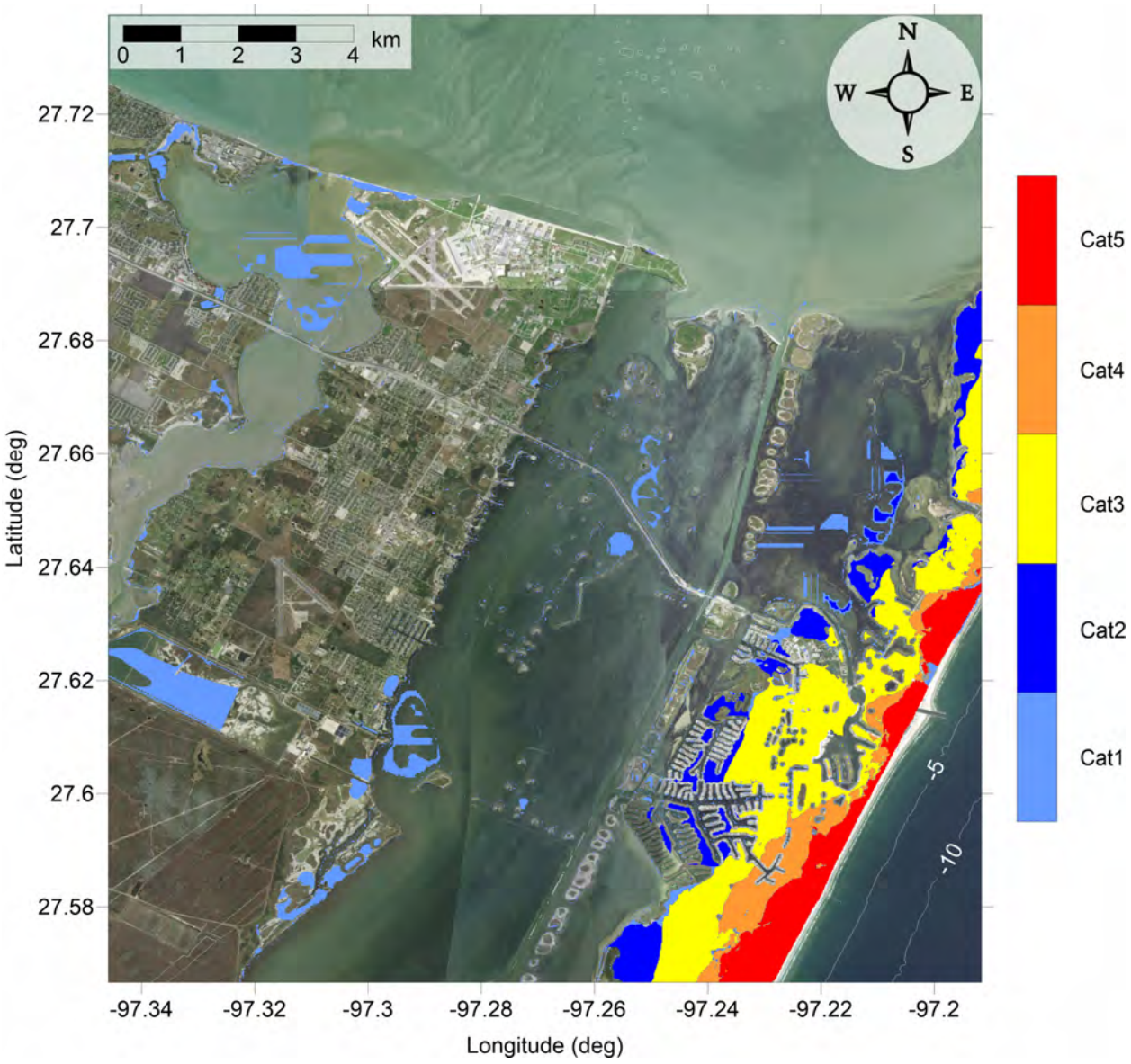


Figure 143: Actual difference $\Delta\zeta$ (in meters) between SLOSH MOM storm surge inundation and MOM tsunami inundation for the best-match hurricane category shown in Figure 144 for South-East Corpus Christi, TX. Note that negative values indicate where tsunami inundation is higher than hurricane inundation, and pale colors indicate relatively good agreement between tsunami and storm surge inundation, i.e. $|\Delta\zeta| \leq 0.5$ m. The contours drawn and labeled are at -5 m, -10 m, and -15 m levels.

## Mustang Island, TX
## All Sources
## SLOSH Storm Surge and MOM Tsunami Inundation Comparison

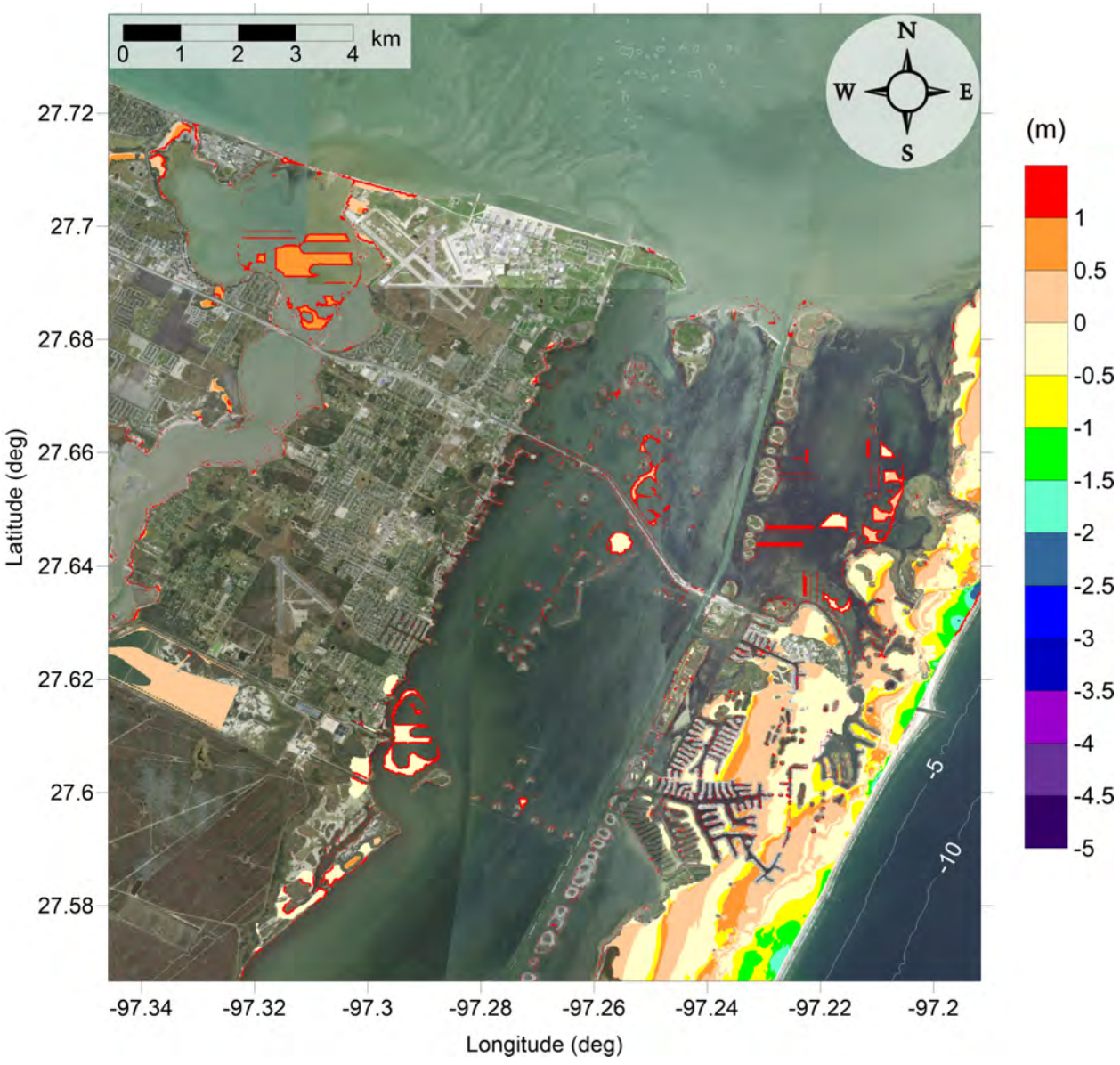


Figure 144: Actual difference $\Delta\zeta$ (in meters) between SLOSH MOM storm surge inundation and MOM tsunami inundation for the best-match hurricane category shown in Figure 143 for South-East Corpus Christi, TX. Note that negative values indicate where tsunami inundation is higher than hurricane inundation, and pale colors indicate relatively good agreement between tsunami and storm surge inundation, i.e. $|\Delta\zeta| \leq 0.5$ m. The contours drawn and labeled are at -5 m, -10 m, and -15 m levels.

# 5 Tsunami Maritime Products

Accurate estimates of tsunami wave amplitude do not necessarily equate to the prediction of localized damaging currents in a basin or harbor [Lynett et al., 2012]. Furthermore, damage potential in ports is strongly related to the current speed. Therefore, tsunami hazard mitigation products need to be advanced to predict damage potential in basins or harbors. Recent tsunamis have shown that the maritime community requires additional information and guidance about tsunami hazards and post-tsunami recovery [Wilson et al., 2012, 2013]. To accomplish mapping and modeling activities to meet NTHMP's planning/response purposes for the maritime community and port emergency management and other customer requirements, it is necessary to start the process to include maritime products in our current inundation map development. These activities will include tsunami hazard products generated by GOM's tsunami sources (submarine landslides) that may impact specifically ship channels, bay inlets, harbors, marinas, and oil infrastructures (e.g., designated lightering and oil tanker waiting zones) by implementing maritime tsunami products. A pilot tsunami hazard maritime study was conducted to predict damage potential in the Galveston Bay in Horrillo et al. [2016], where tsunami hazard maritime products such as tsunami current magnitude, vorticity, safe/hazard zones were included. In this study, nine locations, South Padre Island, TX, Mobile, AL, Panama City, FL, and Tampa Bay, FL, mapped during [Horrillo et al., 2015] (project NA13NWS4670018), and Pensacola, FL, Key West, FL, Okaloosa County, FL, Santa Rosa County, FL and Mustang Island, TX are added to the maritime portfolio in this project.

Lynett et al. [2014] complied a general relationship between tsunami current speed and harbor damage based on observational data, in which the current speed is divided into four ranges of damaging potential, 0 - 3 knots means unharmful currents, 3 - 6 knots corresponds to minor-to-moderate damage, 6 - 9 knots moderate-to-major damage, and over 9 knots extreme damage.

Since the extent of damage is very location-dependent, to make the text concise, we associate 0 - 3 knots to unharmful currents, 3 - 6 knots to minor damage, 6 - 9 knots to moderate damage, and finally over 9 knots to major damage. The four levels are denoted with white, blue, yellow and red colors, respectively, for all the figures within this section.

Using this damage-to-speed relationship, we have plotted the maximum of maximum depth-averaged velocity for each computational subdomain for the nine communities. Since they share the same largest computational domain, which is the entire GOM, the MOM velocity map of the GOM for all locations are the same. Fig. 145 shows the maximum of maximum velocity magnitude contour plot result in the Gulf of Mexico (15 arcsecond resolution) across all the landslide scenarios (Eastbreaks, PSL-A, PSL-B1, PSL-B2, Mississippi Canyon, PSL-C, and West Florida). Potential damaging currents ($>$ 3 knots) tend to be present in most of the area shallower than 200 m, which is approximately 100 fathoms. However, damaging currents could reach areas deeper than 200 m close to most of the landslide generation regions. Major damaging currents can be expected in most of the landslide generation regions, in the continental shelf adjacent to Mississippi Canyon, and offshore northwest Florida. Moderate damaging current areas are scattered over the continental shelf, but mostly close to areas with major damage currents.

**All locations**
**All Sources**
**Maximum of Maximum Velocity Magnitude**

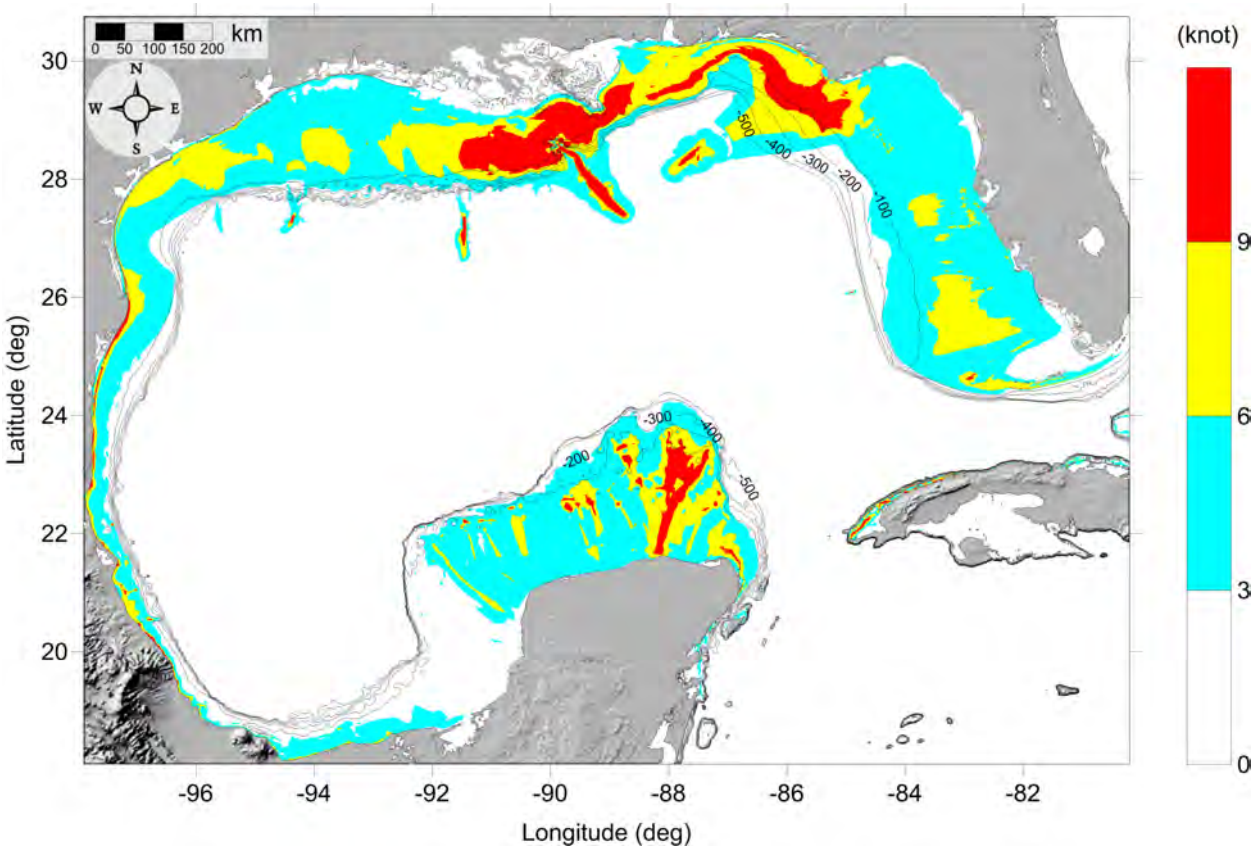


Figure 145: Maximum of maximum velocity magnitude contour in GOM for all landslide scenarios and all locations.

In the following, the numerical results are presented for each community, first MOM velocity magnitude (damaging potential) contour maps, then the MOM vorticity magnitude contour maps of each computational subdomain. The maps are presented in a clockwise order (see Fig. 1, South Padre Island, TX, Mustang Island, TX, Mobile, AL, Pensacola, FL, Santa Rosa County, FL, Okaloosa County, FL, Panama City, FL, Tampa Bay, FL, and Key West, FL).

General trends can be observed from all of the MOM velocity and vorticity maps of the subdomains (from Fig. 146 to Fig. 199). In the nearshore region of the subdomains, there are mostly moderate damaging currents (yellow), with major damaging current (red) bands in Pensacola, FL, Santa Rosa, FL, Okaloosa County, FL, and Key West, FL, probably due to sand bars and reefs. In the surf zone of the barrier island, there are mostly major damaging currents, except for Mobile, AL which has mostly moderate damaging currents and Tampa Bay, FL which has mostly minor damaging currents and few spots of moderate damaging currents. There are usually strong currents flowing through the inlets (some with jetties) which connects the GOM and internal bays, which generates mostly major damaging currents, for example, Pensacola, FL (Fig. 166) and Port Aransas, TX (Fig. 152). However, Tampa Bay, FL inlet only has minor to moderate damaging currents. For internal channel/lagoons, minor damaging currents are most common, and moderate damaging currents appear in South Padre Island, TX, Okaloosa County, FL, and Panama City, FL. In the interior bays, the tsunami currents are less severe which can be used as shelter to minimize tsunami impact.

There is less current impact in the nearshore, surf zone, inlet and channels/lagoons in Tampa Bay, FL, probably because the wider continental shelf dissipates more tsunami energy. It is also worth mentioning that tsunami impact is more severe south of Key West, FL due to tsunami wave refracted by the continental shelf break. The lee side of the islands seems protected also by the wide and shallow continental shelf north of Key West.

## 5.1 South Padre Island, TX

### South Padre Island, TX
### All Sources
### Maximum of Maximum Velocity Magnitude

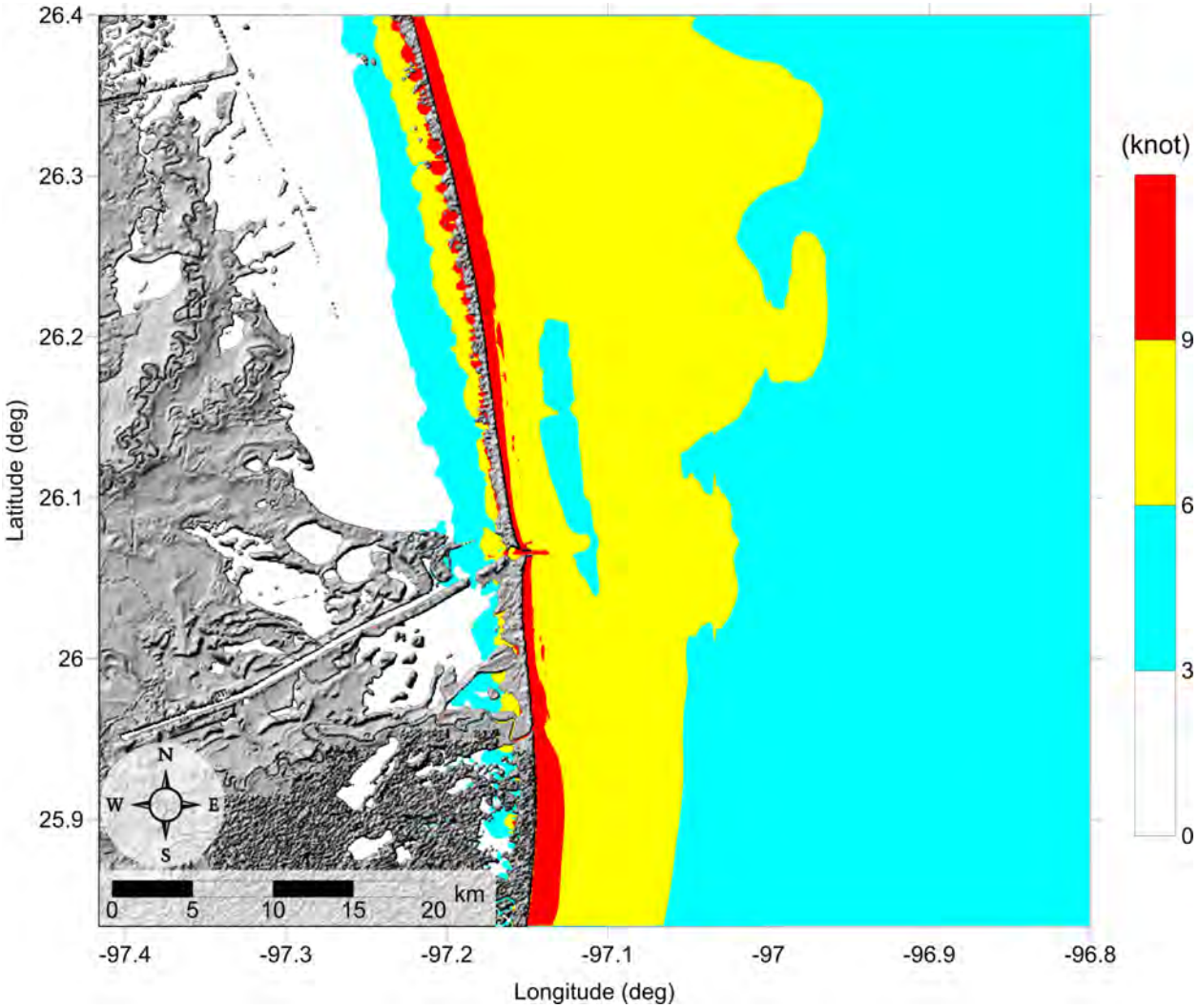


Figure 146: Maximum of maximum velocity magnitude contour in South Padre Island, TX (3 arcsecond) for all landslide scenarios.

**South Padre Island, TX**
**All Sources**
**Maximum of Maximum Velocity Magnitude**

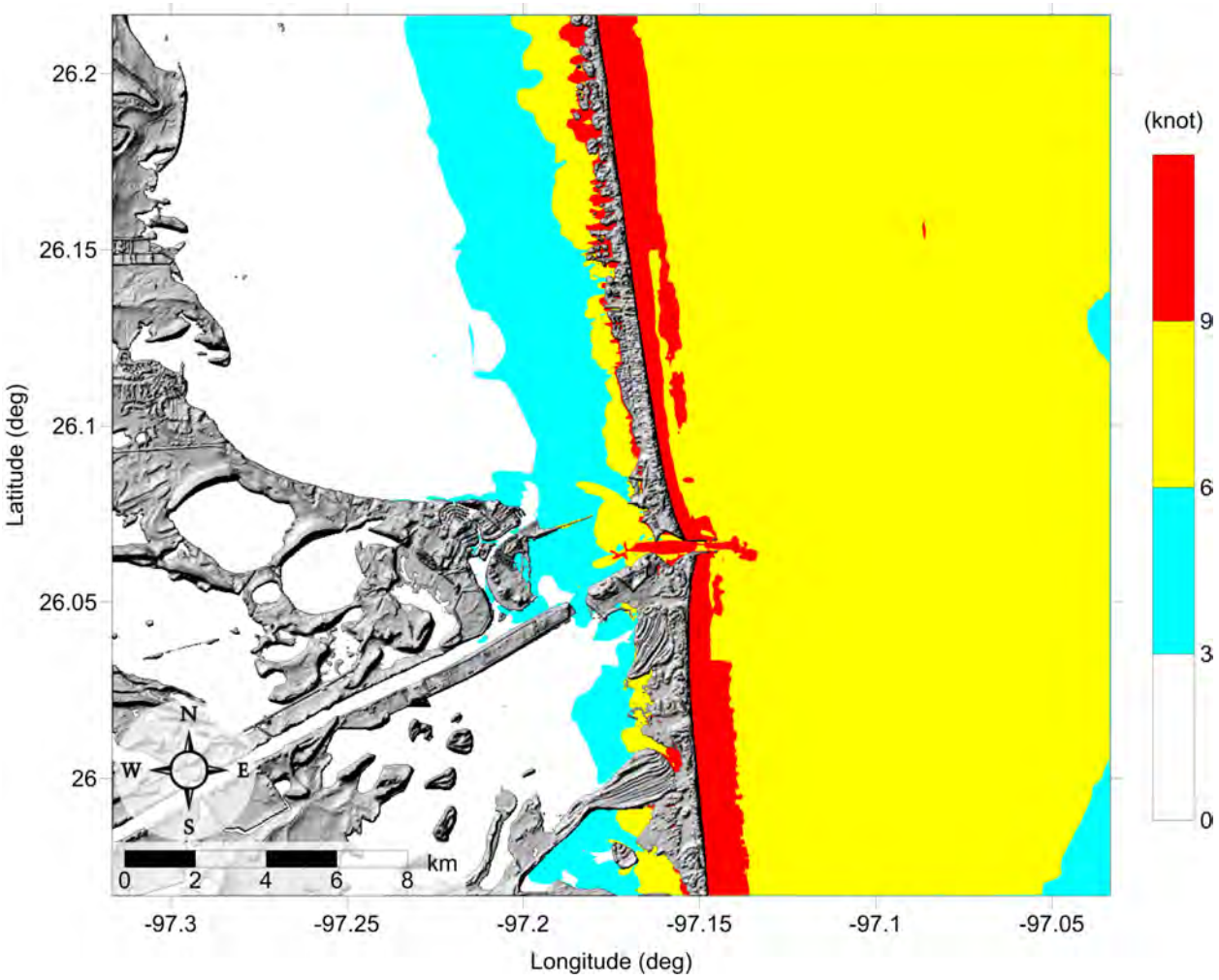


Figure 147: Maximum of maximum velocity magnitude contour in South Padre Island, TX (1 arcsecond) for all landslide scenarios.

## South Padre Island, TX
## All Sources
## Maximum of Maximum Velocity Magnitude

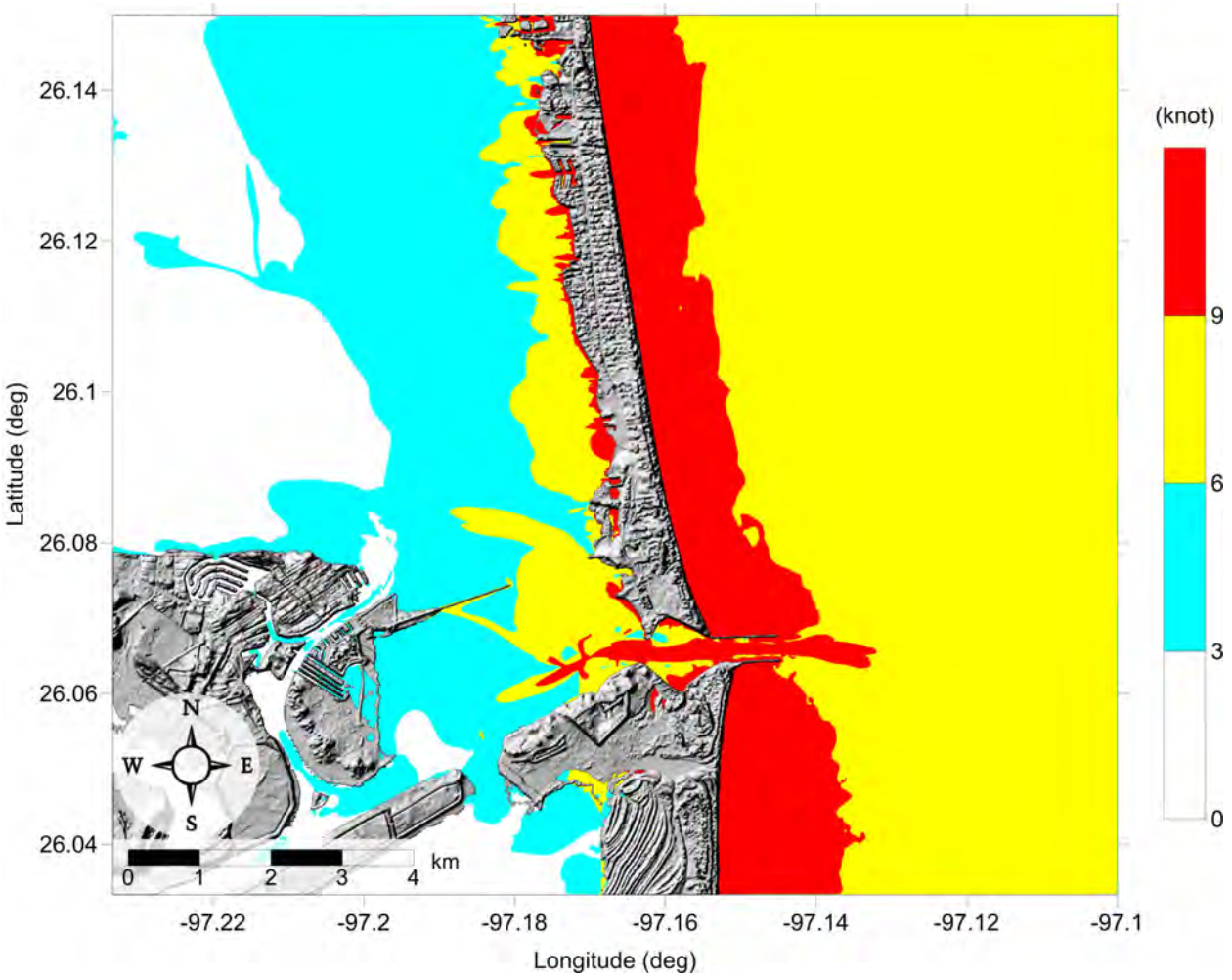


Figure 148: Maximum of maximum velocity magnitude contour in South Padre Island, TX (1/3 arcsecond) for all landslide scenarios.

## South Padre Island, TX
## All Sources
## Maximum of Maximum Vorticity Magnitude

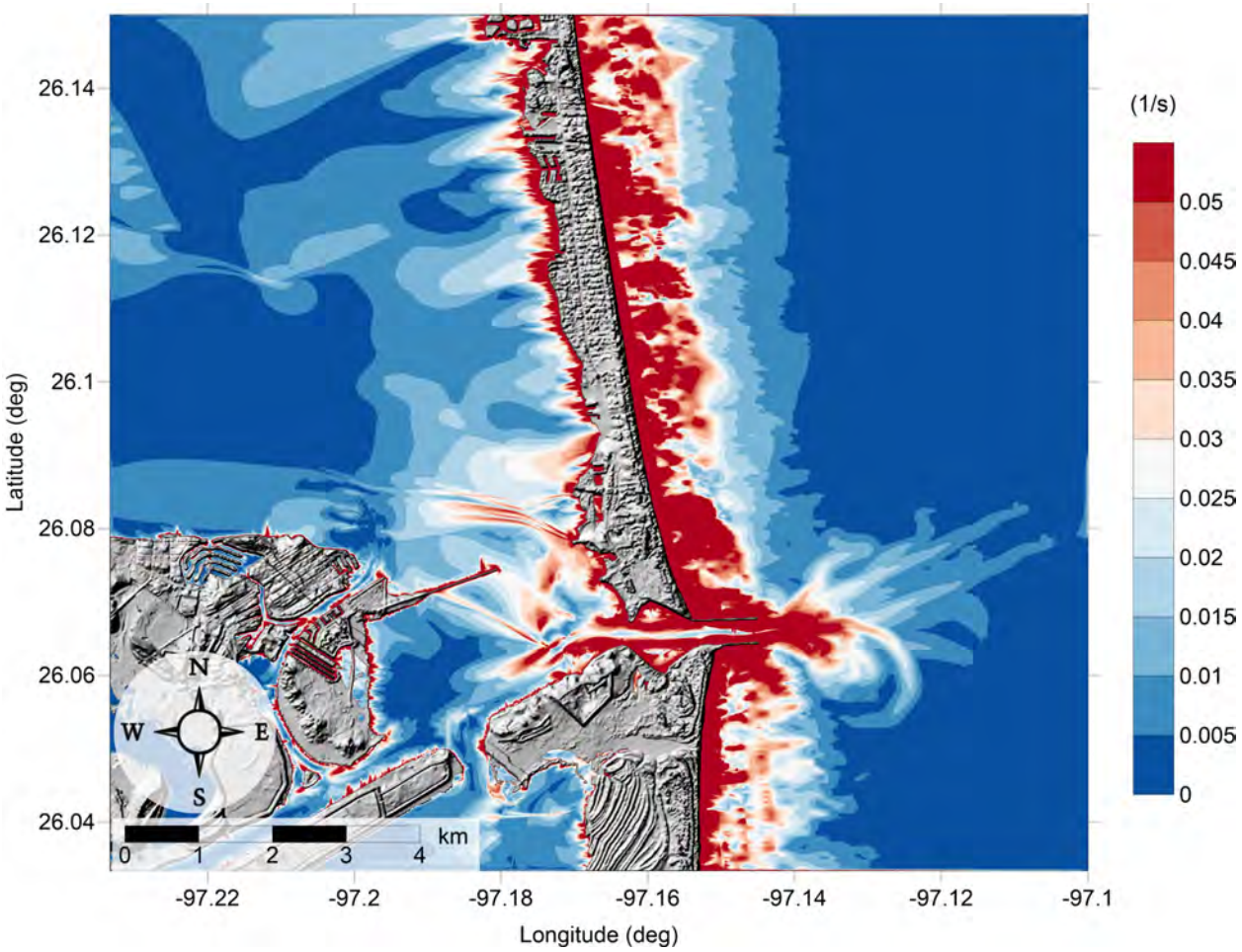


Figure 149: Maximum of maximum vorticity magnitude contour in South Padre Island, TX (1/3 arcsecond) for all landslide scenarios.

## 5.2 Mustang Island, TX

### Mustang Island, TX
### All Sources
### Maximum of Maximum Velocity Magnitude

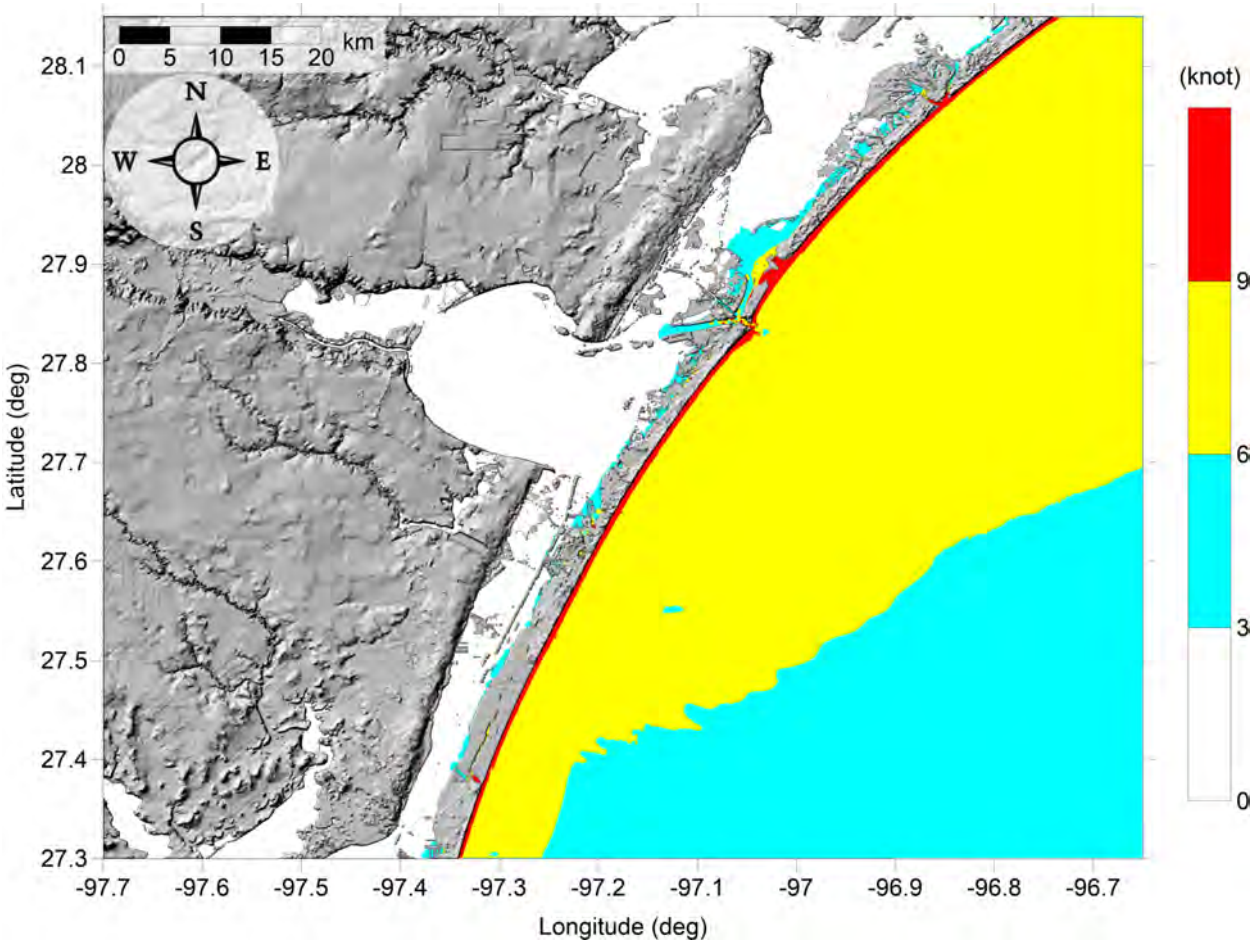


Figure 150: Maximum of maximum velocity magnitude contour in Mustang Island, TX (3 arcsecond) for all landslide scenarios.

## Mustang Island, TX
## All Sources
## Maximum of Maximum Velocity Magnitude

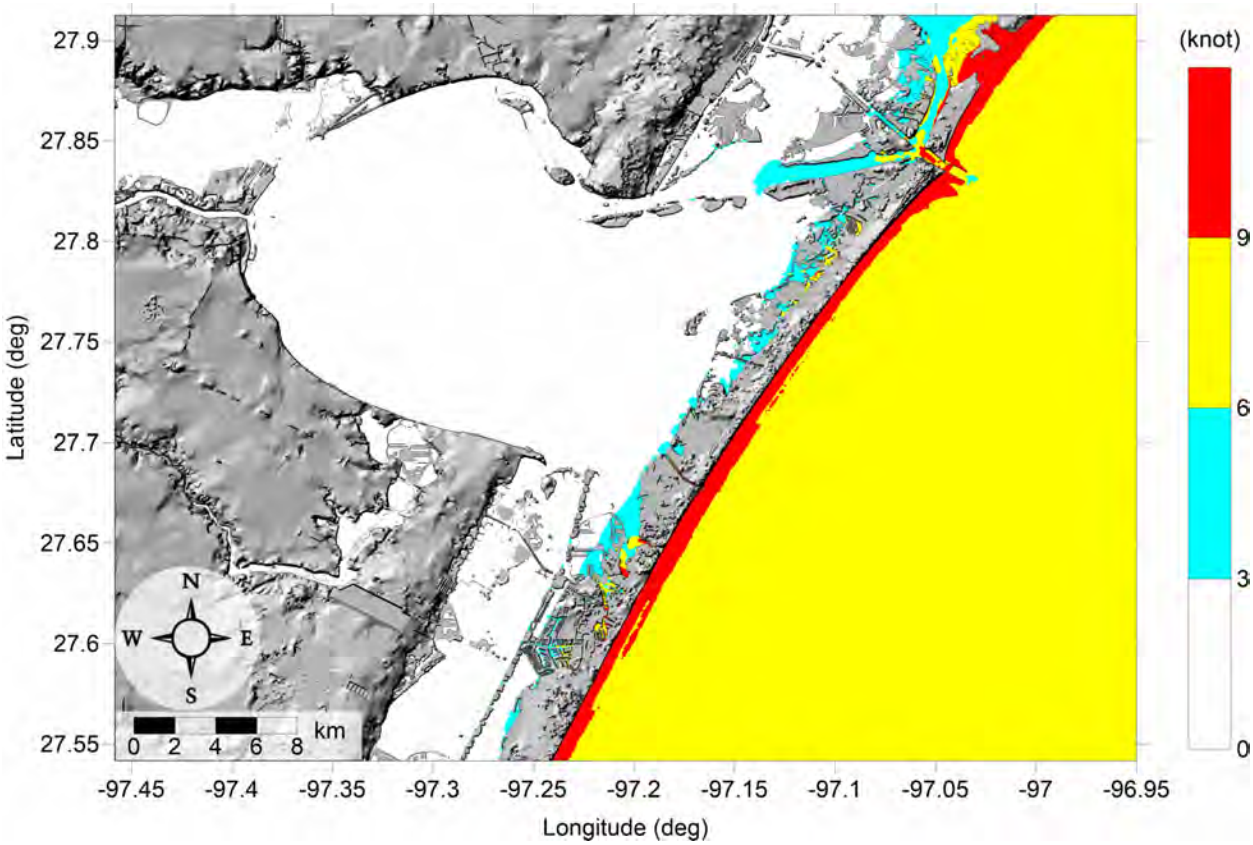


Figure 151: Maximum of maximum velocity magnitude contour in Mustang Island, TX (1 arcsecond) for all landslide scenarios.

## Mustang Island, TX
## All Sources
## Maximum of Maximum Velocity Magnitude

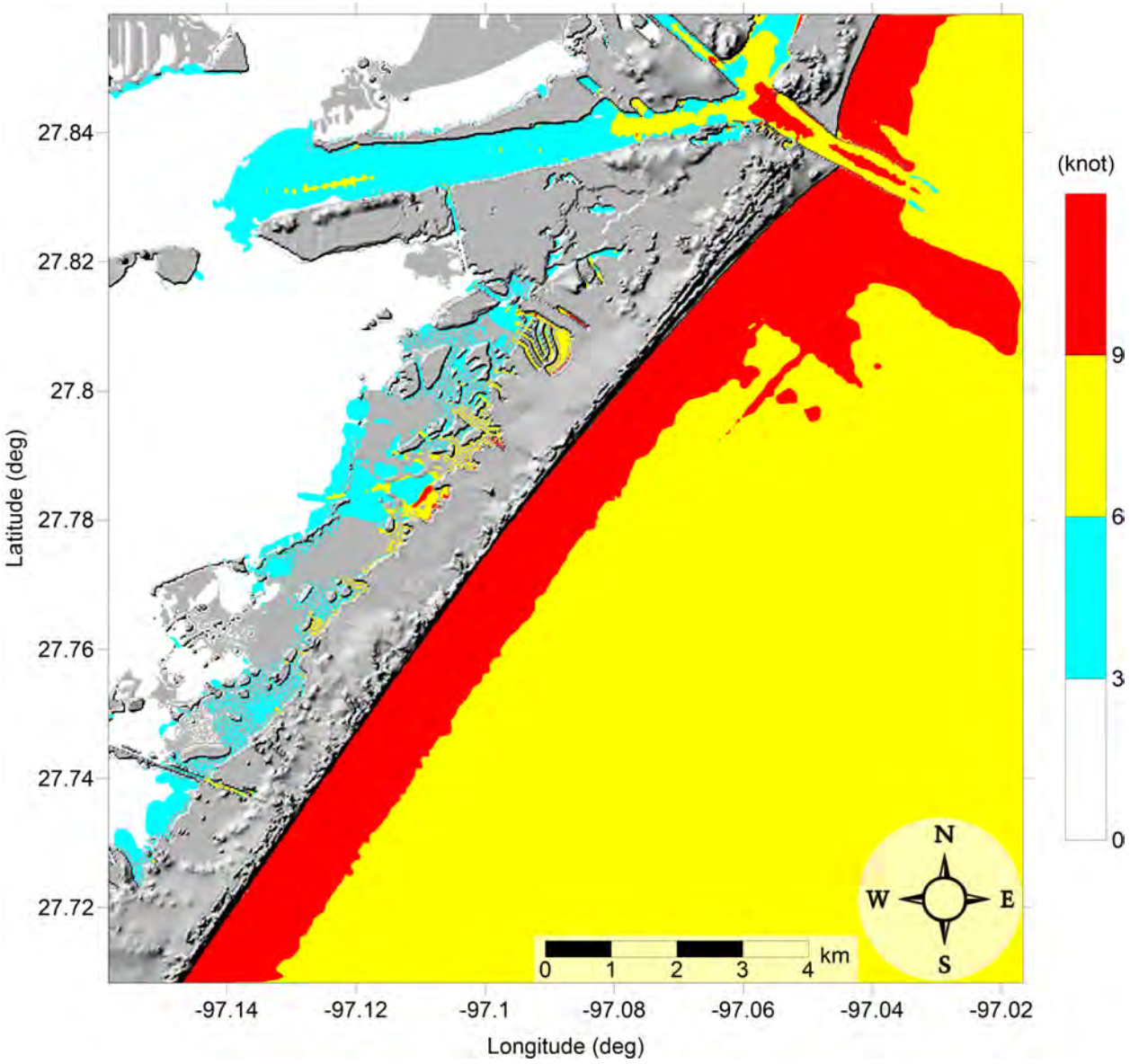


Figure 152: Maximum of maximum velocity magnitude contour in Port Aransas, TX (1/3 arcsecond) for all landslide scenarios.

## Mustang Island, TX
## All Sources
## Maximum of Maximum Velocity Magnitude

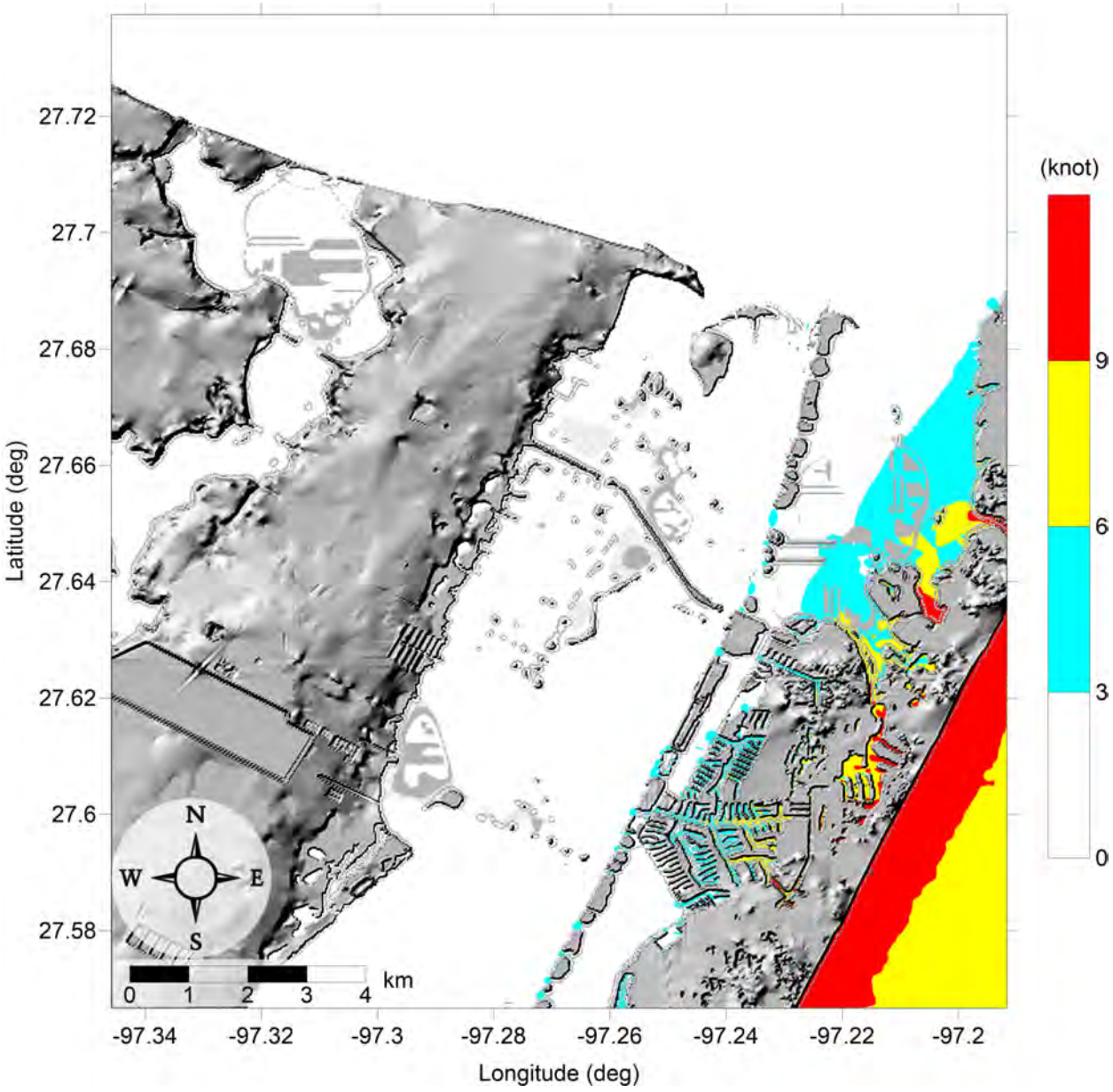


Figure 153: Maximum of maximum velocity magnitude contour in South-East Corpus Christi, TX (1/3 arcsecond) for all landslide scenarios.

## Mustang Island, TX
## All Sources
## Maximum of Maximum Vorticity Magnitude

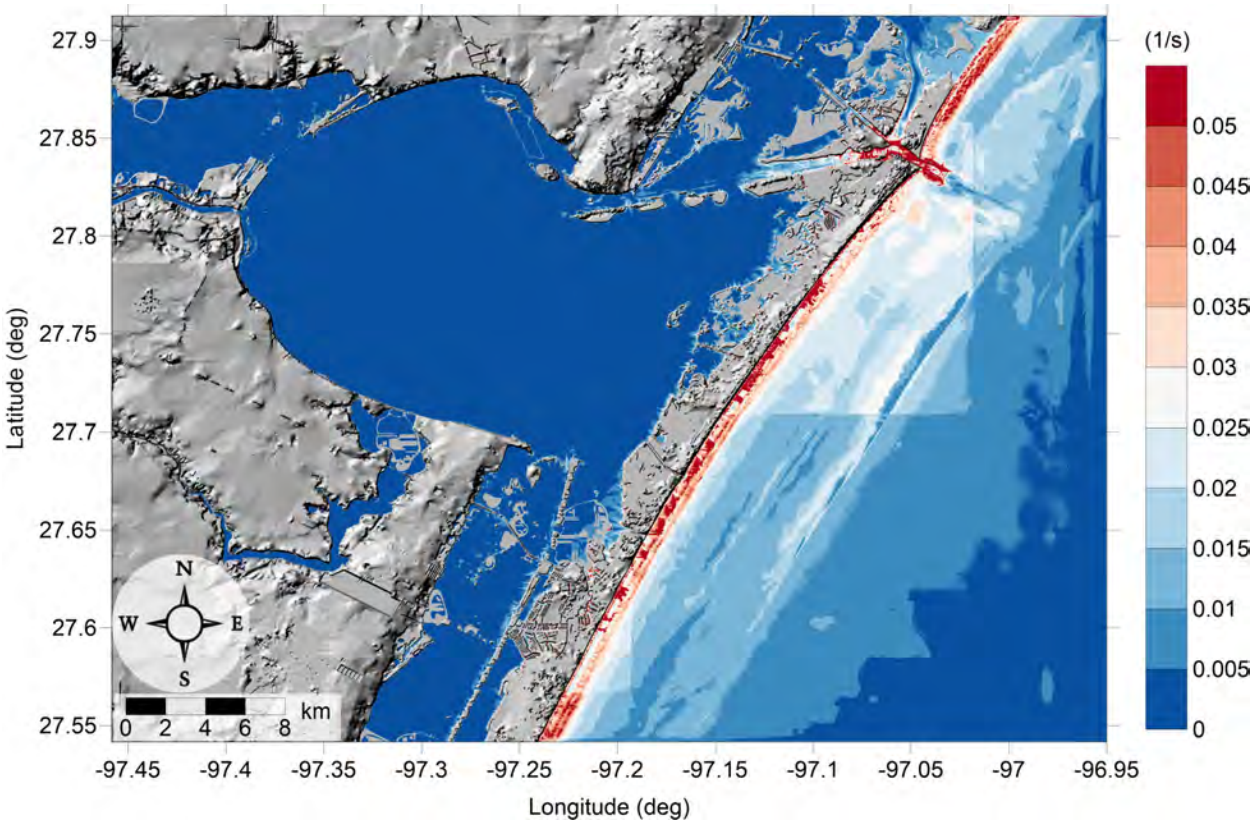


Figure 154: Maximum of maximum vorticity magnitude contour in Mustang Island, TX (1 arcsecond) for all landslide scenarios.

## Mustang Island, TX
## All Sources
## Maximum of Maximum Vorticity Magnitude

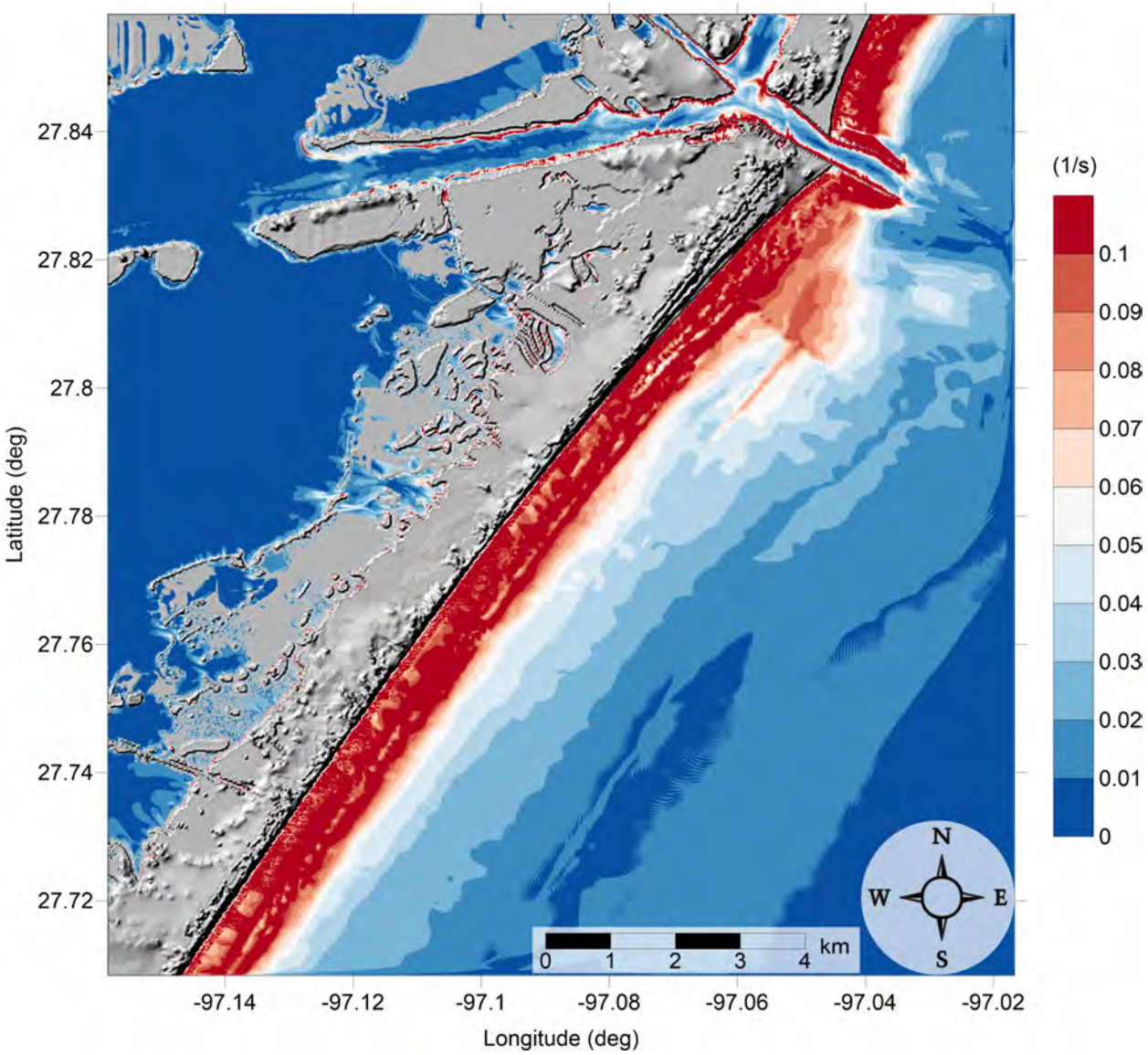


Figure 155: Maximum of maximum vorticity magnitude contour in Port Aransas, TX (1/3 arcsecond) for all landslide scenarios.

## Mustang Island, TX
## All Sources
## Maximum of Maximum Vorticity Magnitude

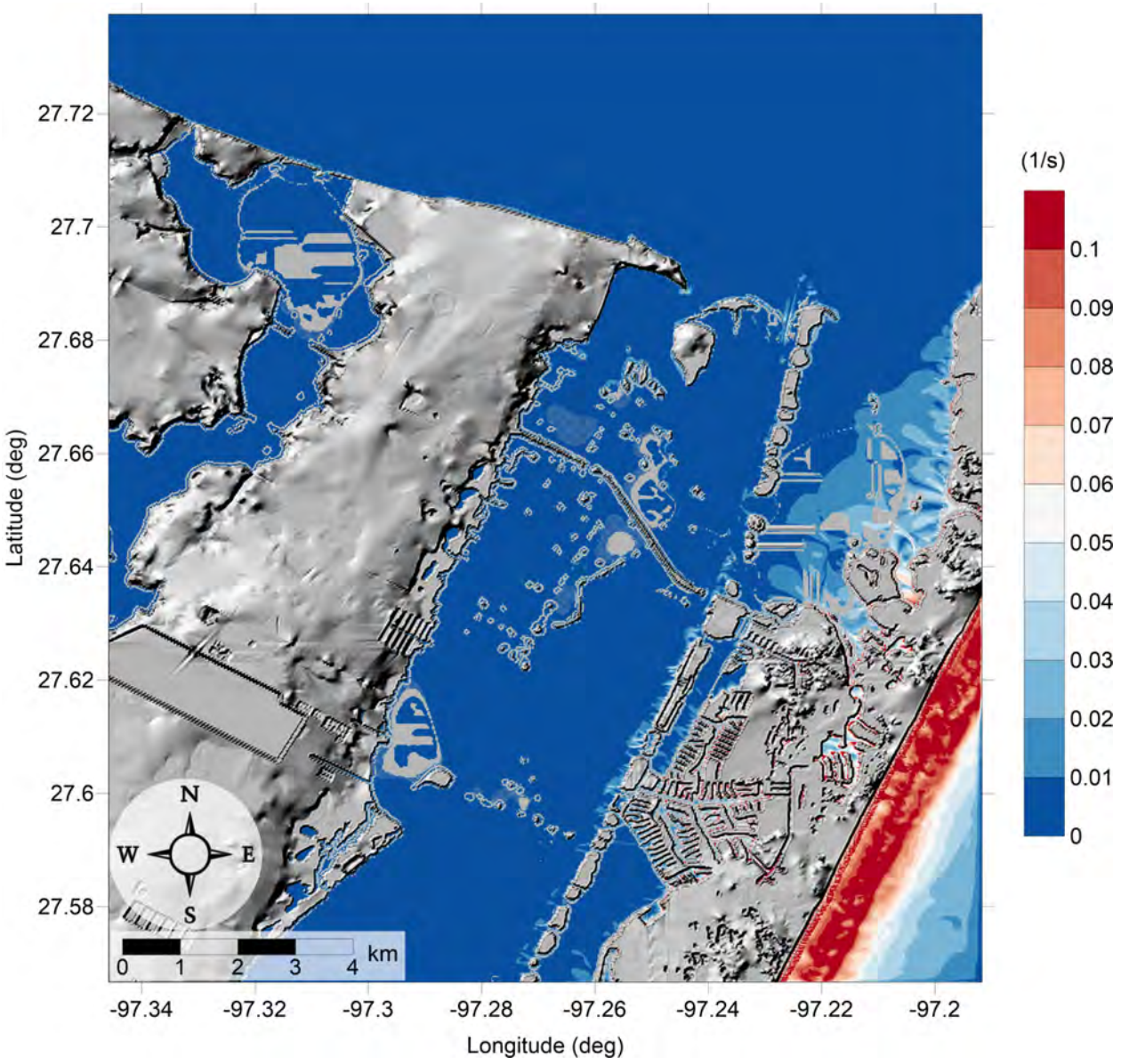


Figure 156: Maximum of maximum vorticity magnitude contour in South-East Corpus Christi, TX (1/3 arcsecond) for all landslide scenarios.

## 5.3 Mobile, AL

### Mobile, AL
### All Sources
### Maximum of Maximum Velocity Magnitude

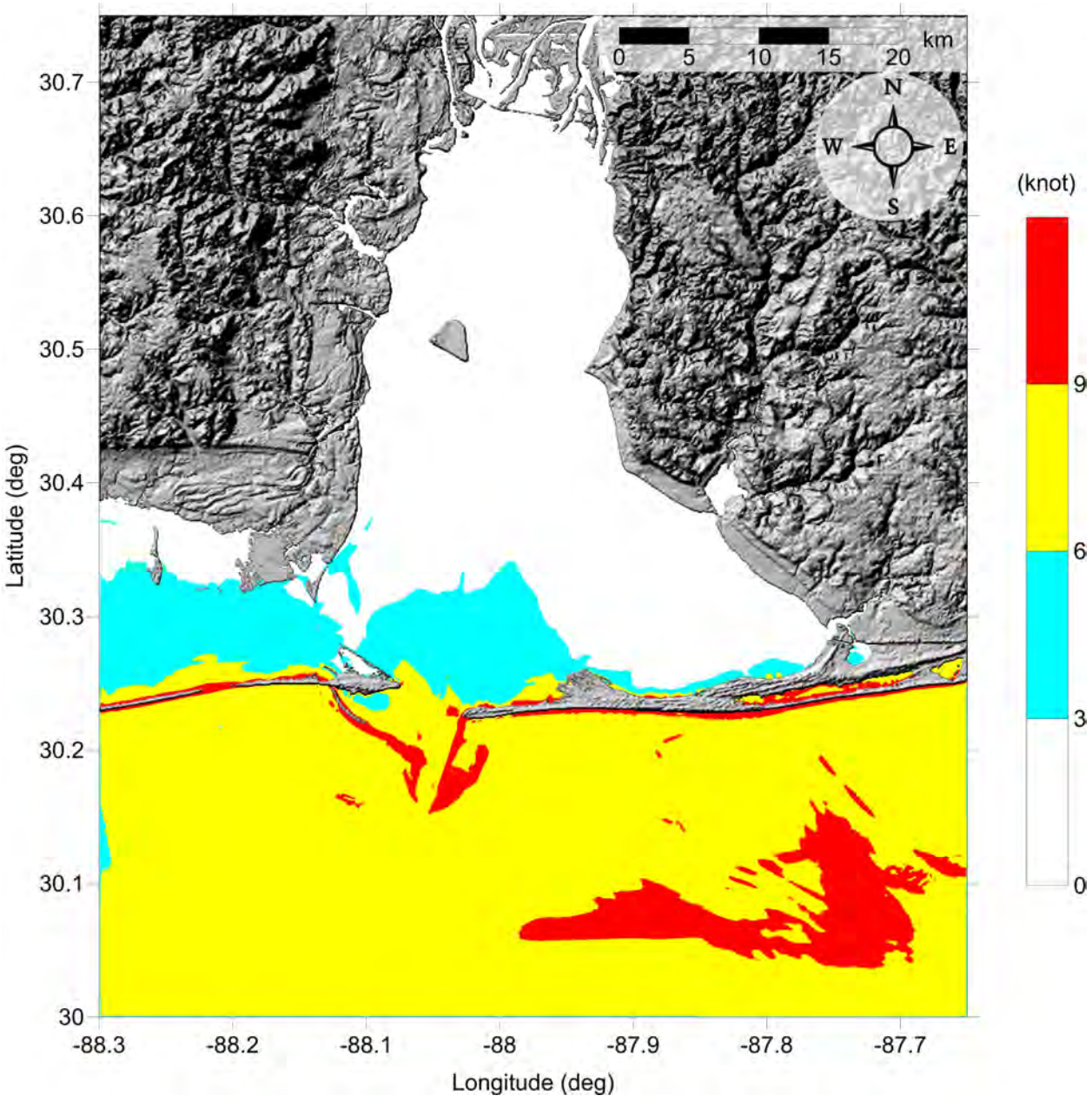


Figure 157: Maximum of maximum velocity magnitude contour in Mobile, AL (3 arcsecond) for all landslide scenarios.

## Mobile, AL
## All Sources
## Maximum of Maximum Velocity Magnitude

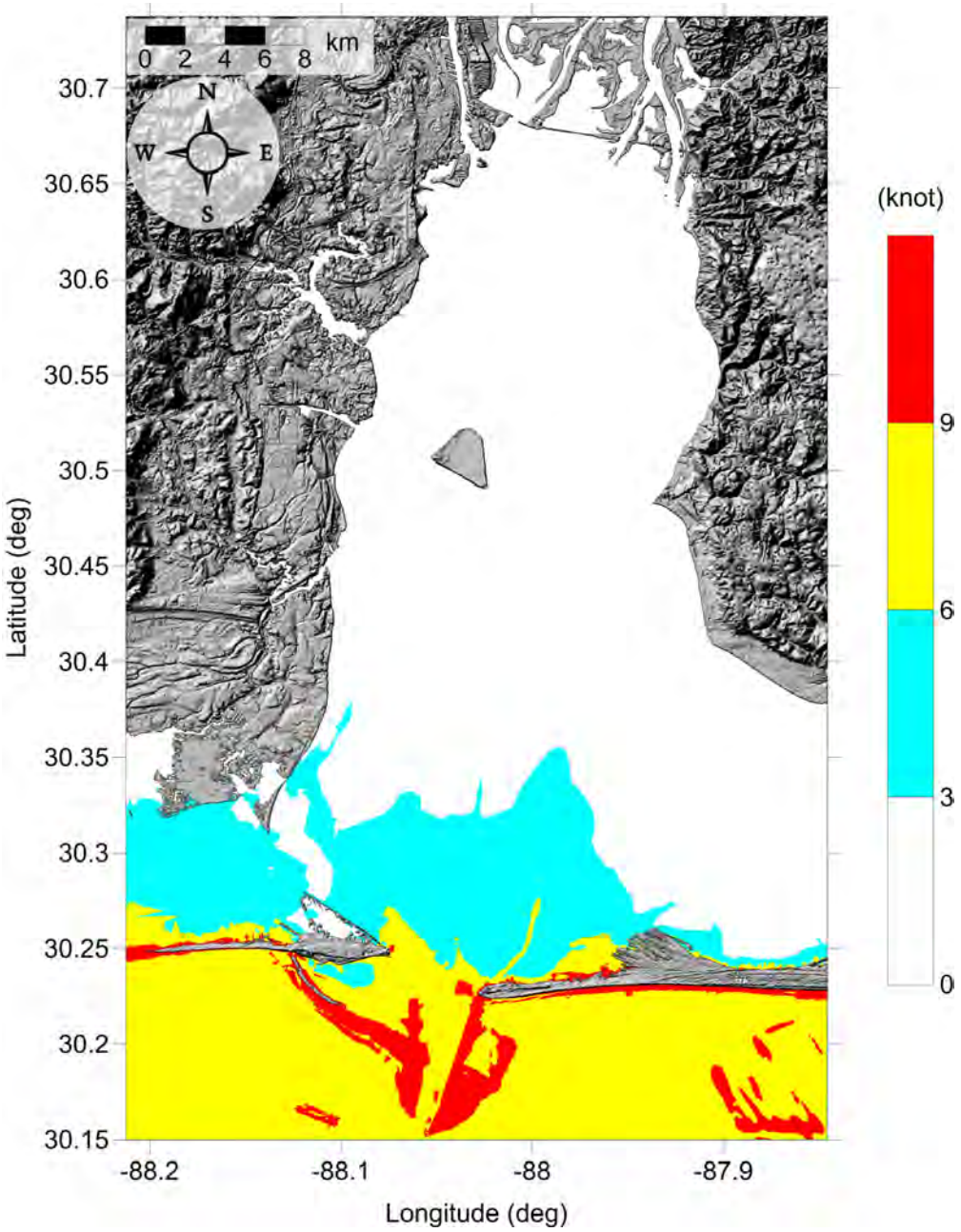


Figure 158: Maximum of maximum velocity magnitude contour in Mobile, AL (1 arcsecond) for all landslide scenarios.

## Mobile, AL
## All Sources
## Maximum of Maximum Velocity Magnitude

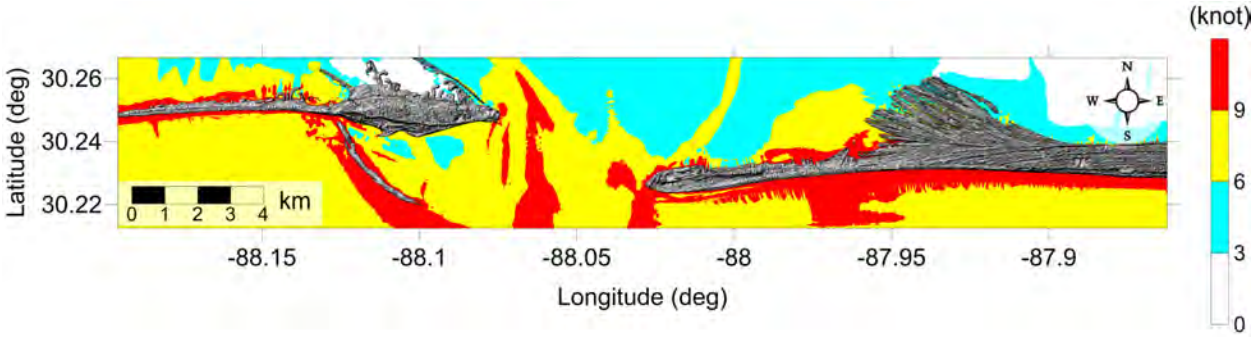


Figure 159: Maximum of maximum velocity magnitude contour in Dauphin Island / Gulf Highlands, AL (1/3 arcsecond) for all landslide scenarios.

## Mobile, AL
## All Sources
## Maximum of Maximum Velocity Magnitude

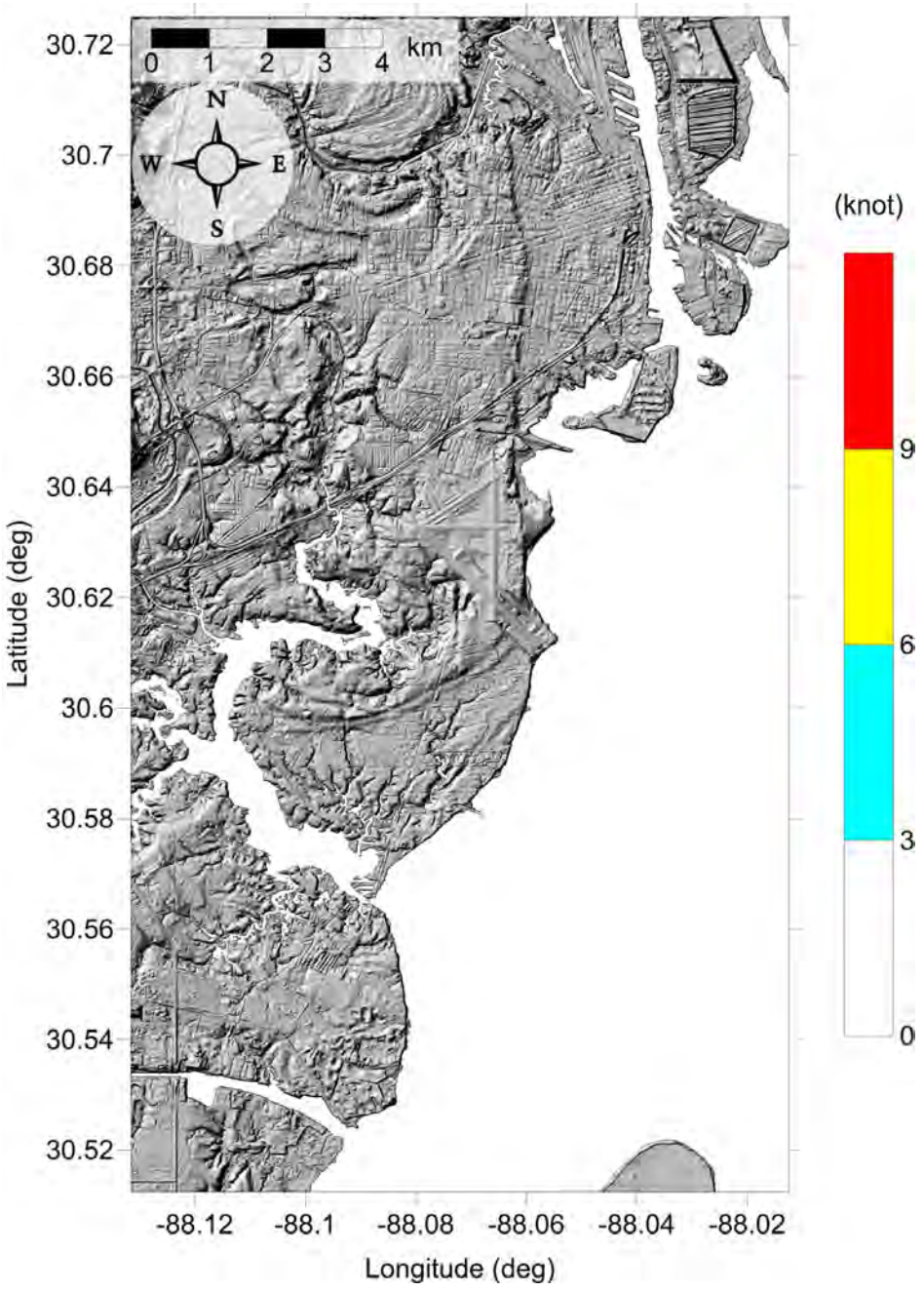


Figure 160: Maximum of maximum velocity magnitude contour in Mobile, AL (1/3 arcsecond) for all landslide scenarios.

## Mobile, AL
## All Sources
## Maximum of Maximum Vorticity Magnitude

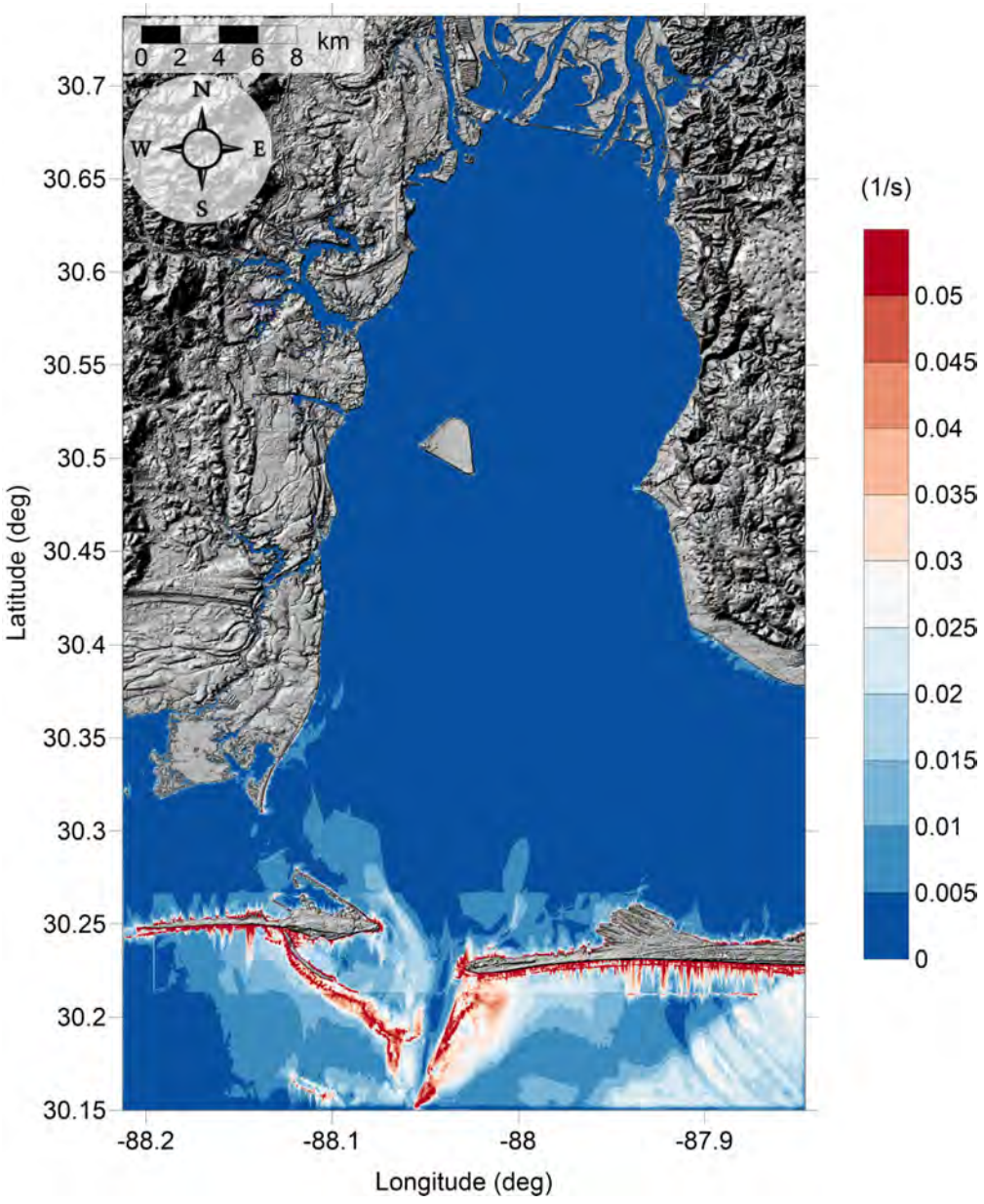


Figure 161: Maximum of maximum vorticity magnitude contour in Mobile, AL (1 arcsecond) for all landslide scenarios.

## Mobile, AL
## All Sources
## Maximum of Maximum Vorticity Magnitude

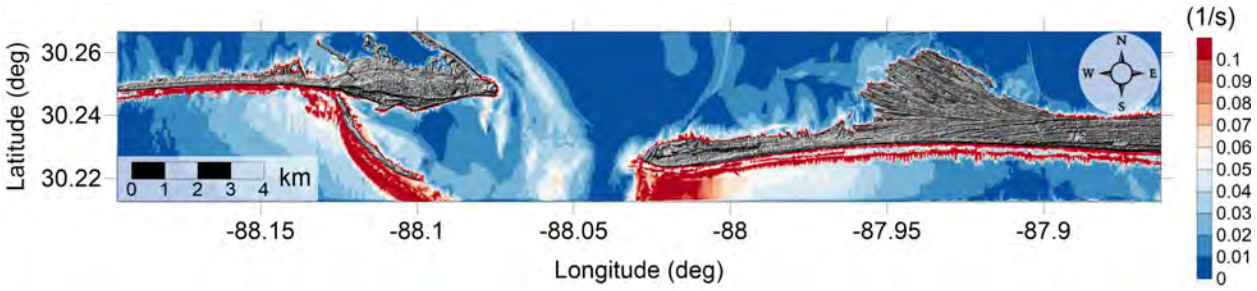


Figure 162: Maximum of maximum vorticity magnitude contour in Dauphin Island / Gulf Highlands, AL (1/3 arcsecond) for all landslide scenarios.

## Mobile, AL
## All Sources
## Maximum of Maximum Vorticity Magnitude

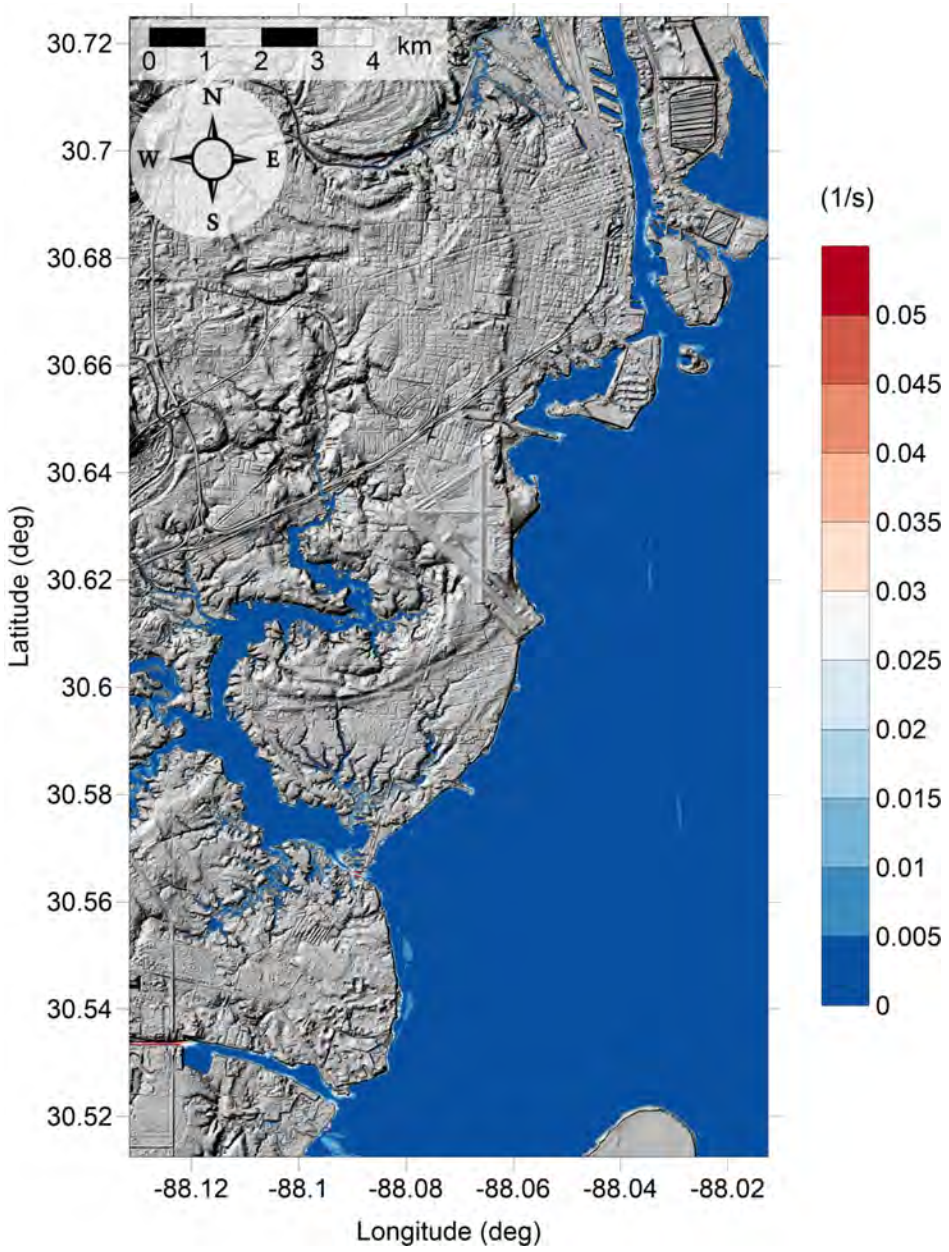


Figure 163: Maximum of maximum vorticity magnitude contour in Mobile, AL (1/3 arcsecond) for all landslide scenarios.

## 5.4 Pensacola, FL

### Pensacola, FL
### All Sources
### Maximum of Maximum Velocity Magnitude

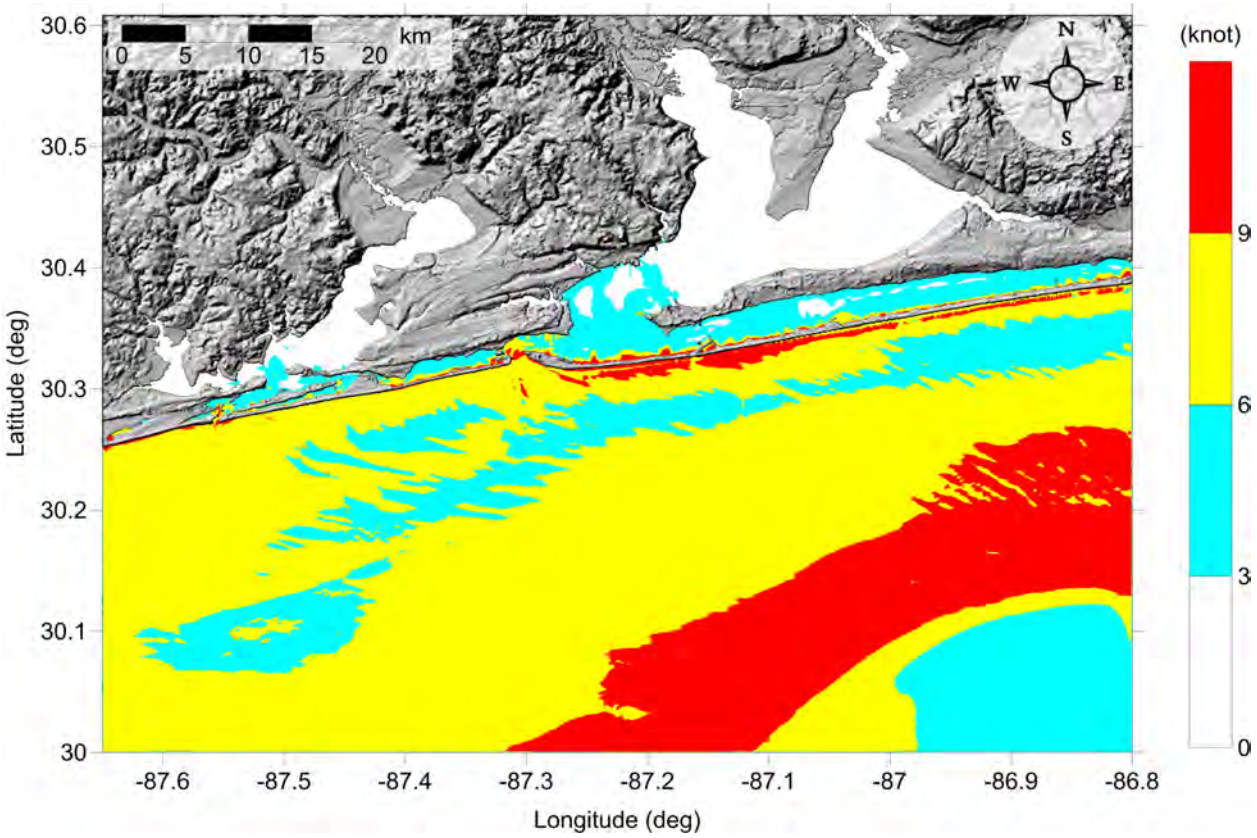


Figure 164: Maximum of maximum velocity magnitude contour in Pensacola, FL (3 arcsecond) for all landslide scenarios.

## Pensacola, FL
## All Sources
## Maximum of Maximum Velocity Magnitude

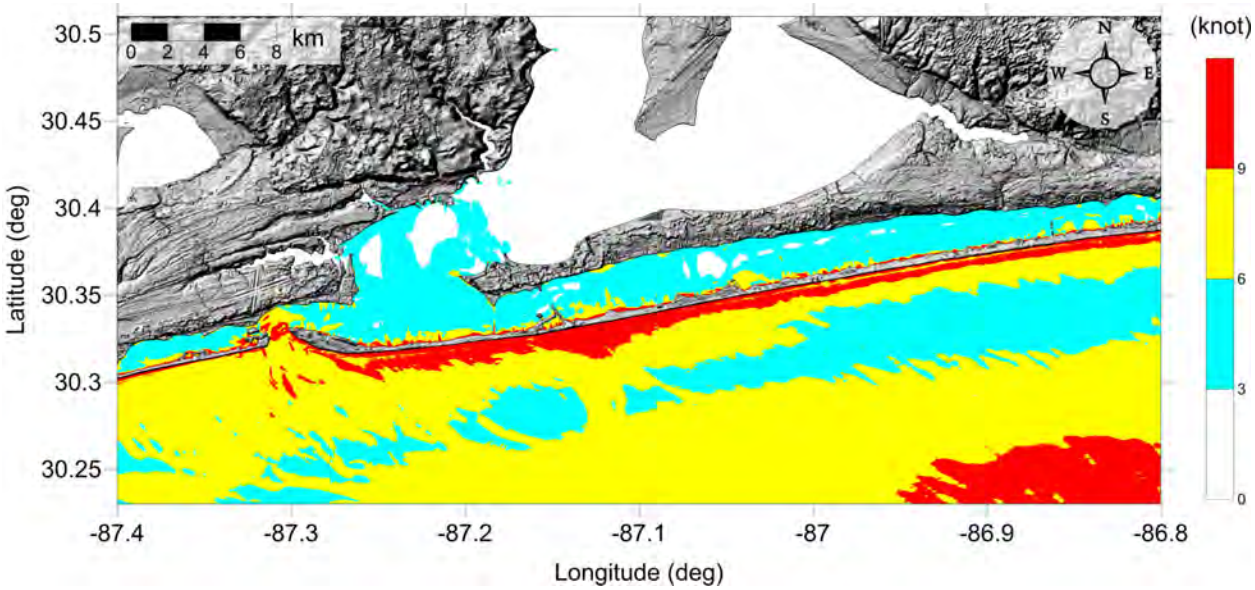


Figure 165: Maximum of maximum velocity magnitude contour in Pensacola, FL (1 arcsecond) for all landslide scenarios.

**Pensacola, FL**
**All Sources**
**Maximum of Maximum Velocity Magnitude**

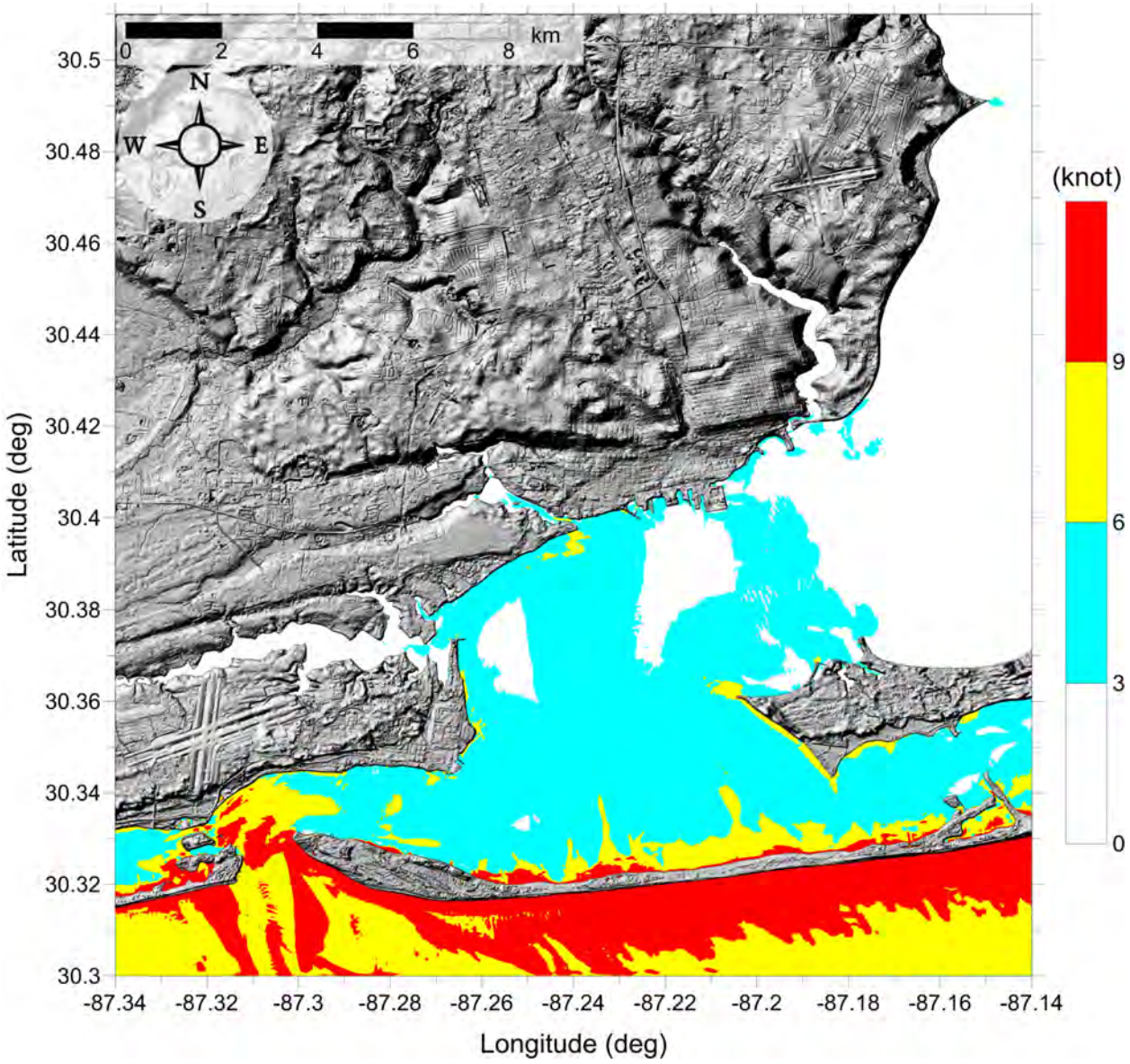


Figure 166: Maximum of maximum velocity magnitude contour in Pensacola, FL (1/3 arc-second) for all landslide scenarios.

## Pensacola, FL
## All Sources
## Maximum of Maximum Vorticity Magnitude

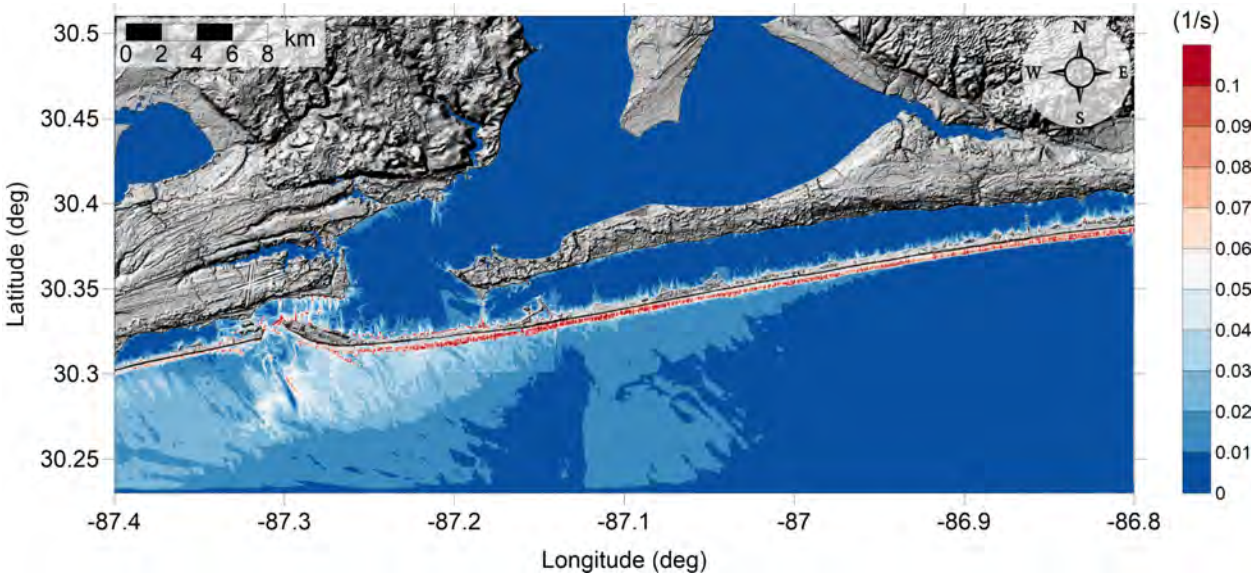


Figure 167: Maximum of maximum vorticity magnitude contour in Pensacola, FL (1 arcsecond) for all landslide scenarios.

## Pensacola, FL
## All Sources
## Maximum of Maximum Vorticity Magnitude

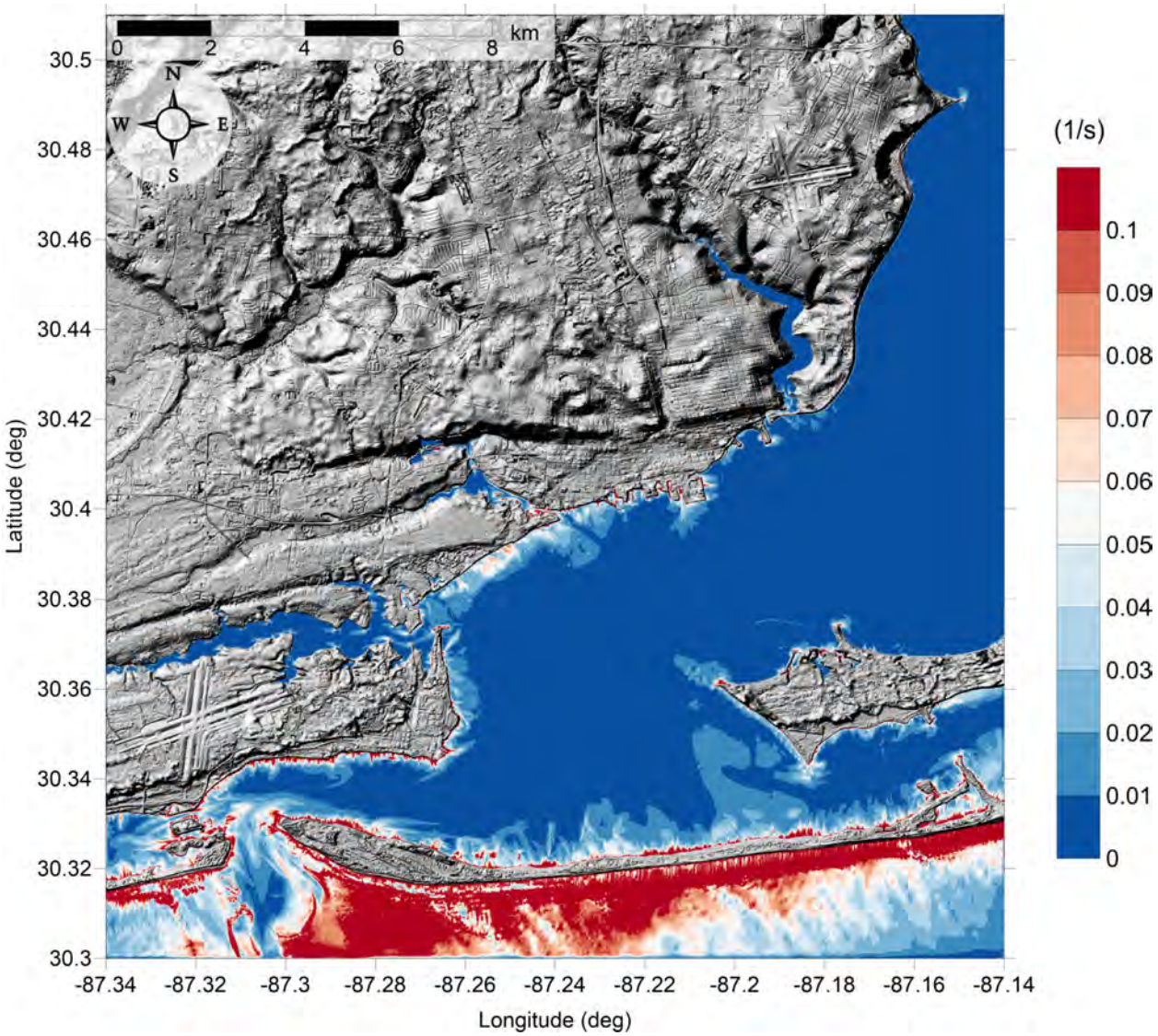


Figure 168: Maximum of maximum vorticity magnitude contour in Pensacola, FL (1/3 arcsecond) for all landslide scenarios.

## 5.5 Santa Rosa County, FL

### Santa Rosa County, FL
### All Sources
### Maximum of Maximum Velocity Magnitude

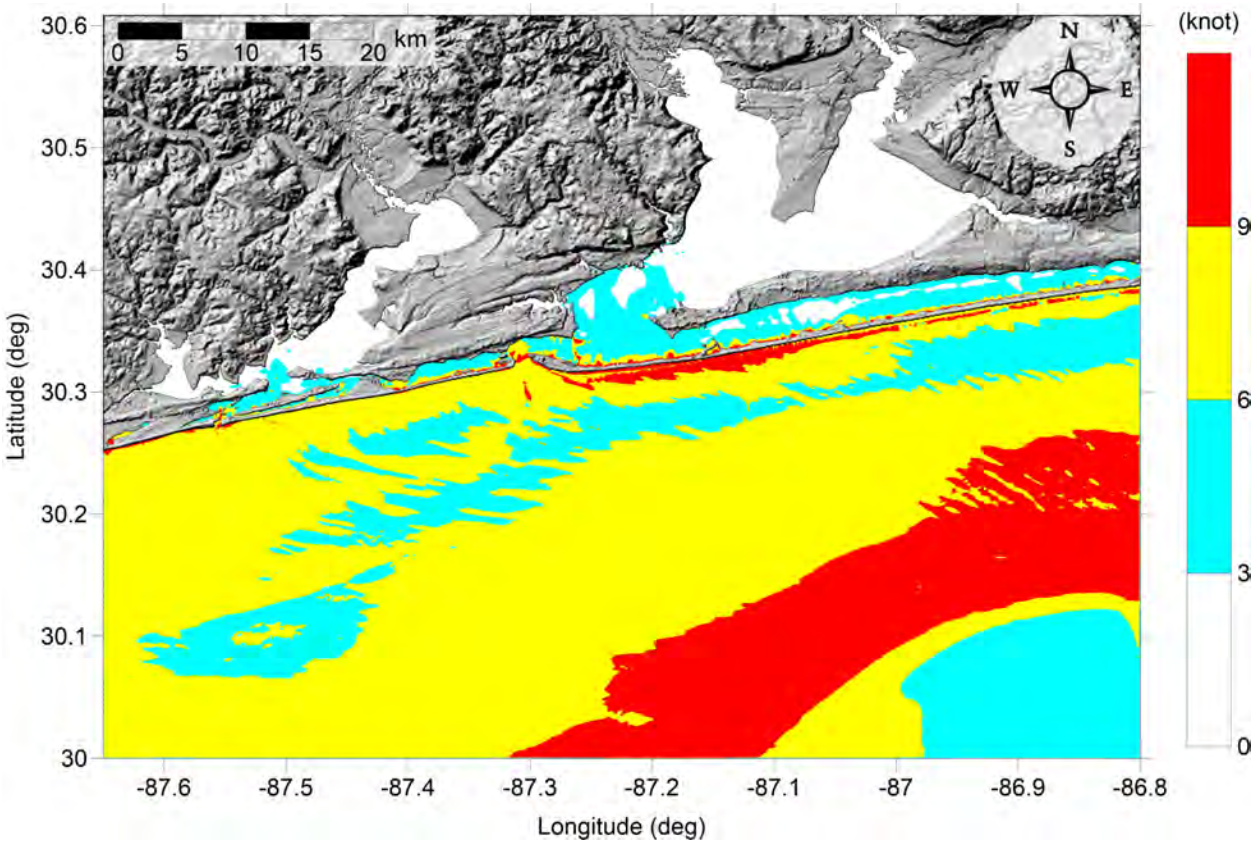


Figure 169: Maximum of maximum velocity magnitude contour in Santa Rosa County, FL (3 arcsecond) for all landslide scenarios.

## Santa Rosa County, FL
## All Sources
## Maximum of Maximum Velocity Magnitude

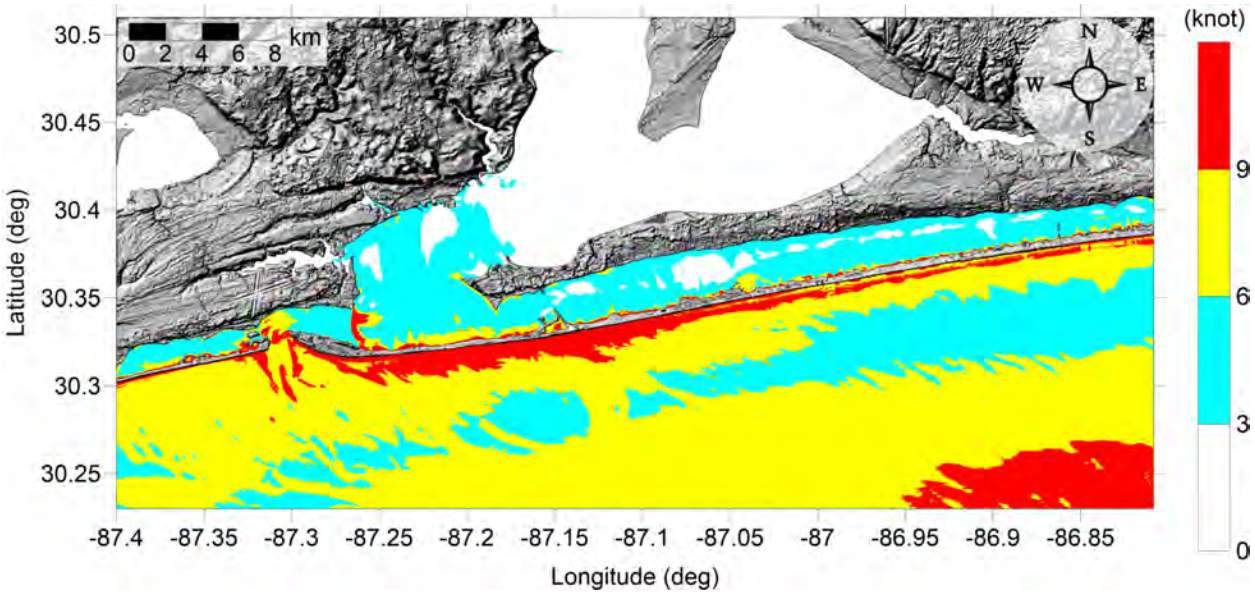


Figure 170: Maximum of maximum velocity magnitude contour in Santa Rosa County, FL (1 arcsecond) for all landslide scenarios.

**Santa Rosa County, FL**
**All Sources**
**Maximum of Maximum Velocity Magnitude**

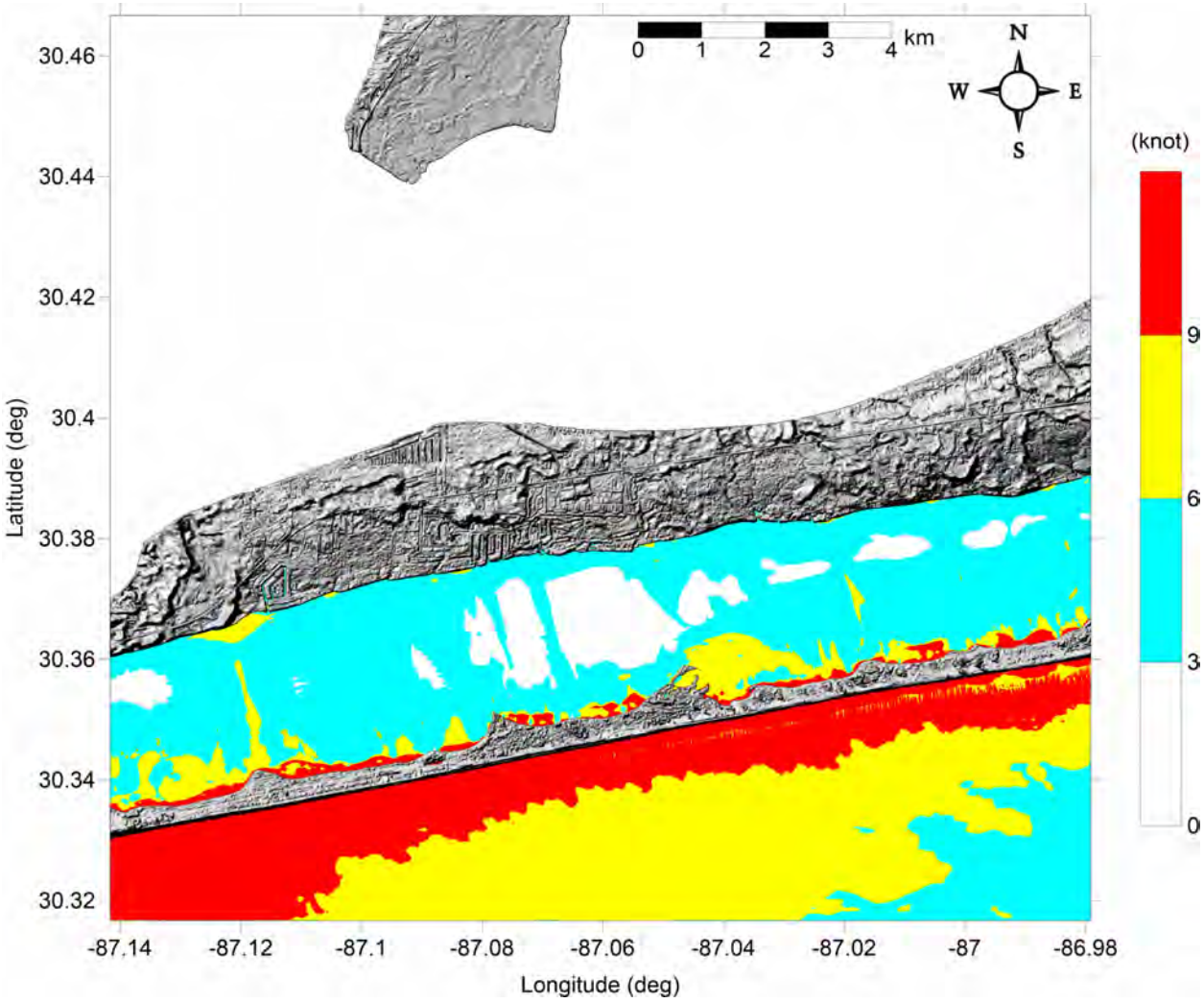


Figure 171: Maximum of maximum velocity magnitude contour in East Gulf Breeze, FL (1/3 arcsecond) for all landslide scenarios.

## Santa Rosa County, FL
## All Sources
## Maximum of Maximum Velocity Magnitude

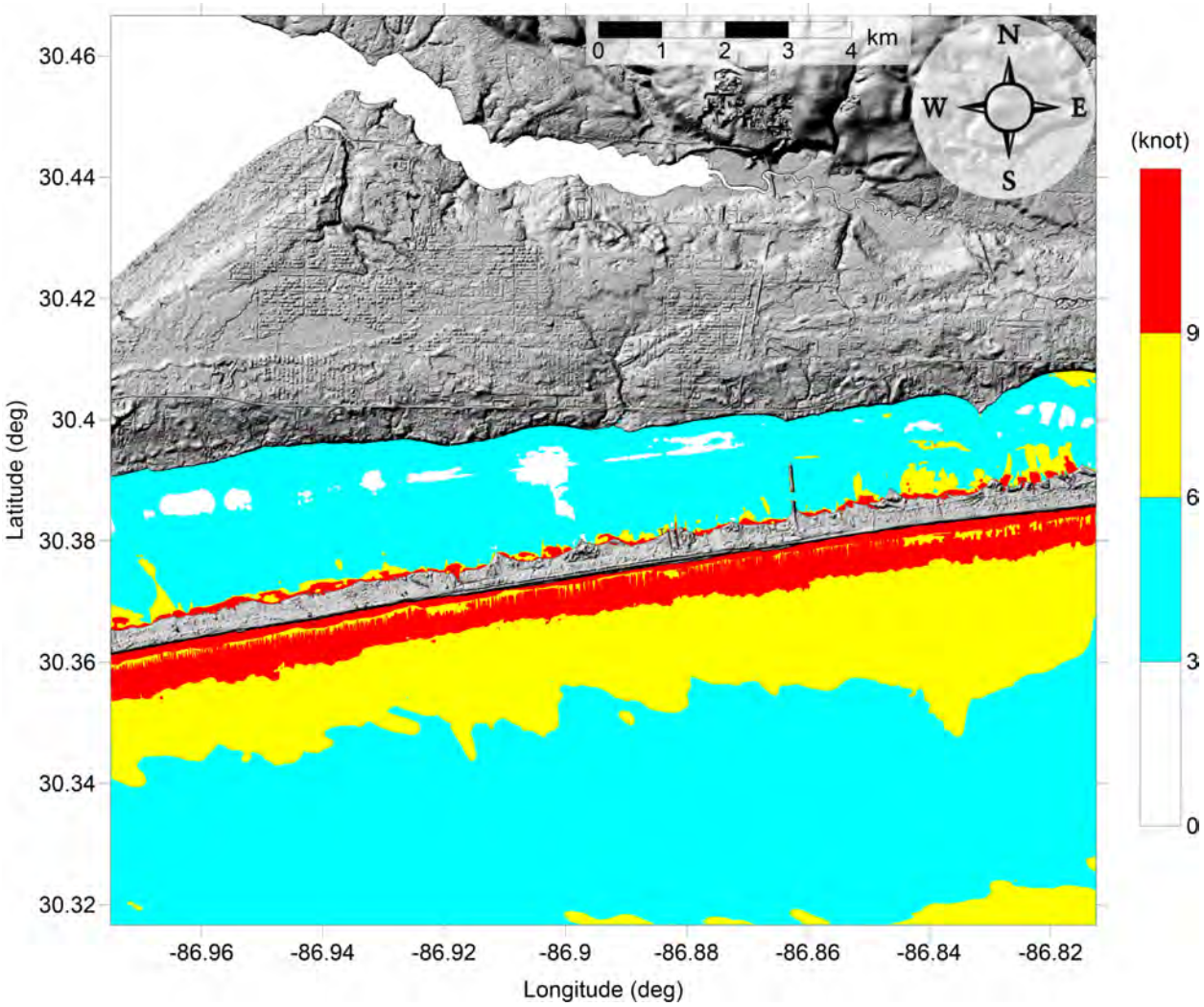


Figure 172: Maximum of maximum velocity magnitude contour in Navarre, FL (1/3 arcsecond) for all landslide scenarios.

## Santa Rosa County, FL
## All Sources
## Maximum of Maximum Vorticity Magnitude

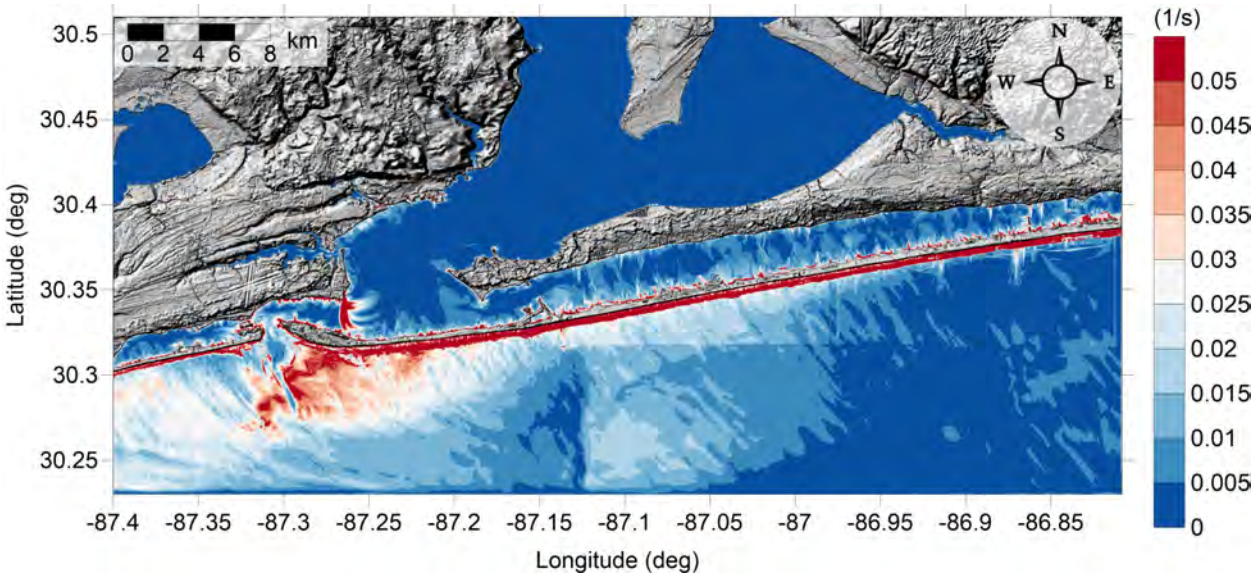


Figure 173: Maximum of maximum vorticity magnitude contour in Santa Rosa County, FL (1 arcsecond) for all landslide scenarios.

## Santa Rosa County, FL
## All Sources
## Maximum of Maximum Vorticity Magnitude

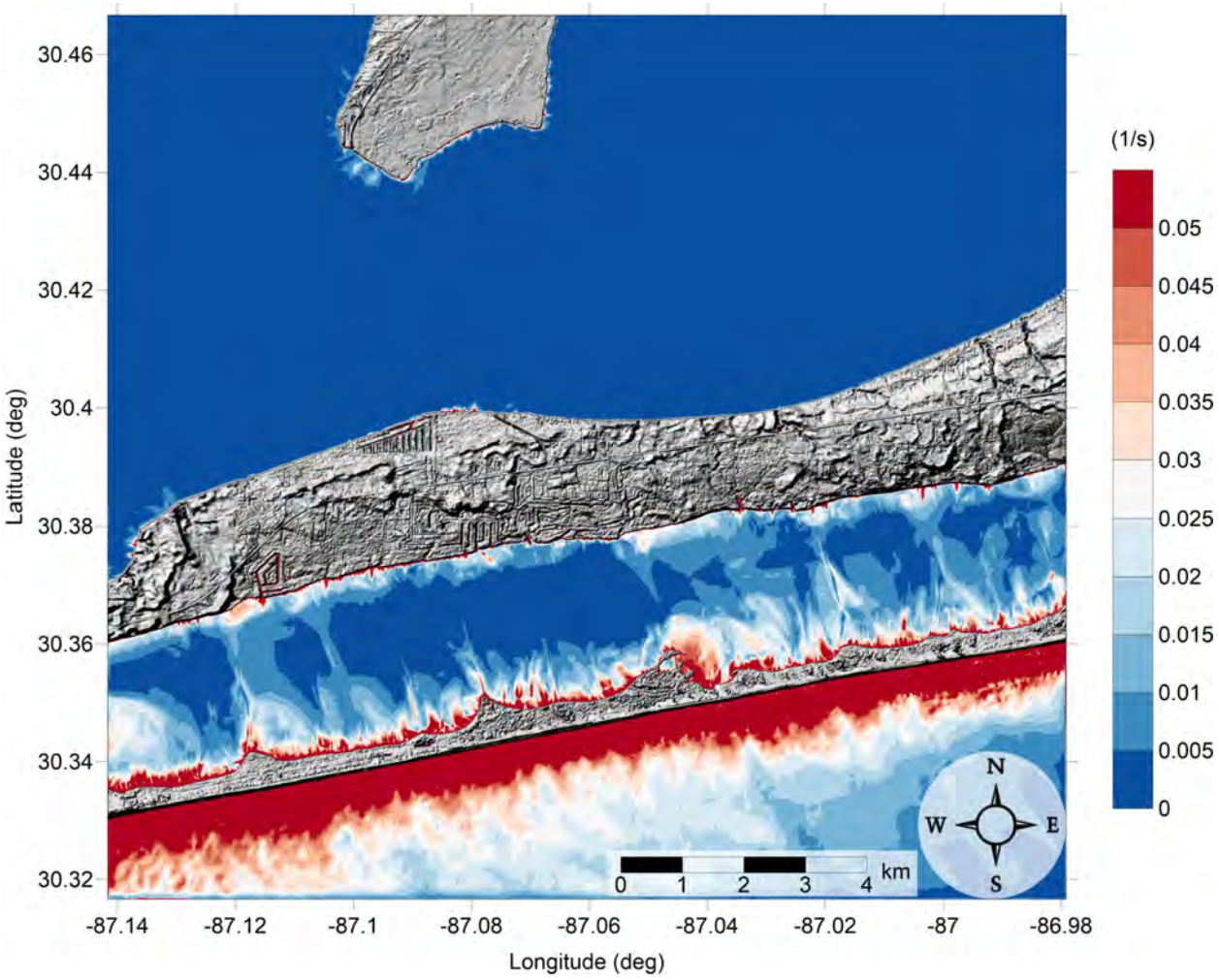


Figure 174: Maximum of maximum vorticity magnitude contour in East Gulf Breeze, FL (1/3 arcsecond) for all landslide scenarios.

## Santa Rosa County, FL
## All Sources
## Maximum of Maximum Vorticity Magnitude

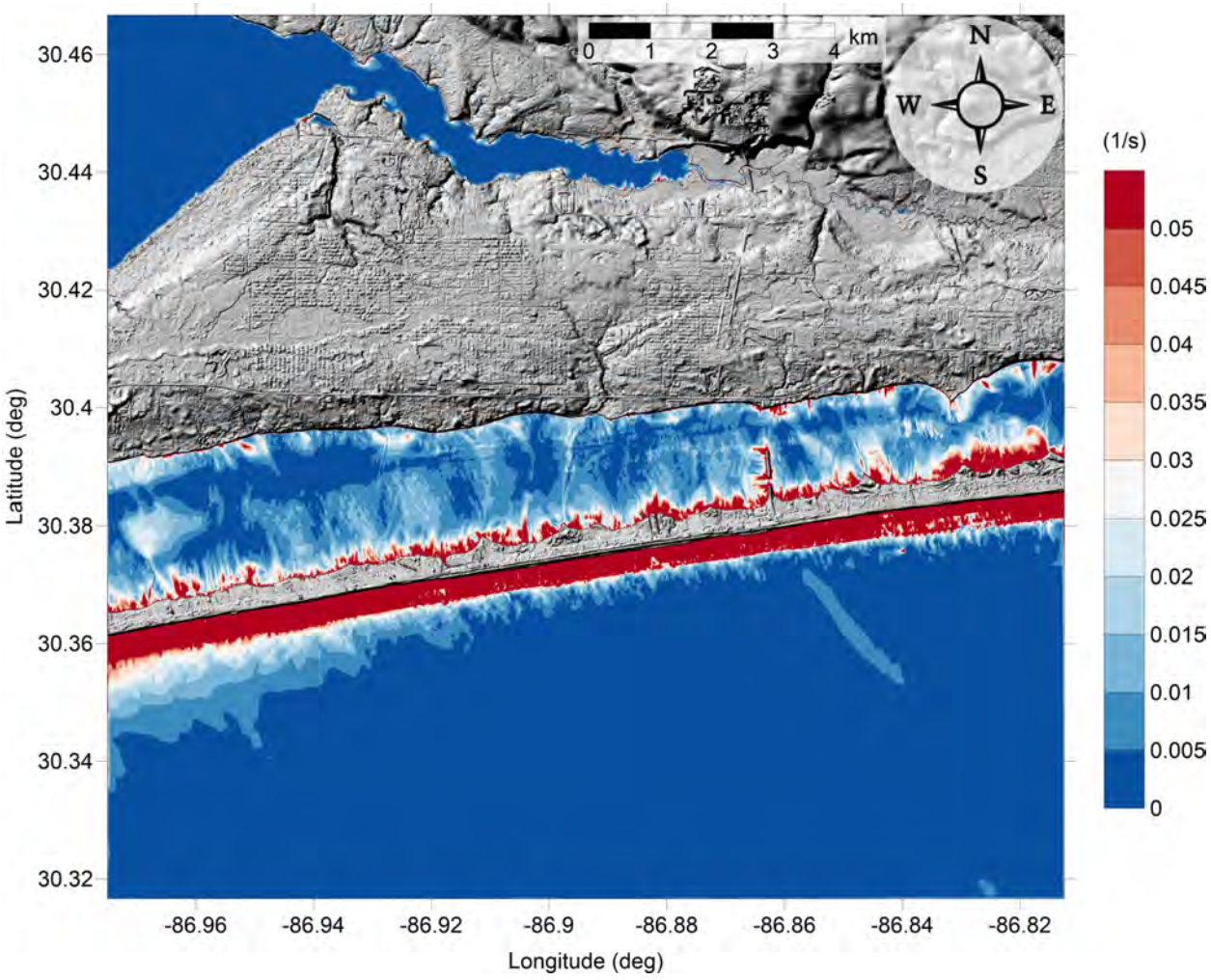


Figure 175: Maximum of maximum vorticity magnitude contour in Navarre, FL (1/3 arc-second) for all landslide scenarios.

## 5.6 Okaloosa County, FL

### Okaloosa County, FL
### All Sources
### Maximum of Maximum Velocity Magnitude

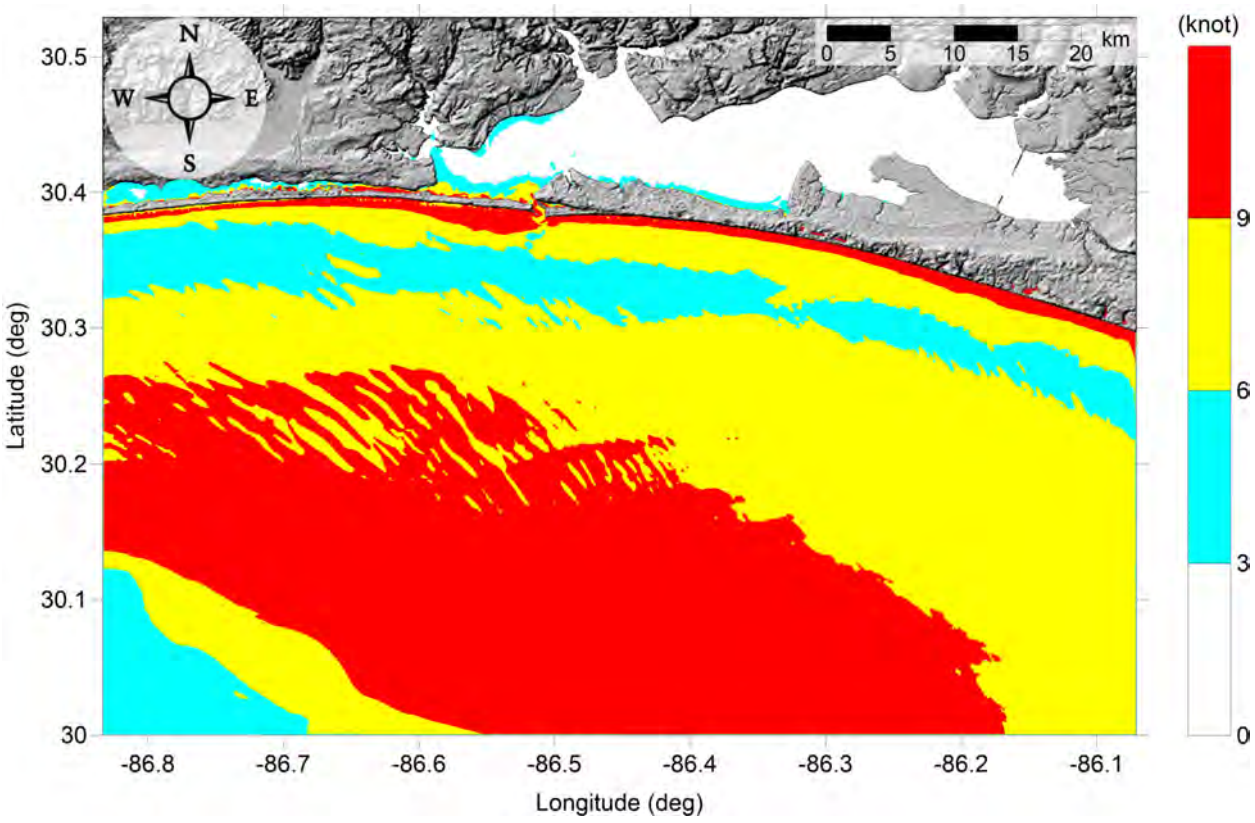


Figure 176: Maximum of maximum velocity magnitude contour in Okaloosa County, FL (3 arcsecond) for all landslide scenarios.

## Okaloosa County, FL
## All Sources
## Maximum of Maximum Velocity Magnitude

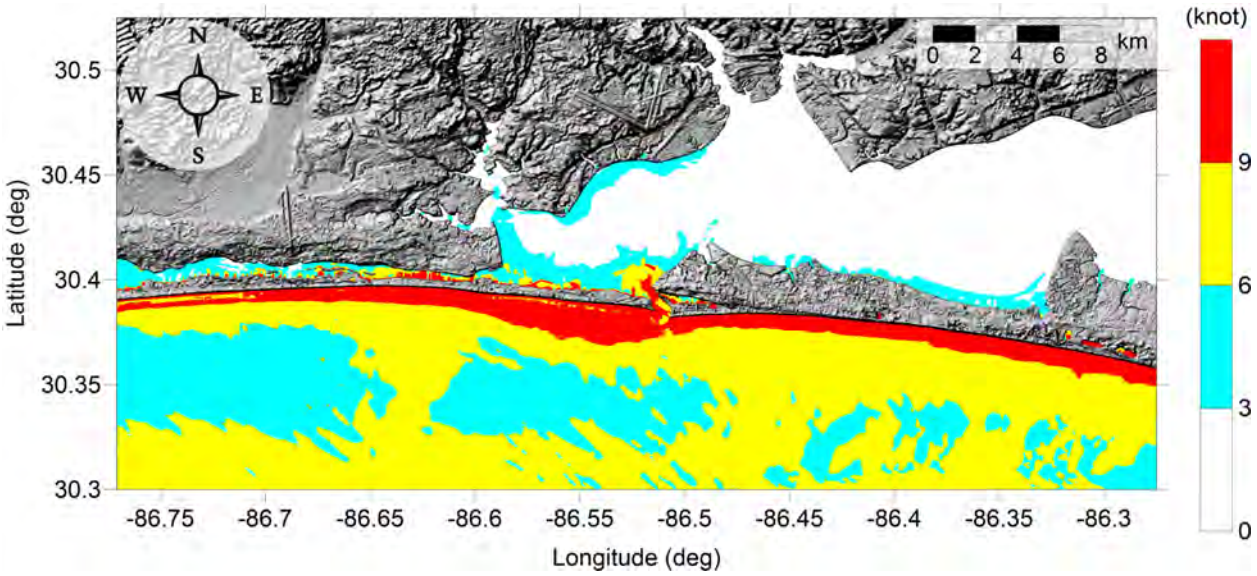


Figure 177: Maximum of maximum velocity magnitude contour in Okaloosa County, FL (1 arcsecond) for all landslide scenarios.

## Okaloosa County, FL
## All Sources
## Maximum of Maximum Velocity Magnitude

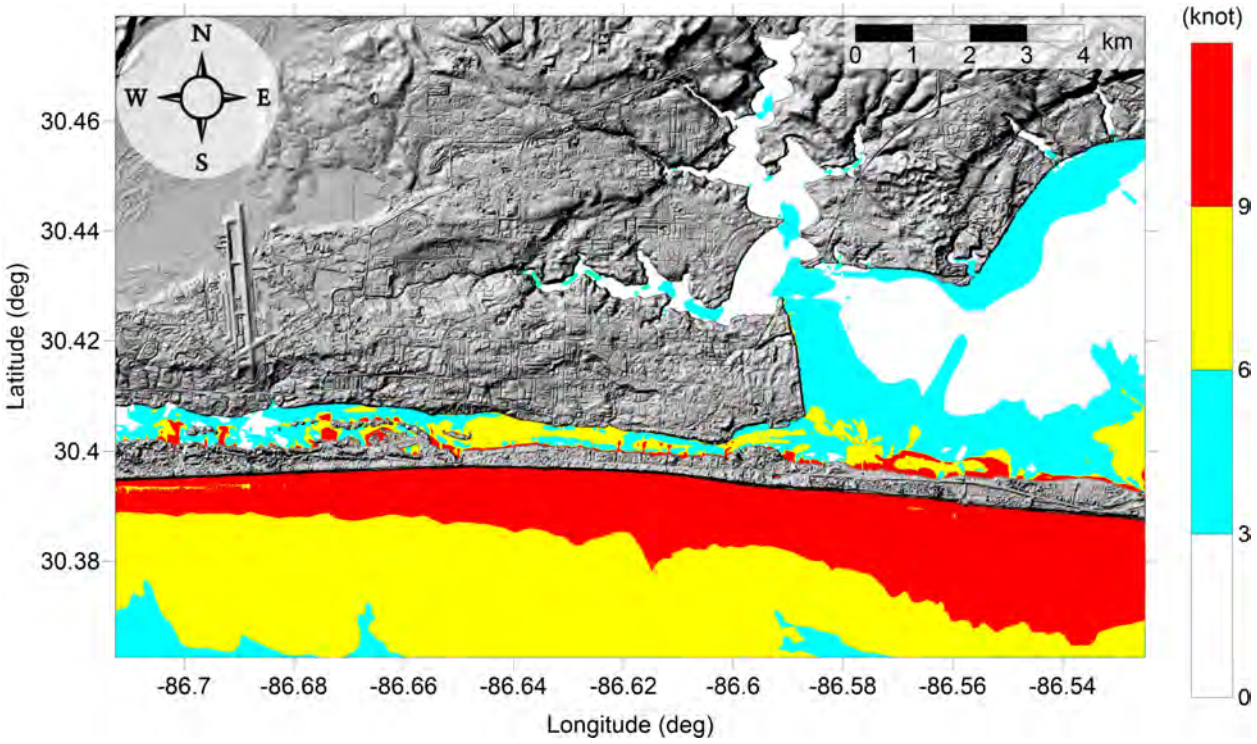


Figure 178: Maximum of maximum velocity magnitude contour in Okaloosa Island, FL (1/3 arcsecond) for all landslide scenarios.

**Okaloosa County, FL**
**All Sources**
**Maximum of Maximum Velocity Magnitude**

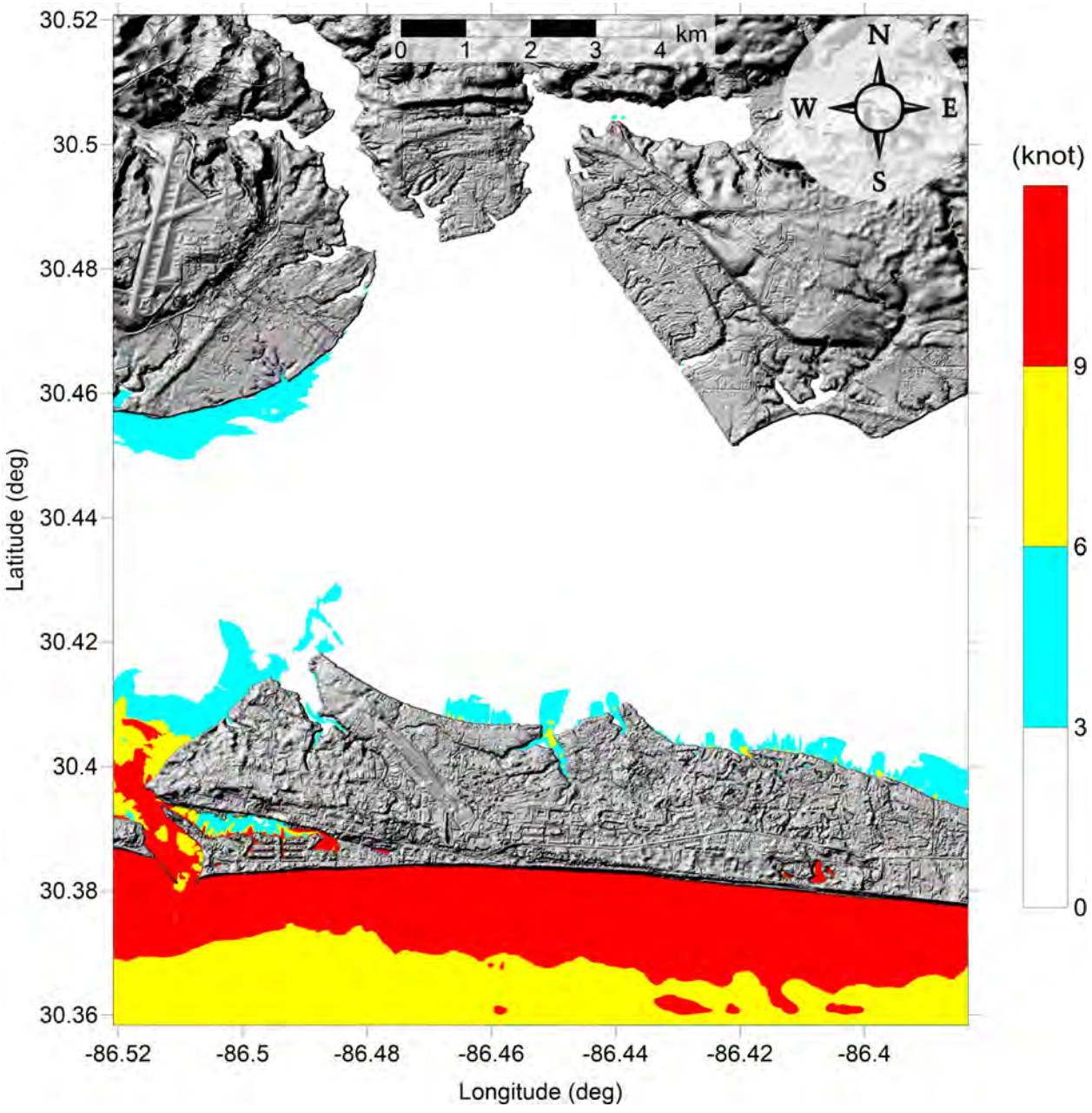


Figure 179: Maximum of maximum velocity magnitude contour in Destin, FL (1/3 arcsecond) for all landslide scenarios.

## Okaloosa County, FL
## All Sources
## Maximum of Maximum Vorticity Magnitude

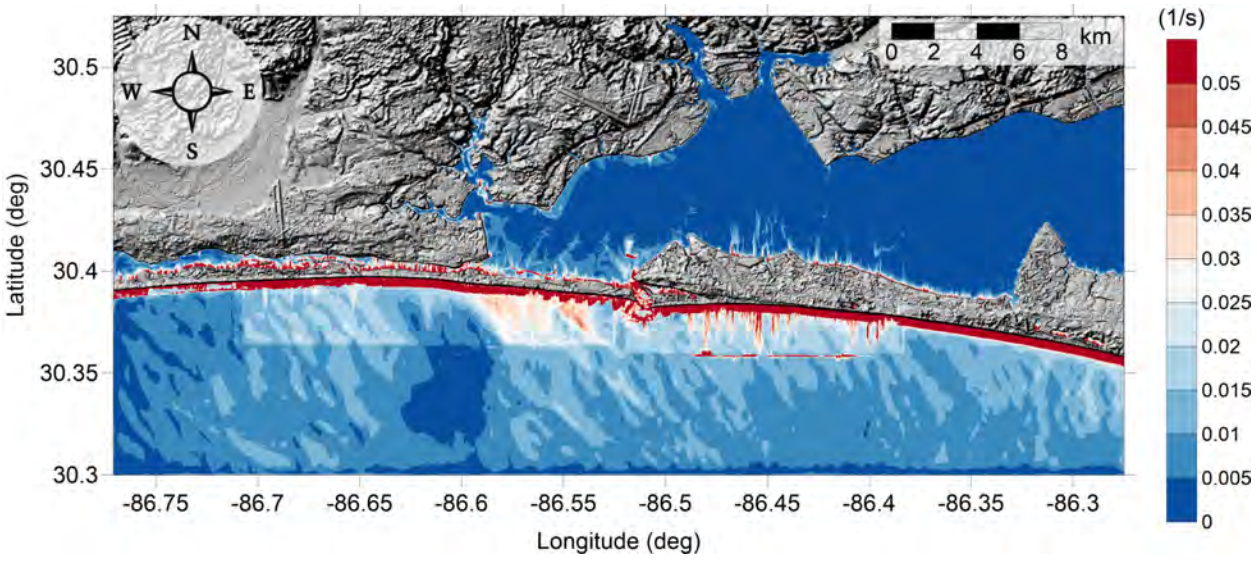


Figure 180: Maximum of maximum vorticity magnitude contour in Okaloosa County, FL (1 arcsecond) for all landslide scenarios.

## Okaloosa County, FL
## All Sources
## Maximum of Maximum Vorticity Magnitude

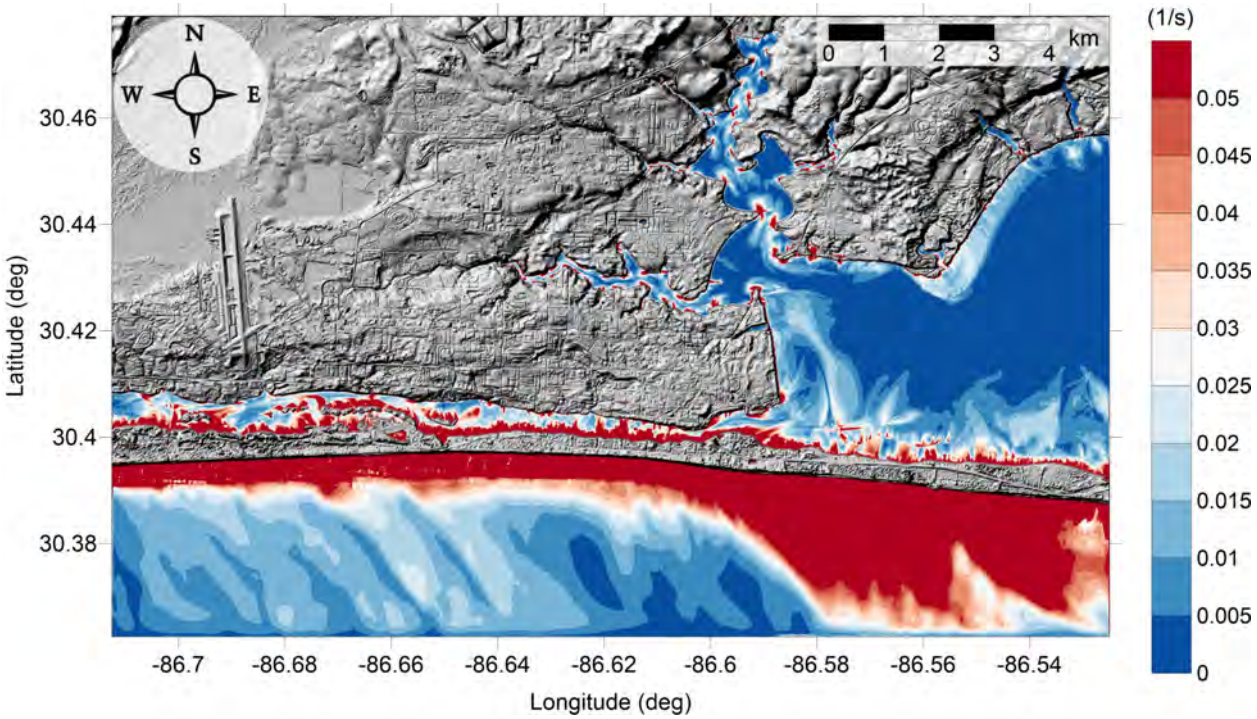


Figure 181: Maximum of maximum vorticity magnitude contour in Okaloosa Island, FL (1/3 arcsecond) for all landslide scenarios.

## Okaloosa County, FL
## All Sources
## Maximum of Maximum Vorticity Magnitude

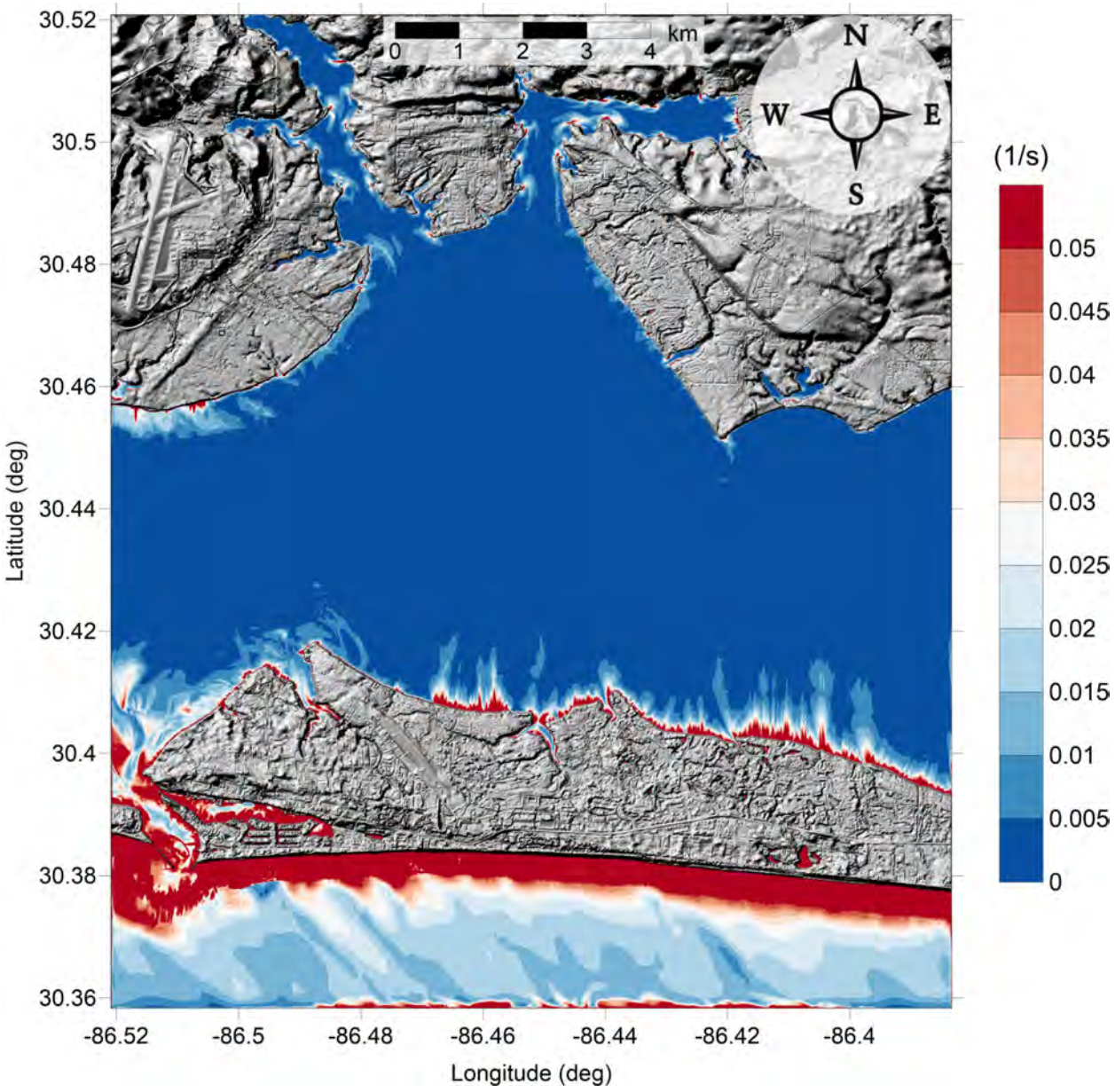


Figure 182: Maximum of maximum vorticity magnitude contour in Destin, FL (1/3 arcsecond) for all landslide scenarios.

## 5.7 Panama City, FL

### Panama City, FL
### All Sources
### Maximum of Maximum Velocity Magnitude

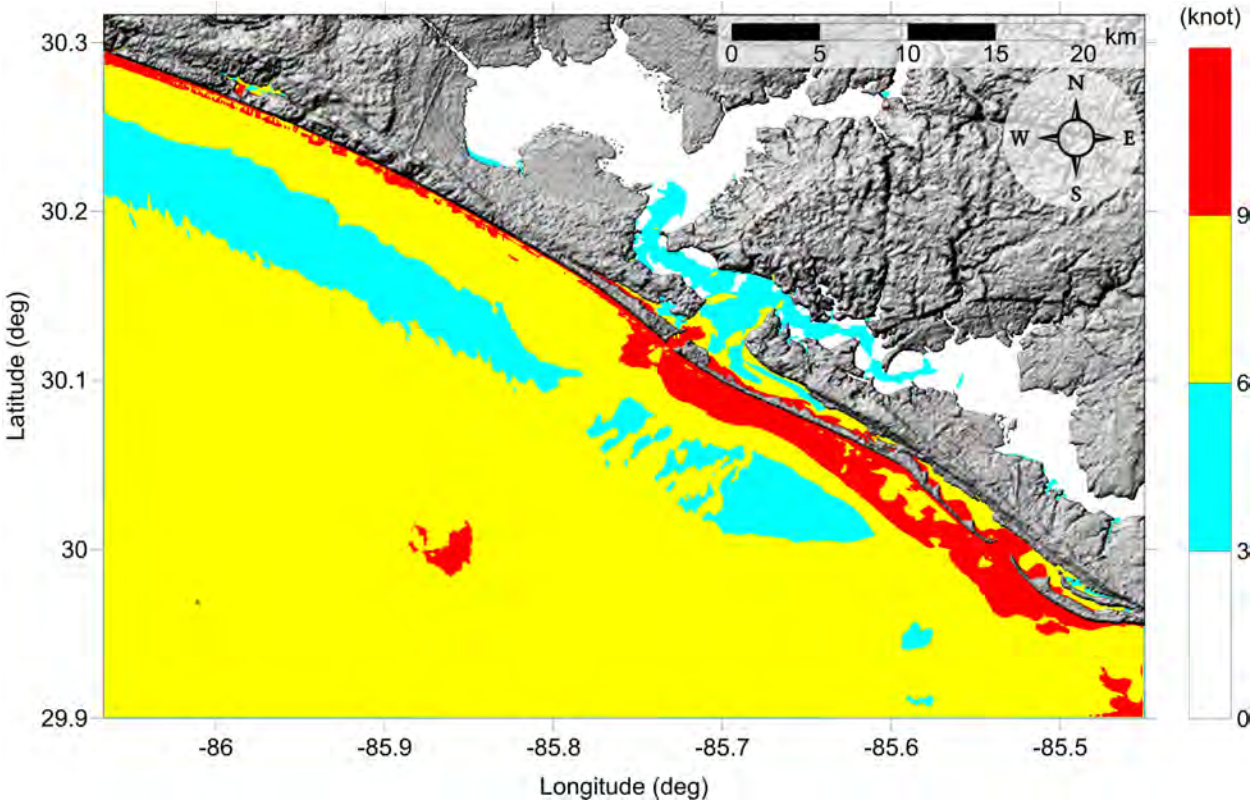


Figure 183: Maximum of maximum velocity magnitude contour in Panama City, FL (3 arcsecond) for all landslide scenarios.

## Panama City, FL
## All Sources
## Maximum of Maximum Velocity Magnitude

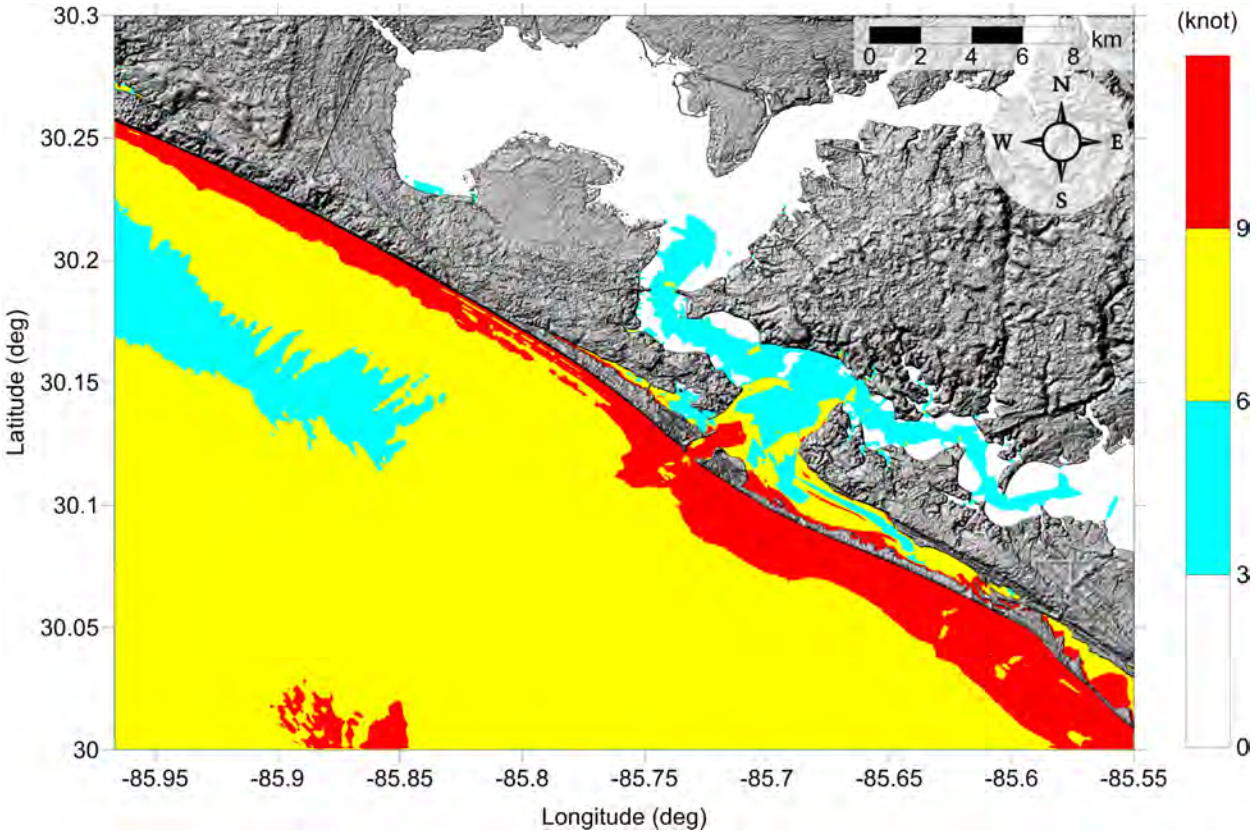


Figure 184: Maximum of maximum velocity magnitude contour in Panama City, FL (1 arcsecond) for all landslide scenarios.

## Panama City, FL
## All Sources
## Maximum of Maximum Velocity Magnitude

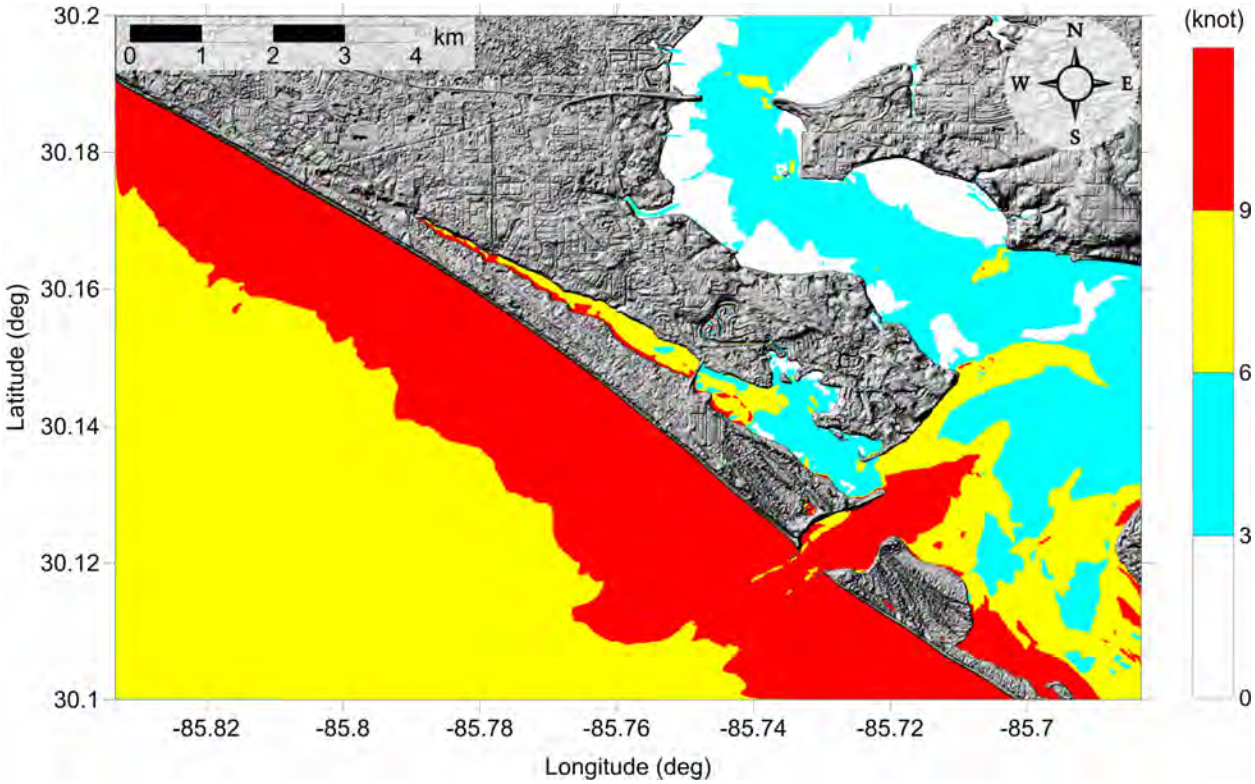


Figure 185: Maximum of maximum velocity magnitude contour in Panama City, FL (1/3 arcsecond) for all landslide scenarios.

## Panama City, FL
## All Sources
## Maximum of Maximum Vorticity Magnitude

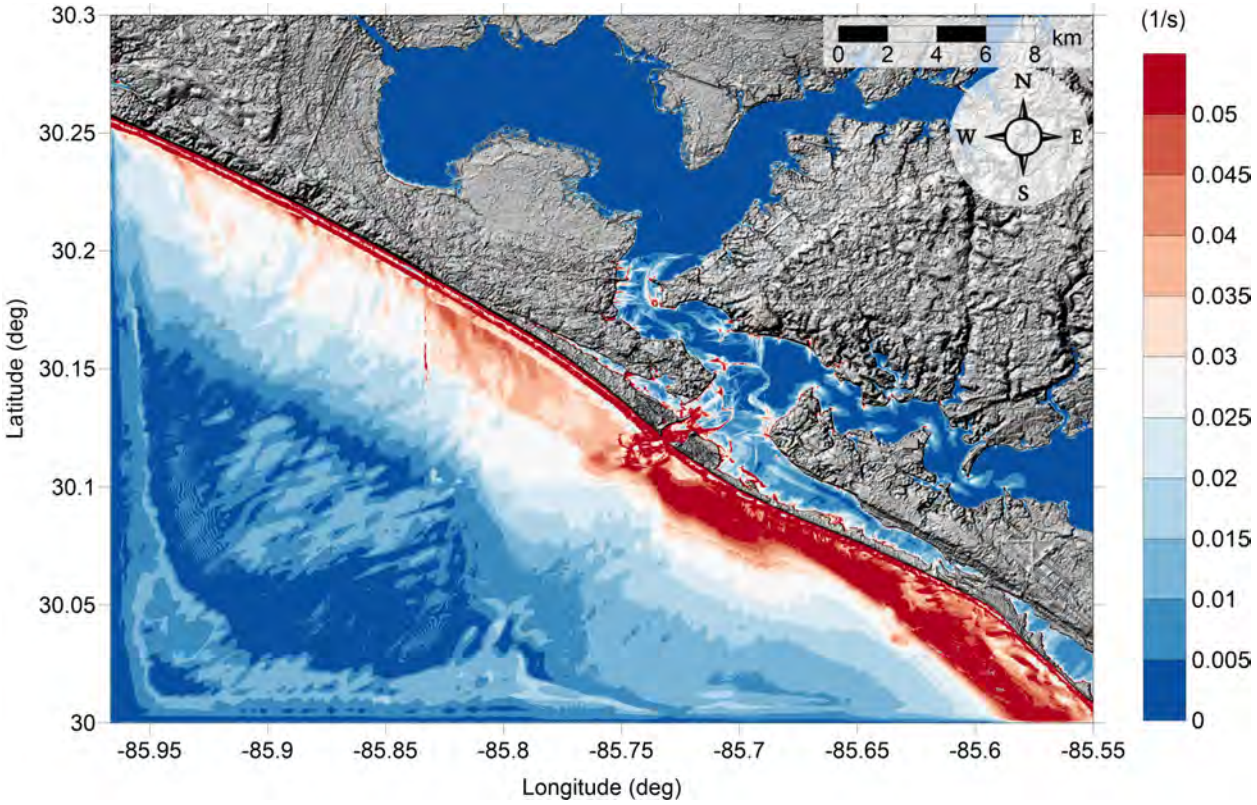


Figure 186: Maximum of maximum vorticity magnitude contour in Panama City, FL (1 arcsecond) for all landslide scenarios.

## Panama City, FL
## All Sources
## Maximum of Maximum Vorticity Magnitude

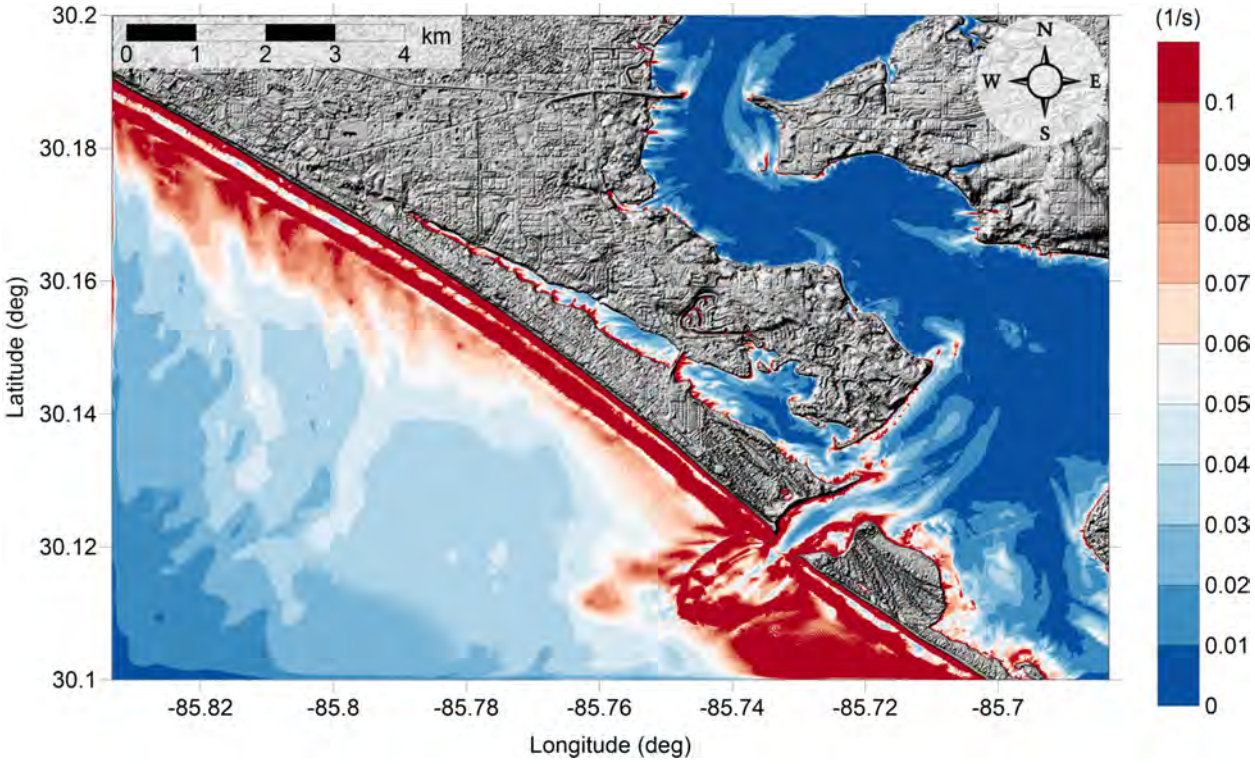


Figure 187: Maximum of maximum vorticity magnitude contour in Panama City, FL (1/3 arcsecond) for all landslide scenarios.

## 5.8 Tampa, FL

### Tampa Bay, FL
### All Sources
### Maximum of Maximum Velocity Magnitude

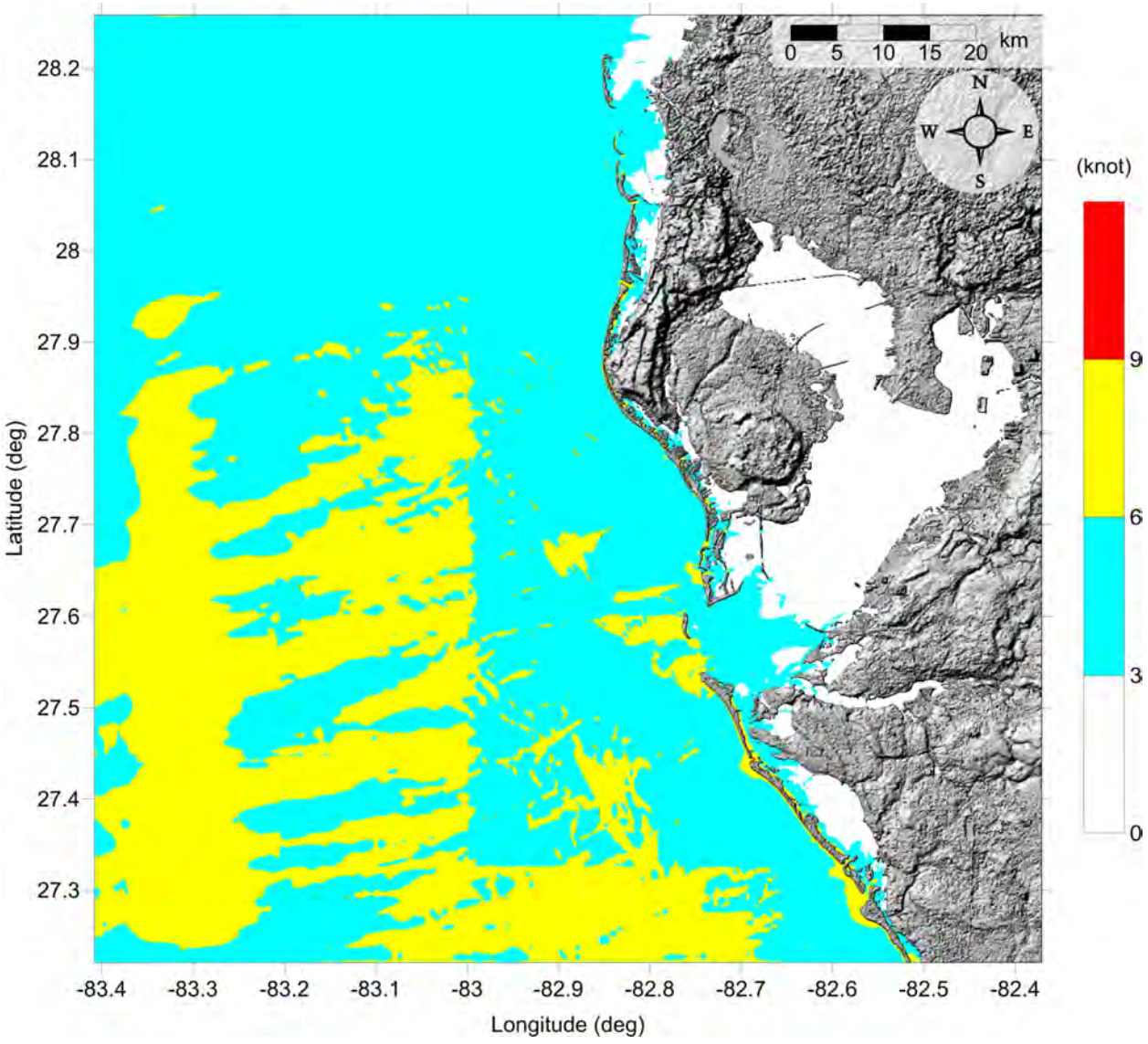


Figure 188: Maximum of maximum velocity magnitude contour in Tampa Bay, FL (3 arc-second) for all landslide scenarios.

## Tampa Bay, FL
## All Sources
## Maximum of Maximum Velocity Magnitude

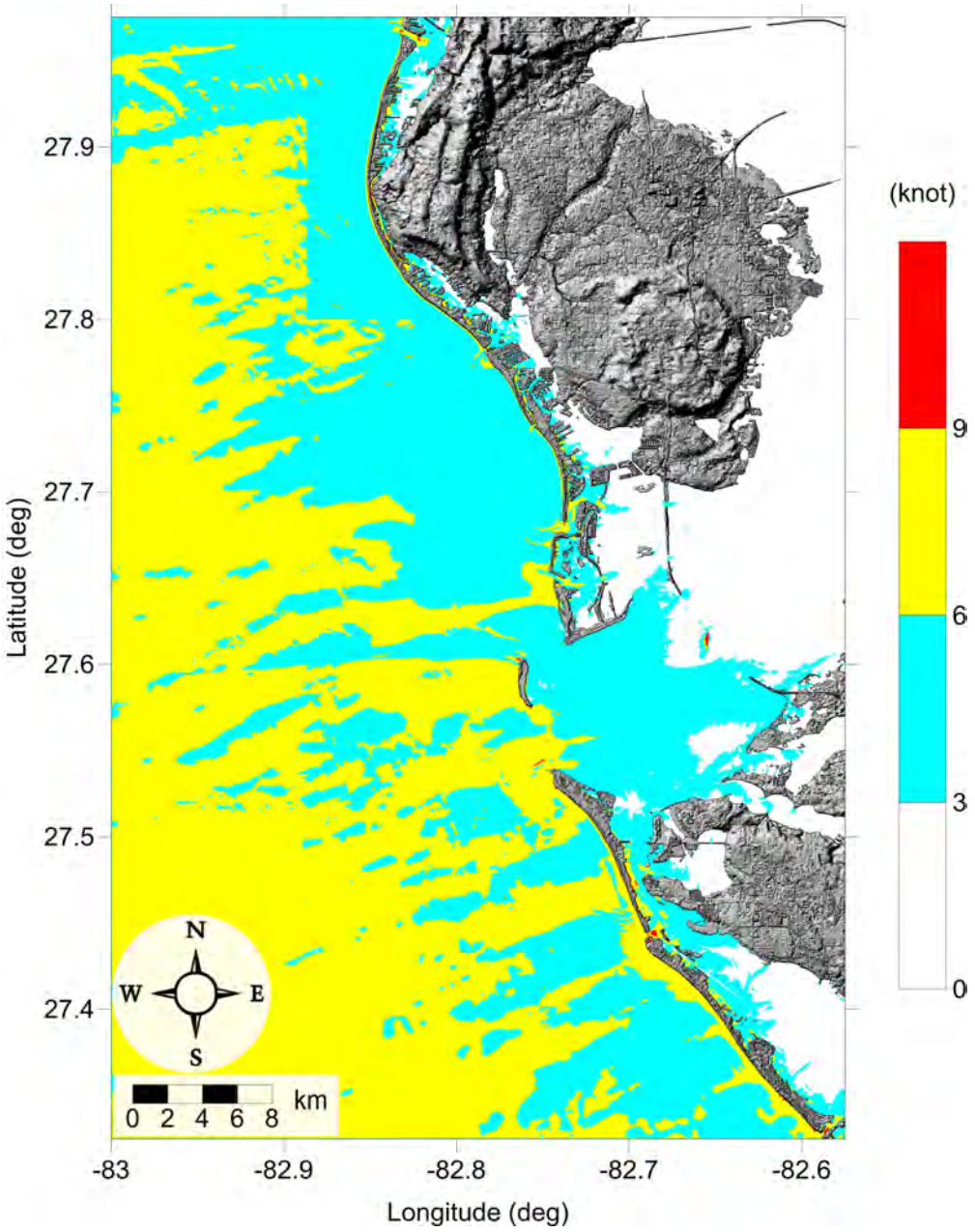


Figure 189: Maximum of maximum velocity magnitude contour in Tampa Bay, FL (1 arc-second) for all landslide scenarios.

## Tampa Bay, FL
## All Sources
## Maximum of Maximum Velocity Magnitude

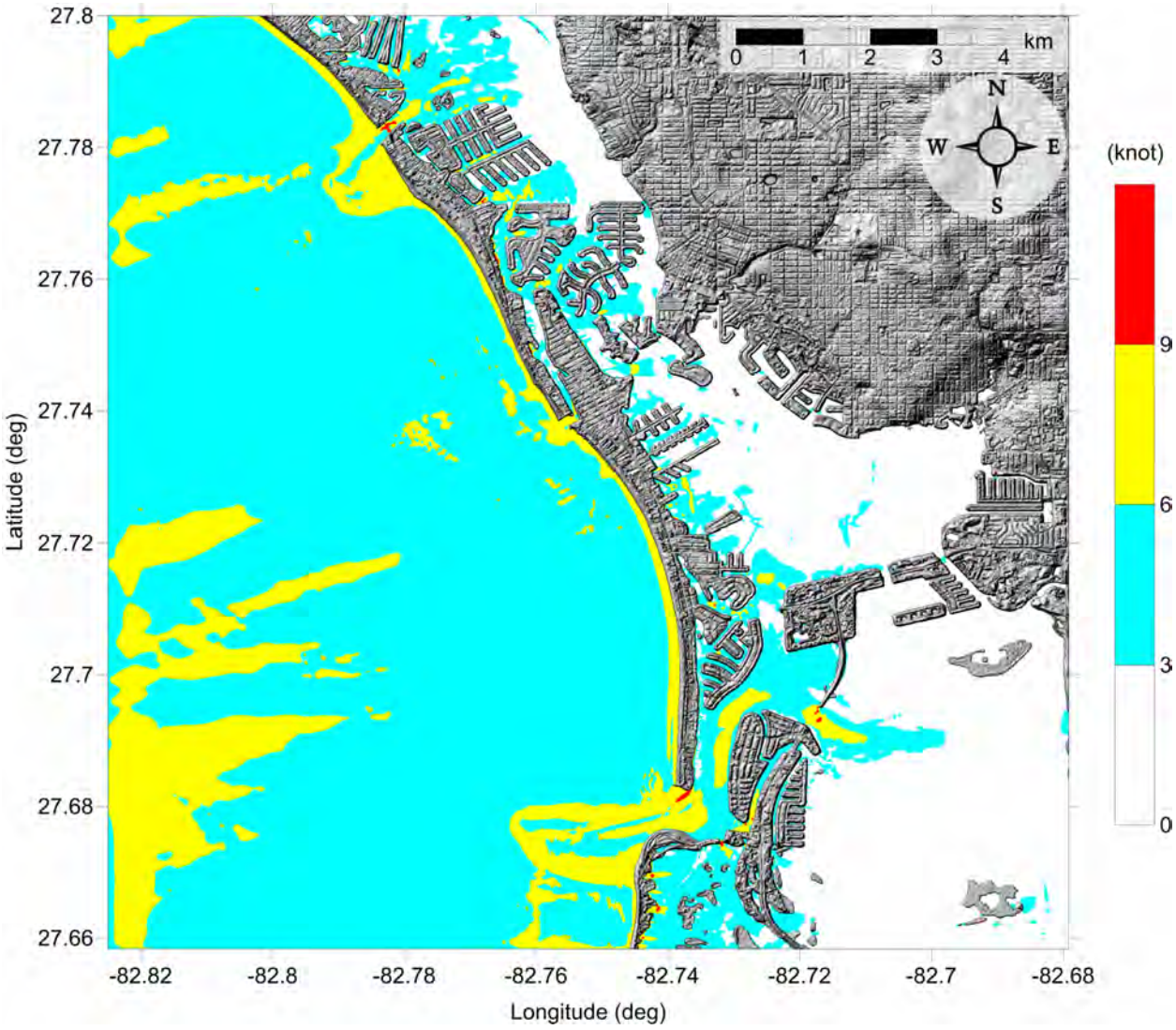


Figure 190: Maximum of maximum velocity magnitude contour in Southern Greater Tampa Area, FL (1/3 arcsecond) for all landslide scenarios.

**Tampa Bay, FL**
**All Sources**
**Maximum of Maximum Velocity Magnitude**

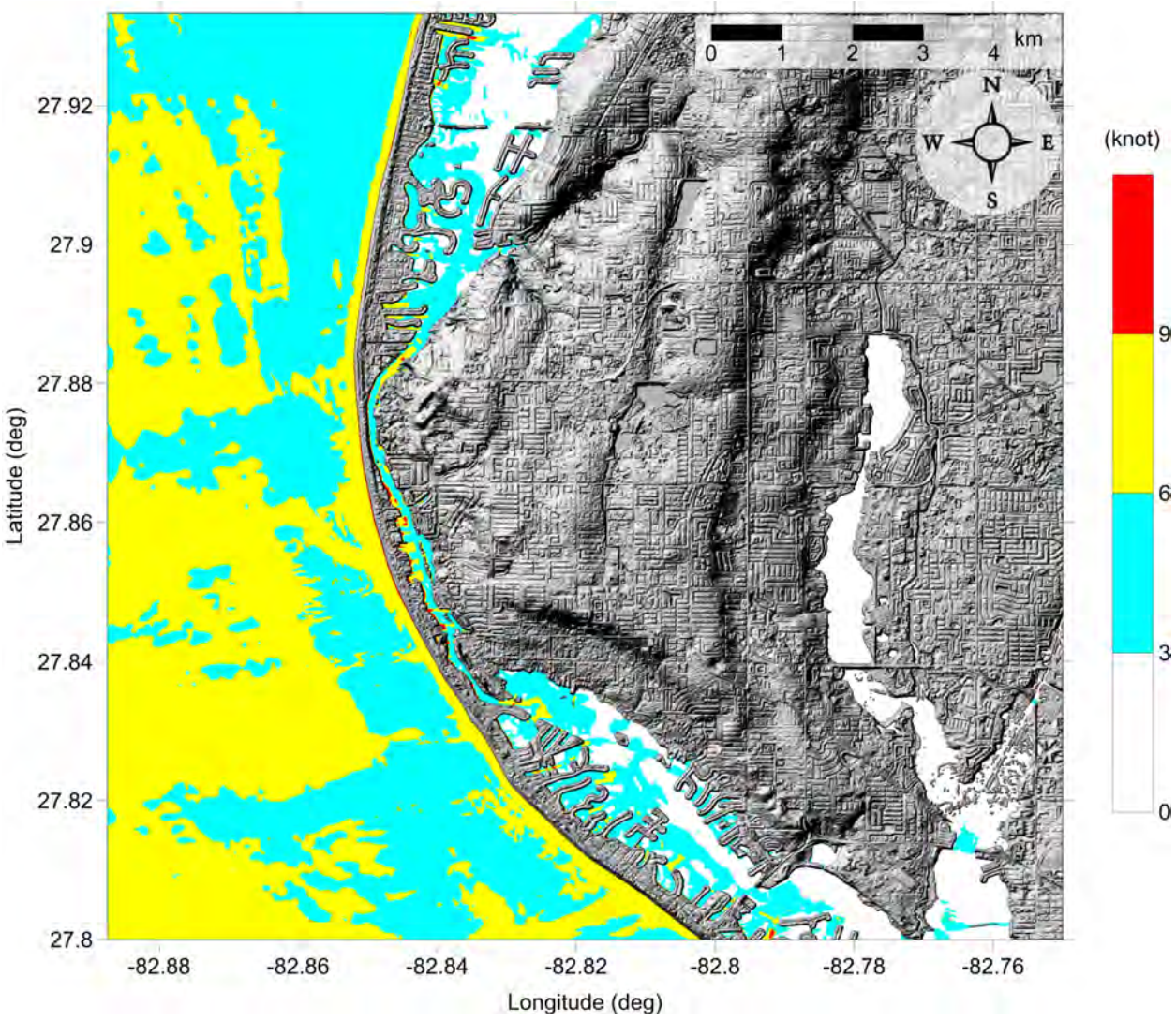


Figure 191: Maximum of maximum velocity magnitude contour in Northern Greater Tampa Area, FL (1/3 arcsecond) for all landslide scenarios.

## Tampa Bay, FL
## All Sources
## Maximum of Maximum Vorticity Magnitude

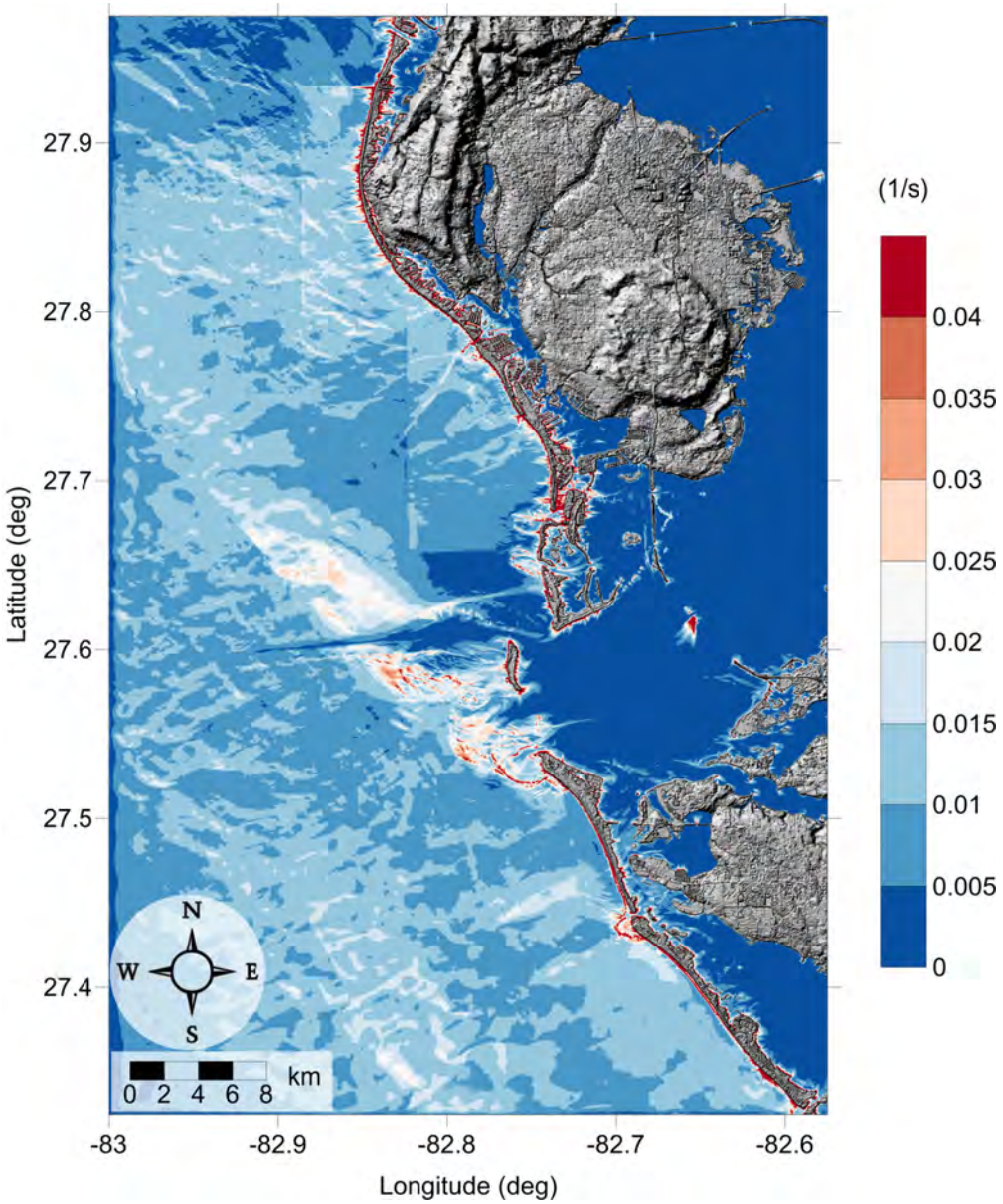


Figure 192: Maximum of maximum vorticity magnitude contour in Tampa Bay, FL (1 arcsecond) for all landslide scenarios.

## Tampa Bay, FL
## All Sources
## Maximum of Maximum Vorticity Magnitude

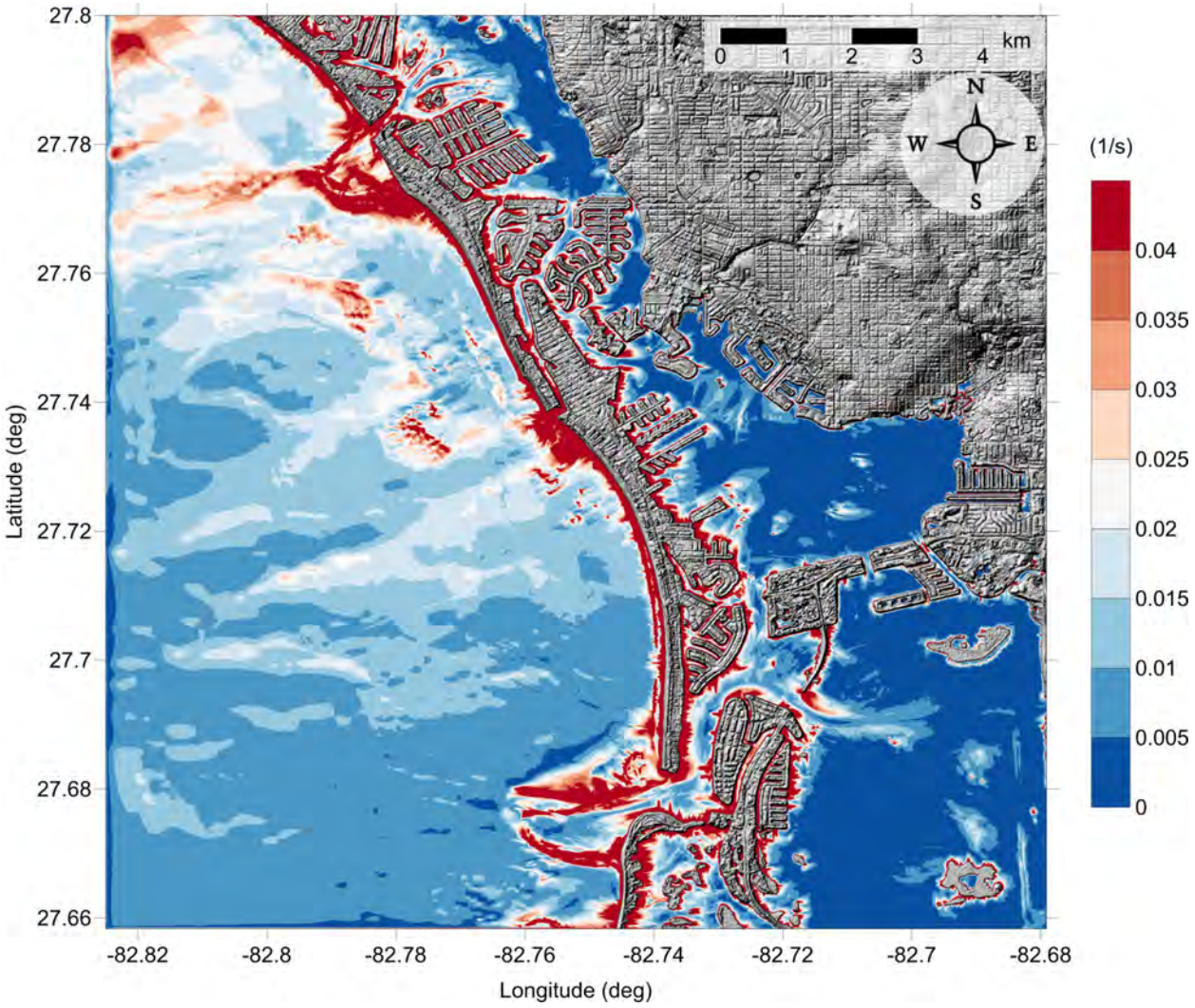


Figure 193: Maximum of maximum vorticity magnitude contour in Southern Greater Tampa Area, FL (1/3 arcsecond) for all landslide scenarios.

## Tampa Bay, FL
## All Sources
## Maximum of Maximum Vorticity Magnitude

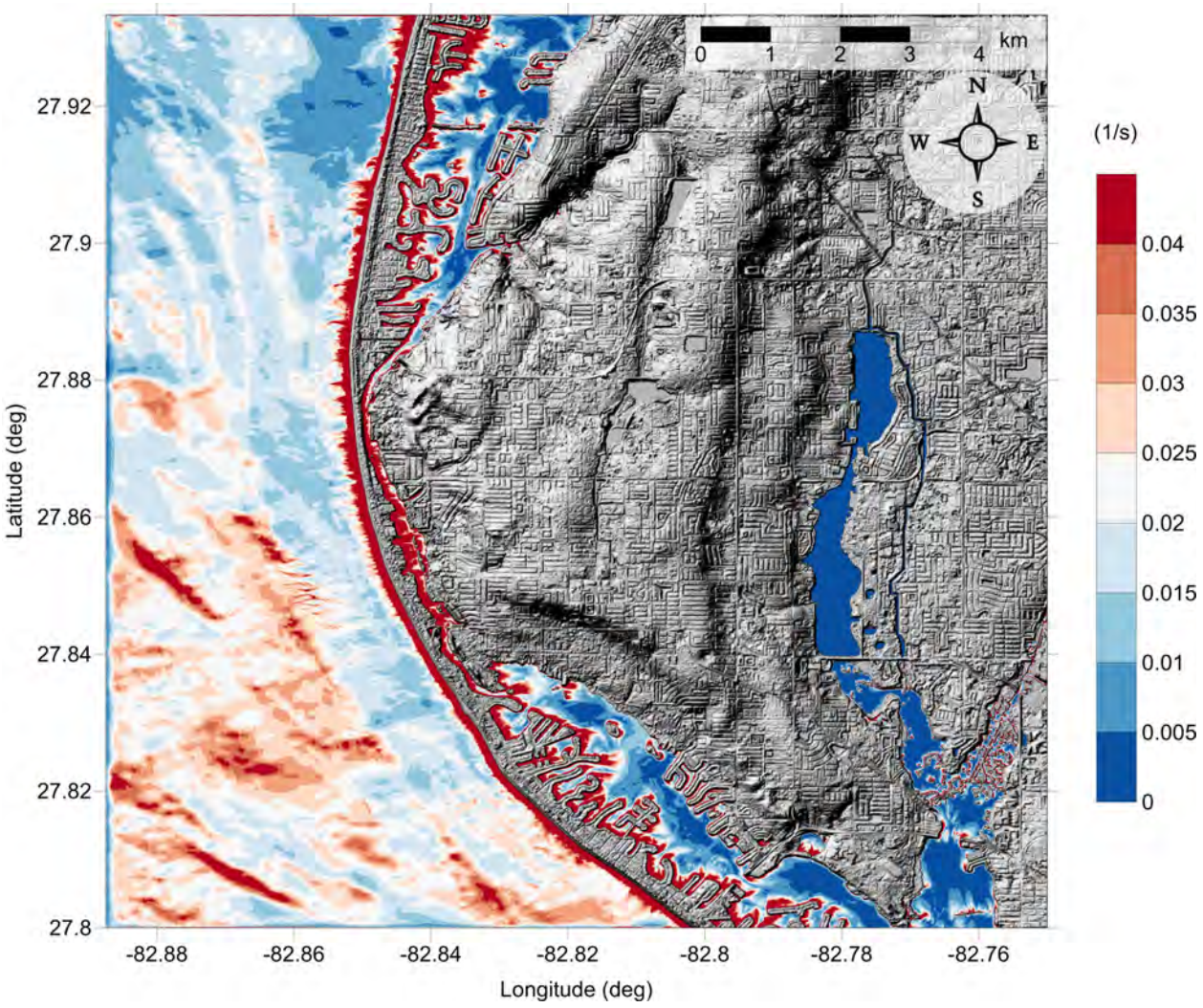


Figure 194: Maximum of maximum vorticity magnitude contour in Northern Greater Tampa Area, FL (1/3 arcsecond) for all landslide scenarios.

## 5.9 Key West, FL

### Key West, FL
### All Sources
### Maximum of Maximum Velocity Magnitude

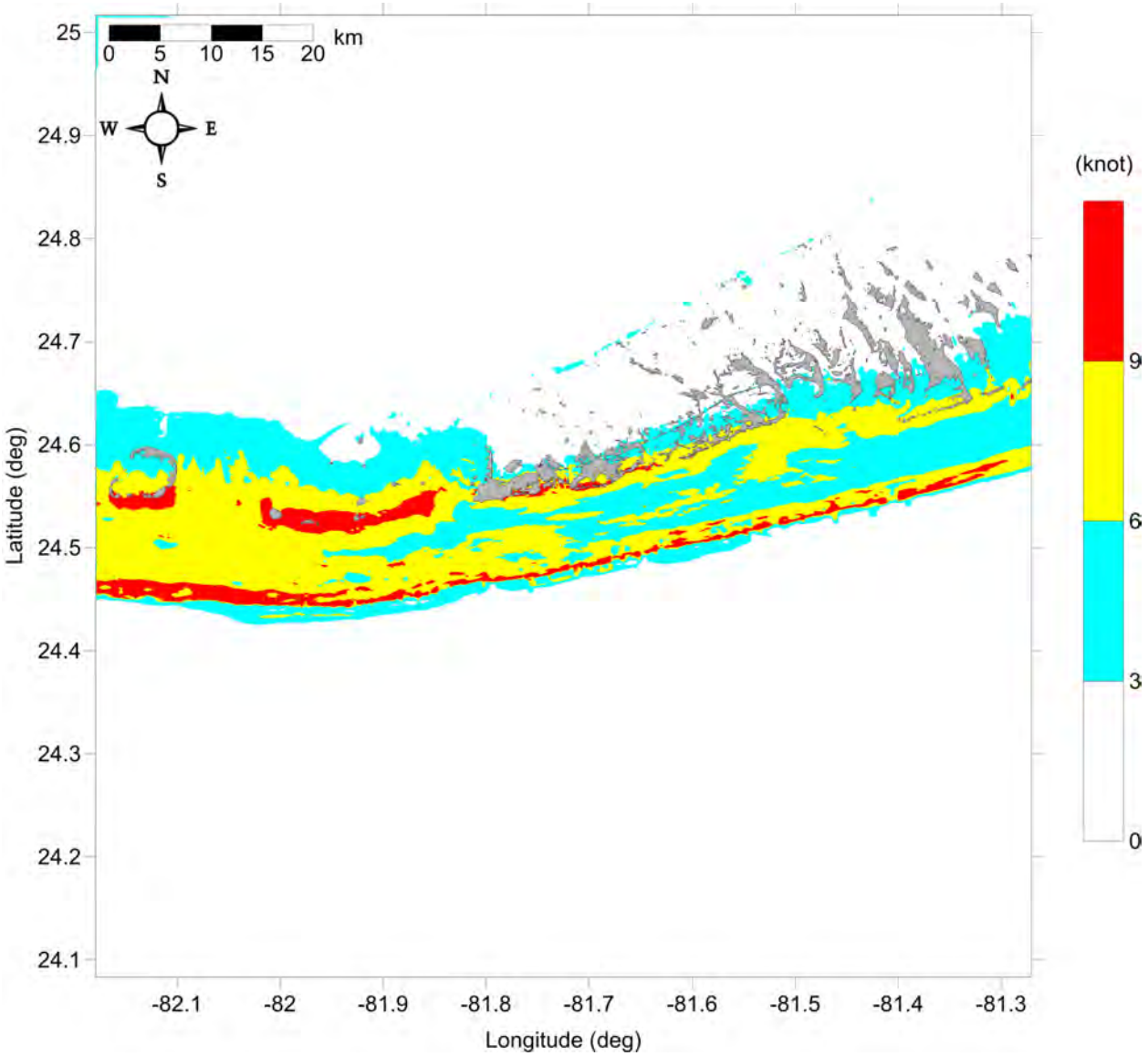


Figure 195: Maximum of maximum velocity magnitude contour in Key West, FL (3 arcsecond) for all landslide scenarios.

## Key West, FL
## All Sources
## Maximum of Maximum Velocity Magnitude

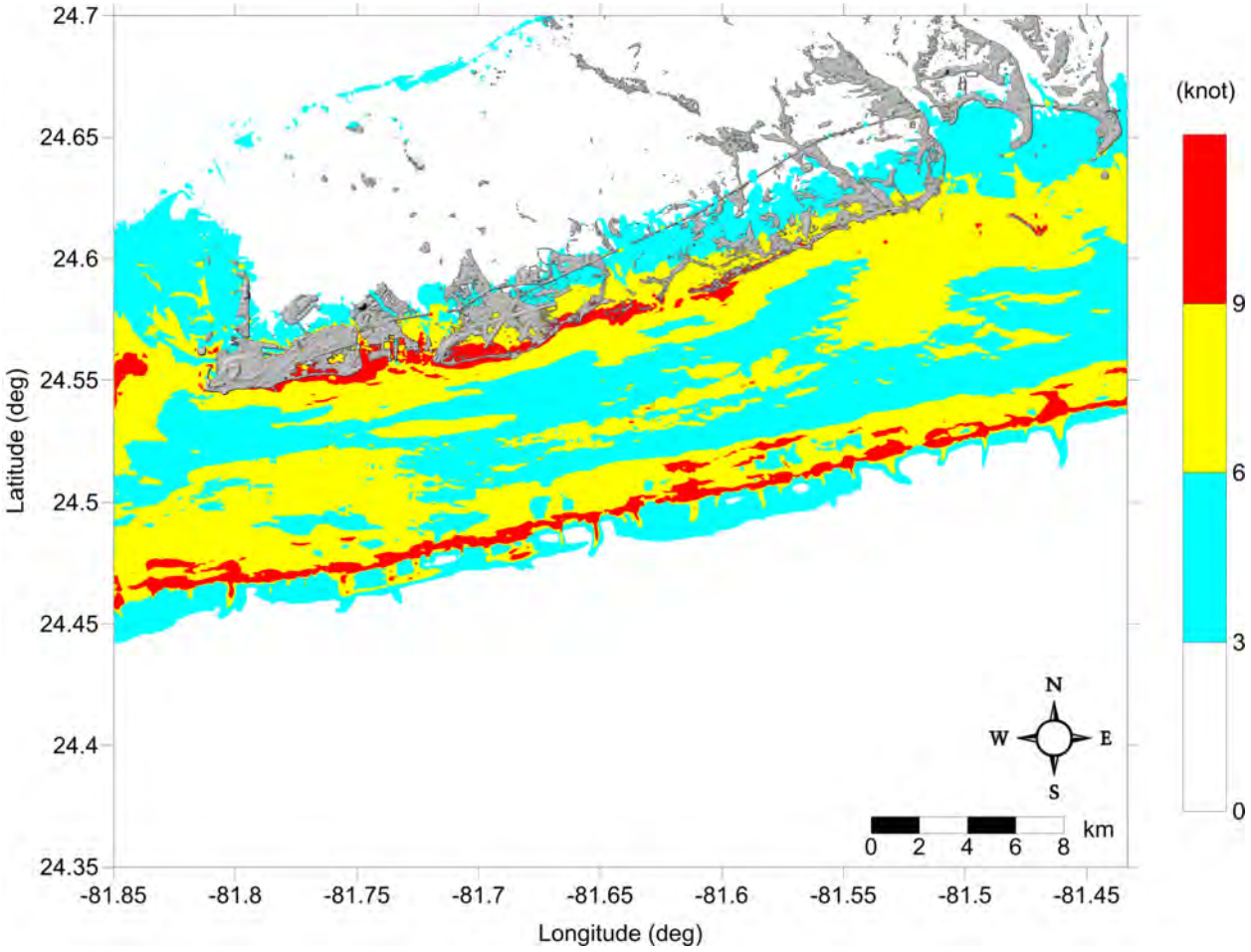


Figure 196: Maximum of maximum velocity magnitude contour in Key West, FL (1 arcsecond) for all landslide scenarios.

## Key West, FL
## All Sources
## Maximum of Maximum Velocity Magnitude

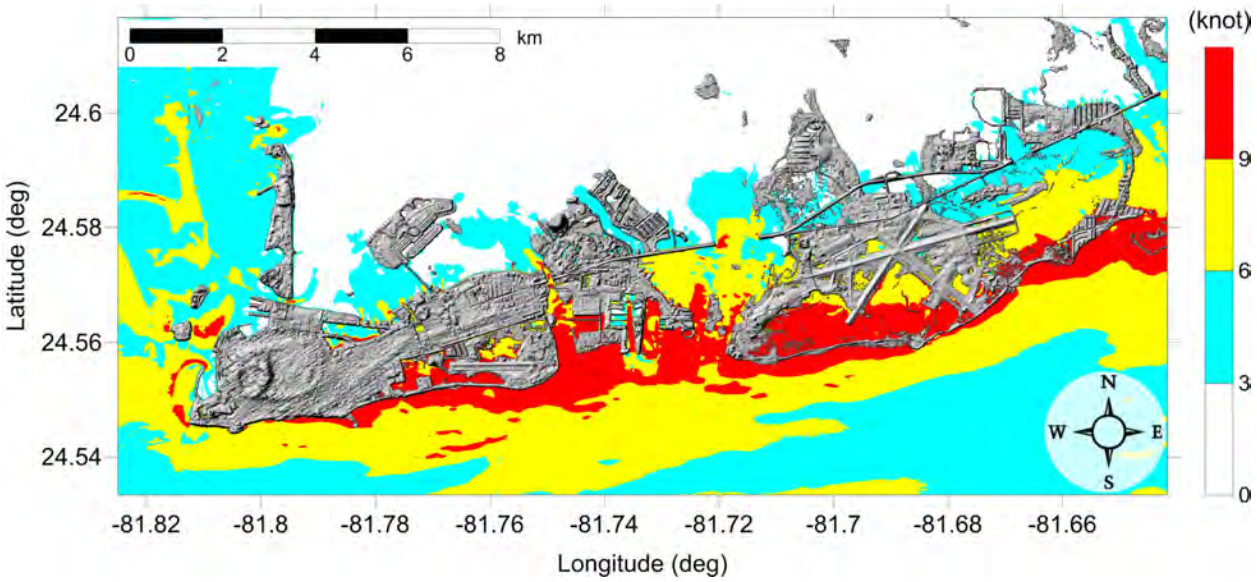


Figure 197: Maximum of maximum velocity magnitude contour in Key West, FL (1/3 arc-second) for all landslide scenarios.

## Key West, FL
## All Sources
## Maximum of Maximum Vorticity Magnitude

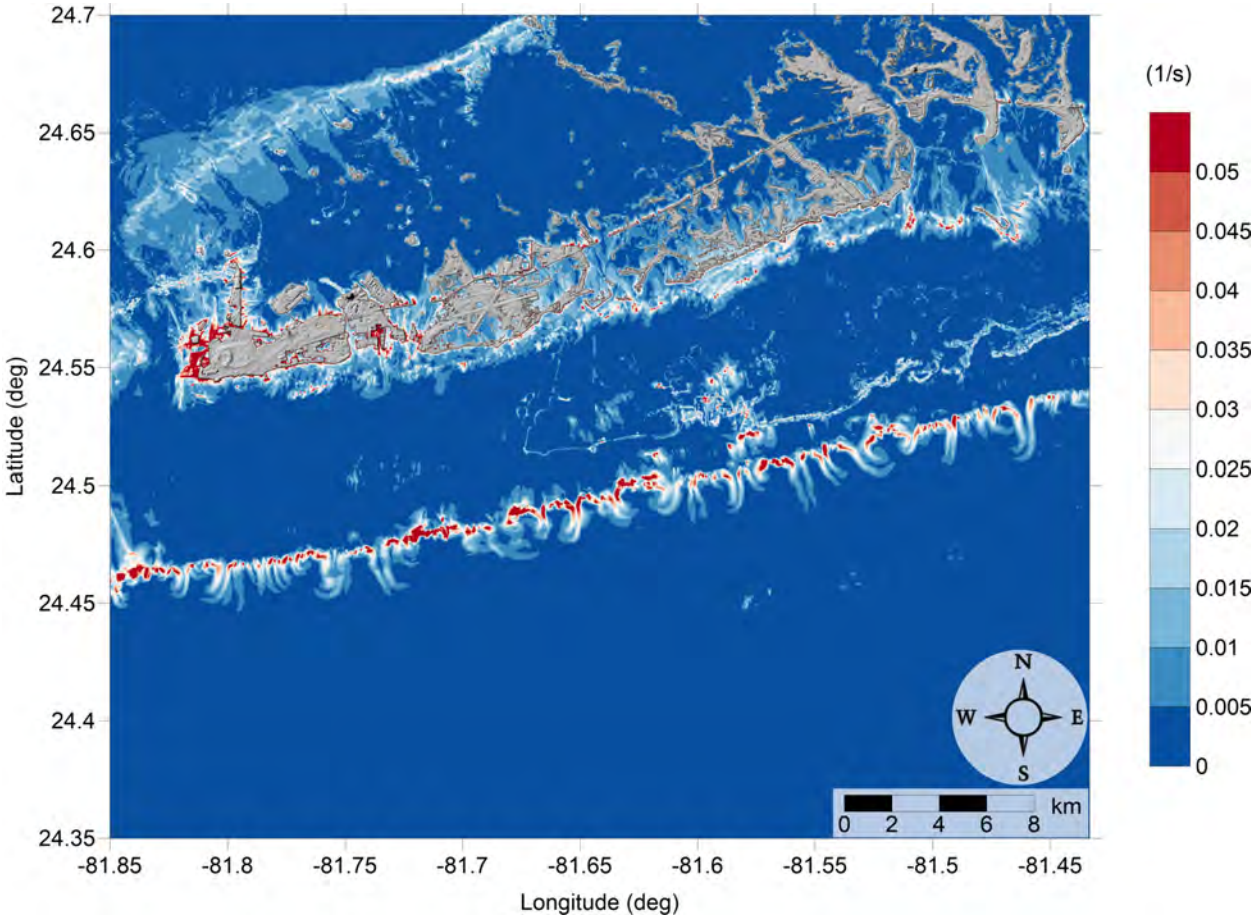


Figure 198: Maximum of maximum vorticity magnitude contour in Key West, FL (1 arcsecond) for all landslide scenarios.

## Key West, FL
## All Sources
## Maximum of Maximum Vorticity Magnitude

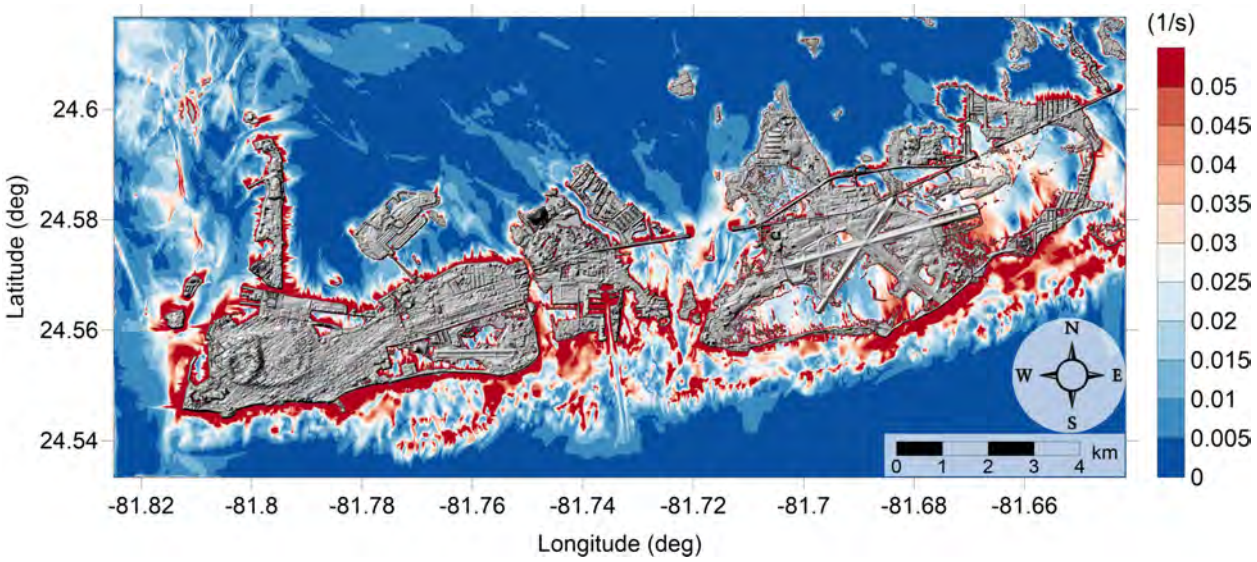


Figure 199: Maximum of maximum vorticity magnitude contour in Key West, FL (1/3 arcsecond) for all landslide scenarios.

# 6 Conclusions

This project focused on the implementation of recent developments in the tsunami science recommended by the National Tsunami Hazard Mitigation Program Modeling - Mapping Subcommittee - Strategic Plan (NTHMP-MMS-SP) into our current Gulf of Mexico (GOM) tsunami mitigation products. Three main developments for tsunami mitigation have been created under this project for communities in the GOM that will provide guidance to state emergency managers for tsunami hazard mitigation and warning purposes. The first is the development of four tsunami inundation maps in Pensacola, FL, Key West, FL Okaloosa County, FL and Santa Rosa County, FL, with revision of Port Aransas, TX (Mustang Island, TX) to account for new landslide sources. The second is a continuing study of the comparison between existing SLOSH hurricane flooding data and our tsunami inundation result, in order to provide temporal-low-order estimate for tsunami hazard areas (community) where inundation studies have not yet been assigned/executed or where little bathymetric and elevation data exists. The third is to produce the velocity field and velocity magnitude maps for all the landslide scenarios, for South Padre Island, TX, Mustang Island, TX, Mobile, AL, Pensacola, FL, Santa Rosa County, FL, Okaloosa County, FL, Panama City, FL, Tampa Bay, FL, and Key West, FL.

Tsunami inundation in four communities, Pensacola, FL, Key West, FL, Okaloosa County, FL and Santa Rosa County, FL with revision of Port Aransas, TX (Mustang Island, TX) was modeled to obtain inundation, momentum flux, current velocity and vorticity maps considering seven landslide sources across the GOM. We found that similar patterns from the maximum of maximum (MOM) inundation results of all communities, that is, barrier islands are completely overtopped by tsunami waves. Also barrier islands provide excellent protection for the mainland against direct tsunami impact. As a result, the mainland only suffers from minor inundation, with water depth mostly under 1.5 m high.

We observed from the modeling results that, of all the communities, Destin, FL has the highest tsunami inundation water depth of greater than 6 m, and South-East Corpus Christi has the lowest of 3 m. Destin's high tsunami inundation was probably caused by the Mississippi-Alabama Shelf break focusing the tsunami wave energy. For all five communities, MOM tsunami inundation is produced solely by the Mississippi Canyon failure. This historical failure is largest in both area and volume of material removed, and therefore produces the highest amplitude wave of all sources simulated. This is most likely due to the location of the Mississippi Canyon landslide being near the center of the GOM, with direction of wave propagation predominantly to the east. The large tsunami amplitude produced by the Mississippi Canyon landslide also causes a widespread effect in the western community of Mustang Island. Other landslide sources can certainly generate large tsunami inundation too, for instance, Mustang Island is significantly threatened by East Breaks, PSL-A and PSL-C landslide with 3 m maximum water depth, despite Mississippi being the highest.

Comparisons of MOM tsunami inundation results to the SLOSH MOM high tide storm surge inundation indicate that while the details of referencing tsunami inundation to hurricane storm surge is dependent on local topographic effects, general regional trends can be identified. Immediate beachfront areas are inundated at levels comparable to major hurricanes (Category 3 or higher) with some places experiencing tsunami inundation that is well

above Category 5 levels (4 m higher or more in some localized places, for instance, south of Highway 98 in Destin, FL). Thin barrier islands, like Santa Rosa Island and Okaloosa Island, experience inundation levels comparable to mostly Category 5 with limited areas Category 4. In contrast, wider island like Destin and Port Aransas, will have levels from Category 5 through 1. Lower hurricane categories, Category 1 and 2, mostly appear along the inundated areas in the mainland, where occasionally see Category 3 level tsunami inundation. However, we observed Category 1 through 5 inundation in mainland Okaloosa County, FL. For most locations, the difference between tsunami inundation and hurricane flooding depth is within 1 m, indicating good match and possible applications to provide temporal-low-order estimate for tsunami hazard areas (community) where inundation studies have not yet been executed or where little bathymetric and elevation data exists. It is possible that some tsunami inundation zone has no hurricane flooding, therefore matching with hurricane category cannot be made, for example Destin, LF (see Fig. 135 and 136).

Since even general, low-resolution inundation information is useful for hazard mitigation efforts, we believe that these results can be extended to provide a preliminary, first-order estimate of potential tsunami hazard zones for other Gulf Coast communities that is accessible and understandable to regional emergency managers and more appropriate for the low-lying Gulf Coast than methods such as the 10 m (33 ft) elevation contour line. We anticipate that communities which lack detailed tsunami inundation maps, but which have modeled hurricane storm surge information, would be able to use the results presented here to estimate their potential tsunami hazard level based on their regional topographical/bathymetric features. We stress, however, that such results should be used only in a broad, regional sense given the differences seen among and within communities based on local details of bathymetry, topography, and geographical location within the GOM basin. There is no guarantee that comparison results will be identical in areas with similar topography, and comparisons should only be made after understanding the limitations and simplifications of the methodology presented here. Improvements to the methodology would clearly improve the reliability of comparisons. For example, given the large difference in resolution of the SLOSH model data (1 km) and tsunami inundation data (1/3 arcsecond $\approx$ 10 m), the comparison between the two datasets would be greatly improved with increased resolution of the SLOSH model runs, or alternate data on category-specific hurricane storm surge. Additionally, a more detailed comparison could also be accomplished by comparison with probabilistic storm surge parameters, e.g. the 100-year or 500-year hurricane surge event, which may provide more/better information in areas where there are large differences between the modeled tsunami inundation and that of the best-match hurricane category. Successful implementation of this approach would certainly require the availability of probabilistic data for the locations of interest in order to develop a generalized probabilistic tsunami - storm surge comparison.

Finally, we produced the velocity field and velocity magnitude maps for all the landslide scenarios, South Padre Island, TX, Mobile, AL, Panama City, FL, and Tampa, FL, mapped during [Horrillo et al., 2015] (project NA13NWS4670018), and Pensacola, FL, Key West, FL, Okaloosa County, FL, Santa Rosa County, FL and Mustang Island, TX, based on a simplified current velocity damage scale where we associate 0 - 3 knots to unharmful currents, 3 - 6 knots to minor damage, 6 - 9 knots to moderate damage, and over 9 knots to major damage.

The four damage levels are denoted with white, blue, yellow and red colors, respectively.

From the MOM velocity magnitude results in the entire Gulf of Mexico (Fig. 145), we found that, potential damaging currents (> 3 knots) tend to be present in most of the area shallower than 200 m, which is approximately 100 fathoms. However, damaging currents could reach areas deeper than 200 m close to most of the landslide generation regions. Major damaging currents can be expected in most of the landslide generation regions, in the continental shelf adjacent to Mississippi Canyon, and offshore northwest Florida. Moderate damaging current areas are scattered over the continental shelf, but mostly close to areas with major damage currents. General trends can be observed from all of the MOM velocity and vorticity maps of all the higher resolution subdomains (see from Fig. 146 to Fig. 199). In the nearshore region of the subdomains, there are mostly moderate damaging currents (yellow), with major damaging current (red) bands in Pensacola, FL, Santa Rosa, FL, Okaloosa County, FL, and Key West, FL, probably due to shallow water, e.g., sand bars and reefs. In the surf zone of the barrier island, there are mostly major damaging currents, except for Mobile, AL which has mostly moderate damaging currents and Tampa Bay, FL which has mostly minor damaging currents and few spots of moderate damaging currents. There are usually strong currents flowing through the inlets (some with jetties) which connects the GOM and internal bays, which generates mostly major damaging currents, for example, Pensacola, FL (Fig. 166) and Port Aransas, TX (Fig. 152). However, Tampa Bay, FL inlet only has minor to moderate damaging currents. For internal channel/lagoons, minor damaging currents are most common, and moderate damaging currents appear in South Padre Island, TX, Okaloosa County, FL, and Panama City, FL. In the interior bays, the tsunami currents are less severe which can be used as shelter to minimize tsunami impact.

There is less current impact in the nearshore, surf zone, inlet and channels/lagoons in Tampa Bay, FL, probably because the wider continental shelf dissipates more tsunami energy. It is also worth mentioning that tsunami impact is more severe south of Key West, FL due to tsunami wave refracted by the continental shelf break. The lee side of the islands seems protected also by the wide and shallow continental shelf north of Key West. The tsunami hazard maritime products such as tsunami current magnitude, vorticity, safe/hazard zones would be central for future developments of maritime hazard maps, maritime emergency response and as well as infrastructure planning.

Although the recurrence of destructive tsunami events have been verified to be quite low in the GOM, our work has confirmed that submarine landslide events with similar characteristics to those used here, have indeed the potential to cause severe damage to GOM coastal communities. Therefore, this work is intended to provide guidance to local emergency managers to help managing urban growth, evacuation planning, and public education with final objective to mitigate potential tsunami hazards in the GOM.

# Acknowledgments

This work was supported by the National Tsunami Hazard Mitigation Program (NTHMP) under awards NA15NWS4670031, "Development of Two Additional Tsunami Inundation Maps and Updating Existing Ones with Maritime Mitigation Hazard Products", and

NA16NWS4670039, "Development of Two Tsunami Inundation Maps in the GOM and Updating Port Aransas, TX Inundation Maps with the Full Set of Tsunami Sources". The authors wish to thank all NTHMP modeling and Mapping Subcommittee members and GOM's emergency manager representatives for their helpful insights. Special thanks go to Chayne Sparagowski for his helpful insight and support. High resolution inundation maps are available from `http://www.tamug.edu/tsunami/NTHMP/NTHMP.html` or by contacting corresponding author upon request.

# References


D. Basco and C. Klentzman. On the classification of coastal storms using principles of momentum conservation. In *Proc. 31st Int. Conf. on Coastal Eng.* ASCE, 2006.

B. Dugan and J. Stigall. Origin of overpressure and slope failure in the Ursa region, northern Gulf of Mexico. In D. C. Mosher, R. C. Shipp, L. Moscardelli, J. D. Chaytor, C. D. P. Baxter, H. J. Lee, and R. Urgeles, editors, *Submarine Mass Movements and Their Consequences*, pages 167–178. Springer Netherlands, 2010.

P. K. Dunbar and C. S. Weaver. *U.S. States and Territories National Tsunami Hazard Assessment: Historical Record and Sources for Waves.* U.S. Department of Commerce, National Oceanic and Atmospheric Administration, National Geophysical Data Center Tech. Rep.No. 3, 2008.

E. L. Geist, J. D. Chaytor, T. Parsons, and U. ten Brink. Estimation of submarine mass failure probability from a sequence of deposits with age dates. *Geosphere*, 9(2):287–298, 2013.

S. T. Grilli, O.-D. S. Taylor, C. D. P. Baxter, and S. Maretzki. A probabilistic approach for determining submarine landslide tsunami hazard along the upper east coast of the United States. *Mar. Geol.*, 264:74–97, 2009.

C. B. Harbitz, F. Løvholt, and H. Bungum. Submarine landslide tsunamis: How extreme and how likely? *Nat. Hazards*, 72(3):1341–1374, 2014.

C. W. Hirt and B. D. Nichols. Volume of fluid method for the dynamics of free boundaries. *J. Comput. Phys.*, 39:201–225, 1981.

J. Horrillo. *Numerical Method for Tsunami calculations using Full Navier-Stokes equations and the Volume of Fluid method.* PhD thesis, University of Alaska Fairbanks, 2006.

J. Horrillo, A. Wood, C. Williams, A. Parambath, and G. Kim. Construction of tsunami inundation maps in the Gulf of Mexico. Technical report, Award Number: NA09NWS4670006 to the National Tsunami Hazard Mitigation Program (NTHMP), National Weather Service Program Office, NOAA, 2011. avail. from http://www.tamug.edu/tsunami/NTHMP.html.

J. Horrillo, A. Wood, G.-B. Kim, and A. Parambath. A simplified 3-D Navier-Stokes numerical model for landslide-tsunami: Application to the Gulf of Mexico. *J. Geophys. Res.-Oceans*, 118:6934–6950, 2013. doi:10.1002/2012JC008689.

J. Horrillo, A. Pampell-Manis, C. Sparagowski, L. Parambath, and Y. Shigihara. Construction of five tsunami inundation maps for the Gulf of Mexico. Technical report, Award Number: NA12NWS4670014 and NA13NWS4670018 to the National Tsunami Hazard Mitigation Program (NTHMP), National Weather Service Program Office, NOAA, 2015. avail. from http://www.tamug.edu/tsunami/NTHMP.html.

J. Horrillo, W. Cheng, A. Pampell-Manis, and J. Figlus. Implementing nthmp-mms strategic plan in tsunami hazard mitigation products for the Gulf of Mexico. Technical report, Award Number: NA14NWS4670049 to the National Tsunami Hazard Mitigation Program (NTHMP), National Weather Service Program Office, NOAA, 2016. avail. from http://www.tamug.edu/tsunami/NTHMP.html.

J. L. Irish and D. T. Resio. A hydrodynamics-based surge scale for hurricanes. *Ocean Eng.*, 37:69–81, 2010.

L. Kantha. Time to replace the Saffir-Simpson hurricane scale? *Eos, Transactions American Geophysical Union*, 87(1):3–6, 2006.

W. Knight. Model predictions of Gulf and Southern Atlantic Coast tsunami impacts from a distribution of sources. *Sci. of Tsunami Hazards*, 24:304–312, 2006.

C. M. Kuehne. *Hurricane Junction: A History of Port Aransas*. St. Mary's University, 1973.

A. M. López-Venegas, J. Horrillo, A. Pampell-Manis, V. Huérfano, and A. Mercado. Advanced tsunami numerical simulations and energy considerations by use of 3D - 2D coupled models: The October 11, 1918, Mona Passage tsunami. *Pure Appl. Geophys.*, 172(6):1679–1698, 2015.

P. J. Lynett, J. C. Borrero, R. Weiss, S. Son, D. Greer, and W. Renteria. Observations and modeling of tsunami-induced currents in ports and harbors. *Earth and Planetary Science Letters*, 327:68–74, 2012.

P. J. Lynett, J. Borrero, S. Son, R. Wilson, and K. Miller. Assessment of the tsunami-induced current hazard. *Geophysical Research Letters*, 41(6):2048–2055, 2014.

S. Maretzki, S. Grilli, and C. D. P. Baxter. Probabilistic SMF tsunami hazard assessment for the upper east coast of the United States. In V. Lykousis, D. Sakellariou, and J. Locat, editors, *Submarine Mass Movements and Their Consequences*, pages 377–385. Springer Netherlands, 2007.

D. Masson, C. Habitz, R. Wynn, G. Pederson, and F. Lovholt. Submarine landslides: Processes, triggers and hazard protection. *Philos. Trans. R. Soc. A*, 364:2009–2039, 2006.

T. Myers, A. E. Butman, and K. Brown. *Port Aransas Historic Resources Survey*. The Port Aransas Preservation and Historical Association, 2006.

A. Pampell-Manis, J. Horrillo, Y. Shigihara, and L. Parambath. Probabilistic assessment of landslide tsunami hazard for the northern Gulf of Mexico. *J. Geophys. Res.-Oceans*, 2016. doi:10.1002/2015JC011261.

V. G. Panchang and D. Li. Large waves in the gulf of mexico caused by hurricane ivan. *Bulletin of the American Meteorological Society*, 87(4):481–489, 2006.

U. S. ten Brink, H. J. Lee, E. L. Geist, and D. Twichell. Assessment of tsunami hazard to the U.S. East Coast using relationships between submarine landslides and earthquakes. *Mar. Geol.*, 264:65–73, 2009a.

U. S. ten Brink, D. Twichell, P. Lynett, E. Geist, J. Chaytor, H. Lee, B. Buczkowski, and C. Flores. Regional assessment of tsunami potential in the Gulf of Mexico. *U. S. Geol. Surv. Admin. Rep.*, 2009b.

R. Wilson, C. Davenport, and B. Jaffe. Sediment scour and deposition within harbors in california (usa), caused by the march 11, 2011 tohoku-oki tsunami. *Sedimentary Geology*, 282:228–240, 2012.

R. I. Wilson, A. R. Admire, J. C. Borrero, L. A. Dengler, M. R. Legg, P. Lynett, T. P. McCrink, K. M. Miller, A. Ritchie, K. Sterling, et al. Observations and impacts from the 2010 chilean and 2011 japanese tsunamis in california (usa). *Pure and Applied Geophysics*, 170(6-8):1127–1147, 2013.

Y. Yamazaki, Z. Kowalik, and K. F. Cheung. Depth-integrated, non-hydrostatic model for wave breaking and run-up. *Int. J. Numer. Meth. Fl.*, 61:473–497, 2008.